In vitro selection of functional DNA for molecular catalysis, conjugation, and sensing

by

Kun Liu

B.Sc., Taiyuan University of Technology, 2009

M.Sc., Tsinghua University, 2012

Thesis Submitted in Partial Fulfillment of the
Requirements for the Degree of
Doctor of Philosophy

in the
Department of Chemistry
Faculty of Science

SIMON FRASER UNIVERSITY
Summer 2021

Declaration of Committee

Name:	**Kun Liu**
Degree:	**Doctor of Philosophy**
Title:	**In vitro selection of functional DNA for molecular catalysis, conjugation, and sensing**
Committee:	**Chair:** Tim Storr Professor, Chemistry
	Hua-Zhong Yu Supervisor Professor, Chemistry
	Dipankar Sen Committee Member Professor, Chemistry
	Jeffrey Warren Committee Member Associate Professor, Chemistry
	David Vocadlo Committee Member Professor, Chemistry
	Gary Leach Examiner Associate Professor, Chemistry
	Maxim V. Berezovski External Examiner Professor Department of Chemistry and Biomolecular Sciences University of Ottawa

Abstract

As the central theme of this thesis research, *in vitro* selection has been performed to isolate functional DNAzymes and DNA aptamers for molecular catalysis and sensing. Not only details of the *in vitro* selection and characterization of functional DNAzymes and aptamers, but also their applications for the catalytic conjugation of biological macromolecules, immobilization of redox functionalities on surfaces, and ultrasensitive detection of total copper in industrial samples are presented.

Copper is known to bind DNA on both negatively charged phosphate backbone and nucleobases; through *in vitro* selection, it has been demonstrated that these interactions can be coordinated in a DNAzyme to catalyze alkyne-azide cycloaddition reaction with ultralow concentrations of either Cu(I) or Cu(II) as a cofactor. The selected DNAzyme, namely, CLICK-17, catalyzes the reaction with high efficiency under both *in cis* (single turn-over) and *in trans* (multi turn-over) conditions. After characterization and kinetics studies, three applications of CLICK-17 have been explored: (1) As a biocompatible coupling reagent for labelling azide-functionalized biological macromolecules; (2) As a highly efficient co-catalyst for the immobilization of electrochemical reporters onto azide-terminated self-assembled monolayers (SAMs); (3) As a superior transducer for the construction of an electrochemical biosensor for copper.

The isolation of DNA aptamers binding to small molecules is challenging, due to their lack of chemical functionalities to interact with DNA strands. Ferrocene is a particularly refractory target, as a mater of fact. Conventional *in vitro* selection method (ferrocene immobilized on a supporting bead) and capture selection method (DNA library immobilized on a supporting bead) in isolating aptamers binding to a water-soluble ferrocene derivative have been compared. A ferrocene binding aptamer with moderate binding affinity was isolated with capture selection method.

In summary, this research achieved the *in vitro selection* of a DNAzyme that is useful for developing different types of applications, and a DNA aptamer that can potentially deepen our understanding of molecular recognition between a DNA aptamer and its target.

Keywords: *In vitro* selection, DNAzyme, DNA aptamer, CuAAC, Copper Sensing, ferrocene

Dedication

This thesis is dedicated to my wife Lihua Cao

Acknowledgements

I would like to thank both my supervisors, Dr. Dipankar Sen and Dr. Hogan Yu, for all the help I got from them, their ever-last patience and enlightening mentorship.

Table of Contents

List of Tables

List of Figures

List of Acronyms

ATP	Adenosine triphosphate
AuNP	Gold Nanoparticle
CLICK-17	CuAAC catalyzing DNAzyme
CTP	Cytidine triphosphate
CuAAC	Copper catalyzed Azide-Alkyne Cycloaddition
GTP	Guanosine triphosphate
LFSE	Ligand field stabilization energy
PAGE	Polyacrylamide gel electrophoresis
SELEX	Systematic evolution of ligands by exponential enrichment
SPAAC	Strain-promoted azide-alkyne cycloaddition
THPTA	Tris(3-hydroxypropyltriazolylmethyl)amine
TTP	Thymidine triphosphate
SAM	Self-assembled monolayer

Chapter 1. General Introduction

In 1869, the Swiss physiological chemist Friedrich Miescher identified a new substance ‘nuclein’ from human white blood cells that were collected from used, pus-coated patient bandages. It took a hundred years after the initial discovery of this substance for elucidation of the actual structure of ‘nuclein’ or deoxyribonucleic acid (as well known today). In 1953,[1] Watson and Crick reported the double helix structure of DNA that has four key features: (1) DNA is double-stranded helix, with both strands consisting of A (adenosine), T (thymidine), G (guanosine), and C (cytidine) dexoyribonucleotides, and connected via hydrogen bonding between A (adenine) and T (thymine) as well as G (guanine) and C (cytosine) bases; (2) The two strands run anti-parallel to each other, i.e., the 5’-end of one strand is paired with the 3’-prime end of the complementary strand; (3) Most DNA double helices that have been obtained under crystallization conditions are right-handed; (4) There are minor grooves and major grooves in the double-helix structure where interactions with other molecules can occur.[2] With the exception of certain types of viruses, DNA carries the hereditary information, or genes, for all living organisms. DNA is chemically and thermally stable, and its unique double helix structure is sturdy and at the same time flexible enough for opening and reforming. All these features make DNA a highly suitable material for the storage and propagation of genetic information. As of now, the nucleic acid research field has grown massively beyond its initial days. Beyond functioning as cellular genomes, DNA analogues have been explored as components of anticancer chemotherapeutics, elegant self-assembled nanostructures, as entities (aptamers) for specific binding to specific molecular targets tightly and, most intriguingly, as new classes of macromolecular catalysts (DNAzymes) for metabolic as well as non-metabolic chemical reactions.

1.1. *In vitro* selection: principle and methodology

1.1.1. *En route* to functional nucleic acids via *in vitro* selection from random pools

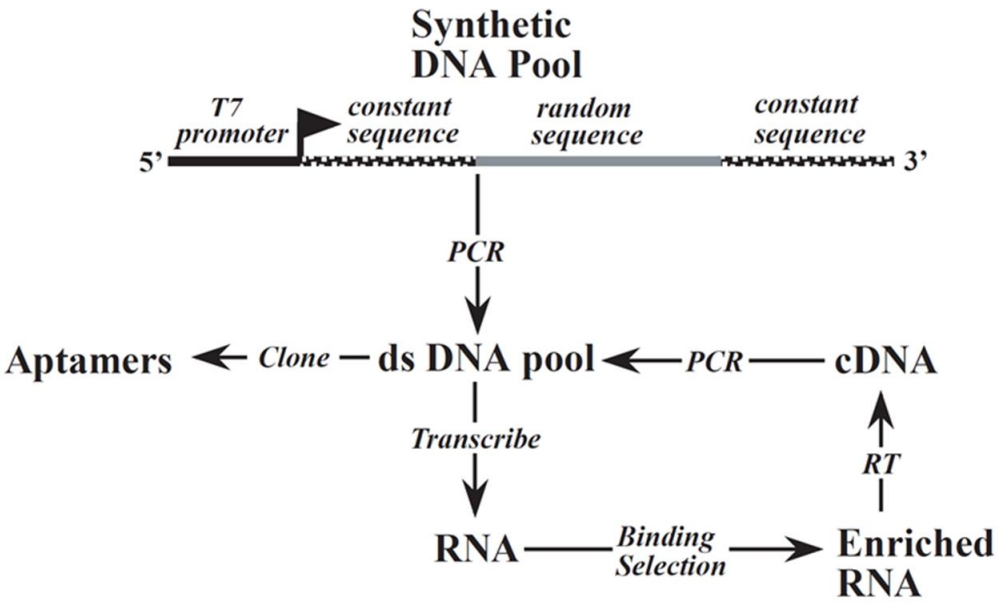

Figure 1.1 Typical aptamer pool structure and scheme for selection process. For selection of RNA aptamers, a DNA pool is chemically synthesized with a region of random sequence flanked on each end by constant sequence and with a T7 RNA polymerase promoter at the 5' end. This DNA is amplified by a few cycles of PCR and subsequently transcribed in vitro to make the RNA pool. The RNA molecules are then partitioned based on whether they bind to the chosen target compound, for example, by passing them through an affinity column derivatized with the target. The retained RNAs are eluted, reverse transcribed, amplified by PCR, transcribed, and then the entire cycle is repeated. For selection of DNA aptamers, DNA pool is used directly without transcribing into RNA.

Note. Reprinted with permission from Wilson, D. S.; Szostak, J. W. *In Vitro* Selection of Functional Nucleic Acids. *Annu. Rev. Biochem.* 1999, 68 (1), 611–647.Copyright 1999. Annual Reviews.

Traditionally, it is believed that catalysis of metabolic reactions within living cells is a function reserved for proteins, with nucleic acids having no role in catalyzing chemical transformations. However, such a hypothesis led to challenging questions in the context of the origin of life on earth, with regard to which macromolecule likely predated others

during the origin of life, i.e., did polypeptides/protein, that are responsible for the catalytic and mechanical work in modern cells, come first, or did nucleic acids (RNA or DNA) that carries the coding information in modern cells for proteins? There is a conjectural stage in the origin of life, where a nucleic acid, capable of carrying the hereditary information, could also serve to carry out catalytic functions. RNAs functioning both as genome and genome-encoded catalysts may have existed, and this was given the name of The RNA World Hypothesis.[3] Indeed, in 1982-1984, first catalytic RNAs, or ribozymes, were reported from living organisms by Thomas Cech from the University of Colorado, and Sidney Altman from Yale University. Independently, they discovered two ribozymes: Cech reported that ribosomal RNA from Tetrahymena thermophila was able to excise introns within itself without the help of proteins;[4] Altman reported a nucleoprotein enzyme, RNase-P, involved in the processing of tRNAs, in which the RNA component of the RNA-protein complex was the catalytic entity.[5] Since the discovery of these two initial ribozymes, the search for RNA-world relevant ribozymes has never stopped. Indeed, many classes of naturally occurring ribozymes have been identified in a variety of organisms; it has been recognized that key and universal cellular processes such as mRNA splicing and ribosome-based protein synthesis are in fact RNA-catalyzed. Both the structure and mechanism of different ribozymes are diverse, owing to the fact that RNA folds to form complex 3D structure (which forms the basis for their diverse functionalities) like their protein counterparts.

With all these pioneering findings, researchers started to ask the question: can any given set of random nucleotide sequences fold into stable 3D structures that manifest some kind of measurable function? Two technological developments in the 1980s made the investigation of this question possible. First, the technology of solid-phase synthesis of DNA makes it relatively easy to prepare randomized DNA pools (for an RNA pool, a DNA pool is synthesized and then transcribed by T7 RNA polymerase) in large quantities for test tube experimentation. Second, the invention of PCR allows the amplification of extremely small amounts of DNA templates. Thus, one can synthesize a randomized DNA pool containing a large (1013-1015) ensemble of sequences that can fold to give unique 3D structures. This large population of 3D-folded DNAs then forms the basis set for a search for novel functionalities of either binding or catalysis. By fishing out potentially rare sequences with a desired functionality and then amplifying them with PCR, functional DNA or RNA were eventually obtained. This process was named as *in vitro* selection (or, Systematic Evolution of Ligands by Exponential Enrichment, SELEX), shown

schematically in Figure 1.1.[6] The first *in vitro* selection was done by Ellington and Szostak,[6] who passed a 3D-folded random RNA library through a set of columns containing covalently immobilized dye molecules. Following removal of the non-specifically bound RNA by a series of washing steps, the bound RNA molecules, which shared a common functional property of binding to specific dye molecules, were eluted, collected, and amplified by RT-PCR (reverse transcription followed by PCR). By iterative and progressive enrichment of dye-binding RNAs, final pools of specific dye-binding RNAs were obtained, which could be subsequently cloned, sequenced, resynthesized, and analyzed for affinity and specificity of binding to the cognate dye targets. Indeed, RNA molecules binding to specific target with high affinity and selectivity were identified. These target binding RNA molecules were named as 'aptamers', which were derived from the Latin *aptus* - fit, and Greek *meros* - part. This seminal work opened a whole field of discovering artificial functional RNA/DNA and their applications.

DNA, a chemically similar biopolymer to RNA, can also form a variety secondary, hierarchical structures. Double-stranded DNA typically forms B-type duplex, while RNA forms A-type duplex most of the time. There are B-type duplex moieties in folded RNA in rare situations, for example, the kissing loop formed in the HIV dimer linkage structure.

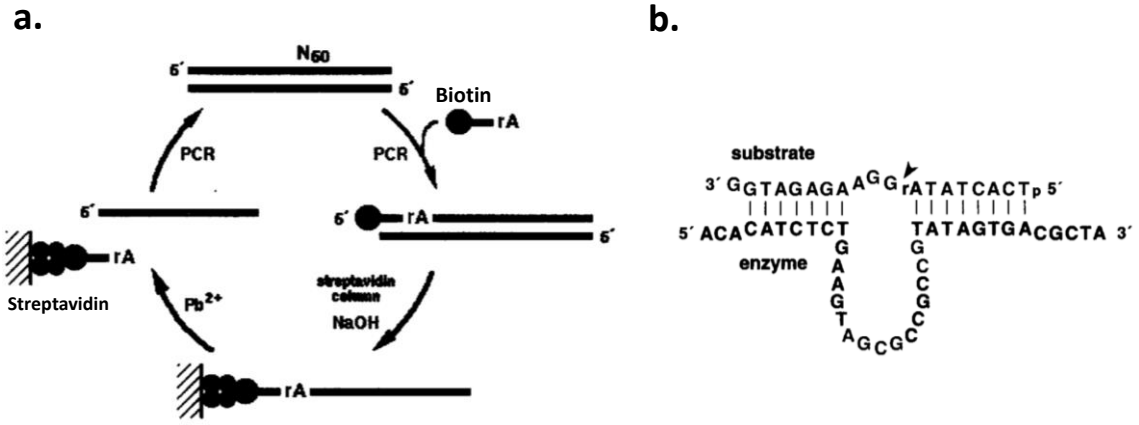

Figure 1.2 The first DNAzyme selection done by Joyce and Breaker. (a) *In vitro* selection procedure: Double-stranded DNA that contains a stretch of 50 random nucleotides is amplified by PCR, employing a 5'-biotinylated DNA primer that is terminated at the 3' end by an adenosine ribonucleotide (rA). This primer is extended by Taq polymerase to yield a DNA product that contains a single embedded ribonucleotide. The resulting double-stranded DNA is immobilized on a streptavidin matrix and the unbiotinylated DNA strand is removed by washing with 0.2 N NaOH. After re-equilibrating the column with a buffered solution, the column is washed with the same solution with added 1 mM PbOAc. DNAs that undergo Pb^{2+}-dependent self-cleavage are released from the column, collected in the

eluate, and amplified by PCR. The PCR products are then used to initiate the next round of selection; (b) the sequence of the Pb(II)-dependent RNA cleaving DNAzyme and its substrate.

Note. Reprinted with permission from Breaker, R. R., Joyce, G. F. A DNA Enzyme That Cleaves RNA. *Chem. Biol.* 1994, 1 (4), 223–229. Copyright 1994 Elsevier Ltd.

In addition to typical double helices as mentioned above, certain sequences can bind to a poly Y • poly R duplex (Y = pyrimidine, R = pyridine) to form triplex structures.[7] Guanine-rich sequences in the presence of appropriate cations (Na^+, K^+) forms a polymorphic family of G-quadraplex structures. Initially, owing to its lack of the C2'-hydroxyl group, DNA was thought to be less potent than RNA in forming the stable tertiary structures needed for complex functionalities. Furthermore, in organisms, unlike RNA, there was no solid experimental evidence for the involvement of DNA in any binding or catalytic processes. However, a large set of artificial functional DNA, both for ligand binding and catalysis, has been isolated from random DNA libraries via *in vitro* selection, with a procedure similar but simpler than that used for selecting RNA aptamers. The first DNA *in vitro* selection was also carried out by Ellington and Szostak, against the same dye molecules used for the first RNA *in vitro* selection.[8,9] Following 5 rounds of selection, single stranded DNA aptamers binding to specific dye columns were identified. The affinity of DNA aptamers to bind to their cognate dyes was found to be comparable to the RNA counterpart. At the end of this work,[9] it was proposed that catalytic DNAs should also, in principle, exist and be amenable to isolation via *in vitro* selection for binding transition-state analogues from reactions of interest — using the approach for generating catalytic antibodies.[9]

However, the first *in vitro* selection-derived catalytic DNA reported was not a transition-state analogue binding aptamer; rather, it was a Pb(II)-dependent RNA cleaving DNAzyme, isolated by Breaker and Joyce in 1994.[9] A randomized DNA library with a rA (ribonucleotide) as the designated cleaving site was prepared, after incubation in the presence of metal cations, catalytic DNA cleaved and released from the solid matrix. These DNA is used as template for the recovery of single-stranded DNA library. As shown in Figure 1.2a, the selection strategy to obtain this family of DNAzymes was based on the premise of a single catalytic turnover which 'tagged' (in this case cleaved) certain members of the DNA random pool. In fact, all the later *in vitro* selection for DNAzymes were based on a single turn-over event, or under the *in cis* condition. Except for a few cases,[10] it usually takes further efforts to convert such a selected DNAzyme to work under

multi turn-over, or *in trans*, conditions. By analyzing the sequences of the enriched library from the final round, a 38nt long DNAzyme that cleaves a 19nt DNA with one rA in the presence of Pb(II) was identified. The DNAzyme cleaves the RNA substrate with a more than 105 -fold higher rate constant than the uncatalyzed reaction (Figure 1.2b).

1.1.2. Structure and binding mode of DNA aptamers

As the first aptamer was reported in 1990 (30 years ago), a large body of literature now exists on nucleic acid aptamers. Chaput recently analyzed papers reporting nucleic acid aptamer published between 1990-2015.[11] 4795 non-redundant articles came out with the term 'nucleic acid aptamer' searched on Web of Science, Google Scholar and PubMed. Out of these, 843 are reporting the discovery of new aptamers, 3152 describing applications of aptamers, and 800 being review articles. These papers were further analyzed in terms of target molecules, backbone chains, and post-SELEX modifications (aptamers generated by private companies were not included). Among the 843 discovery articles, 1003 *in vitro* selection experiments were performed against 705 unique targets ranging from small molecules to whole cells. Protein targets were the most chosen targets, corresponding to 584 entries, followed by small molecules and cells with 234 and 141 entries, respectively. The top five most chosen targets for aptamer development were human α-thrombin, streptavidin, vascular endothelial growth factor (VEGF), influenza haemagglutinin, and adenosine-5´-triphosphate (ATP). In terms of backbone identity, DNA aptamers (428 entries) corresponded to more than 50% of all the aptamers discovered. The number of RNA aptamers listed was 288. In addition to natural DNA and RNA aptamers, 'unnatural' nucleic acids were also prepared for selection of new classes of aptamers. Indeed, 127 instances of such aptamers were listed.

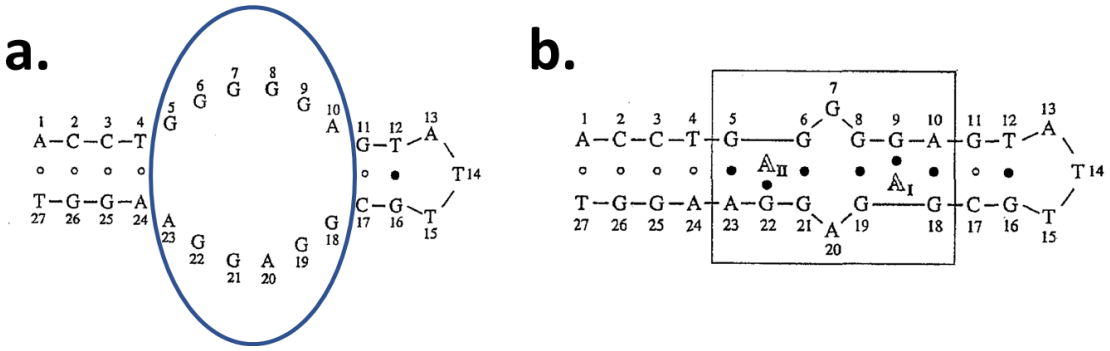

Figure 1.3 (a). Wason-Crick alignment of 27mer AMP binding DNA aptamer. The unstructured asymmetric 'bubble' (circled) zippers up upon AMP binding; (b). the secondary fold of aptamer-AMP complex determined by NMR results.

Note. Reprinted with permission from Lin, C. H.; Patei, D. J. Structural Basis of DNA Folding and Recognition in an AMP-DNA Aptamer Complex: Distinct Architectures but Common Recognition Motifs for DNA and RNA Aptamers Complexed to AMP. *Chem. Biol.* 1997, 4 (11), 817–832.Copyright 1997 Elsevier Ltd.

Natural DNA and RNA consist of five different monomeric nucleotide 'units' (A, T, G, C, and U) linked by deoxyribose/ribose-phosphate backbones. The chemical diversity is limited to the bases and backbone. How does DNA/RNA, with such simple chemical complexity, nevertheless form complex 3D structures capable of recognizing and binding target molecules? The binding mode of the ATP binding DNA aptamer is a good example of how a DNA aptamer recognizes and binds its target. As 'pointed out by Chaput, ATP has been one of the most heavily investigated targets for *in vitro* selection; both DNA and RNA aptamers have been isolated and characterized.[12,13] The binding mode in both cases is clearly elucidated and well understood. Patel and co-workers determined the solution structure of the AMP-binding DNA aptamer complex by NMR, and found that one ATP binding aptamer actually binds to two AMPs (the ATP aptamer binds AMP equally well as ATP) molecules with two non-equivalent binding pockets.[14] The internal unstructured asymmetric 'bubble' (circled in Figure 1.3a) zippers up when the two AMP molecules bind (the adaptive binding seems to be a common feature for both DNA and RNA aptamers binding to their target). As shown in Figure 1.3b, a G•AMP mismatch is responsible for the recognition of AMP in both binding pockets. The G•AMP mismatch is further stacked with a G•G reverse Hoogsteen base pair on one side and an adenine on the other side for both cases. Two three-base platforms (G8•G19) •G20 and (G21•G6) •G7, with three purine bases linearly aligned, are formed to widen the minor groove of the duplex. Together with the sheared G•A mismatch, these alignments form the rectangular binding pockets for

AMP. The structure of the ATP binding RNA aptamer has also been resolved.[15] Comparison between the structures of DNA and RNA aptamer revealed that, despite all the differences in binding, both aptamers utilize a G•AMP mismatch as the recognition alignment. In both cases, the G•AMP mismatch is stacked on one side with a G•G reverse Hoogsteen base pair and on the other side with an adenine. This similarity confirms that both DNA and RNA fundamentally use the same strategies in recognizing the same target. The resolved structure shows that, neither the sugar moiety nor the phosphate group on C5 of the ribose is involved in binding; this explains why both aptamers, selected against ATP, turned out to bind adenine, adenosine, deoxyadenosine, AMP, and ATP with K_d values in the same order of magnitude.

NMR characterization of representative ATP-DNA aptamer complex indicates that aptamers mainly rely on the following interactions in their binding: (1) Shape complementarity, (2) Specific hydrogen bonding, (3) base stacking. A few other interactions such as hydrophobic effect and electrostatic interactions (for charged targets) also play important roles in certain cases.[14]

In many situations, it is needed that aptamers can distinguish structurally related targets, for example, specifically sensing of disease related biomarkers. For example, the ATP-binding DNA aptamer would not be particularly useful in these cases since it recognizes both ATP and AMP, even they are different by two phosphate groups.[14] In fact, negative selections against related target molecules can be adopted to improve the selectivity of aptamers. They work on the assumption that highly specific aptamers exist in the starting random DNA library; one might be able to remove aptamer sequences that lack the desired specificity for the intended target by passing the library through affinity columns containing immobilized unwanted targets, eventually retain only the highly specific binders in the pool. A positive selection, against the desired target compound, can then be used to fish out the highly specific binders. Szostak et al. adopted a related strategy to isolate an RNA aptamer that bound ATP, but not AMP.[16]

Starting with an RNA library with estimated 10^{15} unique sequences, the RNA pool went through an AMP column (negative selection), followed by passing through an ATP column (positive selection). The AMP binders were further selectively discarded by washing the ATP column with buffer containing 5 mM AMP. Finally, the highly specific ATP binders were competitively eluted by a buffer containing 5mM ATP. By such a counter-selection

procedure, an RNA aptamer capable of distinguishing closely related target structures was isolated. Most strikingly, the selection protocol was designed to go against the intrinsic property of negatively charged nucleic acids i.e., bind poorly to negatively charged chemical moieties. Szostak's ATP-specific aptamer showed that an RNA aptamer is able to interact with even a negatively charged phosphate backbone in a way to specifically recognize it. The negative selection and counter-selection approaches have now become a routine for *in vitro* selections in order to isolate highly specificity aptamers.

1.1.3. Expanding the backbone diversity of DNA/RNA

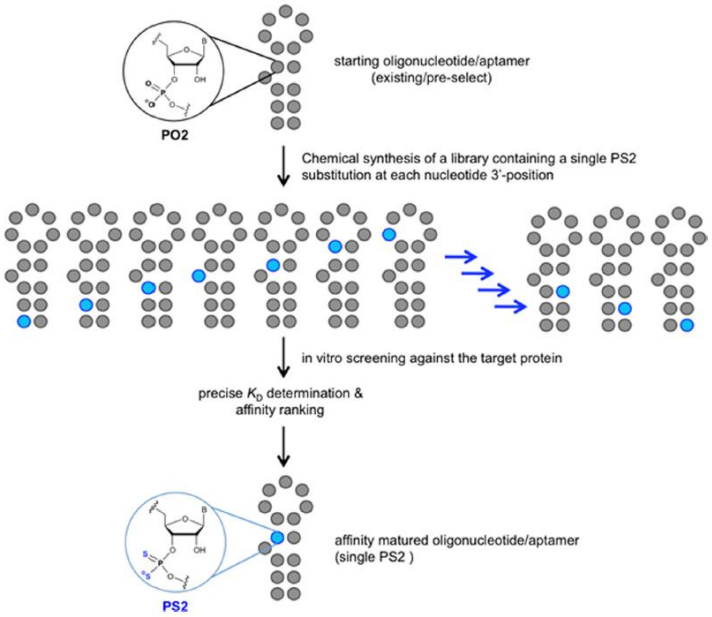

Figure 1.4 Schematic illustration of the PS2-walking experiment using an aptamer library of sequence variants each containing a single PS2 modification. By *in vitro* screening against thrombin, the best binder was identified and characterized.

Note: Reprinted with permission from Abeydeera, N. D. et al. Evoking Picomolar Binding in RNA by a Single Phosphorodithioate Linkage. *Nucleic Acids Res.* 2016, 44 (17), 8052–8064. Copyright 2021 Oxford University Press.

Unlike proteins that are composed of 20 different amino acids, DNA/RNA offer more limited chemical diversity. Indeed, with *in vitro* selection, some targets are poorly 'aptagenic', owing to their lack of chemical functionalities to interact with DNA/RNA. To expand the chemical diversity of DNA/RNA, nucleic acid-like unnatural polymers consisting completely or partially modified nucleobase and/or sugar moieties have been explored. Such broadened chemical diversity has facilitated aptamer isolation against

refractory targets,[17] and helped to enhance the function of aptamers[18] while improve their nuclease stability.[19]

Chemical modifications to DNA can be introduced either after *in vitro* selection, known as post-SELEX modification, or during SELEX using a library of chemically modified DNA. As an example of post-SELEX modification, Yang and co-workers successfully enhanced the binding of thrombin aptamer by introducing a phosphorodithioate (PS2) linkage.[18] Indeed, post-SELEX modifications have been extensively explored as a means to increase the biological stability of DNA and RNA aptamers lately. However, post-SELEX modifications often disturb the natural folding of aptamers; therefore, it needs to be carefully designed and often a trial and error process to allow the introduction of desired modifications while preserving an aptamer's binding property. Yang and co-workers' have shown that the modification with a phosphorodithioate (PS2) linkage enhances the binding property of the well-known thrombin binding DNA aptamer; particularly the two non-bridging phosphate oxygen atoms in the nucleic acids are replaced with sulfurs to form such a PS2 linkage. Crystallographic studies revealed that the introduction of PS2 linkage tends not to change the global structure of folded DNA/RNA.[20] Furthermore, the PS2 linkage modification has been shown to enhance the interaction between the modified DNA/RNA with proteins, owing to the superior hydrophobic interactions among PS2 moieties relative to its phosphate counterpart. To probe the optimal site for the introduction of PS2 modification, Yang et al. chemically synthesized a series of α-thrombin binding RNA aptamers (AF113), each with a single PS2 substitution at the nucleotide 3'-position. These AF113 variants were named as AF113-1(native), AF113-2, until AF113-25 (Figure 1.4). It was found that AF113-18 had a binding affinity ~1000-fold higher than the native aptamer AF113-1, i.e., the K_d is 1871 pM for AF113-1 and 1.8 pM for AF113-18, respectively. was then crystalized, and the crystal structure was resolved to 0.19 nm. The high-resolution (0.19 nm) crystal structure of the AF113-18/α-thrombin complex revealed that the overall conformation of AF113-18 resembles that of the natural AF113, except for new hydrophobic interactions established between the PS2 linkage and bound thrombin. These hydrophobic interactions are likely responsible for the enhanced binding affinity.

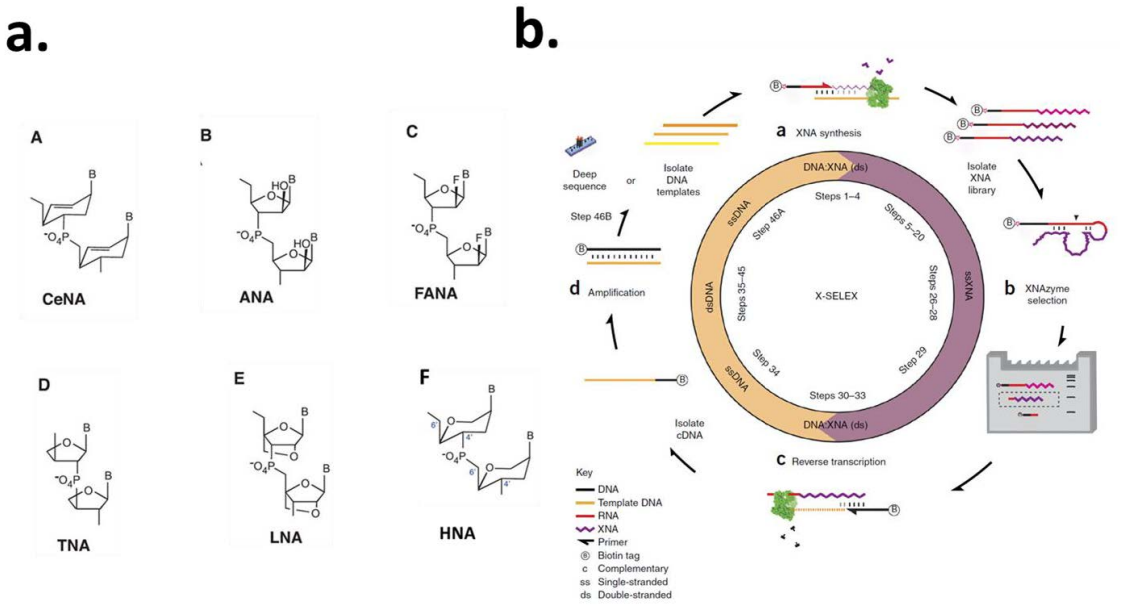

Figure 1.5 (a) Molecular structures of XNA unnatural ribose moiety: 1,5-anhydrohexitol nucleic acids (HNAs), cyclohexenyl nucleic acids (CeNAs), 2'-O,4'-C-methylene-b-D ribonucleic acids [locked nucleic acids (LNAs)], arabinonucleic acids (ANAs), and 2'-fluoro-arabino nucleic acids (FANAs).; (b) overview of X-SELEX procedure: a) Diverse repertoires of XNA molecules may be synthesized (using engineered DNA-dependent XNA polymerases; b) Catalytic XNAs (XNAzymes) may be selected by reacting libraries of XNAs tagged with substrates of interest and isolating on the basis of change in substrate (e.g., urea-PAGE gel shift upon RNA hydrolysis); c,d) XNAzymes may be subsequently reverse-transcribed using engineered XNA-dependent DNA polymerases; c), yielding cDNA that may be amplified to enable either deep sequencing or generation of templates for XNA synthesis; d), and further rounds of X-SELEX.

Note: Reprinted with the permission from Taylor, A. I.; Holliger, P. Directed Evolution of Artificial Enzymes (XNAzymes) from Diverse Repertoires of Synthetic Genetic Polymers. *Nat. Protoc.* 2015, 10 (10), 1625–1642. Copyright 2015. Springer Nature.

Post-SELEX modifications usually have unpredictable, sometimes adverse effect on the binding of aptamers to their targets. That is because it is quite difficult to introduce modifications into aptamer without disturbing its binding property. On the contrary, SELEX done with a DNA library already bearing chemical modifications should be able to counter these problems. Despite all the potential benefits, *in vitro* selection with noncanonical polynucleotides have been sparingly explored owing to the technical difficulties. Both the noncanonical library preparation and the engineering of suitable DNA polymerase(s) capable of amplifying the noncanonical nucleic acid sequences are very difficult to achieve. Holliger and co-workers reported *in vitro* selections carried out with XNA libraries,[21] where XNA refers to a polymer strand made of these unnatural nucleotides. as shown in Figure

5. The canonical ribose of DNA/RNA is a ribofuranose, the authors replaced the ribofuranoses with five- or six-membered congeners, generating 1,5-anhydrohexitol nucleic acids (HNAs), cyclohexenyl nucleic acids (CeNAs), 2'-O,4'-C-methylene-b-D ribonucleic acids [locked nucleic acids (LNAs)], arabinonucleic acids (ANAs), and 2'-fluoro-arabino nucleic acids (FANAs). Then via protein engineering, a DNA polymerase that synthesize XNA from a DNA template was generated. A reverse transcriptase that allows synthesis of complementary DNA from an XNA template was also generated. A library of XNA was prepared by using this XNA polymerase and a synthetic DNA library as template (Figure 1.5a). After being partitioned on a target-bearing affinity column, the column-bound XNA was reverse transcribed into cDNA (Figure 1.5b). This cDNA was then amplified by PCR, followed by regeneration of the XNA library using DNA-dependent XNA polymerase. Using this method, they were able to identify two XNA aptamers, one targeted at a HIV trans-activating response RNA (TAR) and the other directed to hen egg lysozyme (HEL). Both aptamers showed similar binding affinities as their natural aptamer counterparts. However, the XNA aptamers were complete inert to nuclease digestion owing to their unnatural sugar moieties, which makes XNA aptamers ideal candidates for in vivo applications. Natural DNA/RNA has a limited half-life in biological environments (the unmodified DNA aptamer developed as an α-thrombin inhibitor exhibited an in vivo half-life of < 2 min when assayed in a primate animal model).[22]

Holliger's *in vitro* selection required engineered polymerase; modifications that are compatible with traditional DNA polymerase have been explored as well. Tan and co-workers reported *in vitro* selections performed with a DNA library consisting of the 4 canonical nucleotides, GACT and two unnatural nucleotides, Z and P (Figure 1.6a).[23] The DNA library containing GACTZP was prepared and incubated with a breast cancer cell line (MDA-MB-231); the bound oligonucleotides were then amplified using a Taq DNA polymerase. DNA aptamers binding to MDA-MB-231 were successfully isolated. In the mean time, Eaton and co-workers reported *in vitro* selection carried out with a DNA library containing C5-modified uridine (Figure 1.6b).[24] Though PCR under normal conditions can not occur with modified dUTP, primer extension can be done with similar efficiency as canonical dTTP using commercially available DNA polymerases. A DNA aptamer was isolated to bind necrosis factor receptor superfamily member 9 (TNFRSF9), a target they failed to find aptamers with *in vitro* selection using canonical DNA library.[24]

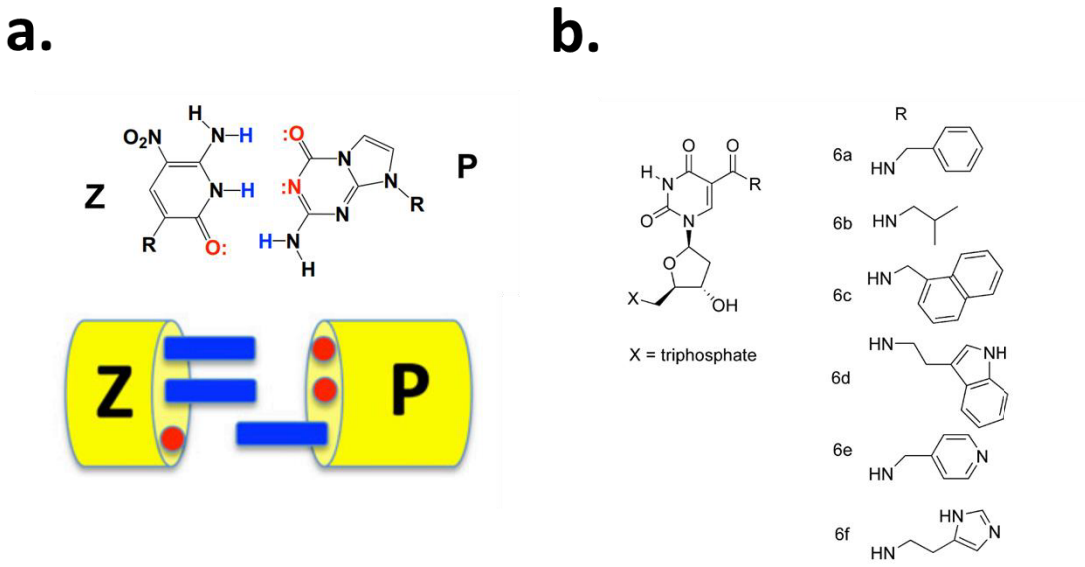

Figure 1.6 a) structure of unnatural nucleotides Z and P. They base pair with each other; b) structures of dUTP derivatives.

Note: Reprinted with the permission from Sefah, K. et al. *In Vitro* Selection with Artificial Expanded Genetic Information Systems. *Proc. Natl. Acad. Sci. U.S.A*. 2014, 111 (4), 1449–1454. Copyright 2021 National Academy of Sciences.

Despite all the potential benefits of chemically modified aptamers, obvious drawbacks hindered the development of unnatural nucleic acid aptamers. Often, organic synthetic skills and apparatus are necessary; also, customized polymerases are usually needed. Unlike regular *in vitro* selection, it is very difficult for most biochemistry labs to carry out unnatural aptamer SELEX. Post-SELEX modifications are relatively easier, but facing the risk of disrupting the function of the aptamer. Before these obstacles are cleared out of the way, natural DNA/RNA aptamers will continue to be the main focus for developing applications. As a matter of fact, the ease of carrying out traditional *in vitro* selection makes it a good starting point for investigating more challenging aptamer selection protocols.

1.1.4. Modified *in vitro* selection procedures

The canonical *in vitro* selection procedure, being easy to conduct, is very tedious and laborious. On average, 8-15 rounds of selection are needed to isolate an aptamer.[25] Furthermore, it is not very effective for poorly aptagenic targets owing to the bead-immobilization method widely used in the canonical *in vitro* selections.

In specific, traditional *in vitro* selection usually involves the use of beads as solid matrix, where targets (from small molecules, peptides to proteins) are immobilized to allow affinity partitioning of the functional oligonucleotides. However, there are some intrinsic problems with this method. Firstly, the derivatized beads themselves are a source for non-specificity in the library; secondly, unpredictable steric hindrance may come in play. One has no control over how the immobilized molecules distribute themselvs on a bead's surface. Target molecules may form clusters, which may make them inaccessible for aptamer binding. Thirdly, the bead's surface is not perfectly even; therefore, steric hindrance from the beads' morphology might also interfere with the nucleic acid library approaching some of the target molecules, especially when the targets are poorly aptagenic.

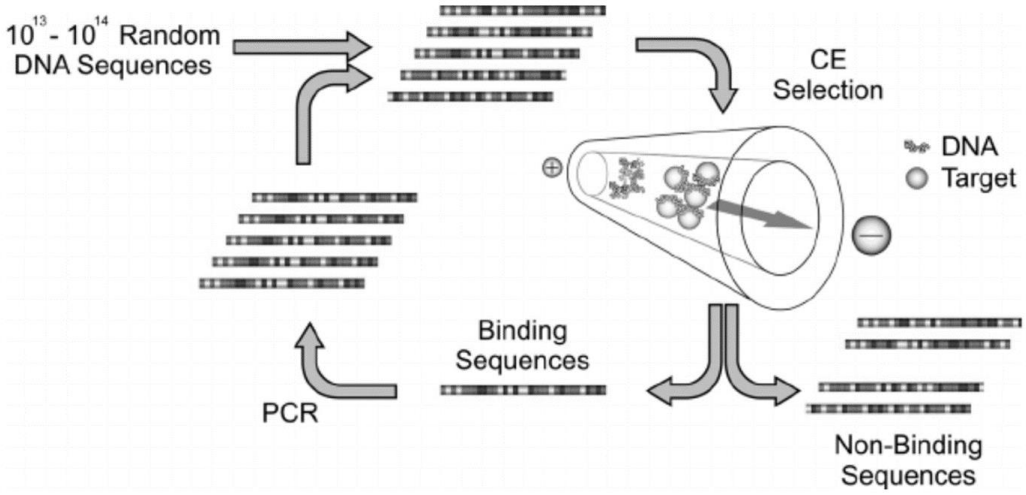

Figure 1.7 Schematic illustration of Capillary SELEX (CE-SELEX) procedure. It uses electrophoresis to separate binding sequences from inactive ones. Active sequences and inactive sequences are partitioned and collected as separate CE fractions.

Note: Reprinted with permission from Mendonsa, S. D.; Bowser, M. T. *In Vitro* Evolution of Functional DNA Using Capillary Electrophoresis. *J. Am. Chem. Soc.* 2004, 126 (1), 20–21. Copyright 2004. The American Association for the Advancement of Science.

Capillary electrophoresis has been explored to replace the bead immobilization method to avoid the biases induced by stationary support and linker.[25,26] Mendonsa and Bowser are the first to incorporate microfluidic approaches into *in vitro* selection. A DNA aptamer binding human IgE with 27 nM K_d was isolated within 4 rounds using a new capillary electrophoresis SELEX(CE-SELEX), for which solution-based capillary electrophoresis was performed to separate binders from non-binders.[26] An extremely small volume (50 nL) of the sample containing 2.3 mM DNA library and 1.0 pM human IgE

was injected into the capillary; protein-bound DNA and unbound DNA were separated owing to their very different retention times (Figure 1.7). Unbound DNA are negatively charged and migrated rapidly in the capillary. The protein/bound DNA complex, in contrast, migrated much slower due the following two factors: (1) the large size of the complex; (2) The pH (8.0) was close to the isoelectric point of IgE. Under this condition, the protein was almost electrically neutral, which made it migrate very slow in the capillary. This separation was so effective that after the first round of selection, the DNA library already showed more than 50% of binding to IgE. The solution-based separation was obviously more advantageous than bead-based separation in reducing the number of rounds needed for the isolation of aptamers. However, the CE-SELEX method has a major limitation on the choice of target molecules. It works only with targets that, when bound to DNA, induce enough retention time difference to allow separation.

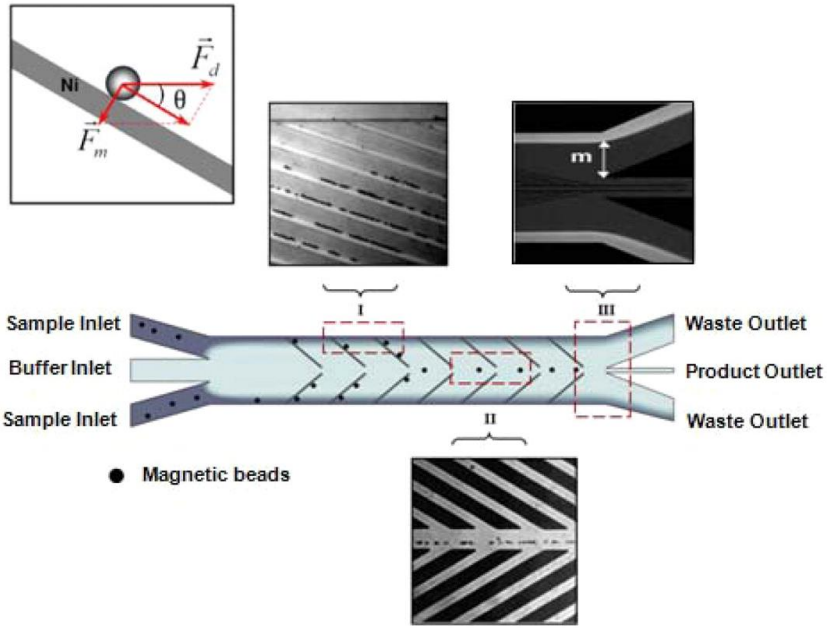

Figure 1.8 Schematic of the hydrodynamic (F_d) and magnetophoretic (F_m) forces on the magnetic particle in the device, relative to the nickel patterns in the microchannel (Top left corner). Schematic of the flow pattern and deflection of magnetic beads within the microchannel. Target protein-coated magnetic beads are selectively guided by the combined mechanical forces along the Ni strips and eluted through the product outlet, whereas unbound aptamers are directed into the waste outlets.

Note: Reprinted with permission from Lou, X.; Qian, J.; Xiao, Y.; Viel, L.; Gerdon, A. E.; Lagally, E. T.; Atzberger, P.; Tarasow, T. M.; Heeger, A. J.; Soh, H. T. Micromagnetic Selection of Aptamers in Microfluidic Channels. *Proc. Natl. Acad. Sci. U.S.A.* 2009, 106 (9), 2989–2994. Copyright 2009. National Academy of Sciences.

Soh and co-workers reported another microfluidic *in vitro* selection method, for which a bead-based traditional selection was carried out in a microfluidic channel.[27] The microfluidic device allowed much higher stringency to be exerted during selection, which enabled good binders to be selected in one round. As shown in Figure 1.8, a microfluidic channel with embedded Ni stripes was prepared; magnetic beads with target molecule attached were incubated with the DNA library before loaded through the two sample inlets. Magnetic beads (with the target molecule and DNA binders bound to it) were attracted onto the Ni strips with the help of a magnet while unbound DNA strands were eluted out and discarded from the waste outlet. The magnetic beads with bound DNA were collected from the product outlet. With one round of selection, a DNA aptamer binding the light chain of recombinant Botulinum neurotoxin type A with a low nM binding affinity was isolated.

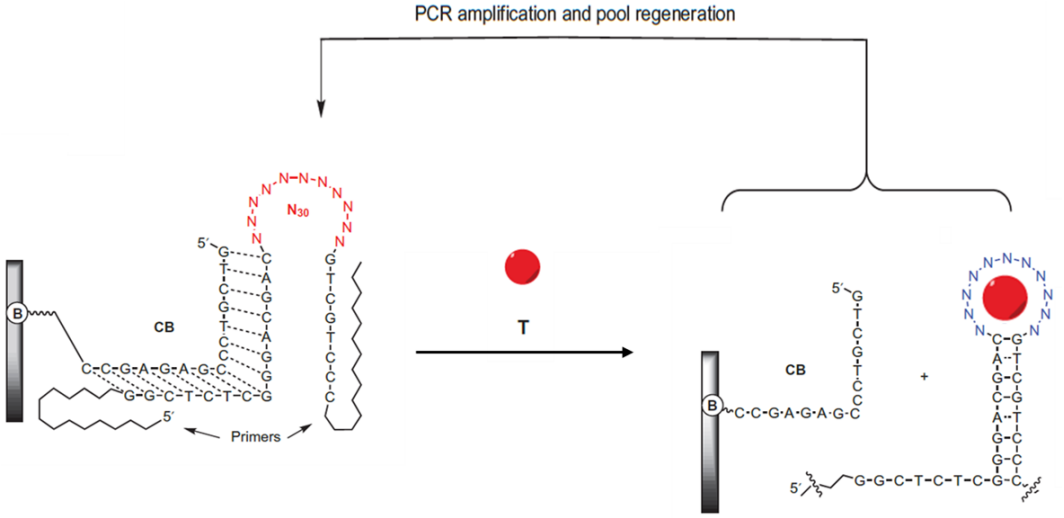

Figure 1.9 A schematic representation of capture selections procedure: a library (for example a randomized region N30 flanked with primers) is attached to an agarose–streptavidin column via a biotinylated complementary oligonucleotide (Capture oligo). On binding to a target molecule (T), aptameric structures are released preferentially from the column as a result of stabilization of the stem formation, PCR amplified and therefore, evolutionarily favoured to survive through multiple selection cycles.

As demonstrated with above two examples and other reported microfluidic SELEX,[25] it is evident that microfluidic SELEX can reduce the number of rounds needed to isolate aptamers from a randomized DNA library. They can be potentially automated to free researchers from the tedious work during *in vitro* selections. However, till now, the microfluidic-based *in vitro* selection methods have not been widely adopted by researchers.

As discussed above, bead-based methods are not quite effective when target molecules are poorly aptagenic. This is partially due to the fact that it is difficult for bulky aptamers to bind to the surface of confined small molecules (steric hindrance from the surface morphology of beads and clustered target molecules). If the DNA library itself was immobilized onto the bead surface, it could be kinetically more favored for a high concentration of target molecules to bind to surface-confined bulky aptamers. In 2014, Stojanovic and co-workers reported such an *in vitro* selection method, known as 'capture selection', which was shown to be effective for the isolation of aptamers against low aptagenic targets.[28] A good target for aptamer isolation would have one or all of the following features: multiple hydrogen boding donor/acceptor, possessing a conjugation moiety for stacking, and positively charges to interact with negatively charged backbone of nucleic acids. Small molecules, such as glucose, one would expect to have very limited interaction with DNA, so that isolation of an aptamer against glucose will be very difficult. To increase the aptagenicity, they complexed glucose with a Shinkai's receptor, which binds to glucose specifically and strongly. The complex was then used as the target for *in vitro* selection with a novel SELEX design. Instead of immobilizing the target onto the surface of beads, the DNA library was annealed onto a biotinylated short oligonucleotide strand ('capture strand') and the duplex was then attached to streptavidin-functionalized agarose beads (Figure 1.9). The bead-bound DNA library was incubated with glucose/Shinkai's receptor complex. Binders that bound to the complex fell off from the beads, possibly through the formation of a DNA three-way junction. The target molecule stabilized the three-way junction, which in turn disrupted the duplex formed between the DNA library and the capture strand, resulting in the release of target binders from the beads. By this method, they were able to isolate aptamers capable of binding refractory targets such as glucose, fructose, and galactose. Another important merit of the abovementioned *in vitro* selection method was that the aptamer selected could be converted into sensors without the requirement of any further development. Since the whole SELEX was done based on strand displacement (shown in Figure 1.9), it is also known as the signalling selection. One needs to note, however, the disadvantages of this method: (1) Only three-way junction stabilizing interactions would be screened, this being a subset of all possible solutions for aptamer binding to the target; (2) the hydrophobic core formed by three way junctions might lead to non-specific binding to other hydrophobic interferences, and (3) it requires high concentration of the small molecules in initial rounds to minimize alternative mechanisms of release of DNA library from the column.[29]

Li and co-workers have reported another capture selection approach with a different design of the DNA library. Their library is annealed onto the beads using a sequence placed in between two randomized nucleotides stretches; binders peel off from the immobilized beads upon target binding.[30] Similar to the capture selection approach of Stojanovic et al.,[27] this method also partially screens the library. Only the binders that induce structural changes capable of disrupting the attaching duplex would be selected.

Compared to RNA aptamers, DNA aptamers have the advantage of being more chemically and biologically stable, commercially available, easy to handle, and amenable to the introduction of a variety of modifications. These collectively make DNA aptamers superior candidates than their RNA counterparts for applications. The only scenario that favors usage of RNA over DNA is in *in vivo* applications. RNA can be readily produced intracellularly, while DNA requires a delivery mechanism. However, these *in vivo* applications usually require modification (affinity tags or reporting tags) of RNA, which to some extent negate the advantage of RNA. In contrast, biosensors using DNA aptamers as their recognition module have been extensively explored.[31] Aptamers isolated from *in vitro* selection, however, usually cannot be used directly for designing sensors. Nevertheless, capture selection techniques provide a promising path for sensor- oriented *in vitro* selection.

1.2. DNAzymes: from mechanism to characterization

1.2.1. DNAzyme overview and its mechanism of catalysis

Although there is not solid evidence yet of naturally occurring DNAzymes, many artificial ones have been discovered by *in vitro* selection. They have been selected to catalyze a wide range of chemical/biochemical reactions and biological transformations. Table 1 summarized the reactions catalyzed by DNAzymes with representative examples. The reactions listed include RNA cleavage,[9] RNA ligation,[32] DNA cleavage,[33] DNA ligation,[34] DNA 5'-phosphorylation,[35] DNA adenylation (capping),[36] nucleopeptide linkage formation,[37] DNA depurination,[38] Diels-Alder reaction,[39] thymine dimer reparing,[40] phosphoramidate cleavage,[41] porphyrin metalation,[42] amide hydrolysis,[43] Friedel–Crafts reaction,[44] peptide phosphatase activity,[45] tyrosine kinase activity.[46] In terms of substrates, the majority of them are nucleotides or nucleotide-derivatives. Only a few of DNAzymes use small molecules, including the DNAzyme for the Diels-Alder reaction, the Friedel-

Crafts reaction, and the oxidative G-quadruplex-hemin complex.[42] The G-quadruplex-hemin DNAzyme is not included in the table because it catalyzes more than one type of reactions; besides the peroxidase- and oxygenase-like activities, it also catalyzes the carbene transfer reaction.[47]

1.2.2. Efforts to enlarge the scope of DNAzyme catalysis

DNAzymes are finding more and more applications in biosensing and in therapeutic applications, particularly many biosensors have been designed based upon.[48] Meanwhile, RNA-cleaving DNAzymes have been adapted for selectively cleaving mRNA to down-regulate gene expression.[49] There are a few advantages of nucleic acids over proteins as catalysts. Firstly, *in vitro* selection with randomized proteins for new functionalities is essentially not practical. In contrast, DNA/RNA *in vitro* selection can be readily carried out with commercially available libraries. Secondly, DNAzymes / RNAzymes can be synthesized with minimal batch to batch difference, at relatively low cost. Thirdly, a large variety of modifications can be readily introduced, especially with DNAzymes.

Table 1 Chemical transformations catalyzed by DNAzymes

Reaction catalyzed	**bond**	**# of random nt**	**Rate enhancement**	**M^{2+} requirement**
RNA cleaving[9]	O-P	50	~10^5	Pb^{2+}
RNA ligation[32]	O-P	40	2 x 10^4	Zn^{2+}
DNA cleavage	C-O	50	~10^6	Cu^{2+}
DNA 5'-phosphorylation[33]	O-P	70	~10^9	Mn^{2+}
DNA adenylation[34]	O-P	70	2 x 10^{10}	Mg^{2+} and Cu^{+}
Nucleopeptide linage formation[35]	O-P	40	5 x 10^5	Mg^{2+} or Mn^{2+}
DNA depurination[36]	O-P	85	9 x 10^5	Ca^{2+}
Diels-Alder reaction[39]	C-C	36	4 x 10^5	Ca^{2+}
Thymine dimer repairing[40]	C-C	40	3 x 10^4	None
Phosphoramidate cleavage[41]	N-P	72	~10^3	Mg^{2+}

Porphyrin metalation[42]	Cu-N	228	1×10^3	Cu^{2+} or Zn^{2+}
Amide hydrolysis[43]	C-N	40		Zn^{2+}/Mn^{2+} or Zn^{2+}/Mg^{2+}
Friedel-crafts reaction[44]	C-C	40		Cu^{2+}
Peptide phosphatase activity[45]	O-P	40		Zn^{2+}
Tyrosine kinase activity[46]	O-P	30/40/50		$Zn^{2+}/Mn^{2+}/Mg^{2+}$

Despite all these advantages, the limited chemical diversity makes DNAzyme incapable of certain catalytic activities, amide hydrolysis as an example. Efforts of selecting DNAzymes for amide hydrolysis led to the incidental discovery of the DNAzyme for catalyzing phosphodiester hydrolysis. Just like the chemically modified aptamers discussed in Section 1.12, efforts have been made to expand the scope of DNAzymes by introducing chemically modified nucleotides. As discussed in previous sections, only chemical modifications that are compatible with natural or evolved DNA polymerases can be explored using *in vitro* selection. Indeed, some modifications on certain atoms of nucleotides do not disrupt their compatibility with standard DNA polymerases. A typical example is the C-5 modification of deoxyuridine (dU); the use of DNA libraries with modified-dUs in place of dT led to the isolation of chemically modified aptamers[24] and DNAzymes.[43,50] Perrin et al. have reported a modified RNA-cleaving DNAzyme with reduced divalent metal ion requirement.[50] Using a similar approach, Silverman and co-workers have successfully isolated a modified DNAzyme capable of catalyzing amide hydrolysis,[43] which was originally considered to be a reaction beyond the reach of chemically unmodified DNAzymes. Overall, it has been explored to expand the chemical diversity of DNA; yet, this is still at very limited level given the limitation on the modification location (only on dU) and a modest scope of additional chemical functionalities that have been essayed (imidazole, amino, carboxyl, and hydroxyl groups). Substantial efforts need to be made beforehand prior to performing SELEX with DNA libraries bearing chemical diversities that are comparable to proteins.

1.2.3. Structural characterization of DNAzymes

Since the Pb^{2+}-dependent RNA-cleaving DNAzyme was reported by Joyce and Breaker in 1994,[9] studies on RNA-cleaving DNAzymes have never been stopped. In fact, it is still the most extensively studied class of catalytic DNAs. Understanding of the structure and mechanism of RNA-cleaving DNAzymes helps us to understand the reaction mechanism of other DNAzymes by analogy.[51] Even so, the structural study of DNAzymes is well behind the development of their applications. Until now, there are only a handful papers reporting crystal structures of DNAzymse.[50-53] The earliest was in 1999, when Joyce and coworkers reported an X-ray crystal structure of the 10-23 DNAzyme at 0.3 nm resolution.[52] However, the structure reported was not the active form of 10-23 DNAzyme; hence, it provided little insight into the mechanism of that RNA-cleaving DNAzyme. It was not until 2016, more than 20 years after the first DNAzyme selected by Breaker and Joyce,[9] that the first high-resolution crystal-structure of a DNAzyme in its active form became available; Höbartner and co-workers reported an X-ray crystal structure the RNA-ligating 9DB1 DNAzyme.[53] This structure revealed several interesting facts on how catalysis can be carried out by DNA. First, the crystal structure proved that a DNAzyme folds into a well-defined tertiary structure. The main structure of 9DB1 is a double pseudoknot, in which two adjacent T residues interact with the A-G RNA nucleotides directly at the ligation junction. Based on these observations, it is possible to re-engineer the DNAzyme to broaden its substrate scope by Watson-Crick covariation. Secondly, the 9DB1 crystal structure revealed that no divalent metal ion is present at its active site. Instead, a non-bridging internucleotide phosphodiester oxygen (between C12 and A13) appeared to make a critical contact. This structure supported the notion that DNAzymes are not obligatory metalloenzymes with regard to the catalytic role of divalent metal ion. Lastly, the new structure revealed that the 9DB1 DNAzyme had a much broader range of sugar-phosphate backbone conformations than those in natural and synthetic ribozymes. Therefore, the missing 2'-hydroxyl groups of DNA, while removing one of the sources of functional interactions, in parallel expand the conformational variability of DNA relative to RNA. Such counteracting effects appear to leave DNA at least as catalytically competent as RNA; indeed, the greater backbone freedom for single-stranded DNA as observed in the 9DB1 crystal structure may enable DNA catalysis in ways not possible for RNA.

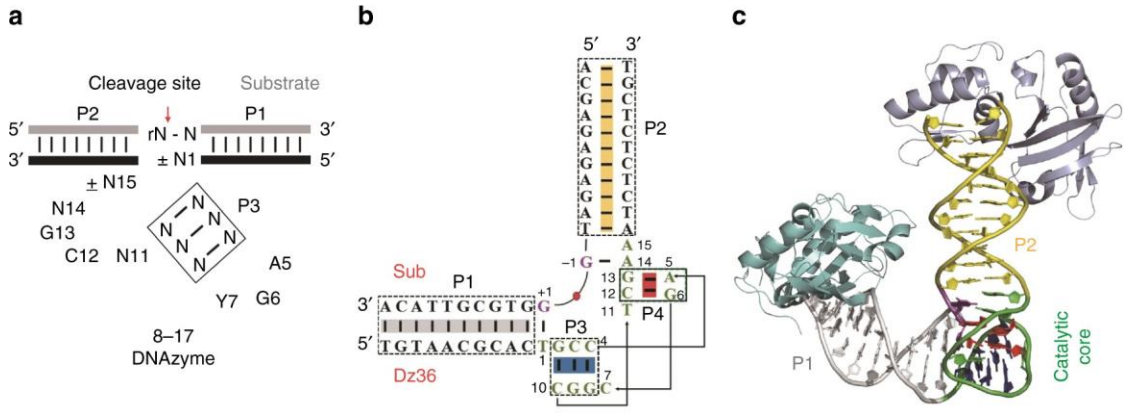

Figure 1.10 a). 8-17 consensus sequence and the predicted secondary structure. b). Sequence and the observed secondary structure of DNAzyme (Dz36)and the substrate (sub) utilized in the structural and the catalytic cleavage studies. c). Cartoon representation showing the overall fold of the DNAzyme/substrate analog complex, based on the high-resolution DNAzyme-Pb^{2+} structure.

Note: Reprinted with permission from Liu, H.; Yu, X.; Chen, Y.; Zhang, J.; Wu, B.; Zheng, L.; Haruehanroengra, P.; Wang, R.; Li, S.; Lin, J.; Li, J.; Sheng, J.; Huang, Z.; Ma, J.; Gan, J. Crystal Structure of an RNA-Cleaving DNAzyme. *Nat. Commun*. 2017, 8 (1), 2016. Copyright 2016. Springer Nature.

The RNA-cleaving motif, 8-17,[54] which has a catalytic core of only 15 nucleotides (nt), is identified independently by a number of researchers under different selection conditions. This motif is thought to be the simplest possible catalytic DNA and its crystal structure has been determined by Liu et al.[55,56] Particularly, the crystal structure of 8-17 DNAzyme shows that it folds into a 'V' shape conformation with two arms oriented about 70° with respect to each other. This structure bends two adjacent Gs (G1 and G-1 in Figure 1.10b) of the RNA substrate (where the DNAzyme cleaves) to form a 'kink'. As shown in Figure 1.10b, the two arms (P1 and P2) are connected by the catalytic core, which forms a compact small DNA pseudoknot (Figure 1.10c). One interesting finding from this structure is that, the metal (Pb^{2+}) binding pocket is pre-formed, not induced by its presence, as revealed by the conformational identicalness of the DNAzyme-Pb^{2+}, and DNAzyme/native DNA without Pb^{2+}. The enzymatic activity of 8-17 depends on the concentration and type of divalent cations. Pb^{2+} is preferred than Mg^{2+}, and both are much preferred than other metal ions. The crystal structure revealed the mechanism behind the metal ion preference; it is not the space availability rendered DNAzyme the preference, but likely the lack of electrostatic interactions around the binding pocket excluded Mg^{2+} and other metal ions. Since besides the O6 of G6 (which interacts with metals like Mg^{2+} poorly), there are no other ligands close enough to the binding pocket to allow coordination interactions with the metal ions inside. The binding of Mg^{2+} or other metal ions may drive

the DNAzyme to adopt an alternative folding which are lower in catalytic activity; this may imply that DNA sequence adaptively folds into different architectures (determined by the co-factors present). A further implication is that it might be possible to design *in vitro* selection for DNAzymes possess two or more desired functionalities, and the functions can be switched by changing the co-factors present. Based on the crystal structure, Liu *et al* further proposed a in-line attacking mechanism, where N1 atom of G13 deprotonates the 2'-OH of attacking G-1 residue.[54] The O6 of G6 coordinate with Pb^{2+}, and the coordinated Pb^{2+} further activate the H_2O ligand of Pb^{2+}, which in turn provides a proton to the O5'' of the leaving group of G+1 (Figure 1.10b). The catalytic mechanism and crystal structure of 8-17 actually share some similarity with RNA-cleaving ribozymes, the shared G-G kink as an example.[56]

1.3. Copper as catalyst for click reaction and its interaction with DNA

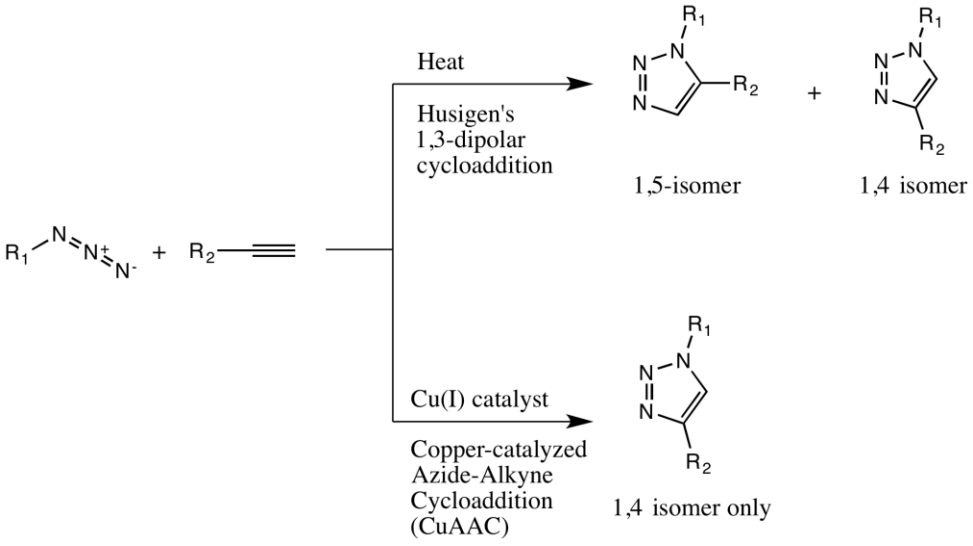

Figure 1.11 Huisgen azide-alkyne cycloaddition activated by heat or Cu(I) catalyst. Two isomers (1,5-isomer and 1,4-isomer) are generated when the reaction is activated by heat.

In 2001， Sharpless et al. proposed the concept of 'Click chemistry' to describe the type of reactions that fulfill certain criteria.[57] These criteria include the requirement for the reaction to be modular, wide in scope, give very high yields, generate only inoffensive byproducts that can be removed by nonchromatographic methods, be stereospecific, use readily available reagents, be insensitive to oxygen and water, and use benign solvents like water. Until now, a handful of reactions have been identified as *bona fide* 'click

chemistry', such as the copper catalyzed azide-alkyne cycloaddition reaction (CuAAC), spring-loaded azide-alkyne cycloaddition, thiol-ene reaction, thiol-yne reaction, inverse electron demand Diels-Alder reaction (tetrazine based cycloaddition), and epoxy-based nucleophilic substitution. Out of these known 'Click chemistry' reactions, CuAAC is undoubtedly the most useful and closest to fulfilling all the criteria specified for a 'Click chemistry'. As a matter of fact, CuAAC has been extensively studied, and has enjoyed great success in both fundamental research and pharmaceutical industry.[58,59]

CuAAC is the copper-catalyzed version of the Huisgen 1,3 dipole cycloaddition, which refers to the reaction between a 1,3-dipole and a dipolarophile to form a five-membered heterocyclic compound. This reaction type was systematically studied and named by Rolf Huisgen in 1960.[60] Nowadays, the name 'Huisgen-1,3 dipole cycloaddition' is often used to specifically refer to the reaction between organic azides and alkynes (Figure 1.12). In 2002, Meldal and Fokin independently reported the catalyzed version of cycloaddition between an organic azide and an alkyne.[61,62] Instead of activating the reaction using elevated temperature, they have shown that the transition metal ion (Cu(I)) can catalyze the reaction efficiently. The catalyzed reaction was found to be regioselective, and form only the 1,4-distributed triazole product. It gave quantitative yield at room temperature or even at low temperature (4 °C), with good reaction rates. The reactivity of azide and alkyne are relatively insensitive to the R group(s) attached and is compatible with many solvents including water. There is almost no byproduct and the product itself can be easily isolated. All these features make CuAAC the most representative and successful 'Click' reaction to date. Since its initial reports, CuAAC has found many applications in synthetic and medicinal chemistry bioconjugations, and polymer chemistry.[59,63,64]

1.3.1. Mechanistic studies

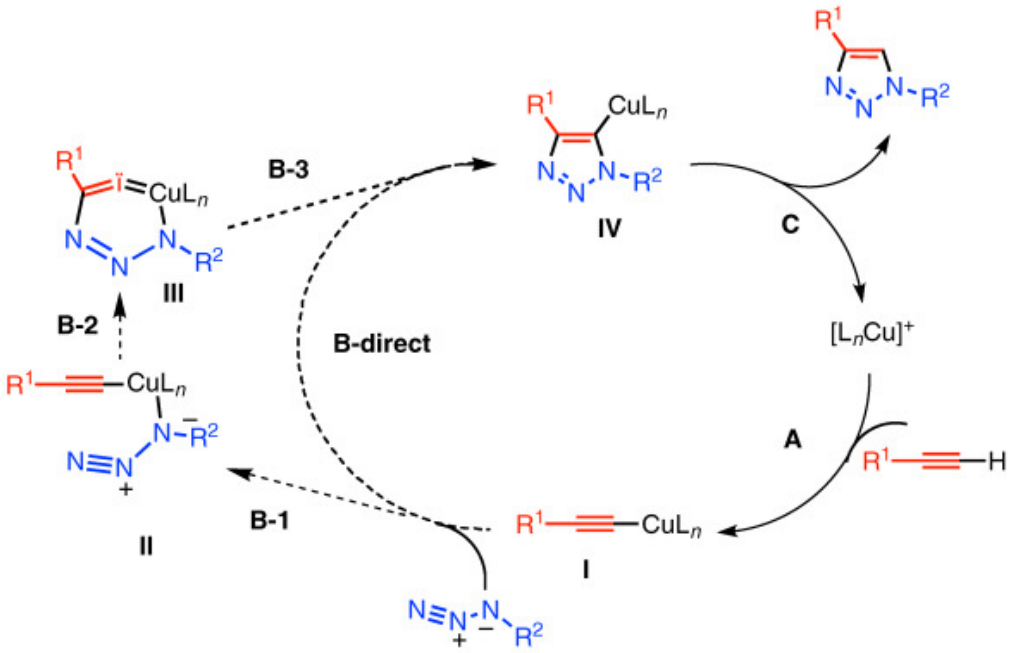

Figure 1.12 Catalytic cycle for the Cu(I)-catalyzed ligation proposed by Fokin and Sharpless in 2002. The reaction cycle starts with the formation of copper(I) acetylide I. Density functional theory calculations offered evidence supporting a stepwise, annealing sequence (B-1→B-2→B-3), which proceeds via the intriguing six‐membered copper-containing intermediate III.

Note: Reprinted with permission from Rostovtse v. V., sevolod V., Green L. G., Fokin V. V., and Sharpless K. B. A Stepwise Huisgen Cycloaddition Process Copper(I)Catalyzed Regioselective Ligation of Azides and Terminal Alkynes. *Angew. Chem.* 2002, 41, 2596-2599. Copyright 2002. John Wiley & Sons, Inc.

Many studies have been carried out to elucidate the mechanism of the CuAAC reaction.[65–68] While the exact pathways and intermediates are still not clear, it is accepted that the CuAAC reaction involves a stepwise annulation with a mono or dinuclear copper intermediate, i.e., it can occur through both one-copper and two-copper pathways, with the two-copper pathway much more kinetically favored.[69]

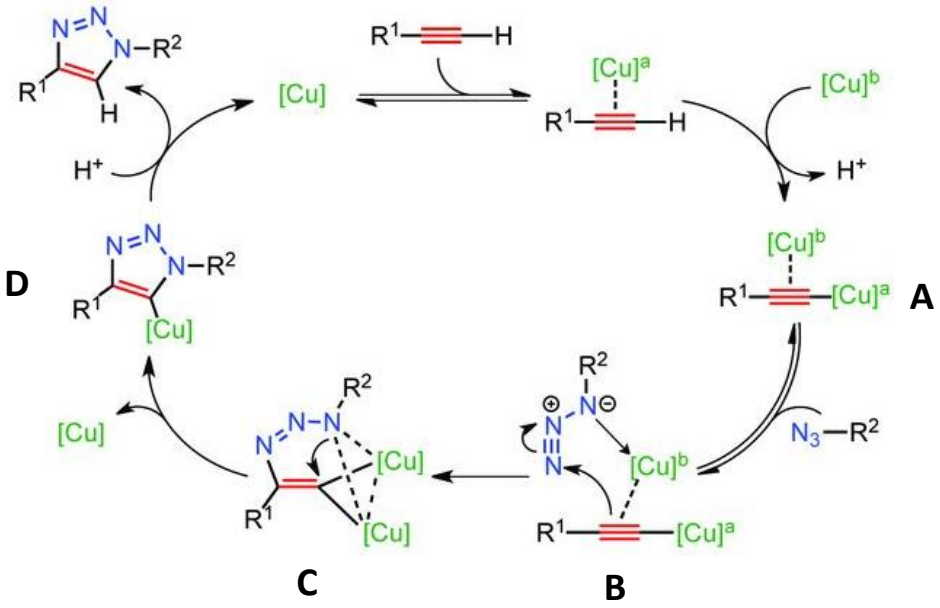

Figure 1.13 Dinuclear intermediate mechanism with direct evidence from isotopic studies. First, the σ-bound copper acetylide bearing the π-bound enriched copper atom (intermediate A) reversibly coordinates an organic azide (B). Following this step, nucleophilic attack at N-3 of the azide by the β-carbon of the acetylide forms the first covalent C–N bond, producing intermediate C. The ligand exchange in this intermediate is faster than the formation of the second covalent C–N bond, which results in ring closure, accounting for the statistical (50%) incorporation of 63Cu into triazolide D.

Note: Reprinted with permission from Worrell, B. T.; Malik, J. A.; Fokin, V. V. Direct Evidence of a Dinuclear Copper Intermediate in Cu(I)-Catalyzed Azide-Alkyne Cycloadditions. *Science*. 2013, 340 (6131), 457–460. Copyright 2013. The American Association for the Advancement of Science.

Based on the observation that this reaction does not work on internal alkynes, but terminal alkynes, along with DFT calculations (the one step concerted [3+2] cycloaddition, B direct in Figure 1.12, is strongly disfavored according to the calculation), Fokin and Sharpless proposed a stepwise annulation process initiated with the formation copper acetylide (I in the scheme of Figure 1.13). In this mechanism, the initiation of the reaction relies on the acidity of proton on the terminal alkyne. However, this was later proved untrue. When the proton on the terminal alkyne is substituted with either a halogen like I,[70] or a transition metal like Au,[71] the Cu(I) complex still catalyzes its cycloaddition with an organic azide to form a 3,4,5-substituted triazole (which means scission of the alkyne-iodide or alkyne-Au bond is not necessary for the reaction to happen).

Both experimental data and calculations indicate a dinuclear mechanism, in which two copper ions are needed for one cycle of the reaction.[47,72,68] Accordingly, Fokin et al.

proposed a dinuclear intermediate mechanism in 2013.[72] This theory is supported by direct evidence from isotopic experiments, and partially explains why the terminal proton is not necessary.

While most of the proposed intermediates involved in CuAAC (from calculations) still have not been isolated, Cu(I)-acetylide and Cu(I)-triazolide can be reliably isolated and characterized.[73] Fokin and coworkers prepared Cu(I)-acetylide and a THF soluble Cu(I) complex [$Cu(PPh_3)_2NO_3$]. When Cu(I)-acetylide was mixed with benzyl azide, no cycloaddition was observed. The reaction only occurred when an exogenous copper complex was added. These results confirmed that Cu(I)-acetylide ([Cu] ^{a} in the scheme) alone does not run through the reaction cycle, i.e., a second Cu(I) ([Cu] ^{b} in the scheme) is necessary. After examining the structure, Fokin and coworkers proposed that the second Cu(I) forming a π-complex with the alkyne group. They thus asked the question: are the two coppers functionally distinct? To answer this question, an isotopically pure ^{63}Cu was used to trace the exogenous copper (natural abundance of ^{63}Cu: ^{65}Cu is 69:31). The copper complex [$Cu(MeCN)_4$]PF_6 was synthesized from commercially available ^{63}CuO. In the final product (Cu(I)-acetylide), the ratio of ^{63}Cu to ^{65}Cu was found to be 85:15, indicating that the second copper can exchange with the Cu(I) in the original Cu(I)-acetylide. Upon excluding the possibility of copper exchange between the Cu(I)-acetylide and exogenous copper, or Cu(I)-triazolide and exogenous copper, a mechanism involving two chemically equivalent copper ions was proposed. First, a copper-alkyne complex formed (**A**), with one σ −bound copper and a second π-bound copper. This complex reversibly coordinates with organic azide to form **B**, then the first C-N bond is formed to give intermediate C. A ligand change happens during intermediate **C**, possibly due to the carbene copper weakening the back bonding to the ligands coordinated to the copper. The ligand exchange is faster than the formation of the second C-N bond, which allowed the enrichment of ^{63}Cu to happen. In protic solvents or if an acid were supplied, the Cu(I)-acetylide (D) would convert into the final 1,4 triazole product. Fokin's model not only emphasized the two-copper pathway, but also clarified the relationship between the two copper ions.[72]

However, the two equivalent Cu(I) mechanism still does not completely explain why the halogen or metal substituted alkyne is compatible with Cu(I) catalysis, given that the formation of acetylide is still involved in the reaction cycle. It seems that the π-complex

of Cu(I)-alkyne plays a critical role in this case, and the π-complexed copper acetylide alone might be able to run through the reaction cycle.

Following Finn's discovery of dinuclear intermediates, other researchers have tried to isolate them directly; in 2015, Laccobuci and co-workers for the first time directly observed the putative dinuclear intermediate by mean of electro-spray ionization mass spectrometry.[74] Later in the same year, Jin and coworkers went one step further to isolate and characterize the dinuclear intermediates.[75]

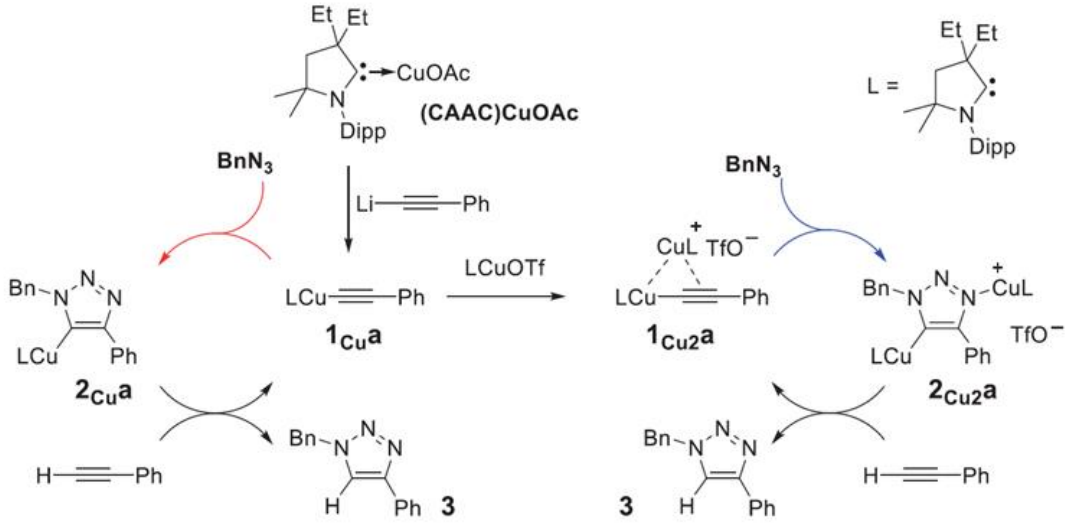

Figure 1.14 Stoichiometric reactions reproducing the different steps of the postulated CuAAC catalytic cycles, which allow for the isolation of a previously postulated π,σ-bis(copper) complex of type 1_{Cu2} and of the never-mentioned bis(copper) triazole 2_{Cu2}. (1_{Cu}a stands for 1_{Cu} acetylide).

Note: Reprinted with permission from Jin, L.; Tolentino, D. R.; Melaimi, M.; Bertrand, G. Isolation of Bis(Copper) Key Intermediates in Cu-Catalyzed Azide-Alkyne 'Click Reaction'. *Sci. Adv.* 2015, 1 (5), e1500304. Copyright 2015. The American Association for the Advancement of Science.

Though contradiction with earlier reports that dinuclear intermediates should be highly unstable, Jin et al. reliably isolated and characterized both the bis-copper acetylide (1_{Cu2}a) and an unexpected bis-copper triazolide (2_{Cu2}a). As shown in Figure 1.14, 1_{Cu2}a reacts with an organic azide readily to form 2_{Cu2}a. Interestingly, it was found that the mononuclear intermediate $\mathbf{1}_{Cu}$a without an exogenous copper (the cycle on the left in Figure 1.14), still slowly reacts with organic azide to afford the 1,2,3-triazole product ($\mathbf{2}_{Cu}$a). Based on these observations, Jin and co-workers proposed that both one-copper and two-copper pathways are possible in CuAAC, with the two-copper pathway kinetically favored.[74] It shoud be noted that the one-copper pathway still happens with terminal

alkynes, but not convinced whether halogen or metal substituted alkynes work or not.

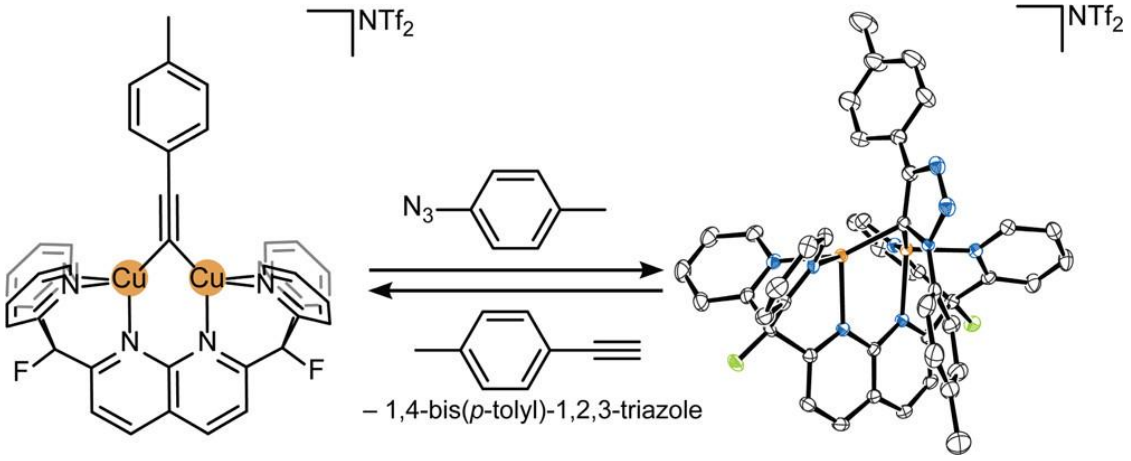

Figure 1.15 Molecular structure of μ-alkynyl complex and its reversible reaction with organic azide and alkyne.

Note: Reprinted with permission from Ziegler M. S., K., Lakshmi V and Tilley T. D. Dicopper Cu(I)Cu(I) and Cu(I)Cu(II) Complexes in Copper-Catalyzed Azide−Alkyne Cycloaddition. *J. Am. Chem. Soc*. 2017, 139, 5378−5386. Copyright 2017. The American Association for the Advancement of Science.

In both Finn's and Jin's dinuclear models, a common feature is that the two copper ions are both cuprous. Do these two copper ions have to be both cuprous? Tilley and coworkers have shown that a mixed-valence pathway is possible, but less likely compared to the two-cuprous pathway owing to its instability as a catalyst.[76] They have synthesized a μ-alkynyl complex **A** as shown in Figure 1.15; this dicopper alkynyl complex not only reacts with an organic azide to form the triazolide product B, but also can be regenerated by reacting B with an alkyne. This process essentially resembles the actual CuAAC reaction cycle. Furthermore, when complex A is mixed with another alkyne and azide, it functions as a competent catalyst to catalyze the cycloaddition between the added alkyne and azide. These results provided further evidence to support the dinuclear mechanism. To probe the mix-valence pathway, Tilley and coworkers synthesized a μ-alkynyl complex contains one Cu(I) and a Cu(II).[75] The mixed valence complex was tested to react with an organic azide, surprisingly it underwent decomposition. Such a decomposition process competes with the cycloaddition catalysis which makes determining the reactivity of this complex not possible. In contrast, the μ-alkynyl complex with two coppers both cuprous is stable during the reaction with organic azide (to form a stable dicuprous triazolide). These findings suggest that the mix-valence pathway is less likely in comparison with the two-cuprous pathway.

1.3.2. Efforts to make CuAAC bio-compatible

The azide and alkyne moieties are not naturally occurring in biological systems, which makes CuAAC a bioorthogonal reaction. Together with the 'Click reaction' attributes of CuAAC, this reaction has been explored as a means for labelling in the context of living cells.

Finn and co-workers have reported an optimized condition for CuAAC to be used for bio-conjugation.[77] The reaction should be performed in the presence of 100 μM $CuSO_4$, 2.5 mM sodium ascorbate (the preferred reducing agent), at least 5 equivalents of Tris-hydroxypropyltriazolylmethylamine (THPTA, a water-soluble copper ligand) and aminoguanidine (an optional additive for extra protection from oxidative damage). Phosphate or carbonate are suitable buffers; Tris should be avoided since it competes with THPTA for binding copper. For the azide and alkyne substrates, it was found that a high concentration of alkyne (over 5 mM) is inhibitive for the reaction. High concentration of thiols is also inhibitive. These conditions proved to be suitable for bioconjugation in most cases. However, it is not suitable for cross-linking reactions involves live cells, especially reactions to take place inside cells. Copper of the concentration needed for copper-THPTA (or other simple Cu(I) stabilizing ligands) system is high enough to induce unpredictable changes to the normal growth of cells. The toxicity of copper is believed to be mainly due to the reactive oxygen species generated by copper mediated processes.[78,79] As a matter of fact, 1,10-phenanthroline/Cu(I) shows DNAase activity and is used as a DNA foot-printing reagent.[80] Although it is reported that THPTA (and other copper ligands) neutralize the oxidative damage induced by copper to some extent, experimental data have shown that the cytotoxicity is still severe enough to jeopardize cells. Copper interacts strongly with cysteine and histidine; non-specific copper binding to enzymes inside cells may also have adverse effect on normal biological processes of cells.

In general, for a given process, it is difficult to decrease the toxicity while maintaining its efficiency. Better biocompatibility would be normally accompanied with a compromised efficiency. Bertozzi and co-workers developed a copper-free azide alkyne cycloaddition reaction, which completely avoids the toxic Cu(I) catalyst at the price of inefficient kinetics and selectivity.[80] Instead of activating the terminal alkyne by Cu(I), the alkyne group was activated by the 'ring strain', and this method is named as strain promoted azide alkyne cycloaddition (SPAAC). Internal alkynes (cyclooctynes) are

relatively reactive towards organic azides,[81] as such the strain-promoted azide alkyne cycloaddition has been widely used for labelling reactions involves living cells. However, the efficiency of this reaction is much lower compared to that of the CuAAC. The Staudinger reaction, a phosphine bioorthogonal process often used for live cell labelling, has shown disappointing reaction kinetics, i.e., it requires long incubation time (overnight); the SPAAC reaction has about 50% of labelling efficiency of the phosphine reaction within same incubation time.[81] The reaction kinetics can be greatly enhanced by introducing electronegative atoms onto the cyclooctyne ring, the difluorinated cyclooctyne (DIFO) shows a 17-63 times higher rate constant than the Staudinger reaction or the un-substituted cyclooctyne reaction.[82] Another cyclooctyne, biarylazacyclooctynone (BARAC), displays even better kinetics, with a rate constant around 1 $M^{-1}s^{-1}$,[83] though it is still at least 10 times slower than CuAAC with 10-100 μM of copper (10-100 $M^{-1}s^{-1}$).[84] Another shortcoming of SPAAC is the compromised selectivity of the strained alkyne; it reacts, to a varying extent, with biological functionalities in an azide-independent manner,[85] the thiol-yne addition for example.[86]

An alternative way of making CuAAC more biocompatible is to reduce the copper concentration required to be biocompatible. One way is to link either alkyne or azide to a copper binding ligand so that the effective copper concentration is increased to work as well as bulk addition of copper. Ting et al. reported that picolyl azides (the picolyl group is a copper binding moiety) react with alkyne substrates in the presence of THPTA and as low as 10 μM of Cu(I).[87] Picolyl azide alone gives modest enhancement of the reaction and requires a higher copper concentration (40 μM) to achieve cell surface labelling. Based on this pioneering work, Taran and coworkers took one step further to examine the reaction efficiency of azide attached to a whole series of N-donor ligands (azide-copper chelating ligands of different copper chelating capabilities, shown in Figure 1.16), other than the picolyl azide alone (A2 in Figure 1.16). It was found that A20 catalyzes the reaction with 17.5 μM of Cu(I) to achieve 59% conversion within 40 s.[88] With the same concentration of copper and one equivalent of BTTE, A2 (pycolyl azide) shows 39% conversion within 7 min. Taran and coworkers further tested the A20 reaction in complex media that contained cell lysates, and found that A20 kept its ability to catalyze the reaction

with 40% percent conversion within 30 sec.

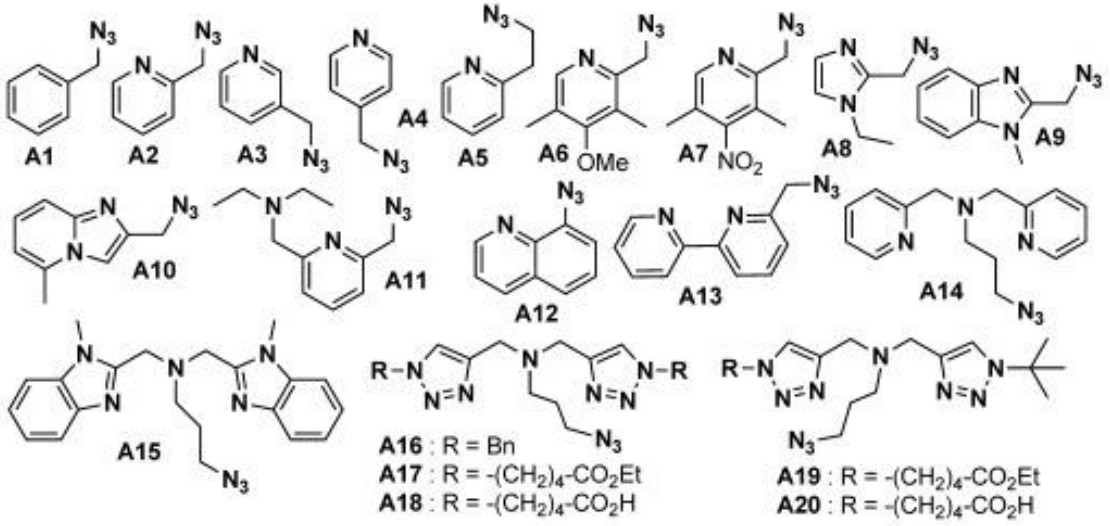

Figure 1.16 Azide-copper chelating ligand conjugates tested.

Note: Reprinted with permission from Valentina B. et al. Copper-Chelating Azides for Efficient Click Conjugation Reactions in Complex Media. *Angew. chem.* 2014, 126, 5982 –5986. Copyright 2014. John Wiley & Sons, Inc.

1.3.3. Copper as co-factor for protein and nucleic acid enzymes

Copper is a transition metal that has an atomic number of 29 and atomic mass of 63.54 Da. The electron configuration of copper is $[Ar]3d^{10}4s^{1}$ and has stable oxidation states, Cu(I) and Cu(II). As one of the most important metals for industrial applications, copper's favorite properties include low corrosion, alloying ability, high thermal conductivity, and high electrical conductivity. As such, copper has been popularly used either as pure metal or alloy in machinery, construction, transportation, and military weapons.[89] Chemically, copper ions coordinate with various ligands to form complexes, and the preferred binding geometries for Cu(I) and Cu(II) are different. Cu(I) is a d10 system and therefore does not experience, or have geometric preference based on, the ligand field stabilization energy (LFSE). It is often found coordinated by 2, 3, or 4 ligands in linear, trigonal planar, or tetrahedral geometries. Cu(II) is a d9 system that exhibits geometric preferences based in part on LFSE. It is often found coordinated by 4, 5, or 6 ligands, in square planar, square pyramidal, or axially distorted octahedral geometries, the last being the result of Jahn–Teller distortion. Rubino and Franz examined a number of redox-active copper proteins that cycle between Cu(I) and Cu(II) states, where the metal

is found predominately in the tetrahedral geometry.[90]

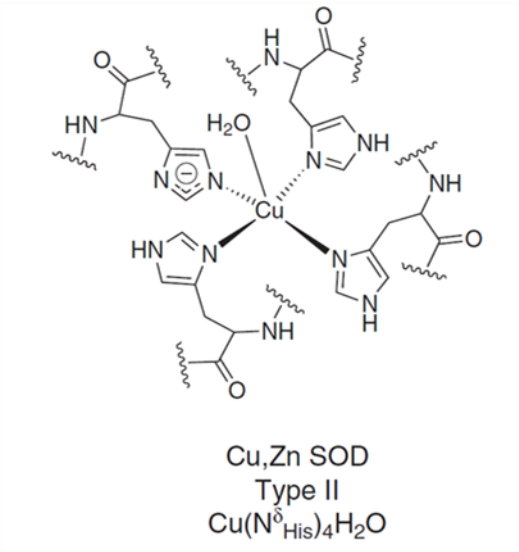

Figure 1.17 Coordination sphere of Cu Zn SOD. It has a square pyramidal coordination geometry.

Note: Reprinted with permission from Rubino, J. T.; Franz, K. J. Coordination Chemistry of Copper Proteins: How Nature Handles a Toxic Cargo for Essential Function. *J. Inorg. Biochem*. 2012, 107 (1), 129–143. Copyright 2012. Elsevier Inc.

Biologically, copper is an essential nutrient for humans, which is the co-factor for enzymes such as Cu-Zn superoxide dismutase, ceruloplasmin, cytochrome c oxidase, tyrosinase, dopamine β-hydroxylase and so on. Proper concentration of cellular copper is essential for copper-dependent protein enzymes, however, excess level of copper not only adversely interacts with biomolecules, but also mediates the generation of reactive oxygen species (ROS). Cu(II) alone is not very cytotoxic, it is the redox cycle between Cu(II) and Cu(I) that causes the oxidative damage to biomolecules and cells. Particularly, when Cu(I) is oxidized by O_2 or H_2O_2, the damage-causing hydroxyl radicals are generated. Therefore, the homeostasis of copper needs to be strictly maintained in the healthy human body. The concentration of copper in the human brain is estimated to be in the range of 100-150 μM and about 14.4 μM in serum,[91] which are delicately maintained by a whole set of proteins and enzymes. The disruption of copper homeostasis is linked to diseases such as Menkes, Wilson's, and Alzheimer's diseases.[57]

Copper-proteins have been extensively studied and are categorized into two types: proteins that utilize copper as cofactor to perform biological functions, and proteins transport copper as cargo.[90] Proteins utilizing copper as a cofactor can be further classified into groups based on ligand compositions and the geometry of the metal center. As listed

in Table 2, three amino acid residues, cysteine, methionine and histidine dominate the binding sites of various copper enzymes/proteins. The chemical properties of this small ligand set actually provide a choice of nitrogen or sulfur donor, neutral or negative charge (methionine and deprotonated cysteine respectively), pH dependent versus independent metal coordination, hydrophobic versus hydrophilic character, the ability to bridge multiple metal centers, as well as different susceptibilities and consequences of oxidation of both the ligand and metal. Figure 1.17 shows a representative type II copper center, which has a square-planar geometry with 4 histidine and one water as ligands.

Table 2 Summary of different classes copper proteins (Adopted with permission from Rubino, J. T. et al. Coordination Chemistry of Copper Proteins: How Nature Handles a Toxic Cargo for Essential Function. *J. Inorg. Biochem*. 2012, 107 (1), 129–143. Copyright 2012. Elsevier Inc.)

Center	**#Cu**	**Geometry**	**Example**	**Coordination environment**
Type I				
Class I	1	Tetrahedral	Plastocyanin	$Cu(N^{\delta}_{His})_2S^{\gamma}_{Cys}S^{\delta}_{Met}$
Class II	1	Tetrahedral	Umecyanin	$Cu(N^{\delta}_{His})_2S^{\gamma}_{Cys}\ O^{\varepsilon}_{Glu}$
Class III	1	Trigonal bipyramidal	Azurin	$Cu(N^{\delta}_{His})_2S^{\gamma}_{Cys}S^{\delta}_{Met}O_{Gly}$
Type II	1	Square pyramidal	Cu, Zn SOD	$Cu(N^{\delta}_{His})_4H_2O$
Type III	2	Trigonal bipyramidal	Hemocyanin	$\mu O_2[Cu(N^{\delta}_{His})_3]_2$
Cu_A	2	Tetrahedral	Cytochrome c oxidase	$\mu(S^{\gamma}_{Cys})_2[CuN^{\delta}_{His}S^{\delta}_{Met}][CuN^{\delta}_{His}O_{Glu}]$
Cu_B	1	Trigonal bipyramidal	Cytochrome c oxidase	$Cu(N^{\delta}His)_3$
Cu_C	4	Tetrahedral	N2O reductase	$\mu S^{2-}[4Cu(N^{\delta}His)_7O]$

It should be noted that the redox potential of copper is usually positively shifted when bound to protein enzymes; for example, the redox potential of Cu, Zn SOD is ~+0.40V with respect to the standard hydrogen electrode.[89]

For Alzheimer's Disease, the formation of senile plaques precipitated in the brain is a pathological marker. Their core element is an aggregated form of a peptide containing 39–43 amino acid residues, which is termed as the Aβ peptide.[90] The aggregated Aβ peptides have been described as metal sinks because of their high metal contents: Cu,

0.44 mM; Zn, 1 mM; Fe,1 mM.[92] Huang and coworkers in 1999 showed that the Aβ1-42 shifts the formal potential of the bound copper from -80 mV to +500-550 mV. This allows the reduction of Cu(II) to Cu(I) by Aβ1-42 in a phosphate buffer. Moreover, the reduction of Cu(II) is accompanied by the generation of H_2O_2 which further reacts with Cu(I) to generate a hydroxyl radical. Hydroxyl radicals will cause oxidative damage to neural cells. Clearly the redox potential of copper is tuned by the copper protein through providing specific coordinating environment, which in turn enables the function of copper enzymes.

As mentioned in the last section, DNAzymes need specific cations for folding and/or acting as catalytic centers. For example, the 8-17 DNAzyme cleaves RNA substrate about 200 times faster with Pb^{2+} than that with Mg^{2+}, although the initial *in vitro* selection was carried out in the presence of Mg^{2+}.[54] Not only 8-17, but all catalytic nucleic acids exhibit large differences in folding and catalytic activity depending on the concentration and type of metal ions available. Positively charge species, mostly metal ions, not only compensate the negative charges of the sugar phosphate backbone, but also induce folding of intricate nucleic acid secondary and tertiary structures. Furthermore, metal ions bind to specific sites, stabilize local motifs, and position themselves correctly to aid (or even enable) a catalytic mechanism.

As shown in Table 1, a number of DNAzymes require copper as their co-factor, just like copper-dependent protein enzymes. The copper-dependent DNAzymes were shown to catalyze the follow reactions: oxidative DNA cleavage,[93] DNA ligation,[34] DNA capping,[36] porphyrin metalation,[42] and the Friedel–Crafts reaction.[44]

1.3.4. Interaction between copper and DNA

Owing to the instability of Cu(I), most studies have focused on the interaction between DNA and Cu(II). Although it is questionable to extrapolate the conclusions for Cu(II) to Cu(I), these studies are certainly informative for understanding the interaction of Cu(I) with DNA. Direct techniques such as X-ray crystallography, NMR, EPR and indirect methods such as UV spectrophotometry, electrochemistry, and computational analysis have revealed many aspects of DNA and copper - mainly Cu(II), interactions. There are three basic questions to be addressed: first, how copper binding change the property of DNA, both structurally and functionally; second, what is the exact binding mode of copper to DNA; and the third, how does DNA binding change the property of copper.

The first question has been well answered. While most cations increase the stability of a DNA duplex, Cu(II) in high enough concentration effectively does the opposite.[94] Cu(II) induces unwinding and rewinding of DNA duplex depending on the solution conditions.[95] The binding of Cu(II) to poly $d(GC)_2$ induces the transformation from the canonical B-form duplex to the Z-form duplex[96]. Cu(I) binds to DNA strongly and this complex effectively reduces H_2O_2 to generate reactive oxygen species (ROS), which in turn damages DNA at the vicinity sites. Cu(I)/H_2O_2-mediated damage impacts consecutive Gs preferentially, with 5'-TGG-3' stretches being the most susceptible.[97,98] For the second question, as shown by the crystal structure of Cu(II) complexed with DNA nucleotides and derivatives, Cu(II) forms either square-pyramidal or octahedral coordination geometries. For the two purines (guanine and adenosine), similar square-pyramidal geometry was observed, with three water molecules and one phosphate oxygen atom forming the equatorial ligands and purine N-7 the single axial position. These results may reflect more, though, on how Cu(II) interacts with single stranded DNA. Cu(II) complexes double stranded DNA in a quite different manner, it associates with a short Z-type duplex (dCGCGCG) in an octahedral coordination geometry, with four equatorial water molecules, one axial water molecule, and one axial N7 of guanine. Along the DNA strand, both the copper distribution and the exact coordination geometry are not uniform. For the third question, there is a very limited literature available.

Interaction between DNA and Cu(I)

Prutz and co-workers carried out quite a few studies, both on the interaction of Cu(I) with DNA and copper/H_2O_2 induced DNA damage.[99-101] DNA forms particularly stable complexes with Cu(I), which shows a characteristic UV absorbance band. Therefore, the association and dissociation of Cu(I) to DNA can be followed by monitoring the differential spectra (using the spectra of Cu(II) samples as reference). Prutz et al. used the following model DNAs: poly(dG-dC), poly(dG).poly(dC), poly(dA-dT), polyA, polyT, polyG, polyC, and native helical DNA to prepare various DNA-Cu(I) complexes by in situ radiolysis reduction of Cu(II).[99] Radiolysis reduction was used to avoid interfering effects potentially caused by chemical reductants such as ascorbates. A few interesting facts of DNA and Cu(I) interaction were revealed: (1) Cu(I) can be transferred from one nucleotide to another dependent on the strength of binding, which increases in the order of poly(U) < poly(dT) < poly(A) < poly(G) ~ poly(C) < DNA < poly(dG-dC) < poly(I). Prutz and co-workers showed experimentally that Cu(I) ions randomly bound to DNA initially, then

quickly transferred to specific bases on the timescale of 10 ms within the same DNA strand. Cu(I) could also transfer intermolecularly, but that happens on a timescale of minutes; (2) EDTA extracted Cu(I) from Cu(I)/DNA complexes with an apparent first order rate constant of 0.019 s^{-1}. The reaction rate is independent of the concentration of EDTA, indicating that the rate-determining step is the dissociation of Cu(I) from the Cu(I)/DNA complex. The formation constant of Cu(I) binding to DNA was determined from these kinetics data, which is ~2×10^9 mol/L. (3) DNA competes favourably with protein in binding to Cu(I). A mixture of Cu(I) and H_2O_2 causes degradation of the DNA, and likely happens via the reaction below:

Equation 1.

$$DNA{-}Cu(I) + H_2O_2 \rightarrow DNA{-}\bullet OH + Cu(II) + OH^-$$

When RNase or BSA was added to Cu(I)/H_2O_2 and DNA mixture, the DNA degradation was not affected, implying that the tested protein is not able to deprive Cu(I) from Cu(I)-DNA complex. In fact, the identity of the ROS is still debatable, it could be the hydroxyl radical as shown in the equation above. Yamamoto et al. showed that the reactivity of this species is similar to that of a singlet oxygen.[102]

To the best of my knowledge, besides a few computational studies[100,103], there are no experimental data concerning the binding of Cu(I) to DNA strands or DNA nucleotides. However, the binding of Cu(II) to DNA and DNA nucleotides has been well established as detailed below.

Interaction between DNA and Cu(II)

Studies on the interaction between Cu(II) with DNA can be traced back to the 1960s, when Cu(II) was found to bind to DNA bases with an affinity higher than any other divalent cation.[104] Since then, the affected thermal stability of DNA duplexes upon Cu(II) binding has been extensively studied.[94] At low Cu:DNA ratios, Cu(II) stabilizes the DNA duplexes, while higher Cu:DNA ratios dramatically decreased the T_m value; with 0.1 mM Cu(II), the T_m of tested DNA decreased from 69 to 36 ˚C (in the presence of 5 mM NaCl). Cu(II) destabilized the DNA duplexes in a cooperative manner and GC base pairs were essential for such a destabilization effect. When a DNA duplex were free of GC, i.e., polydA-polydT, the T_m value would not decrease, even slightly increase. These studies

provided the first evidence that Cu(II) interact directly with guanine-cytosine base pairs in double stranded DNA.[93, 103]

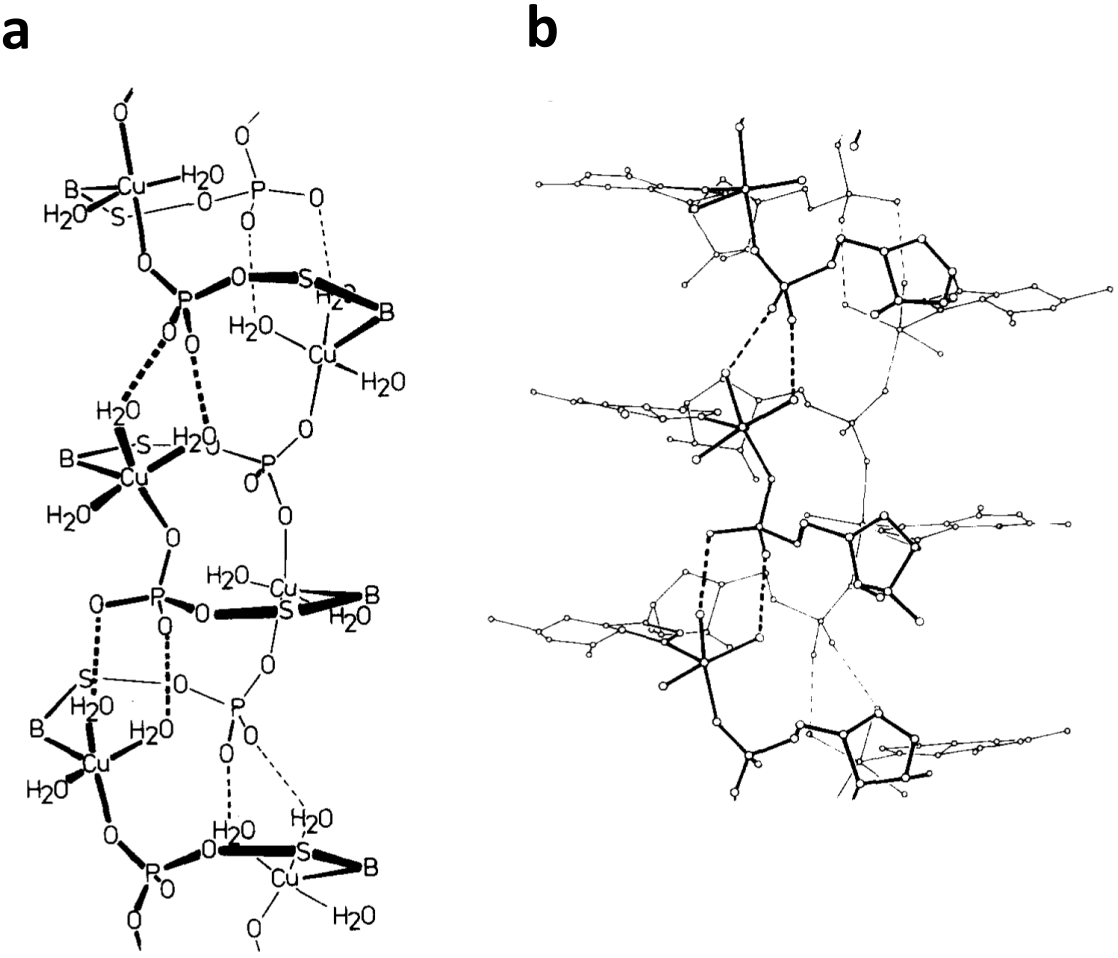

Figure 1.18 Polymeric crystal structure of copper(II) and guanosine 5'-monophosphate complex, in which each copper atom is square pyramidal with binding to N7 of the base and with both direct and indirect bonding to the phosphates. (a). Schematic representation of a segment of the polymeric chain structure of $[Cu_2(5'\text{-}GMP)_3(8H_2O)\ 4H_2O]_n$. The sugar and base groups are depicted as S and B respectively. Broken lines represent hydrogen bonds. Non-coordinated water molecules have been omitted; (b) Stereoscopic representation of a segment of the polymeric chain structure of $[Cu_2(5'\text{-}GMP)_3(8H_2O)\ 4H_2O]_n$.

Note: Reprinted with permission from Aoki, K. et al. Metal-Phosphate Bonding *in Trans*ition Metal nucleotide Complexes. The Crystal and Molecular Structures of the Polymeric Copper(II) Complex of Guanosine 5'-Monophosphate. *Biochim. Biophys. Acta*. 1976, 425 (3), 369–371.

Since 1970s, X-ray crystallographic studies on complexes of Cu(II) with nucleotides and their derivatives have been extensive.[104-107] Of the four DNA nucleotides, the two purines (guanine and adenine) attracted much more attention since the interaction

of copper with cytosine and thymine is much weaker. In 1976, Aoki and co-workers reported the crystal structure of Cu(II) complexed with guanosine 5'-monophophate (GMP).[105] As shown in Figure 1.18, Cu(II) bound to GMP to form a chain-like (base stacking) polymeric structure with three crystallographically different metal-nucleotide units. Cu(II) coordinates to four oxygen atoms equatorially, with either three oxygens from H_2O and the fourth from the phosphate, or two oxygens from H_2O and the remaining two from phosphates. In all cases, both direct and indirect phosphate interactions are involved. The axial ligand is always the N7 of guanine. As a matter of fact, besides copper, other transition metal-guanosine phosphate complexes have been reported, including nickel, cobalt, cadmium, and manganese.[106]

Ho and coworkers first solved the crystal structure of a complex between Cu(II) and the double stranded Z-DNA sequence d(CGCGCGG) shown in Figure 1.19A.[107] A few interesting observations are: (1) the overall structure of Z-DNA is not disrupted by the binding of copper, as compared with the native Z-DNA structure; (2) copper formed an octahedral geometry with four water molecules as equatorial ligands and another water along with the N7 of guanine at the axial positions; (3) The 6 guanines (G2, G4, G6, G8, G10 and G12) along the Z-DNA duplex, each forms a crystallographically different copper binding site. The geometry of these copper complexes are either distorted versions of octahedral or ambiguously assigned -- both the bond length of Cu-N7 and angle between Cu-N7 and Cu-water varying between different binding sites. (4) With about 1.9 Cu(II) ions per hexamer duplex on average, the distribution of Cu(II) along the duplex strand is not uniform. The guanine at the end of the sequence has the highest copper occupancy, indicating that the binding affinity of DNA to copper could be modulated by the exact microenvironment defined by the crystal packing of the hexamer duplex; (5) Based on the structural information from a Cu(II)/Z-DNA complex, Ho and coworkers proposed models for how Cu(II) could complex with B-DNA in solution. According to these models, two adjacent guanines on the same B-DNA strand are the energetically favored binding site for Cu(II), accommodating the octahedral copper complex in the major groove with minimal distortion on the structure of both B-DNA and the complex's own geometry.

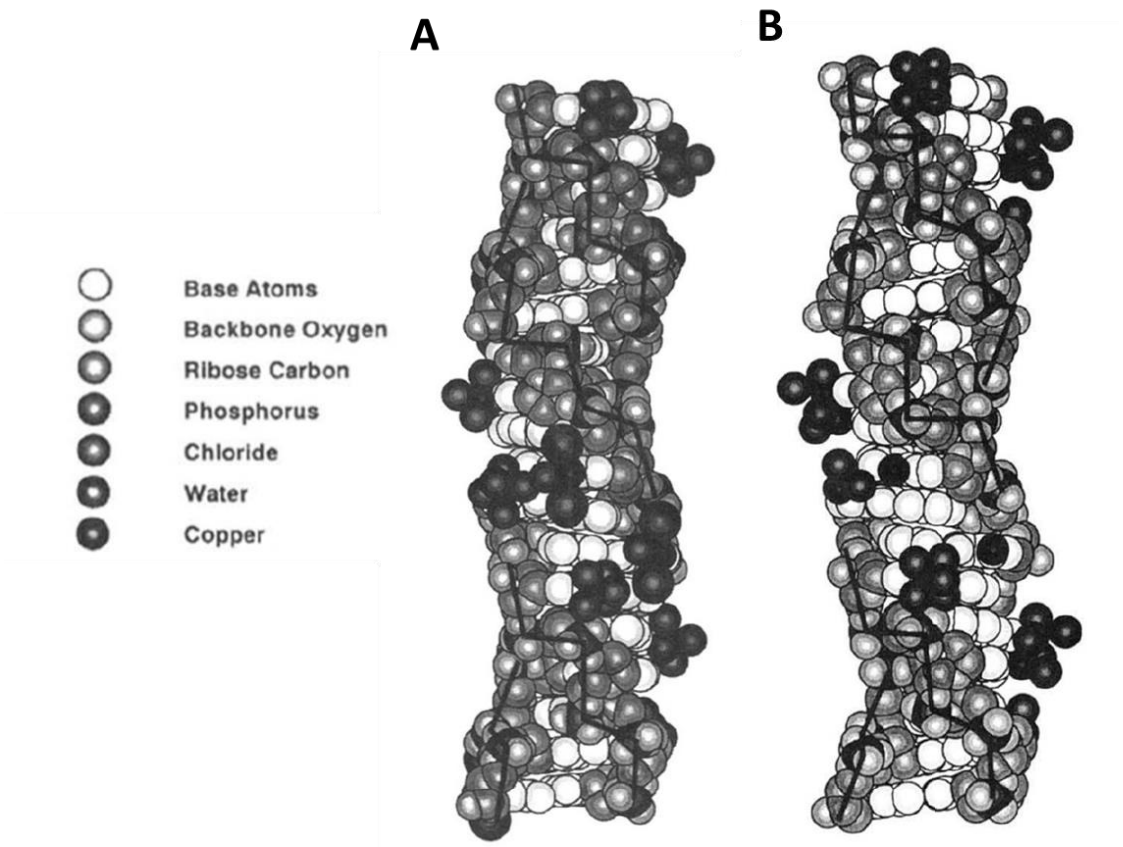

Figure 1.19 Stereo van der Waals diagram of copper(II) chloride-soaked d(CGCGCG); (B). Stereo van der Waals diagram of copper(II) chloride-soaked d(m5CGUAm5CG) as Z-DNA. Three hexamers are shown as they are aligned along the crystallographic c axis to define 1.5 turns of Z-DNA along the molecular helix axis. Each hexamer duplex defines 0.5 turn of Z-DNA. Each copper is shown as fully occupied. The DNA atoms are shaded as indicated, and the copper atoms of the copper complexes are shown as dark shaded spheres. The phosphorus atoms (including the approximate positions of the phosphorus atoms of the missing phosphate groups on the 5'- and 3'-ends of the hexamers) of the DNA backbone are connected to illustrate the zig-zag pattern of the Z-DNA backbone.

Note: Reprinted with permission from Bernhard H. et al. Base-specific Binding of Copper(I1) to Z-DNA *J. Biol. Chem.* 1991 266 (3) 20185-20191. Copyright 1991. The American Society for Biochemistry and Molecular Biology.

In their two consecutive publications in 1991, Ho and coworkers reported the crystal structure of another Cu(II)-Z-DNA complex, d(m5CGUAm5CG) (Figure 1.19A).[107] Different from the first Z-DNA-copper complex, which contained DNA with only CG, this Z-DNA contained UA base pairs as well. It was clear that copper binds purine much more preferentially than pyrimidines, but the question was raised: did copper bind to the two purines, A and G, with different preferences? It seemed to be the case, as copper /H_2O_2

selectively damage consecutive Gs, while adenines are quite resistant to such damage.[108] Such a hypothesis is supported by the resolved crystal structures as discussed below.

The crystal structure of Cu(II)/d(m5CGUAm5CG) shares a lot in common with that of Cu(II)/d(CGCGCG) (the numbering of this duplex follows the same rule as mentioned before for d(CGCGCG)). All four guanines (G2, G4, G8, G12) on the hexamer duplex bound to a copper complex with N7, the distribution of copper is primarily based on the availability of N7 of guanine in the crystal (the more exposed in the crystal structure, the high copper occupancy it will have). For the two adenines (A4 and A10), they behave differently in terms of binding to the copper complex. A4 was not observed to be complexed with any copper, and it is located at an open solvent channel in the crystal. In contrast, A10 binds to Cu(II) to certain extent, however, not independently. It shares a copper complex with G12 of the adjacent hexamer duplex in the crystal. These data imply that in a dilute solution of DNA, adenines are not susceptible to be bound by Cu(II). Furthermore, the adenine modification of copper can happen with the help of specific DNA-DNA interaction (to provide the Guanines needed).

Equation 2

$$M^{2+} + Ns \leftrightarrow M(Ns)^{2+} \quad (1)$$

$$K^{M}_{M(Ns)} = [M(Ns)^{2+}]/([M^{2+}][Ns]) \quad (2)$$

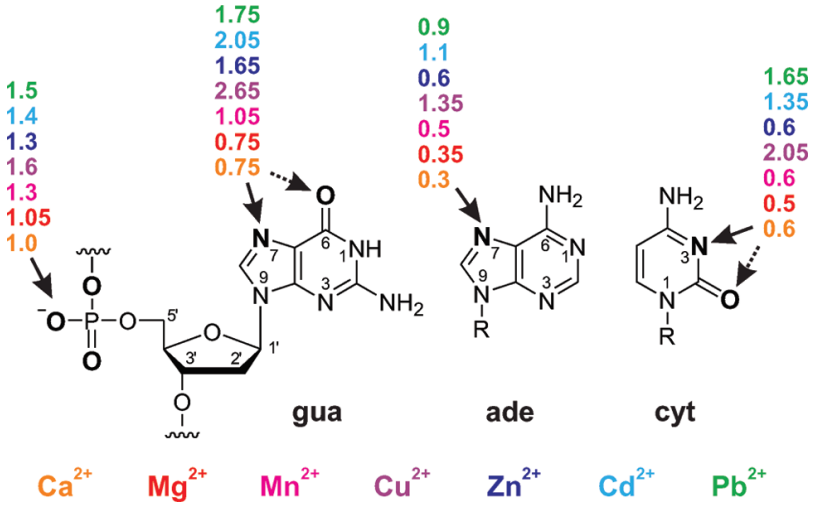

Figure 1.20 Log stability constant of divalent metal ions to binding sites on nucleotide residues.

Note: Reprinted with permission from Sigel, R. K., et al. A Stability Concept for Metal Ion Coordination to Single-Stranded Nucleic Acids and Affinities of Individual Sites. *Acc. Chem. Res.* 2010, 43 (7), 974–984. Copyright 2010. The American Chemical Society.

The above crystal data identified the preferred Cu(II) binding site on DNA; a remaining question is the relative binding affinity of all potential copper binding sites, namely, N7, oxygen on C6 of guanine, N7 of adenine, N3 of cytosine and the phosphate backbone. Amino groups of cytosine and adenine are not basic, thus they are essentially inert to metal binding. N3 of thymine is not suitable for copper binding since it is deprotonated under neutral pH. Sigel and coworkers proposed a model to estimate the overall binding affinity of divalent cations to DNA in considering all binding sites.[108] They estimated the binding affinity of Cu(II) to the nitrogen atoms of bases based on published potentiometric pH titration data;[109] the stability constant of what was determined based on published potentiometric pH titration datausing Equation 1.2. The log ($K_{M(Ns)}$) values are shown in Figure 1.20 and listed in Table 3.[110–112] Particularly, Cu(II) binds to N7 of guanine with a K_d of around 7.58 mM (converted from the log$K_{M(Ns)}$ value in Table 3) to N7 of adenine with a K_d of around 44.68 mM, and to N3 of cytosine with a K_d of around 8.91 mM. These values may not represent the actual binding affinities of Cu(II) to DNA, but provide a reasonable comparison. As indicated by the K_d values, N7 of guanine has the highest binding affinity to Cu(II), i.e., higher than any other metals in the list to any of the binding sites.

Table 3 Log stability constants of divalent metal ions to nucleobase residues calculated based on published potentiometric pH titration data and eq 1.2. Note: Adopted with permission from Sigel, R. K., et al. *Acc. Chem. Res*. 2010, 43 (7), 974–984. Copyright 2010. The American Chemical Society.

M^{2+}	**Guo**	**Cyd**	**Ado**
Mg^{2+}	0.35 ± 0.25	0.12 ± 0.04	-0.06 ± 0.15
Ca^{2+}	0.35 ± 0.26	0.18 ± 0.06	-0.12 ± 0.12
Mn^{2+}	0.57 ± 0.2	0.19 ± 0.08	0.04 ± 0.09
Cu^{2+}	2.12 ± 0.14	1.56 ± 0.06	0.84 ± 0.04
Zn^{2+}	1.16 ± 0.11	0.20 ± 0.11	0.15 ± 0.04
Cd^{2+}	1.53 ± 0.07	0.91 ± 0.07	0.64 ± 0.03
Pb^{2+}	1.25 ± 0.17	1.20 ± 0.07	0.4 ± 0.3

To summarize, for copper dependent DNAzymes, since there are potentially single stranded loops, duplex moieties, bulges, and other DNA secondary and tertiary structures, the interaction between copper and DNA can be rather complicate. Copper could function as structural ions to help DNAzymes to fold into the active conformation (as copper of right concentration stabilizes duplex DNA), or as a mechanistic player in the active site where the catalyzed reaction takes place. It is reasonable to conclude that these binding sites must involve one or more N7 of guanines. In certain cases, where specific DNA-DNA interaction is achieved by DNA folding, N7 of adenine is also possible to serve as the binding site. Thymine and cytosine are less likely to directly interact with copper in the presence of guanine and adenine. Copper/H_2O_2 induced site-specific DNA degradation might be a reliable way to probe the copper binding sites on DNA.

1.3.5. Possibility of DNAzyme-assisted CuAAC

As has been discussed above, substantial efforts have been made to make CuAAC more biocompatible. With limited improvements, none of the above strategies are free of obvious drawbacks. We believe that an enzyme (in our case DNAzyme)-catalyzed CuAAC, if possible, could eliminate a number of the above drawbacks.

As has been reported, certain N-donor ligands stabilizes Cu(I) and accelerate the CuAAC reactions.[63,88] In the most frequently used water-soluble ligand (THPTA) and other tris-triazole based ligands, the central tertiary amine provides strong and stable coordination with copper, while the imine nitrogen atoms on the triazole ring provide labile and transient interaction with copper to allow coordination between copper and azide and alkyne substrates. DNA has coordination sites with different affinities for copper as well—for example the N7 positions of guanine and adenine, N3 of thymine, and the negatively charged phosphate backbone, which will be discussed in detail in next section. These may allow a similar range of interactions with copper as THPTA. Furthermore, as has been discussed in previous sections, copper dependent DNAzymes catalyzing DNA ligation, DNA cleavage, DNA capping as well as a few other chemical transformations have been successfully isolated and characterized.[32,35] We postulated that through *in vitro* selection, DNA with optimal ligand environment for copper to maximize its catalytic ability for CuAAC could be isolated.

Furthermore, DNAzymes that are activated by specific type of metal ions can be readily converted into biosensors for them. A copper dependent DNAzyme catalyzing a coupling reaction may offer new opportunity for construction of new copper biosensor. (see more detail in the next section)

1.4. Research objectives and thesis structure

As discussed above, Cu(II) is the required co-factor for most of DNAzymes, except for oxidative DNA cleavage DNAzyme, which requires Cu(I) as its cofactor. It would be interesting to investigate the consensus sequences shared by different copper dependent DNAzymes; from the structural characterization of DNA and RNA aptamers of ATP, it is known that both aptamers share very similar strategies in recognizing their target (as discussed earlier in this thesis). It would not be surprising if different copper dependent DNAzymes share common copper-binding motifs. Furthermore, the existence of copper dependent DNAzymes indicates that DNA can interact with copper in constructive ways to enable new functionalities. Based on this notion, we proposed the selection of DNAzymes that could enable superior catalysis of the alkyne-azide cycloaddition reaction. The objective of this research includes (1) through *in vitro* selection, isolate DNAzyme for azide-alkyne cycloaddition; (2) develop applications using the selected DNAzyme.

Chapter 2 will describe the *in vitro* selection that leads us to the DNAzyme; the kinetics studies under both *in cis* and *in trans* conditions; the labelling of azide-functionalized lysozyme which is confirmed by mass spectrometry; the cell surface labelling of E. coli under biocompatible conditions. Chapter 3 will describe the application of the *in trans* CLICK-17 reaction as a new method to functionalize azide-terminated SAMs on gold with electrochemical reporter. Chapter 4 will describe the development of an electrochemical copper biosensor based on the *in cis* CLICK-17 reaction. Chapter 5 will describe our attempts for the isolation of DNA aptamers binding to a water-soluble ferrocene derivative. General concluding remarks and future work will be presented in Chapter 6.

Chapter 2. CLICK-17, a DNA enzyme that harnesses ultra-low concentrations of either Cu(I) or Cu(II) to catalyze the azide-alkyne 'click' reaction in water

To enable the optimal, biocompatible and non-destructive application of the highly useful copper (Cu(I))-mediated alkyne-azide 'click' cycloaddition in water, we have isolated and characterized a 79- nucleotide DNA enzyme or DNAzyme, 'CLICK-17', that harnesses as low as sub-micromolar Cu(I); or, surprisingly, Cu(II) (without added reductants such as ascorbate) to catalyze conjugation between a variety of alkyne and azide substrates, including small molecules, proteins and nucleic acids. CLICK-17's Cu(I) catalysis is orders of magnitude faster than that of either Cu(I) alone or of Cu(I) complexed to PERMUT-17, a sequence-permuted DNA isomer of CLICK-17. With the less toxic Cu(II), CLICK-17 attains rates comparable to Cu(I), under conditions where both Cu(II) alone and Cu(II) complexed with a classic accelerating ligand, THPTA, are wholly inactive. Cyclic voltammetry shows that CLICK-17, unlike PERMUT-17, powerfully perturbs the Cu(II)/Cu(I) redox potential. CLICK-17 thus provides a unique, DNA-derived ligand environment for catalytic copper within its active site. As a bona fide Cu(II)-driven enzyme, with potential for being evolved to accept only designated substrates, CLICK-17 and future variants promise the fast, safe, and substrate-specific catalysis of 'click' bioconjugations, potentially on the surfaces of living cell. [†]

[†] Adapted from: Liu, K.; Lat, P. K.; Yu, H.-Z.; Sen, D. Nucleic Acids Research. **2020,** 48 (30), 7356–7370. D. Sen supervised the project in all aspects and conceived the initial concept. I have performed all the experiments. P. Kumar Lat participated in constructive discussions. D. Sen, H.-Z. Yu and I composed the manuscript.

2.1. Introduction

The copper (Cu(I))-dependent azide-alkyne cycloaddition ('CuAAC') reaction is perhaps the most versatile and widely used of the 'click' chemistries used for bioconjugations, and more generally for coupling together two molecules of interest, in this case, a terminal alkyne and an organic azide.[61,113,114] The CuAAC reaction has found many applications, including bioconjugations involving living cells. Powerful and versatile as it is, the requirement for Cu(I) ions in CuAAC can be problematic, owing to the concomitant generation of destructive reactive oxygen species (ROS) by Cu(I).[115,116] This, and the desirability for ~100 μM–1 mM concentrations of Cu(I) (toxic to most living cells), have inhibited the full-blown use of CuAAC in biological applications. A number of innovative approaches to minimize or abrogate the toxic effect of Cu(I), and of copper in general, have been developed in recent years. These include (i) utilization of specific ligands to bind and stabilize Cu(I); such ligands, including the water-soluble tris(3-hydroxypropyltriazolylmethyl)amine (THPTA), accelerate the reaction by perturbing the Cu(II)/Cu(I) redox potential toward Cu(I) as well as serving as sacrificial oxidation substrates for the generated ROS;[77,117] (ii) developing Cu(I)-chelating azides as participating reagents and (iii) the use of enforcedly proximal azide and alkyne[87] or strained alkynes,[81,82] both under copper-free conditions. These novel approaches afford substantial benefits; nevertheless, they continue to show collateral disadvantages—for instance, the relatively promiscuous reactivity (such as with thiols) of the strained alkynes used for copper-free AAC. Biological transformations of any kind are most optimally facilitated by enzymes. If there were to exist an enzyme (protein or nucleic acid) capable of catalyzing the azide-alkyne cycloaddition (AAC) reaction with high efficiency under low-to-zero copper concentrations, it should prove to be a highly useful reagent for catalyzing this powerful coupling reaction, especially in biological contexts. However, AAC or CuAAC are not metabolic reactions per se; and out of the large number of naturally occurring copper-utilizing proteins, it is difficult to identify an obvious candidate that could be 'evolved' towards catalyzing CuAAC. Nevertheless, powerful methodologies exist, such as *in vitro* selection from vast, random sequence, single-stranded RNA or DNA libraries ('SELEX') for de novo identification of RNA or DNA biocatalysts (ribozymes and DNAzymes) suitable for catalyzing even nonmetabolic reactions.[118-120] Currently, standard conditions for CuAAC in water involve generation of Cu(I) in situ via reduction of 100 μM–1 mM of an added Cu(II) salt by a reducing agent (commonly, ascorbate), generally in the

presence of a 5-fold excess (over copper) of a ligand such as THPTA.[57,58] We hypothesized that efficient catalytic DNAs capable of harnessing very low Cu(I) concentrations could, in principle, be identified despite the propensity of Cu(II) and Cu(I) for non-specific binding to DNA (to the backbone phosphodiesters as well as to sites on the heterocyclic nucleobases).[99,109] Figure 2.1 shows the design of a randomized DNA library for our selection, consisting of $\sim 10^{14}$ distinct 80-nt sequences, each incorporating 40 random deoxynucleotides ('N40') flanked on either side by 20-nt fixed sequences suitable for primer-binding for PCR-amplification (Figure 2.1). Herein, we present the selection of a highly copper efficient catalytic DNA (DNA enzyme, deoxyribozyme, or DNAzyme), 'CLICK-17', which catalyzes CuAAC *in cis* with as little as 50–200 nM Cu(I). Such an initial, single turnover version of CLICK-17 (operating '*in cis*', as 5'-hexynyl-CLICK-17 or ≡-CLICK-17) was then converted to a true enzyme, catalyzing multiple turnovers of a variety of small molecule as well as macromolecule substrates '*in trans*'.[119] The most intriguing result we report is that CLICK-17 is catalytic with either Cu(I) or Cu(II) as added cofactors (the latter in the absence of added ascorbate). The Cu(II) reaction is optimal in the 5–20 μM copper ion concentration range; under which conditions, neither a sequence permuted isomer of CLICK-17 ('PERMUT-17') DNA nor a 5-fold excess THPTA are found to support the CuAAC reaction at any level.

2.2. Results and Discussion

2.2.1. *DNAzyme design and selection*

The key design strategy for identifying catalytic DNA sequences out of a large random-sequence library is to select first for quasi-catalytic DNAs, that carry out a single catalytic turnover (i.e. work '*in cis*'); and are in the process chemically modified (tagged) such that they can be sequestered away from non-active DNAs within the library. Our single-stranded DNA (ssDNA) pool was synthesized with a 5'-hexynyl attachment on each DNA (Figure 1). These sequences were allowed to fold to form their distinctive secondary/tertiary structures in an aqueous buffer solution ('S Buffer': 50 mM HEPES, pH 7.4, 300 mM NaCl, 50 mM KCl, 20 mM $MgCl_2$), then supplemented with 5 μM Cu(I) and freely diffusible azide-biotin for 2 h at 22 °C(Figure 1). DNA sequences capable of catalyzing CuAAC in this very low-copper regime self-tagged with biotin, and were separated on that basis from the unreacted DNAs (the biotin 'tag' binds tightly to the

protein streptavidin, which in turn retards the electrophoretic mobility of biotinylated DNAs in a gel). Figure A1 in appendix A provides a schematic diagram for the entire SELEX procedure.

Forward primer	5’-Hexynyl_GGATCGTCAGTGCATTGAGA-3’
Reverse primer	5’-TACCCGTTGC GGATrACCACC-3’
DNA pool	5’-GGATCGTCAGTGCATTGAGA-(N_{40})-GGTGGTATCCGCAACGGGTA-3’

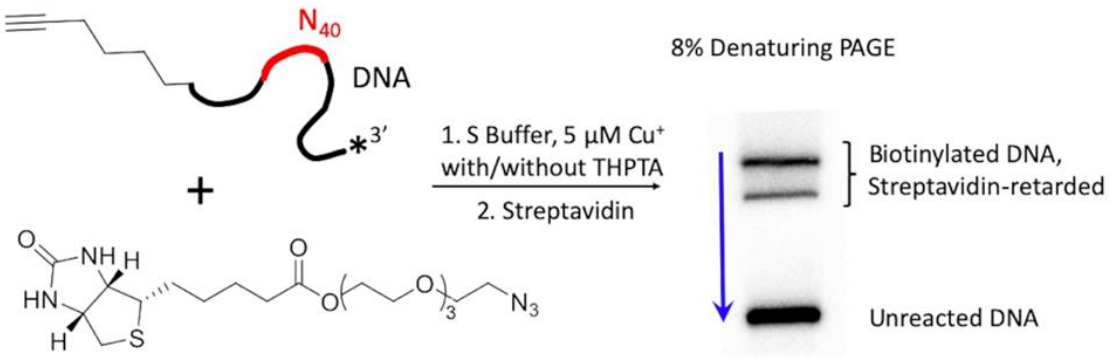

Figure 2.1 PAGE gel-based method for a CuAAC-catalyzing DNAzyme. The ‘N40’ region shown in red indicates the location of the randomized stretch of DNA sequence present within each individual DNA molecule (~10^{14} total such molecules within the starting selection ‘library’). The blue arrow (right) shows the direction of electrophoretic migration of DNA in a denaturing polyacrylamide gel (PAGE).

A total of 25 rounds *in vitro* selection were carried out. Two parallel selection experiments were conducted, one with Cu(I) as the catalytic cofactor, and another with THPTA/Cu(I) as the cofactor. The enrichment of CuAAC active DNAs through the selection rounds could be tracked by monitoring the overall conversion percentage of pool DNA in rounds 1–7 (Figure A2 in Appendix A). The enrichment trends observed for both selections were roughly comparable; by round 7, > 50% of the input 5’ -hexynyl-DNA had reacted with the input azide-biotin within 2 h. By Round 25, pool enrichment had stabilized. Forty clones of the Round 25 pool were picked and sequenced, and the results are compiled in Figure A3 in appendix A. A number of the sequenced clones showed identical sequences, and five families of sequence were identified. Clones were picked from each family and prepared as 5’ hexynyl-labeled-ssDNA (‘≡-DNA’), then tested for *in cis* CuAAC-promoting activities. Testing was carried out in S buffer, used for the *in vitro* selection, and clone CLICK-17 was picked as a promising catalytic candidate. 5’-hexynyl-

CLICK-17 (‘≡-CLICK-17’) was then studied intensively. It was found that ≡-CLICK-17’s reaction kinetics in a relatively simple reaction buffer (‘R buffer’: 50mMLi-HEPES, pH 7.4, 20 mM $MgCl_2$) were comparable to those in the higher ionic-strength S buffer. Consequently, all detailed characterization studies on ≡-CLICK-17 were carried out, except where explicitly stated to be otherwise, in R buffer. *In cis* reaction of CLICK-17.

2.2.2. The *in cis* reaction of 5’ -hexynyl-CLICK-17 DNA (≡-CLICK-17)

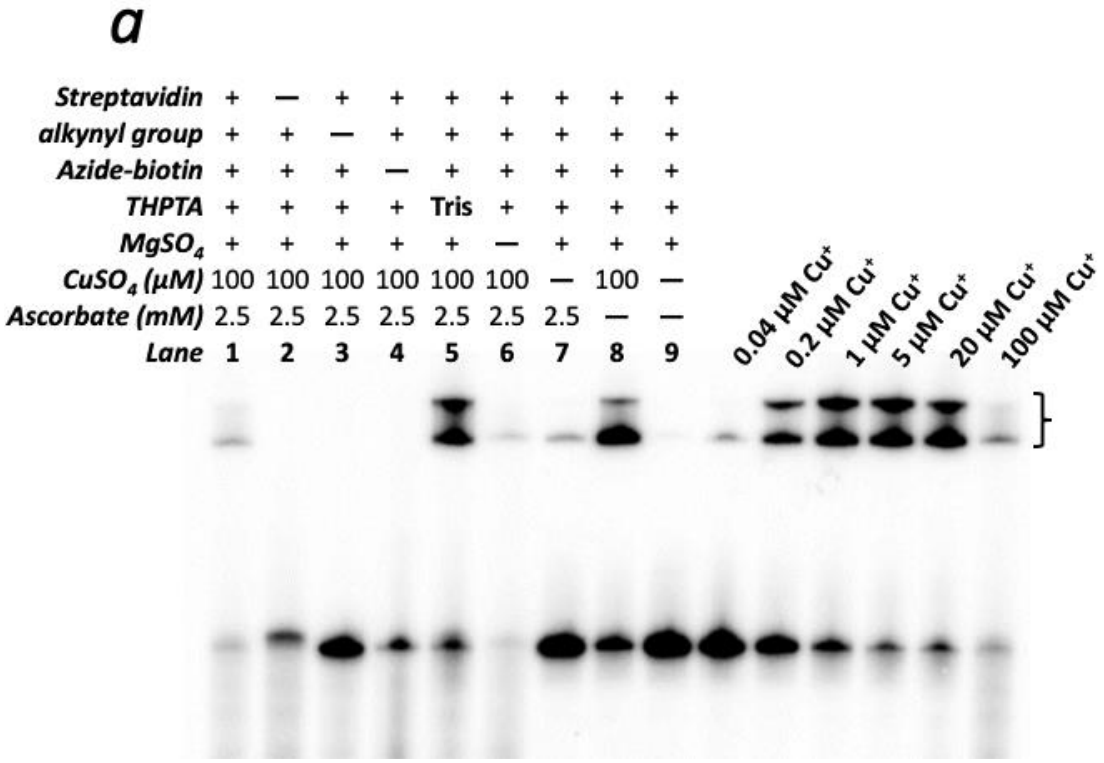

Figure 2.2 *In cis* catalysis by 5’-hexynyl-CLICK-17 DNA (≡-CLICK-17). 5’-hexynyl-CLICK-17 DNA (≡-CLICK-17) catalyzes CuAAC *in cis* in R buffer. Reaction conditions were: 2 μM ≡-CLICK-17 and 2.5 mM azide-biotin in R buffer, to which 100 μM $CuSO_4$ (the default concentration, unless indicated), and 2.5 mM sodium ascorbate were added. Reactions proceeded at 22 °C for 1 h except in the copper titration lanes (where they proceeded for 30 min).

As Figure 2a shows the CuAAC capabilities of 3’-32P-labeled ≡-CLICK-17 DNA under different reaction conditions. ≡-CLICK-17 was heat-denatured and refolded in R buffer. The generic *in cis* reaction with azide-biotin consisted of 2 μM folded ≡-CLICK-17, to which was added 100 μM $CuSO_4$, 5 mM azide-biotin and 2.5 mM of sodium ascorbate. These solutions were incubated at 22°C for 1 h for the various control experiments (first

nine lanes from the left in Figure 2.2), and for 0.5 h for the copper titration (0.04–100 μM Cu^{+}) experiments (Figure 2.2). In all lanes (excepting lane 2), the reaction was terminated by ethanol precipitation, and the recovered and redissolved DNA was treated with streptavidin prior to loading into a non-denaturing PAGE gel. Identical values of ^{32}P counts were loaded into each lane. Biotinylation of DNA gave rise to two or more DNA bands of retarded electrophoretic mobility by virtue of streptavidin binding (indicated by brackets in Figure 2.2; the different retarded bands represent different stoichiometries of these robust complexes, one streptavidin protein is capable of binding up to four biotinylated DNAs).

Although precisely equal amounts of DNA (corresponding to ^{32}P counts) were loaded in each lane, the different incubations show different levels of DNA in the different lanes of the gel. The first six lanes of the experiment show that in all incubations carried out with 100 μM Cu(I), significant degradation of the ≡-CLICK-17 DNA occurs, particularly in the absence of THPTA, presumably via ROS generation in the solution. Substitution of Li-HEPES by Tris as the buffering reagent lowers this degradation (‘Tris buffer’ lane in Figure 2.2, this protective effect of Tris buffer may be due to the competitively binding of copper to Tris). The presence of magnesium is required in the reaction buffer, presumably for the catalytically relevant folding of ≡-CLICK-17. The absence of magnesium ions also leads to a high level of≡-CLICK-17 degradation; presumably, Mg^{2+} modulates the binding (and degradative effect) of Cu(I) to the DNA. Curiously, the complete absence of copper (‘-$CuSO_4$’) does generate a small amount of streptavidin-retarded product, presumably from very low levels of copper-free AAC catalyzed by the folded ≡-CLICK-17. The most curious, yet reproducible, result is the high level of CuAAC product seen in the presence of 100 μM $CuSO_4$ in the absence of any added ascorbate (‘- sodium ascorbate’, Figure 2.2). This phenomenon was investigated in later section. The six lanes on the extreme right side of Figure 2.2 show the yield of the CuAAC product formed from≡-CLICK-17 as a function of Cu(I) concentration. With as little as 200 nM Cu(I), ~50% biotinylation of ≡-CLICK-17 is reached within 0.5 h; with 1 μM Cu(I), conversion is ~80% complete in this time frame. While DNA degradation is modest at ⩽20 μM Cu(I), at 100 μM Cu(I), such degradation is heavy (as shown by the smears at the bottom of the gel).

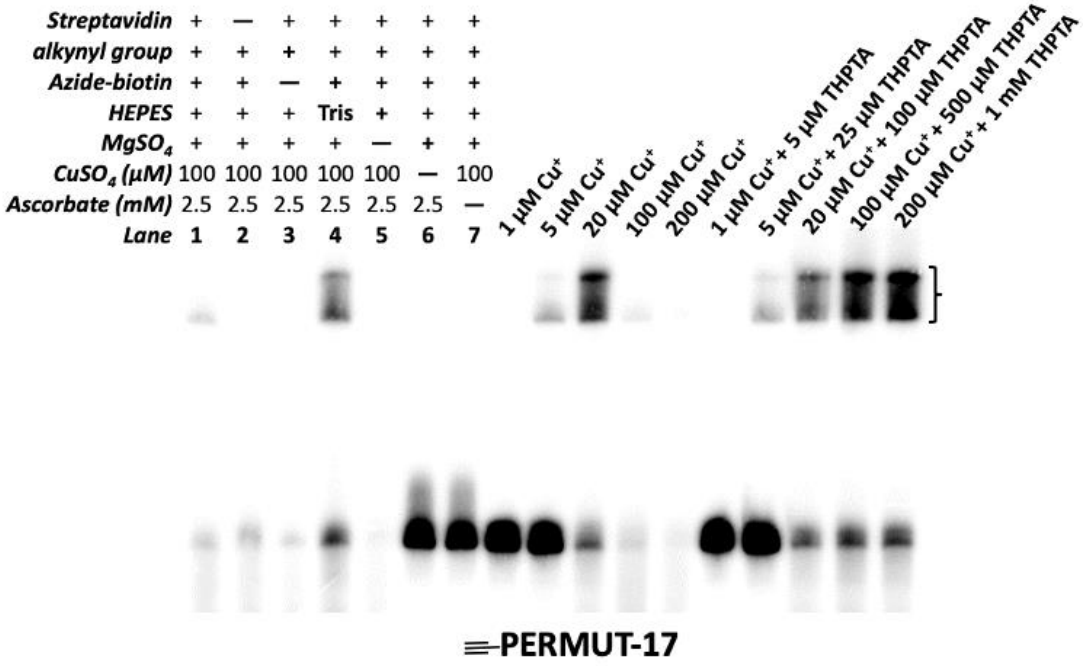

Figure 2.3 *In cis* catalysis by 5'-hexynyl-PERMUT-17 DNA (≡-PERMUT-17). 5'-hexynyl-PERMUT-17 DNA (≡-PERMUT-17) catalyzes CuAAC *in cis* in R buffer. Reaction conditions were: 2 μM ≡-PERMUT-17 and 2.5 mM azide-biotin in R buffer, to which 100 μM $CuSO_4$ (the default concentration, unless indicated), and 2.5 mM sodium ascorbate were added. Reactions proceeded at 22 °C for 1 h except in the copper titration lanes (where they proceeded for 30 min).

To determine if the above results are specific to ≡-CLICK-17, as opposed to 5'-hexynylated ssDNAs in general, we carried out analogous experiments with a nucleotide-sequence permuted DNA isomer of ≡-CLICK-17 ('≡-PERMUT-17' ; nucleotide sequence given in the material and methods section). Figure 2.3 shows these results. Here, again, Tris buffer generates less DNA degradation than does HEPES buffer. With ≡-PERMUT-17, unlike ≡-CLICK-17, however, (a) no biotinylation is evident with 100 μM $CuSO_4$ in the absence of ascorbate and (b) quantitative biotinylation of ≡-PERMUT-17 requires ~20 μM Cu(I), between 20- and 100-fold higher than required for ≡-CLICK-17. The impact of THPTA (present at 5-fold > [Cu(I)]) on ≡-PERMUT-17 biotinylation is not majorly different from that in the absence of THPTA; only, at high copper concentrations

(100 and 200 μM Cu(I)), THPTA reduces ≡ -PERMUT-17 degradation.

	5 μM copper Initial rate (μM/min)	20 μM copper Initial rate (μM/min)
≡-CLICK-17	4.2	0.14
≡-PERMUT-17	0.0019	0.094

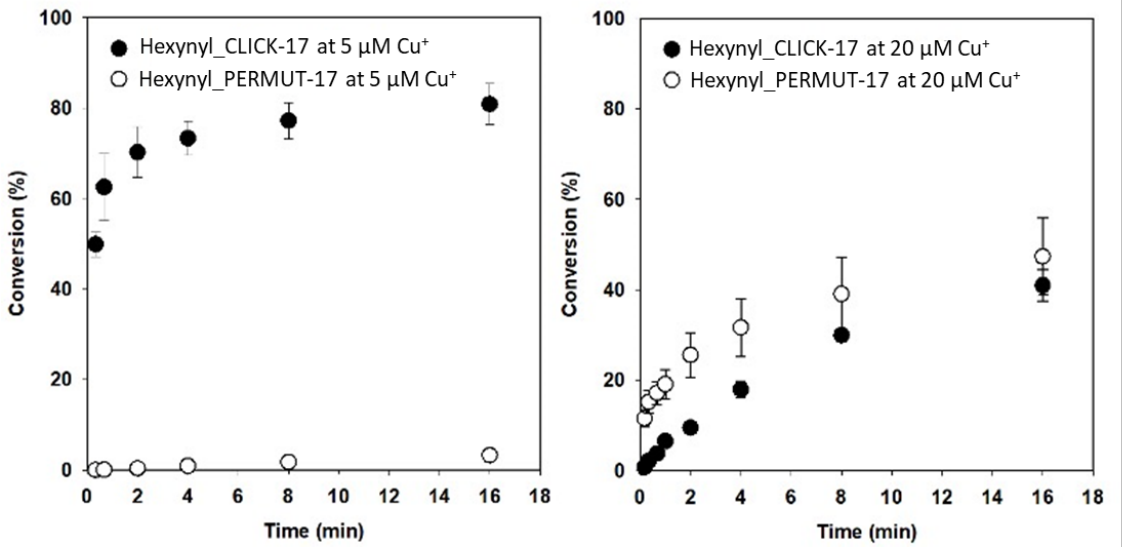

Figure 2.4 Plots of the reaction time-dependences of 2 μM ≡-CLICK-17 and ≡-PERMUT-17 in the presence of 5 μM and 20 μM Cu(I), respectively. The error bars shown represent one standard deviation from the mean, determined from three independent experiments.

Detailed time-dependence measurements of *in cis* CuAAC (biotinylation) experiments were carried out for the first 100 min of reaction, for both 2 μM ≡-CLICK-17 and 2 μM ≡-PERMUT-17, at different Cu(I) concentrations (Figures A4 and A5 in appendix A). Figure A4 in appendix A shows that in the presence of as little as 5 μM Cu(I), the ≡-CLICK-17 reaction is 80% complete within 20min; with 8 nM Cu(I), >20% conversion occurs in 2 h. A striking observation about the Cu(I)-dependence of the ≡-CLICK-17 reaction is that highest catalytic activity is observed with ~ 5 μM Cu(I). Reaction with 20 μM Cu(I) is dramatically slower (slower than with 1 μM or 5 μM Cu(I)). The most plausible explanation is that at ~20 μM Cu(I), ≡-CLICK-17 forms an alternatively folded conformer that is either non-catalytic or poorly catalytic. As a matter of fact, high copper inhibition is a common observation among copper dependent DNAzymes. Indeed, Figure 2.4, which plots *in cis* biotinylation rates for ≡-CLICK-17 and for ≡-PERMUT-17 for the first 16 min of reaction, shows that at 5 μM Cu(I), the ≡-CLICK-17 reaction is ~2000-fold

more rapid than the ≡-PERMUT-17 reaction. However, at 20 μM Cu(I), the ≡-CLICK-17 and ≡-PERMUT-17 rates are comparable, likely representing baseline CuAAC rates observable with 2 μM of any 79-nt long ≡-ssDNA. Figure A6 in appendix A shows ESI mass spectrometry data that confirm that the streptavidin-retarded products on gels, such as shown in Figure 2.2, are indeed the CuAAC adduct of ≡-CLICK-17 and azide-biotin. To facilitate ESI mass spectrometry of the conjugation product, the CuAAC reacted mixture was subjected to complete digestion with Nuclease P1, an endonuclease that cleaves DNA into 5'-deoxyribonucleotide monophosphates. The resulting residual structure from the expected conjugation product of ≡-CLICK-17 with azide-biotin incoporates the 5'-most deoxyriboguanosine monophosphate residue of the CLICK-17 DNA sequence linked to biotin via the triazole and linker atoms shown in Figure A6.

2.2.3. The *in trans* reaction: CLICK-17 is a true enzyme

Given that ≡-CLICK-17 is capable of harnessing very low (≤5 μM) concentrations of Cu(I) to efficiently catalyze the CuAAC reaction *in cis*, two questions arose immediately: (a) what mechanistic role does the CLICK-17 DNA play? A 'minimal' hypothesis would be that CLICK-17 plays a role similar to Cu(I)-stabilizing ligands such as THPTA. (b) Can CLICK-17 DNA (now underivatized with the hexynyl moiety) catalyze CuAAC *in trans*, utilizing both diffusible alkyne and azide substrates? To investigate whether folded CLICK-17 DNA can catalyze CuAAC *in trans*, we first explored suitable assays for making such a determination. We picked 5-hexyn-1-ol ('hexynol') as a diffusible alkyne substrate on the basis of its similarity to the 5-hexynyl moiety within ≡-CLICK-17. However, azide-biotin here was not a particularly useful substrate, because its expected triazole product with hexynol would be a low molecular weight compound requiring specialized detection procedures. We therefore examined a structurally distinct, fluorogenic azide (3-azido-7-hydroxycoumarin or 'azide-coumarin') as a potential substrate for CLICK-17. Experiments were carried out in R buffer with 2 μM CLICK-17 DNA, 8 mM hexynol and 50 μM (limiting) azide-coumarin. The progress of any reaction could be followed using fluorescence measurements (excitation at 404 nm and emission at 480 nm). A fluorescence calibration curve, quantitatively linking measured fluorescence to triazole product concentration, is shown in Figure A7a in appendix A.

Figure A8 in appendix A shows that both azide-coumarin and hexynol were diffusible substrates acceptable to CLICK-17 for CuAAC catalysis *in trans*. The initial rate for the CLICK-17-catalyzed reaction with 5 μM Cu(I) was 0.24 μM min^{-1}; that for PERMUT-17 DNA was < 0.01 μM min^{-1}; that in the absence of all DNA was 0.03 μM min^{-1}. We compared CuAAC kinetics measured with a fixed Cu(I) concentration (5 μM) in the presence of: 2 μM CLICK-17 and no THPTA; 25 μM THPTA and no DNA; neither DNA nor THPTA; as well as with both DNA and THPTA present together. Figure 2.14a shows that 2 μM CLICK-17 is ~1.2-fold more efficient as a catalyst than 25 μM THPTA under these conditions. Interestingly, CLICK-17 and THPTA together do not show any synergy. Moreover, the complete lack of catalysis observed with 2 μM of the control PERMUT-17 DNA cannot be rescued by the presence of THPTA. The above results suggest that for its catalytic action using Cu(I), CLICK-17 likely provides privileged binding site(s) as well as significant redox stabilization for one or more catalytically important Cu(I) ion(s) within its active site. As the data on the non-catalytic PERMUT-17 DNA demonstrate, beyond such privileged binding, DNA sequesters and renders CuAAC-unavailable any residual Cu(I) in the solution under these reaction conditions. Not only does PERMUT-17DNA kill CuAAC comprehensively; in addition, its likely non-specific sequestration of copper can not be reversed or rescued by THPTA.

To optimize *in trans* catalysis by CLICK-17, we explored whether the inhibition imposed by higher (20 μM) Cu(I) on the activity of 2 μM CLICK-17 could be overcome by varying the CLICK-17 concentration in the fixed presence of 20 μM Cu(I). Figure A7b in appendix A shows that, indeed, CuAAC levels obtained with 4μM CLICK-17 are >3-fold higher than those obtained with 2 μM CLICK-17. The complex dependence of CuAAC rates as a function of CLICK-17 concentration (at fixed [Cu(I)]) likely results from the distinct modes of Cu(I) binding to CLICK-17, i.e., tight binding to the active site as well as non-specific binding along the length of the DNA.

2.2.4. CLICK-17 is catalytic with added Cu(II) in the absence of explicit reductants

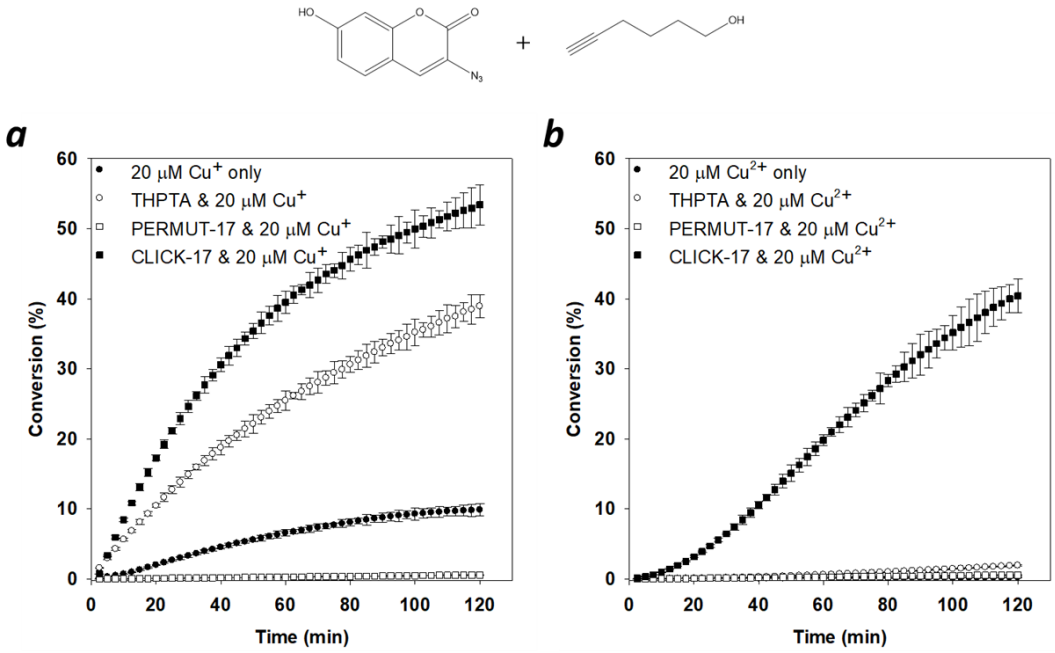

Figure 2.5 CLICK-17 also catalyzes the in trans reaction with either added Cu(I) or Cu(II). The reactions were carried out in R buffer (50 mM Li-HEPES, pH 7.4, 20 mM MgCl2) with 4 μM DNA (CLICK-17 or PERMUT-17). Panels A and B show time-courses of the CuAAC reaction between hexynol and azide-coumarin catalyzed by CLICK-17 DNA, compared to PERMUT-17 DNA, THPTA, or in the absence altogether of added ligand or DNA. Concentrations of the fluorescent triazole product are shown as percentages of the starting concentration (50 μM) of the limiting substrate, azide-coumarin. Whereas the kinetic curves in the presence of added Cu(I) are hyperbolic (panel A), in the presence of Cu(II), the CLICK-17-catalyzed time-dependence is sigmoidal in shape (panel B). The error bars shown represent one standard deviation from the mean, determined from three independent experiments

The most striking observation from the *in cis* experiments with ≡-CLICK-17 (Figure 2.2) was that in the presence of 100 μM $CuSO_4$, with no ascorbate (or other extrinsic reducing agent) added, CuAAC was still catalyzed to a high level. By contrast, under those same conditions, no *in cis* reaction was seen with the control alkynyl DNA, ≡-PERMUT-17 (Figure 2.3).To further understand these observations, a thorough investigation was carried out with (unalkynated) CLICK-17 DNA, first, under *in trans* conditions.

Figure 2.5a and 2.5b shows side-by-side comparisons of CuAAC catalyzed in the presence of 20 μM Cu(I) (generated in situ by 2.5 mM ascorbate—panel (A); and, in the

presence of 20 μM Cu(II) in the absence of ascorbate (panel B). 4 μM of either CLICK-17 or PERMUT-17 DNA (at 4 μM), CLICK-17 is optimally active with 20 μM Cu(I), with hexynol and azide-coumarin as diffusible substrates. Panel A shows that (a) Cu(I) in the absence of either THPTA or CLICK-17 DNA was poor at promoting CuAAC (10% conversion after 2 h); (b) either 100 μM THPTA (~40% conversion) or 4 μM CLICK-17 (~55% conversion) accelerated CuAAC significantly and (c) the presence of 4 μM of the control PERMUT-17 DNA abrogated the reaction completely.

The Cu(II) data shown in Figure 2.5b, however, were strikingly different. With 20 μM $CuSO_4$ in the reaction (in the absence of added ascorbate), only CLICK-17 was able to catalyze the reaction (~40% conversion after 2 h). All the other controls (Cu(II) alone; Cu(II) plus THPTA; and Cu(II) plus PERMUT-17 DNA) failed to support the reaction. A striking feature of the time-dependence of the CLICK-17/Cu(II) combination is its sigmoidal rather than hyperbolic shape, indicative of an initial 'lag' or 'induction' phase. Such kinetics are consistent with the need to reduce Cu(II) and the *in situ* generation of a sufficient concentration of catalytically obligatory Cu(I), stabilized by CLICK-17, to promote CuAAC (a comparison of the relative efficacies of added Cu(I) versus Cu(II) under optimized reaction conditions, where CuAAC proceeds to completion in 30–40 min, is shown in Figure A9 in appendix A).

2.2.5. *In trans*- and *in cis*- labeling of macromolecules (proteins) using the CLICK-17 DNAzyme

We wished to explore the utility of the CLICK-17 DNAzyme (i) to catalyze the conjugation of an azido-protein *in trans* with an alkynated fluorescent dye; as well as (ii) to catalyze the *in cis* conjugation of a fluorescently labeled version of itself (≡-CLICK-17-Fluorescein) to the azido-protein. We wished to test for these activities under the very low Cu(I) and Cu(II) concentration regimes that were shown in Figure, to be characteristic of CLICK-17's activity with small molecule substrates.

First, we labeled the protein lysozyme (14,305 Da) with Azido-PEG2-NHS Ester. The purified products were analyzed by LC–mass spectrometry (ESI). Figure A10 in appendix A shows a near-complete conversion of the unlabeled lysozyme to three new products of MW14,489, 14,674 and 14,859 Da, corresponding to derivatized lysozymes with one, two, and three appended azide functionalities, respectively (each label adds

~185 Da to the protein). This mixture of azido-lysozymes (hereafter referred to as lysozyme- $(N3)_{1–3}$) was then tested first, for *in trans* coupling with alkyne labeled Alexa Fluor Dye 546 (≡-AFDye 546). Figure 2.7 shows an SDS PAGE gel with the results of Cu(II) and CLICK-17-catalyzed *in trans* coupling of 4 μM lysozyme-$(N3)_{1-3}$ with 20 μM≡-AFDye 546, in R buffer for 2.5 h, at 22 ºC. Panel A shows Coomassie Blue-labeled protein bands, while panel B shows the fluorescence of AFDye 546. The second lane from the left in the gel was loaded with ≡-AFDye 546 alone. Panel B therefore identifies the lower of the two fluorescent bands in the gel as free ≡-AFDye 546 ('≡-Dye'). The upper fluorescent band, generated with 5–50 μM Cu(II) in the presence of CLICK-17 (but not with PERMUT-17 nor a 5-fold molar excess of THPTA), was therefore hypothesized to represent the protein–dye conjugate. Indeed, panel C, which overlaps the protein mobility data of panel A with the dye fluorescence data of panel B, shows that this hypothesis is correct. The gel band to the extreme right in all panels shows a positive control, CuAAC under standard conditions used in the field (100 μM Cu(I) in the presence of 500 μM THPTA). Although the yield of lysozyme-dye conjugate catalyzed by CLICK-17/Cu(II) under these conditions is ~40% of that achieved with the positive control, it must be

emphasized that the CLICK-17 here is using Cu(II) as its exclusive

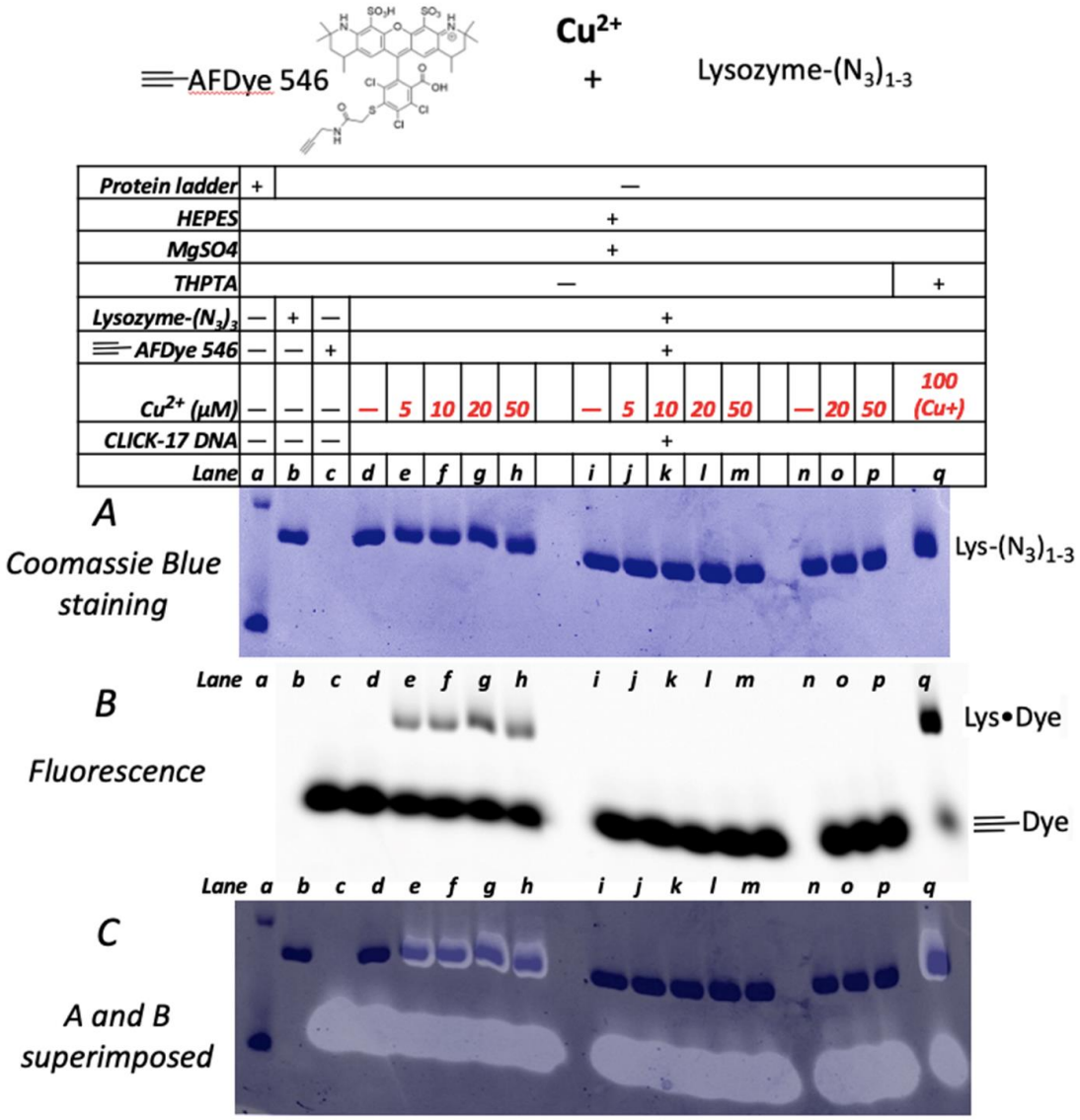

Figure 2.6 SDS-PAGE gel showing Cu(II)-dependence of *in trans*-catalyzed coupling by CLICK-17 of alkynated Alexa Fluor 546 dye (≡AFDye 546) to an azide-labeled protein (lysozyme-$(N3)_{1-3}$). Coomassie Blue-staining patterns for protein in (A); AFDye 546 fluorescence is shown in (B); and overlap of the two gels is shown in (C). Lanes, from left to right, show a protein ladder (the reference bands seen in this lane in panels (B) and (C) represent 10 and 15 kDa standards); lysozyme-$(N3)_{1-3}$ only; ≡-AFDye 546 only; lysozyme-(N3)1-3 incubated for 2 h with ≡-AFDye 546 in the absence of added copper; the two reactants incubated for 2 h in the presence of 5 μM Cu(II); 10 μM Cu(II); 20 μM Cu(II); and, a positive control of the two reactants with 0.1 mM Cu(I)/0.5 mM THPTA for 2 h.

cofactor (in the absence of any explicit reductant). In the presence of Cu(I), CLICK-17 performs comparably to the positive control. LC–MS analysis of the dye-lysozyme CuAAC

conjugates obtained, as shown in Figure 2.6, are given in Figure A11 and Figure A12 in appendix A.

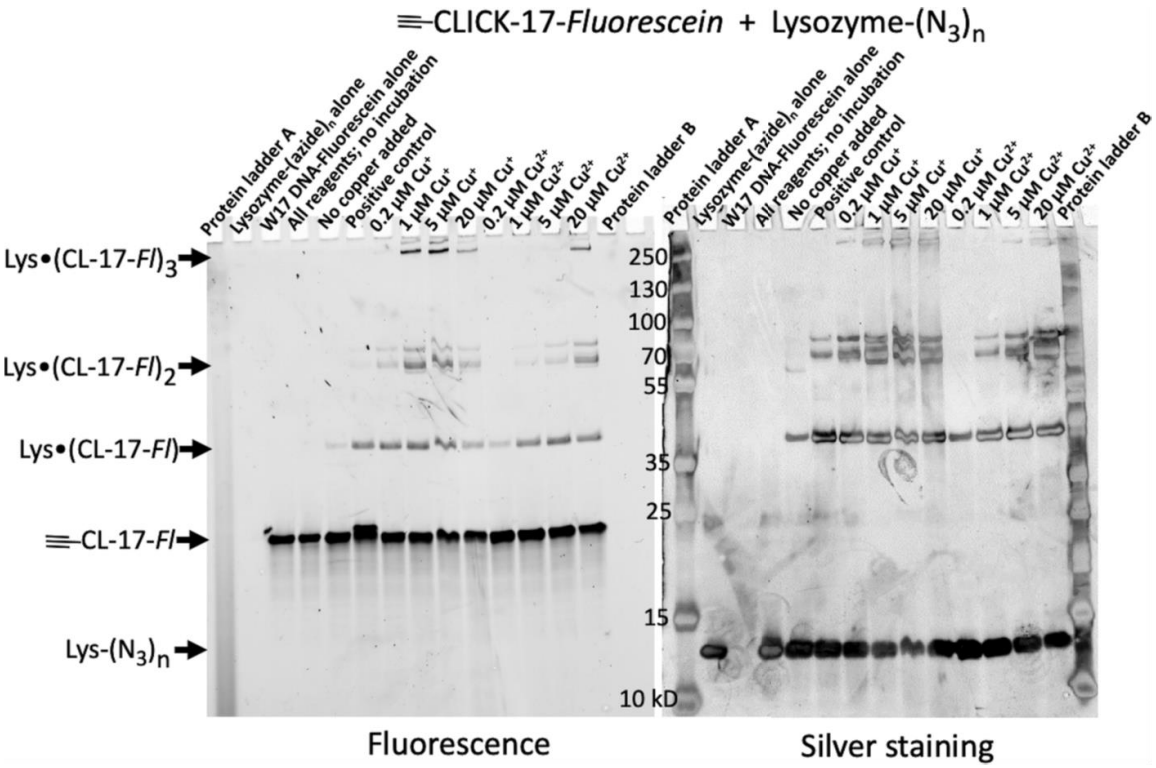

Figure 2.7 SDS-PAGE gel showing Cu(I)- and Cu(II)-dependence of *in cis*-catalyzed clicking of fluoresceinated ≡-CLICK-17 DNA to an azide-labeled protein (lysozyme-$(N3)_{1-3}$). Both fluorescein fluorescence, indicative of DNA (left) and silver staining patterns for protein (right) are shown, both in grey scale. Lanes, from left to right, show Protein Ladder A; lysozyme-$(N3)_{1-3}$ only; ≡-CLICK-17-Fluorescein only; lysozyme-$(N3)_{1-3}$ mixed with ≡-CLICK-17-Fluorescein in the absence of either added copper or incubation; lysozyme-(N3)1 – 3 and ≡-CLICK-17-Fluorescein without added copper but incubated for 2.5 h; a positive control of the two reactants with 1 mM Cu(I)/5 mM THPTA for 2.5 h; the two reactants incubated for 2 h in the presence of 0.2 μM Cu(I); 1 μM Cu(I); 5 μM Cu(I); 20 μM Cu(I); 0.2 μM Cu(II); 1 μM Cu(II); 5 μM Cu(II); 20 μM Cu(II); and, Protein Ladder B.

Figure 2.7 shows the results of the ≡-CLICK-17-catalyzed *in cis* conjugation of lysozyme-$(N3)_{1-3}$ to the fluorescein labeled≡-CLICK-17 DNAzyme itself. The SDS PAGE gel shows the results of incubation of 1 μM lysozyme- $(N3)_{1-3}$ and 2 μM ≡-CLICK-17-Fluorescein DNA, in R buffer for 2.5 h at 22 ^{O}C. Both fluorescein fluorescence (from DNA, Figure 2.8, left) and protein silver staining (rather than Coomassie staining, because of the very low protein concentrations used) patterns (Figure 2.8, right) are shown. The positive control experiment here is the reaction of 2 μM≡-CLICK-17-Fluorescein with 1

μM lysozyme-$(N3)_{1-3}$ under 'normal' CuAAC conditions (i.e. with 1 mM Cu(I) and 5 mM THPTA). The key observation in Figure 2.7 is the appearance of three sets of product bands, visible with both fluorescence and silver staining detection (i.e. these products contain both DNA and protein, hypothesized to be the 1:1, 1:2 and 1:3 protein: DNA adducts; confirmatory mass spectra are shown in Figures A14). These products are labeled, accordingly, as 'Lys•(CL-17-Fl)', 'Lys•$(CL\text{-}17\text{-}Fl)_2$' and 'Lys•$(CL\text{-}17\text{-}Fl)_3$'. There is a single band associated with 'Lys•(CL-17-Fl)', consistent with it showing a 1:1 protein–DNA conjugate; two or more closely spaced bands can be seen for 'Lys•$(CL\text{-}17\text{-}Fl)_2$' (and for 'Lys•$(CL\text{-}17\text{-}Fl)_3$'), likely representing protein-DNA conjugates of the same molecular weight but with variable sites of attachment (and hence, diverse geometries and gel mobilities) of two or three ≡-CLICK-17 DNAs conjugated to one lysozyme-$(N3)_{1–3}$ molecule. What the Figure 2.7 gel strikingly shows—seen particularly clearly from the DNA fluorescence bands on the left—is that (i) under our experimental conditions, as little as 0.2 μM Cu(I) or 1 μM Cu(II) catalyze formation of the 1:1 ≡-CLICK-17-lysozyme conjugate ('Lys•(CL-17-Fl)') comparably as well as the positive control (under optimal CuAAC conditions: 1 mM Cu(I)/5 mM THPTA). (ii) Somewhat higher Cu(I) (1 μM) or Cu(II) (5 μM) catalyze the formation of the 2:1 and 3:1 ≡-CLICK-17-lysozyme conjugates at significantly higher levels than does the positive control. As seen earlier, with ≡-CLICK-17 *cis*-catalyzed small molecule conjugations (Figure 2.2), even in incubations wholly lacking copper, ≡-CLICK-17 does promote a low level of DNA-protein conjugate-formation—consistent, again, with the existence of an active site within folded CLICK-17/≡-CLICK-17. Given that CLICK-17 is macromolecular catalyst, with a catalytically relevant folded structure, we see in Figure 2.7 (as also in Figures 2.2) that higher concentrations of Cu(I) (for example, 20 μM in Figure 2.7) disfavor CLICK-17's catalysis. Again, this is because at such higher [Cu(I)], CLICK-17 forms an alternative, less catalytic or non-catalytic fold. We carried out ESI mass spectrometry analysis on the mixture of species formed in the above *in cis* catalyzed conjugation of≡-CLICK-17DNAwith lysozyme-$(N3)_{1-3}$. Figure A13, panels a and b, show, respectively, schematic diagrams of unmodified lysozyme and lysozyme-$(N3)_n$ (where n = 1). Panel C shows the expected *in cis* conjugated product of lysozyme-$(N3)_1$ reacted with ≡-CLICK-17 (the full length of the conjugated CLICK-17 is show as 'DNA'). To facilitate ESI mass spectrometry identification of this latter product, the DNA component of the protein–DNA conjugate was digested to completion with Nuclease P1, an endonuclease that cleaves DNA into 5'-

deoxyribonucleotide monophosphates. The portion of the appended CLICK-17 DNA expected to be removed by the nuclease is indicated by a red bracket. The resulting residual structure incorporates the 5'-most deoxyribo guanosine residue of the CLICK-17 sequence conjugated to the lysozyme via the triazole and linker atoms, as indicated. Panel d provides the schematics of symbols used for the ESI mass spectrometry data for conjugation of *in cis* catalyzed conjugation of ≡-CLICK-17 DNA with lysozyme-$(N3)_{1-3}$ shown in Figure A14 in appendix A. In this last figure, in addition to low amounts of the starting materials, underivatized lysozyme ('A'), lysozyme-(N3) ('B'), lysozyme-$(N3)_2$ ('C') and lysozyme-$(N3)_3$ ('D'), bands corresponding to five DNA conjugated (following nuclease digestion) species, 'E' to 'I', can be seen, by far the most abundant of which is 'F' [lysozyme-$(N3)_2$•(CLICK-17 digestion residue)$_1$].

2.2.6. Specific nucleotide sequences and foldings are required for CLICK-17 and CLICK-16 catalytic activity

To further confirm that correct folding of CLICK-17 DNA is a key factor for its catalytic competence, we examined the catalytic activity of two other DNA clones from our original SELEX experiment, CLICK-16 and CLICK-20, both with sequences closely related to that of CLICK-17. Second, we tested a number of rationally designed mutants derived from CLICK-17, CLICK-16, and CLICK-20. Third, we subjected the nucleotide sequences of CLICK-17, CLICK-16 and CLICK-20 to the folding algorithm, Mfold, to try and correlate catalytic activity with their predicted folded structures. Figure A15, upper, shows the nucleotide sequences of the SELEX-derived DNA clones CLICK-17, CLICK-16 and CLICK-20, as well of the three mutants, CLICK-17 T24G, CLICK-20 C39G and CLICK-20 G24T. 77-nucleotide long CLICK-16 differs from 79-nt CLICK-17 in a single point mutation and in lacking two adjacent thymines present in CLICK-17. 79-nt CLICK-20 varies from CLICK-17 in having three non-adjacent point mutations. The three further sequences tested restore some of the nucleotide differences between CLICK-17, CLICK-16 and CLICK-20, listed above.

Figure A15, lower, shows that these oligonucleotides are notably different in their ability to utilize either Cu(I) or Cu(II) to catalyze CuAAC *in trans*. Specifically, CLICK-16 is catalytic, though less so than CLICK-17; while CLICK-20, CLICK- 20 C39G and CLICK-20 G24T are inactive under these reaction conditions. These data further emphasize that CLICK-17's catalytic properties are precisely dependent on its nucleotide sequence and

its concomitantly folded structure. The nucleotide sequences of the catalytic CLICK-17 and CLICK-16 as well as the non-catalytic CLICK-20 were subjected to the Mfold program used for predicting the most stably folded structures of single-stranded DNAs[121]. Figure A16 in appendix A shows the thermodynamically most stable predicted folds for the three DNAs. It is interesting to note that the catalytically active CLICK-17 and CLICK-16 share a common fold, whereas the inactive CLICK-20 shows a divergent folded structure.

2.2.7. Investigations into the mode of action of CLICK-17

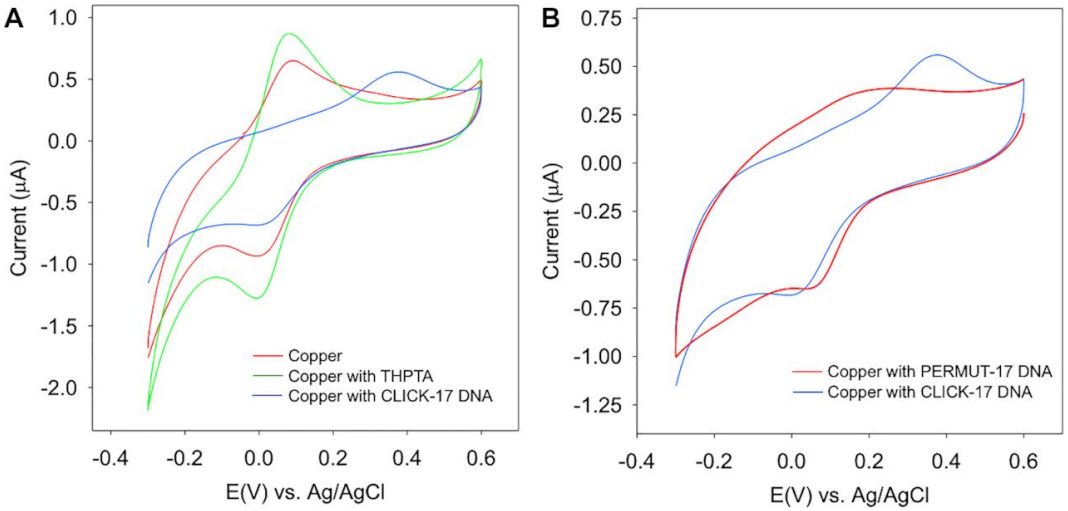

Figure 2.8 Cyclic voltammetry of Cu(II)/Cu(I) with different ligands. (A) cyclic voltammetry of 0.1 mM $CuSO_4$ in HEPES buffer (red); 0.1 mM $CuSO_4$ with 0.5 mM THPTA in HEPES buffer (green); 0.2 mM $CuSO_4$ with folded 0.1 mM CLICK-17 DNA (blue). (B) 0.2 mM $CuSO_4$ with folded 0.1 mM CLICK-17 DNA (blue); and 0.2 mM $CuSO_4$ with folded 0.1 mM PERMUT-17 DNA (red). The initial potential was held at - 0.3 V for 20 sec, and then scanned positively.

The data shown above cumulatively encourage a hypothesis that CLICK-17 is a DNA enzyme with a precise, catalytically active fold, and an active site that offers one or more privileged bindings sites for Cu(II) or Cu(I). It is hypothesized that such a binding site/sites powerfully impacts the redox potential of Cu(II)/Cu(I) in a positive direction, i.e. toward Cu(I). Therefore, CLICK-17 shows catalytic activity (both *in cis* and *in trans*) with added Cu(II) alone, in the absence of any explicit reductant such as ascorbate. Conceivably, one or more Cu(II) ion/ions bound to the active site are then relatively easily

reduced to the CuAAC-capable Cu(I) species not by a classic reductant such as ascorbate, but an available buffer solution component, such as HEPES.

To test, first, the redox potential of copper ion bound to CLICK-17, we carried out cyclic voltammetry (CV) experiments. Figure 2.8 shows the results. The presence of the DNAzyme, CLICK-17, significantly influences the redox property of the Cu(II)/Cu(I) couple in the HEPES buffer. While there are no discernible changes in either the reduction or the oxidation peak with added THPTA, the oxidation peak appears 301 mV more positive when CLICK-17 is introduced to the electrolyte. This corresponds to a ~150 mV shift in the formation potential of Cu(II)/(I), indicative of the much improved stability of Cu(I). In addition, the much larger separation between the oxidation and reduction peaks indicates slower electron-transfer rates between the two forms as well. In comparison, the presence of the folded, non catalytic DNA strand (PERMUT-17) induces no such substantial changes to the CV, i.e., the formal potential shift is not as significant; and, the oxidation peak becomes broad. The above observations are consistent with the binding of Cu(I)/Cu(II) species to the CLICK-17 DNAzyme as being both strong and unique.

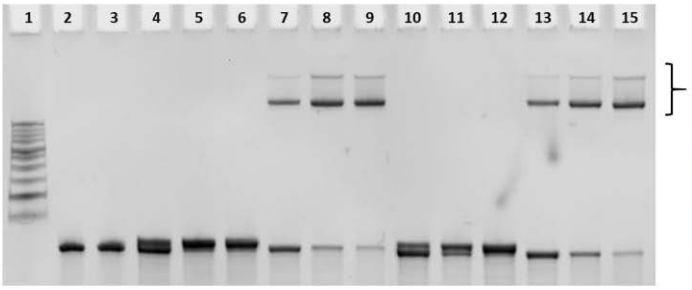

Lane	1	2	3	4	5	6	7	8	9	10	11	12	13	14	15
Cu^{+} (μM)		No RXN	No RXN	-	-	-	-	-	-	0.2	1	5	0.2	1	5
Cu^{2+}(μM)	DNA Ladder			1	5	20	1	5	20	-	-	-	-	-	-
StAV		-	+	-	-	-	+	+	+	-	-	-	+	+	+

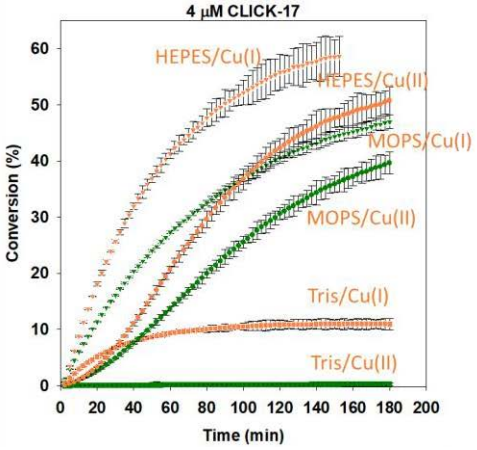

Figure 2.9 Investigation of Cu(II)-induced alkyne homocoupling and the role of buffer components in the generation of Cu(I) for CuAAC by CLICK-17 and ≡-CLICK-17. (A) Investigation of alkyne homocoupling using the *in cis* reaction of ≡-CLICK-17 with azide-biotin. The bracket indicates streptavidin-shifted bands of biotinylated ≡-CLICK-17. The DNA band running just above the unreacted ≡-CLICK-17 represents the triazole product formed between ≡-CLICK-17 and azide-streptavidin. However, no additional DNA band corresponding to a CLICK-17-≡-≡-CLICK-17 product can be seen in any of the lanes. (B) Table of reagents used for the data shown in (A). (C) Investigation of the effectiveness of different buffering agents in promoting the *in trans* catalysis of conjugation between hexynol and azide-coumarin (for all buffer, pH=7.4), catalyzed by CLICK-17, in the presence of either Cu(I) or Cu(II). The error bars represent one standard deviation from the mean obtained from three independent experiments.

An examination of the extant literature for other reported instances of CuAAC observed in the presence of Cu(II) (in the absence of extrinsic reducing reagents) revealed a small number of reports of such events[122]. Unsuspected reductants were, however, ultimately identified in those systems—most notably, excess alkyne, capable of reducing Cu(II) to Cu(I) via alkyne homocoupling[72]; alternatively, a role for alcohol oxidation has also been proposed. To investigate whether alkyne homocoupling might be responsible for our observed CLICK-17/'Cu(II)' catalysis, a close investigation of the *in cis* reaction of ≡-CLICK-17 was made. In the *in cis* reaction, the only alkynes present are the hexynyl moieties covalently appended to CLICK-17 DNA. If alkyne homocoupling were indeed occurring, two ≡-CLICK-17 strands would be joined end-to-end to yield a product ('CLICK-17-≡-≡-CLICK-17') of twice the length and molecular weight of 2 x CLICK-17 (strictly, a molecular weight of [(2 x CLICK-17)-2]), which should show a predictable electrophoretic mobility that should be observable in a denaturing polyacrylamide gel. Figure 2.10, panel A, shows that in the presence of either Cu(II) or Cu(I), only streptavidin retarded bands but no additional DNA band corresponding to a 158-nt DNA product is present in the gel (lanes 4–6). DNA bands of very slightly higher molecular weight, running just above the unmodified ≡-CLICK-17 bands, are discernable with both Cu(II) (lanes 4–6) and Cu(I) (lanes 10–12)—this is the triazole product formed by≡-CLICK-17 with azide-biotin. We have shown that binding to CLICK-17 DNA (but not to PERMUT-17 DNA) dramatically shifts the redox potential of Cu(II)/Cu(I) towards Cu(I). There nevertheless remains the requirement of an electron source for the reduction. It is clear that a powerful reductant such as ascorbate is not required by CLICK-17/Cu(II). Figure 2.9, panel C, shows the effectiveness of different buffer solutions in promoting CLICK-17-catalyzed *in trans* CuAAC by Cu(I) as well as by Cu(II). It is evident that while the Cu(I) reaction works in all three buffers tested (albeit less well in Tris), the CLICK-17/Cu(II) catalysis is promoted by HEPES and MOPS but not at all by Tris. It has been reported that HEPES can act as a mild reductant[123]—thus, it is plausible that it acts as the mild reductant necessary to convert sufficient CLICK-17-bound Cu(II) to the required CuAAC-active Cu(I).

To address a potential role for alcohol oxidation in this catalytic system, a number of our substrates were indeed alcohols (hexynol, propargyl alcohol). Nevertheless, deliberate supplementations of the *in trans* reaction with exogenous methanol (5% and 15%, v/v, respectively) led to less effective CuAAC rather than to rate acceleration (Figure

A17, panel A). Crucially, the sigmoidal shapes of the rate profiles (and unchanging lag-times of 20–30 min) persisted irrespective of the alcohol content of these reactions, discouraging the hypothesis of a determining role for alcohol oxidation in CLICK-17's Cu(II) reaction. We also tested for whether any residual azide anion or a contamination of amines in the commercially synthesized azide substrates that we have used, could act as reductants for CLICK-17's 'Cu(II)' reaction. Figure A17 shows that supplementations of up to 20 μM of either the N3− anion or of methylamine did not change the catalytic rate profiles of CLICK-17, nor did they change the characteristic sigmoidal shapes of these profiles. Given that CLICK-17 is catalytic both *in cis* (as ≡-CLICK-17) and *in trans* and is able to accept structurally divergent azide substrates (azide-biotin, azide-coumarin, and azide-labeled lysozyme) and alkynes (hexynol, propargyl alcohol, Alexa Fluor Dye 546), we attempted to determine a putative K_M value for one of our substrates, hexynol. Figure 2.28 shows the reaction profiles of Cu(I)/CLICK-17-catalyzed CuAAC with a fixed concentration (50 μM) of azide-coumarin and varying concentrations (0.1–20 mM) of hexynol. It was concluded that the K_M for hexynol with respect to CLICK-17 was >20 mM.

2.3. Conclusion

The data reported herein demonstrate that the 79-nt DNA oligonucleotide, CLICK-17, is a bona fide enzyme for the copper-dependent azide-alkyne cycloaddition (CuAAC) reaction. Folded CLICK-17 is a metalloenzyme, able of harness ascorbate-generated Cu(I), as well as added Cu(II) in the absence of ascorbate, with buffer components as likely reductants for CLICK-17 catalyzed CuAAC. Curiously, guanine bases in DNA and RNA are relatively easily oxidized and are ready sources of electrons for such phenomena as the recently discovered intrinsic photoreactivation of cyclobutene thymine dimers within DNA[40,124]. It is therefore conceivable that one or more guanines bases within CLICK-17's sequence may also contribute to the Cu(II) to Cu(I) reduction. This will be the subject of further investigation. We show, using cyclic voltammetry, that complexation of copper ions to CLICK-17 DNA (but not to a sequence-permuted DNA isomer, PERMUT-17) perturbs the Cu(II)/Cu(I) redox potential, by approximately 150 mV relative to that of copper ions in the presence of either HEPES buffer alone or containing THPTA. These data are consistent with folded CLICK-17 DNA (but not folded PERMUT-17 DNA) providing one or more high-affinity and catalytically relevant copper ion binding sites within CLICK-17's active site. CLICK-17 is CuAAC-active with Cu(II) in reaction solutions buffered by the

mildly reducing HEPES and MOPS, but not by Tris. Likely, HEPES and MOPS are sufficiently reducing for the CLICK-17's bound (and redox-potential shifted Cu(II) ion/ions––see above) but not for Cu(II) bound to PERMUT-17 or to THPTA. Above, we also show that neither alkyne homocoupling nor adventitious reduction of Cu(II) to Cu(I) by primary alcohols—two alternative mechanisms invoked for Cu(II)-dependent CuAAC observed in other experimental systems that have been described in the literature, is responsible for the observed Cu(II)-dependent activity of CLICK-17. We do not yet know any details of the ligand environment or environments provided by CLICK-17. CLICK-17 has 79 heterocyclic nucleobases (of which 23 are guanines); and, at pH 7.4, 79 full negative charges. Several studies have examined the preferred copper-binding sites in DNA. Sigel and Sigel[109] have described that the guanine N7 and O6 positions, together with a negatively charged phosphate oxygen, provides a tight multidentate binding site for Cu(II) (with estimated formation constant of $\sim 10^4$ M^{-1}). The binding of Cu(I) to DNA may be stronger yet; association constants of $\sim 10^9$ M^{-1} have been reported[99]. A viable cytosine-Cu(I)-cytosine complex has also been reported in DNA[125]. However, the ligand environment in CLICK-17's active site for binding one or more Cu(II)/Cu(I) ions may be yet more intricate, conceivably involving Cu(I)/Cu(I) or Cu(II)/Cu(I) bimetallic binding sites such as have been discussed in the introduction section.

Future work will focus on generating and studying truncated pieces of CLICK-17 that may be still capable of efficiently catalyzing CuAAC with both Cu(I) and added Cu(II). These, and other studies will help us to fully understand the mechanism of CLICK-17. A major advantage we foresee for the utilization of very low 10–20 μM concentrations of Cu(II) (and not Cu(I) generated in situ by a strong reductant such as ascorbate), is lower production (and lower concomitant damage from) ROS species. Being a macromolecule, the DNAzyme is furthermore likely to act as a superior sacrificial scavenger itself for any level of ROS species that may still be generated.

2.4. Material and Methods

2.4.1. Chemicals

HEPES (Sigma-Aldrich, 99.5% purity, copper $\leqslant$ 5 ppm); $MgCl_2.H_2O$ (Sigma-Aldrich, 99% purity, copper $\leqslant$ 5 ppm); $LiOH \cdot H_2O$ (Sigma-Aldrich, $\geqslant$ 99% purity, copper

$\leqslant$ 5 ppm); sodium ascorbate (Sigma-Aldrich, 98% purity); NaCl (Sigma-Aldrich, 99% purity); KCl (ACP Chemicals, 99%); sodium acetate (Bio Basic, 99% purity); 5-hexyn-1-ol (Sigma-Aldrich, 96% purity); propargyl alcohol (Sigma- Aldrich, 99% purity); 3-azido-7-hydroxycoumarin (AK Scientific 98% purity); azide-PEG3-biotin conjugate (Sigma- Aldrich, purity not specified by the manufacturer); NaOH (Sigma-Aldrich, 99% purity); $CuSO_4$ (Fisher Scientific, 99% purity); Azido-PEG2-NHS ester (BroadPharm, 98% purity); Fluorescein-NHS ester (BroadPharm, 95% purity); AFDye 546 (Click Chemistry Tools, $\geqslant$ 95%); Lysozyme, from chicken egg white (Sigma-Aldrich, $\geqslant$98% purity); Nuclease P1 (NEB, 100,000 Units/mL).

2.4.2. DNA and 3' end-labeling

An 80-deoxynucleotide (80-nt) single-stranded DNA library (5'-GGATCGTCAGTGCATTGAGAN40GGTGGTATCCGCAACGGGTA) was designed to contain a central stretch of 40 randomized deoxynucleotides ('N40'). flanked by two fixed, 20-nt primer binding sequences (Core DNA Services Inc., Calgary, Canada). All other DNAs, modified or unmodified, were from Integrated DNA Technologies (Illinois, USA). Oligonucleotides were size-purified using denaturing gel-electrophoresis, followed by ethanol precipitation(s) and scrupulous 70% aqueous ethanol washes to remove residual urea. The 5'-hexynyl moiety was linked to the 'forward' PCR primer sequence (5'-hexynyl-GGATCGTCAGTGCATTGAGA-3') during automated DNA synthesis. The reverse primer had the sequence: 5'-TACCCGTTGCGGrATACCACC-3' (where 'rA' shows the location of a single ribonucleotide placed within the DNA oligonucleotide). Azide-PEG3-biotin (Sigma)was chosen as a substrate based on its solubility in water and because, following CuAAC, azide-clicked 5'-hexynyl-DNA molecules would be tagged with biotin, enabling their separation from unreacted DNA via binding to streptavidin (Figure 1). For 3'-end radioactive labelling, 50 pmol of a given oligonucleotide was dissolved in 10 mM Li-HEPES·(pH 7.4) buffer and denatured by boiling for 5 min. The cooled DNA was then 3'-32P labeled using a standard protocol for use of Terminal Deoxynucleotidyl Transferase (Thermo Fisher Scientific, Vilnius, Lithuania). 1 µl of [α-^{32}P]-dCTP (Perkin-Elmer) was added, and the reaction mixture was incubated for 1 h at 37 ^{o}C. The 3'-^{32}P labeled oligonucleotide was then size-purified in 8%denaturing gels containing 7M urea.

2.4.3. *In vitro* selection

5 μM CuI was the concentration chosen for the first round of *in vitro* selection, to encourage selection of DNAzymes that worked with ultra-low Cu(I) concentrations or required it not at all. 500 pmol of the DNA library was amplified b a large-scale (20 mL) PCR in order to incorporate the 'forward' 5'-hexynyl primer in one of the two strands. The 'reverse' primer contained an internal riboside nucleotide. 2.5 mL PCR reactions were used for round 2 and for all subsequent rounds of selection. 5'-Hexynyl-labeled single stranded DNA was recovered following NaOH-catalyzed ribonucleotide cleavage of one of the two component strands of the DNA duplexes, and then size-purification of the 5'-hexynyl-modified strand away from the cleaved complementary strand by preparative denaturing polyacrylamide gel electrophoresis. The entirety of the recovered 5'-hexynyl labeled ssDNA pool, doped with a portion of the same strand pool 3'-labeled with ^{32}P using terminal transferase (ThermoFisher Scientific, Vilnius, Lithuania) was used for the first round of *in vitro* selection, with parallel selections being performed with and without added THPTA (25 μM). The 5'-hexynyl labeled ssDNA was first heated to 100 ^{o}C in S buffer (50 mM HEPES, pH 7.4, 300 mM NaCl, 50 mM KCl, 20 mM $MgCl_2$), then cooled down to 22 ^{o}C over a period of 10 min in a thermal cycler. Azide-PEG3-biotin ('azide-biotin') to a final concentration of 2.5 mM was then added, followed by $CuSO_4$ to 5 μM. The CuAAC reaction was initiated at 22 ^{o}C by addition of sodium ascorbate to 2.5 mM. The DNA solution was incubated at 22 ^{o}C in a thermal cycler for 2 h, following which the DNA was ethanol precipitated, washed with 70% ethanol, air-dried, and dissolved in 5 μl of 10 mM HEPES buffer, pH 7.4 containing ~1.9 nmol dissolved streptavidin. The solution was loaded directly onto a denaturing gel (8% acrylamide, 7 M urea), and the streptavidin-retarded DNA bands, visualized by phosphorimagery (Typhoon 9410 Phosphorimager, Amersham Biosciences), were excised from the gel, eluted into TE buffer (10 mM Tris, pH 7.4, 0.1 mM EDTA) and collected by ethanol precipitation. The recovered DNA was PCR amplified, again using one 5'-hexynyl labeled primer and one internal ribonucleotide containing primer, followed by base treatment and gel purification (as above), to generate an enriched pool of 5'-hexynyl labelled ssDNA for next round of *in vitro* selection. Following 25 rounds of selection, the enriched DNA sequences were cloned into Escherichia coli and 40 clones picked for sequencing (Genewiz, Canada). Preliminary CuAAC experiments were done with individual DNA clones (all 5'-hexynyl labeled), and clone CLICK-17, 79-nt long, was picked as a promising catalytic candidate. CLICK-17 had the

nucleotide sequence: 5'-GGATCGTCAGTGCATTGAGATTATTATGCAACTCTATGGGTCCACTCTGTGAATGTGACGGTGGTATCCGCAACGGGTA-3'. A sequence-permuted variant of CLICK-17 DNA, named 'PERMUT-17', was used as a control DNA throughout; PERMUT-17 had the nucleotide sequence: 5'-GGATCGTCAGTGCATTGAGAGACATACATGTTATCGGTATGTTCGAGCTCTATATCTCGTACCCGTTGCGGATACCACC.

2.4.4. *In cis* reactions

51-Hexynyl-CLICK-17 DNA ('≡-CLICK-17') or 51-hexynyl-PERMUT-17 DNA ('≡-PERMUT-17'), either 3'-^{32}P-labeled or not, were denatured and refolded in R buffer (50 mM Li-HEPES, pH 7.4, 20 mM $MgCl_2$) by boiling the solution and cooling down to 22°C, over 10 min, in a thermal cycler. 2.5 mM azide-PEG3-biotin ('azide-biotin') was then added. To start the reaction, a mixture of $CuSO_4$ and sodium ascorbate in 10 mM Li- HEPES, pH 7.4 was added. For Cu(II)-catalyzed reactions, only $CuSO_4$ in 10 mM Li-HEPES, pH 7.4 was added. Following incubation at 22°C in a thermal cycler for the indicated reaction time, the DNA was ethanol precipitated, washed thoroughly with cold 70% ethanol, air-dried, redissolved and treated with streptavidin (2 µl from a 5 mg/mL stock). The resulting solutions were loaded directly onto a denaturing 10% polyacrylamide gel. DNA bands in the gel following electrophoresis were visualized either by phosphorimagery or by ethidium bromide staining followed by fluorescence imagery (fluorescent gel images were recorded with a GENi gel imaging system, Syngene, Frederick, Maryland). For *in cis* reactions of lysozyme-$(N_3)_n$ (see below) with≡-CLICK-17, 1 µM lysozyme-(N_3)n was mixed with 2 µM ≡-CLICK-17 DNA, along with copper salts (or not) with or without ascorbate, as indicated in the text. Reactions were carried out in R buffer, at 22 °C, for 2.5 h. *In trans* reactions: 2 µM DNA oligonucleotides were refolded in R buffer. 50 µM 3-azido-7-hydroxycoumarin ('azide-coumarin', Jena Bioscience,Germany), from a fresh stockmade in dimethylsulfoxide, was then added followed by a mixture of appropriate concentrations of $CuSO_4$ and sodium ascorbate in 10 mM Li-HEPES, pH7.4 (for the Cu(I) reactions). For Cu(II) reactions, $CuSO_4$ alone (and, no ascorbate) in 10 mM Li-HEPES, pH 7.4, was added. The solutions were transferred to the wells of a 384-well Falcon plate (black, flat bottomed, from Corning) and incubated at 22◦C for 5 min. 5-Hexyn-1-ol ('hexynol') or propargyl alcohol was finally added to initiate the reaction. End-point fluorescence readings were

carried out in a fluorescence plate reader (InfiniteM200 Pro, Tecan). Excitation was at 403 nm, and emission was monitored at 480 nm. For *in trans* reaction of lysozyme-(N_3)n (see below) with alkynated Alexa Fluor Dye 546 (≡-AFDye 54) catalyzed by CLICK-17, 20 μM lysozyme-(N_3)n was mixed with 200 μM ≡-AFDye 546, 4 μM folded CLICK-17 DNA, along with copper salts (or not) with or without ascorbate, as indicated in the text. Reactions were carried out in R buffer, at 22 °C, for 2.5 h.

2.4.5. Mass spectrometry

An Agilent 1200 HPLC couple to a Bruker maXis Impact Ultra-High Resolution tandem TOF (UHR-Qq-TOF) mass spectrometer was used. The software used was: Compass 1.5. The ionization mode used was positive electrospray ionization (+ESI), with gas temperature (180 °C);Gas Flow (8 l/min); nebulizer (2 bar); capillary voltage (4200 V); mass range (300–2500 Da). The calibrant used was: Agilent Tune Mix L. For HPLC, the column used was: Zorbax 300SB-C8 particle size 3.5 micron, 50 mm length × 2.1 mm diameter (Agilent Technologies).

2.4.6. Mass spectrometry of *in cis* ≡-CLICK-17 DNA-labeled lysozyme

Mass spectrometry was carried out in a Bruker maXis Impact Quadrupole Time-of-Flight LC/MS System. For unconjugated lysozyme-(N_3)n, 1 mg/mL solution was prepared in ddH_2O, and loaded directly. For ≡-CLICK-17/lysozyme-(N_3)n conjugates, the DNA was first cleaved by Nuclease P1 (New England Biolabs, MA, USA) to leave one guanosine (the 5'-most deoxyguanosine of the CLICK-17 sequence) per conjugated DNA still attached to lysozyme. For mass-spectrometry, *in cis* conjugation of ≡-CLICK- 17 and lysozyme-(N_3)n, 2 μM ≡-CLICK-17 DNA, 2 μM lysozyme-(N_3)n, were reacted together at 22 °C for 1 h in R Buffer supplemented with 4 μM $CuSO_4$ and 100 μM sodium ascorbate. The reaction mixturewas passed through Microcon-10K centrifugal filter to desalt. The concentrated solution was diluted with ddH_2O, supplemented with 1/10 volume of 10×nuclease P1 reaction buffer, and 0.1 μl nuclease P1 per 50 μl reaction. Digestion was carried out at 37 °C for 15 min, and the reaction quenched by heating at 75 °C for 10 min. The resulting solution was cleaned up by passing through a Microcon-10K centrifugal filter.After adjusting the sample volume to make the concentration of protein ~1 mg/mL, samples were analyzed by mass spectrometry.

2.4.7. Cyclic voltammetry

The buffer solution for all CV measurements was: 20 mM HEPES, pH 7.4, and 20 mM $MgCl_2$ (R Buffer). The dissolved DNA was folded as described above. Prior to making CV measurements, $CuSO_4$ was added and rested for 5 min. All samples were degassed with argon. Cyclic voltammetry measurements were carried out in a three-electrode, single chamber glass cell with a CHI 1040A Electrochemical Analyzer (Austin, TX). A platinum wire and an Ag|AgCl|3 M NaCl electrode were used as counter electrode and reference electrode, respectively. A glassy carbon electrode was used as the working electrode. All CV measurements were performed in a Faraday cage at 22 ^{o}C, in R Buffer, which had been subjected to deoxygenation for at least 15 min. The scan rate for all CV measurements was maintained at 50 mV/s.

Chapter 3. DNAzyme-Catalyzed Click Chemistry for Facilitated Immobilization of Redox Functionalities on Self-Assembled Monolayers

Cu(I)-catalyzed azide-alkyne cycloaddition (CuAAC), the representative reaction of modern 'click chemistry', has been broadly employed in organic synthesis, bio-labeling, and surface functionalization. Nevertheless, it has limitations such as posing a dilemma of either using high concentrations of Cu(I) catalyst or suffering from slow kinetics. Herein, we demonstrate that a newly selected DNAzyme (CLICK-17; a 79-nucleotide, catalytic DNA single strand) can rapidly catalyze CuAAC to tether redox functionalities onto an electrode surface using low concentrations of either Cu(I) or Cu (II). Particularly, the CLICK-17 DNAzyme, at μM concentrations, facilitated the covalent immobilization of ethynylferrocene (Fc-C ≡ CH) onto 1-azido-11-undecanethiolate self-assembled monolayers on gold (N3C11S-Au SAMs); as low as 50 μM Cu(I) together with 4 μM DNAzyme was able to complete the coupling reaction within 30 min and the pseudo first-order reaction rate constant is 7 times higher than that using the Cu(I) catalyst alone. It was also remarkable that the CLICK-17 DNAzyme is functional with Cu(II) in the absence of an explicit reductant for the catalyzed surface immobilization of Fc-C≡CH on N3C11S-Au SAMs. [†]

[†] Adapted from: Gan, N.; Liu, K.; Qi, L.; Zhang, G.; Guo, Y.; Sen, D.; Yu, H.-Z. J. Phys. Chem. C 2020, 124 (35), 19083–19090. Copy 2020 American Chemical Society. H. Yu, D. Sen, and Y. Guo supervised the project in all aspects and I have conceived the initial concept. N. Gan performed major parts of the electrochemical experiments; G. Zhang and I repeated some of the electrochemical experiments and I performed all biochemical tests. N. Gan and I prepared the initial draft, D. Sen and H. Yu reviewed and reviewed the manuscript.

3.1. Introduction

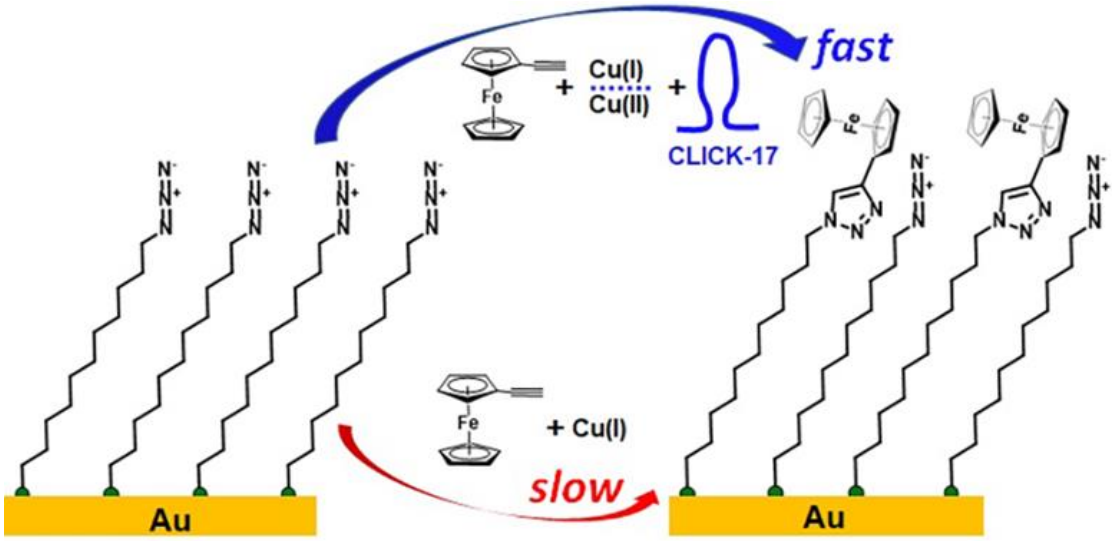

Figure 3.1 Schematic View of the CLICK-17 DNAzyme Catalyzed CuAAC Reaction for the Facilitated Immobilization of Redox Functionalities (Fc-C ≡ CH) on 1-Azido-11-Undecanethiolate Self-Assembled Monolayers on Gold.

Click chemistry, introduced by Sharpless and Meldal almost two decades ago, encompasses a set of powerful, reliable, and selective reactions for the facilitated synthesis of functional new compounds and combinatorial libraries through heteroatom links (C-X-C).[61,62] In practice, the copper(I)-catalyzed azide-alkyne cycloaddition (CuAAC) is regarded as the most representative example of click reactions, as it is simple and efficient in creating new molecular architectures via the formation of triazole bridges from readily available chemical and biochemical reagents. The fact that the CuAAC reaction enables rapid coupling of azide and alkyne-containing moieties leads to its indispensable role in drug development and other diverse molecular biology applications[126].

Click chemistry has been also adapted for the immobilization of redox and biorecognition functionalities on surfaces[127]. Chidsey and co-workers initiated the derivatization of azide terminated self-assembled monolayers (SAMs) on gold with ethynylferrocene (Fc-CCH) and demonstrated the effectiveness of click chemistry to modify a well-defined electrode surface; they also showed that the CuAAC reaction could be adapted as a rapid and straightforward procedure for creating structurally well-defined DNA microarrays via the controlled coupling of acetylene-bearing oligonucleotides and azide functionalized SAMs on gold.[128-130] Gooding and co-workers reported the

functionalization of alkyne-terminated alkyl monolayers on silicon with azides in an aqueous environment,[131] and later demonstrated the remarkable stability of redox-active monolayers formed from the click reaction between 1-methylazidoferrocene and alkyne-terminated SAMs on oxide-free silicon.[132] Recently, Aidello et al. have shown that redox functionalities can be grafted on SiO_2 surfaces via an indirect but efficient procedure comprising salinization followed by a click reaction;[133] Mpeta et al. reported the derivatization of glassy carbon electrode via CuAAC using 4-ethynylbenzyl-substituted cobalt phthalocyanine for applications in electrocatalysis;[134] Mishyn et al. demonstrated the CuAAC-assisted surface functionalization of propargyl-terminated Au/rGO (reduced graphene oxide) electrodes with azidomethylferrocene, which is an essential step in the fabrication of graphene-based sensing platforms.[135]

Building upon the abovementioned progress in the fabrication of functional surfaces, click chemistry has been subsequently explored for applications in the area of quantitative analysis. Qiu and co-workers, reported the determination of Cu(II) electrochemically based on the CuAAC reaction of propargyl-functionalized Fc with azide-terminated SAMs; their differential pulse voltammetry detection of Cu(II) in spiked, diluted yoghurt samples showed both good sensitivity and selectivity.[136] De Leener et al. immobilized a copper calix[6]azacrypt and funnel complex via CuAAC on alkyne-terminated, thiol-modified gold electrodes, which displays a well-defined quasi-reversible CV response and triggers selective and sensitive detection of primary alkylamines at the μM level; and, Dai and coworkers adapted CuAAC to tether cucurbituril and azide co-functionalized graphene oxides to electrode surfaces (modified with alkyne-derivatized oligonucleotides) as an ultrasensitive ‘electro-click’ biosensing platform for protein detection (VEGF165, vascular endothelial growth factor 165, as example).[137] Extended from SAM modified gold electrodes, Galan et al. developed a label-free electrochemical DNA sensor based on poly (3,4-ethylenedioyxthiophene) (PEDOT)-modified electrodes, where acetylene-terminated DNA probes were immobilized on the azido derivatized PEDOT electrodes using click chemistry for the detection of sub-nM Hepatitis C virus sequences;[138] Tang et al. reported the ‘click’ of azide-functionalized and nanogold derivatized PAMAM dendrimers to an alkyne-modified carbon electrode, by which the detection limit of copper was claimed to be improved to 2.8 pM via stripping voltammetry measurements.[139] Conceptually different from SAM-modified gold electrodes for electrochemical sensing, Jiang and co-workers reported their colorimetric method for the

detection of Cu(II) ions using two types (azide- and alkyne-functionalized) of gold nanoparticles in water using click chemistry.[140]

Although the CuAAC reaction has been shown to be convenient and powerful for fabricating functionalized molecular interfaces, as mentioned above, limitations still exist. In particular, it presents a dilemma of either using high concentration of Cu(I) catalyst or suffering from rather slow kinetics; the use of a high concentration of Cu(I) prohibits its application in bioconjugation, as the unstable Cu(I) can produce reactive oxygen species that are highly toxic to most living cells and biological macromolecules[141]. However, at low concentrations of the Cu(I) catalyst, the reaction can take several hours to complete.[128] To date, a number of organic ligands have been found to be beneficial in reducing the concentration of Cu(I) required for the click reaction without unduly jeopardizing the reaction kinetics, such as tris (hydroxypropyltriazolyl) methylamine (THPTA), tris (2-pyridylmethyl)amine, and tris [(1-benzyl-1H-1,2,3- triazol-4-yl)methyl)]amine (TBTA).These ligands were confirmed to accelerates the reaction by stabilizing Cu(I). Unfortunately, most of these organic ligands have poor solubility in water and their concentrations need to be several times higher than the Cu(I) concentration.[128,141]

Derived from *in vitro* selection experiments, out of large, random-sequence DNA pools ('SELEX'), DNAzymes are single-stranded oligonucleotides that fold into intricate 3Dstructures and catalyze a wide range of chemical transformations.[6] To date, DNAzymes have found applications mostly in biosensing and in vivo gene silencing, but have been sparingly used as a tool to catalyze a reaction that is practically useful for downstream applications.[51] To expand the scope of DNAzyme application, we explore the application of the newly selected CLICK-17 DNAzyme as a superior tool for conjugating redox functionalizes onto pre-assembled SAMs. Notably, in the presence of Cu(I) and CLICK-17, at the μM level, the initial reaction rate of solution-based CuAAC was improved by three orders of magnitude relative to the use of Cu(I) alone.

Herein, for this purpose, the catalytic performance of CLICK-17 towards the CuAAC reaction with both Cu(I) and Cu(II) at organized molecular interfaces was evaluated, aiming at facilitating the immobilization of functionalities onto electrode surfaces. In particular, 1-azido-11-undecanethiolate SAMs on gold (N3C11S-Au) was adopted as the trial platform for grafting alkyne-tethered redox molecules (i.e., Fc-C≡CH) in the presence of both Cu ions and CLICK-17 DNAzyme (Figure 3.1).

3.2. Results and Discussion

3.2.1. DNAzyme-Facilitated CuAAC Derivatization of N3C11S-Au with Fc-C≡CH

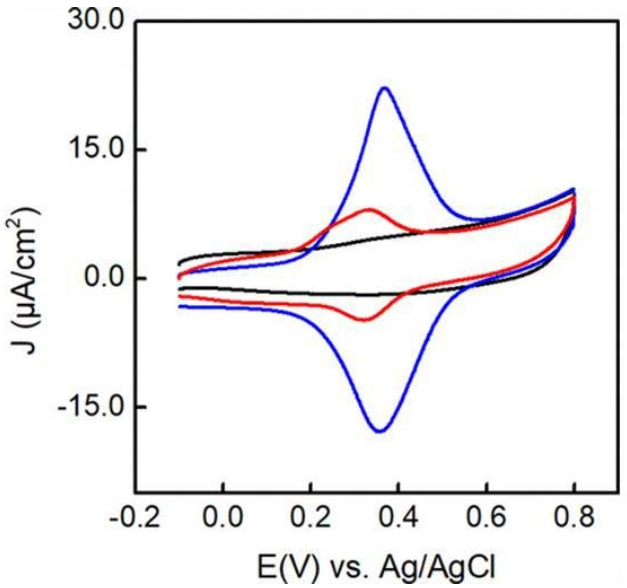

Figure 3.2 Representative CV responses of N3C11S-Au (black curve); N3C11S-Au derivatized with 250 M Fc-C≡CH in the presence of 50 μM Cu(I) for 30 min (red curve); N3C11S-Au treated with 250 μM Fc-C≡CH in the presence of both 50 μM Cu(I) + 4.0 μM CLICK-17 DNAzyme for 30 min (blue curve). The derivatization reaction was performed in 25 mM HEPES buffer at pH 7.4 (2.5 mM AA and 20 mM $MgCl_2$ were added). The supporting electrolyte for CV measurements was 0.1 M $NaClO_4$, and the scan rate (v) was kept at 0.1 V/s. The potential was held at – 0.1 V for 10 sec and then scanned positively.

We have demonstrated that the CLICK-17 DNAzyme can significantly enhance the efficiency of click reactions between both small molecules and biological macromolecules in the presence only μM-Cu(I) or Cu(II) under homogeneous aqueous conditions in last chapter; it was our hope that this novel DNAzyme would work for CuAAC at organized molecular interfaces, e.g., the derivatization of SAMs to introduce various functionalities (e.g., redox centers). Figure 3.2 shows our first set of experiments for such an effort. Whereas no faradic responses are evident for N3C11S-Au (black curve), clear-cut redox peaks corresponding to the oxidation and reduction of Fc/Fc^+ were observed upon reacting with Fc-C≡CH for 30 min in the presence of Cu(I) together with CLICK-17 DNAzyme (blue curve). At the same concentration of Cu(I) (50 μM) but in the absence of the DNAzyme, the CV responses are remarkably different, i.e., much weaker redox peaks

were observed (red curve). To quantitate such a difference, we have determined the surface density of immobilized Fc groups based on Equation 2,

Equation 3.

$$\Gamma_{FC} = Q/nFA$$

where F is the faraday constant, n is the number of electrons of the redox reaction, and A is the real electrode area. With 4.0 μM CLICK-17 added to the derivatization solution, the surface density of Fc ($2.2 \pm 0.3 \times 10^{-10}$ mol/cm^2) achieved in 30 min is more than 4 times higher than that of the reaction without using the DNAzyme ($\Gamma_{Fc} = 0.52 \pm 0.07 \times 10^{-10}$ mol/cm^2). Only with a prolonged reaction time (4 h), we can achieve a similar Γ_{Fc} ($2.1 \pm 0.2 \times 10^{-10}$ mol/cm2) by using Cu(I) alone, which is close to the value reported by Mishyn et al. (2.5×10^{-10} mol/cm^2).[135]

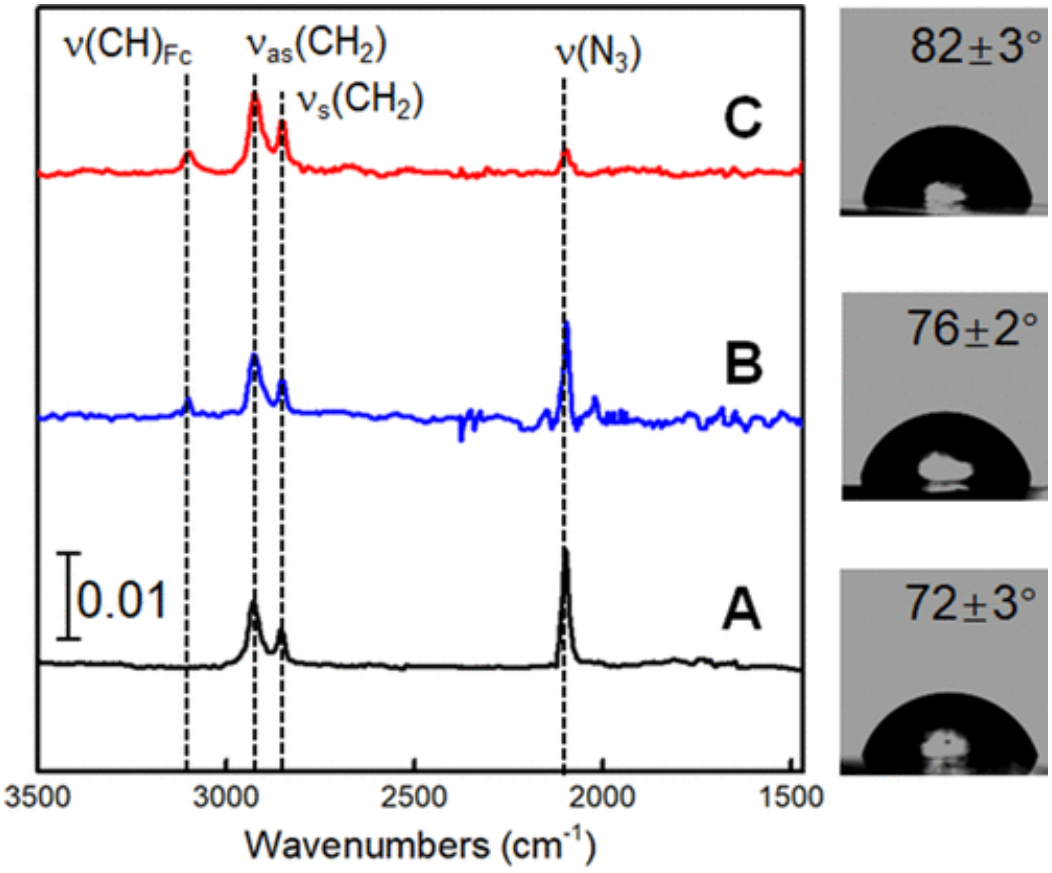

Figure 3.3 Reflection absorption IR spectra of (A) N3C11S-Au (black curve); (B) N3C11S-Au treated with Fc-C≡CH in the presence of the Cu(I) catalyst (blue curve). (C) N3C11S-Au treated with Fc-C≡CH in the presence of both Cu(I) and CLICK-17 DNAzyme (red curve). The insets on the right are photos of water droplets on the corresponding surface with the measured contact angle listed. The detailed buffer conditions for the surface reactions and and CV measurements are the same as those mentioned in Figure 3.2.

In order to further confirm the efficient immobilization of Fc-C≡CH on $N_3C_{11}S$-Au via Cu(I)/CLICK-17 catalyzed CuAAC, reflectance absorbance infrared (IR) spectroscopy and water contact angle measurements were performed. As shown in Figure 3.3, the appearance of a strong peak at 2102 cm^{-1} can be attributed to the stretching vibration of the azide group ($v(N_3)$)[141], and the two signature peaks at 2925 and 2850 cm^{-1}, corresponding to the asymmetric and symmetric vibrations of $-CH_2-$ groups, essentially confirm the formation of $N_3C^{11}S$-Au[142,143]. Upon derivatization with Fc-C≡CH in the presence of the Cu(I) catalyst (Figure 3.2B), we can observe a new peak at 3101 cm^{-1} (characteristic of the stretching vibration of −CH groups of Fc (v(CH)Fc), while the v(N3) peak decreases slightly. More significantly, upon derivatization in the presence of Cu(I) and CLICK-17 DNAzyme, not only does the v(CH)Fc peak become stronger, but also the v(N3) peak is much weaker. For 30 min of reaction, the intensity of the v(N3) peak decreases by ~ 70%, indicating that only ~30% of the azide terminal groups of $N_3C_{11}S$-Au remain unreacted. In contrast, the peaks corresponding to the $-CH_2-$ stretching regions do not vary in either position or intensity, confirming that the orientation of alkyl chains is not disrupted upon the immobilization of Fc groups via CuAAC.

The contact angle measurement is a simple method to monitor the wettability of a solid surface[144]. The right insets in Figure 3.3 show how water contact angles change upon the derivatization of $N_3C_{11}S$-Au with Fc-C≡CH. It was found that the water contact angle of $N_3C_{11}S$-Au only shows a moderate increase from 72 ± 3° to 76 ± 2° upon being catalyzed by Cu(I) only; in contrast, a more significant increase (to 82 ± 3°) was observed when the Cu(I) catalysis is accompanied by CLICK-17 DNAzyme. The water contact angle on the original $N_3C_{11}S$-Au is almost the same as that observed by Chidsey and co-workers (77°)[128]. The slightly higher water contact angles after Fc immobilization are consistent with those (79 to 83°) reported for ferrocenyl alkanethiolate SAMs on gold,[143] due to the fact that Fc groups are less polar than azides. These structural characterization results, together with CV measurements described above, illustrate unambiguously the enhanced CuAAC by CLICK-17 DNAzyme to immobilize redox functionalities on SAMs.

3.2.2. Catalytic performance of DNAzyme

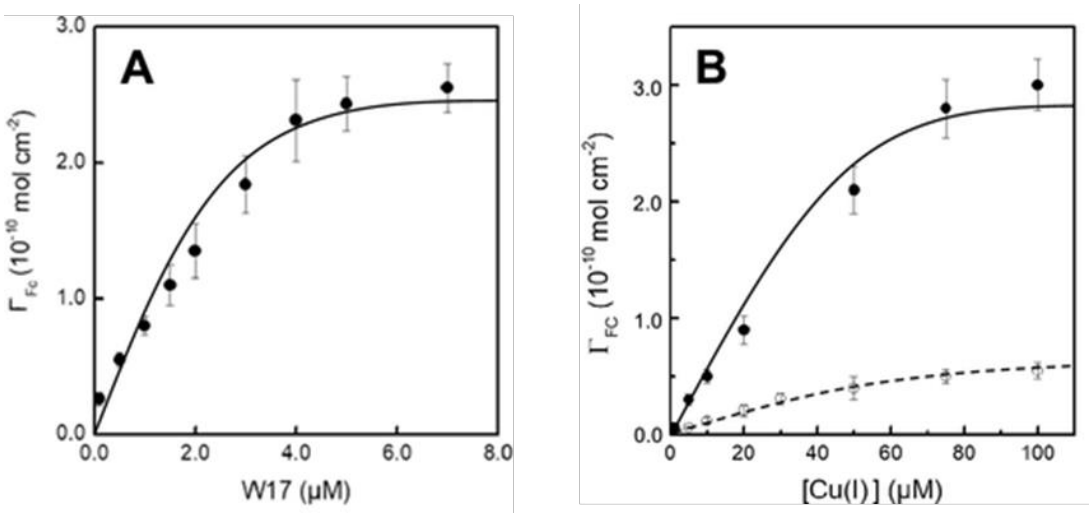

Figure 3.4 Γ_{Fc} as a function of CLICK-17 DNAzyme concentration in the presence of 50 μM Cu(I)A); Γ_{Fc} as a function of Cu(I) concentration with (solid circles) and without (open circles) CLICK-17 DNAzyme (4.0 μM) added B). Other detailed buffer conditions for the surface reactions and CV measurements are the same as those mentioned in Figure 3.2. The reaction time was kept as 30 min. The solid and dashed lines are to guide the eyes only.

One of the advantages of using CLICK-17 DNAzyme is to reduce the amount of Cu(I) catalyst for the CuAAC reaction; we therefore systematically investigated the catalysis performance for immobilizing redox functionalities on surfaces when different amounts of DNAzyme and the Cu(I) catalyst were present. At the same concentration of the Cu(I) catalyst (50 μM) and for the same reaction time (30 min), it was observed in Figure 3.4 that, at the initial stage, the Γ_{Fc} after immobilization increases dramatically with increased concentration of CLICK-17 DNAzyme; after it reaches 4.0 μM, the Γ_{Fc} begins to level off (i.e., no further increase was evident by considering the experimental uncertainties).On the other hand, when the concentration of CLICK-17 DNAzyme was fixed (still at 30 min reaction time), we found that the catalytic efficiency was in fact dictated by the amount of Cu(I) added to the derivatization solution (Figure 3.2B). For comparison, the data obtained without adding CLICK-17 DNAzyme were also plotted, which shows a much lower efficiency (lower Γ_{Fc}) across the entire concentration range of Cu(I) studied. The immediate conclusions that can be derived from these results include: (1) the surface CuAAC reaction can occur with low concentrations of CLICK-17 DNAzyme and Cu(I). When the DNAzyme concentration is fixed at 4 μM, the saturated Cu(I) concentration lies in the 50−75 μM range, somewhat higher than the saturating concentration (20 μM)

observed for the reaction carried out in solution, implying a higher complexity of the CuAAC reaction on surfaces catalyzed by a DNAzyme. (2) The electrochemically determined Γ_{Fc} is a quantitative measure of the catalytic efficiency, based on which we can further investigate the binding/interaction between Cu(I)/CLICK-17 and the reaction precursors. Particularly, the correlation between Γ_{Fc} and CLICK-17 in solution is essentially a binding isotherm, which we can use to extend mechanistic studies of DNAzyme-facilitated catalysis as well as to screen other DNAzyme sequences.

The other potential advantage of using the CLICK-17 DNAzyme to facilitate CuAAC reactions on surfaces is to shorten the reaction time, i.e., we hope that the reaction will become much faster in the presence of CLICK-17 compared with using the Cu(I) catalyst alone. As for the derivatization of N3C11S-Au with Fc-C≡CH, not only the surface density of azide groups (Γazide), but also the concentration of Fc-C≡CH in solution ([Fc-C≡CH]) dictates the reaction rate. It indicates that, this surface CuAAC is, in fact, a second-order reaction, for which the differential rate law is expressed as:

Equation 4

$$Rate = k\Gamma_{azide}[Fc - C \equiv CH]$$

where k is the second order reaction rate constant for the surface CuAAC. The [Fc-C≡CH] is in the μM range (here, 250 μM), which is in great excess with respect to Γ_{azide} (less than 7×10^{-10} mol/cm^2). Therefore, it can be considered to remain constant during the entire reaction process. We can simplify the reaction into a pseudo first-order case, for which

Equation 5

$$Rate = k'\Gamma_{azide} \qquad (1)$$

$$k = k'[Fc - C \equiv CH] \qquad (2)$$

where k' is the pseudo first-order reaction rate constant for the surface CuAAC, and its value can be obtained from the integrated rate law,

Equation 6

$$In\Gamma_{azide}/\Gamma_{azide(0)} = -k't + c$$

Although the initial surface density of azide ($\Gamma_{azide\ (0)}$) and its surface density at any time during the reaction (Γ_{azide}) cannot be directly obtained from the electrochemical measurements, they can be derived from the surface density of Fc groups that are 'clicked' to the surface azide groups in a 1:1 ratio. With the assumption that all azide groups are reacted for tethering Fc groups via CuAAC upon prolonged reaction time, the initial surface density of azide can be approximated to the experimentally achieved maximum surface density of Fc, i.e., $\Gamma_{azide\ (0)} = \Gamma_{Fc\ (max)}$; and the value of Γ_{azide} can be determined from:

Equation 7

$$\Gamma_{azide} = \Gamma_{Fc(max)} - \Gamma_{Fc}$$

In Figure 3.5, we have shown the kinetic data of the CLICK-17 DNAzyme facilitated surface CuAAC and its comparison with the situation using Cu(I) only. It is expected that the value of Γ_{Fc} determined from the CV measurements would rise monotonically with respect to the reaction time in both cases (with and without CLICK-17) (Figure 3.5A), and the initial rise in the case of adding CLICK-17 is much more rapid (solid circles in Figure 4A). As shown in Figure 3.5B, the Γ_{azide} determined based on eq 6 decreases as a function of the reaction time, and a much faster rate of decrease is evident for the situation when CLICK-17 is present (solid circles in Figure 3.5B). More importantly, based on the best linear fits (R2 > 0.99) presented in Figure 3.5C, we were able to obtain the k' values for both cases (i.e., with and without CLICK-17 added to the Cu(I) catalyst). As listed in Table 1, the k' values with and without adding CLICK-17 are (1.4 ± 0.1) × 10^{-3} s^{-1} and (2.0± 0.1) × 10^{-4} s^{-1}, respectively. The former is about 7 times faster than the latter. Chidsey and co-workers reported a k' value of 0.01 s^{-1} for a similar click reaction on surfaces[129], though it was performed with a much higher concentration of the ligand-protected Cu(I) complex as the catalyst (i.e., 400 μM Cu(I)-tris(benzyltriazolylmethyl) amine tetrafluoroboride, Cu(I)(TBTA)-BF4). More importantly, the second-order rate constant determined herein is much faster than the initial rate constant determined for the '*in trans*' reaction between 50 μM azide coumarin and excess amount of hexynol in solution (a lower concentrations of

both Cu(I) and CLICK-17)[145].

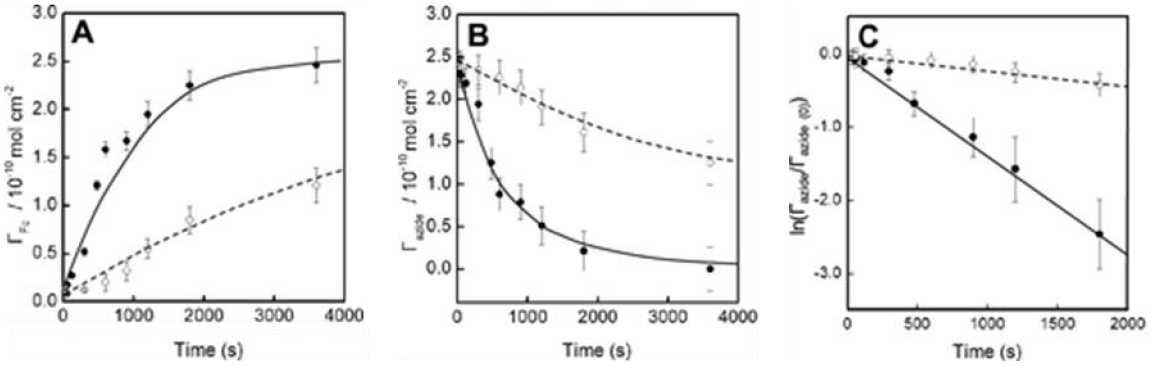

Figure 3.5 Kinetic studies of CLICK-17 DNAzyme-facilitated CuAAC reaction between Fc-C≡CH and N3C11S-Au. Dependence of (A) Γ_{Fc}, (B) Γ_{azide}, and (C) ln (Γ_{azide} / $\Gamma_{azide(0)}$) as a function of the reaction time. The solid circles represent the data obtained in the presence of 4.0 μM CLICK-17 DNAzyme, while the open circles are for the reaction in the presence of 50 μM Cu(I) only. The solid and dashed lines in (A) and (B) are to guide the eyes only, while those in (C) are the best linear fits to the experimental data. Other detailed conditions for the surface reaction and CV measurements are the same as those described in Figure 3.2.

3.2.3. DNAzyme-Facilitated Cu(II) Catalysis for Surface CuAAC and Beyond

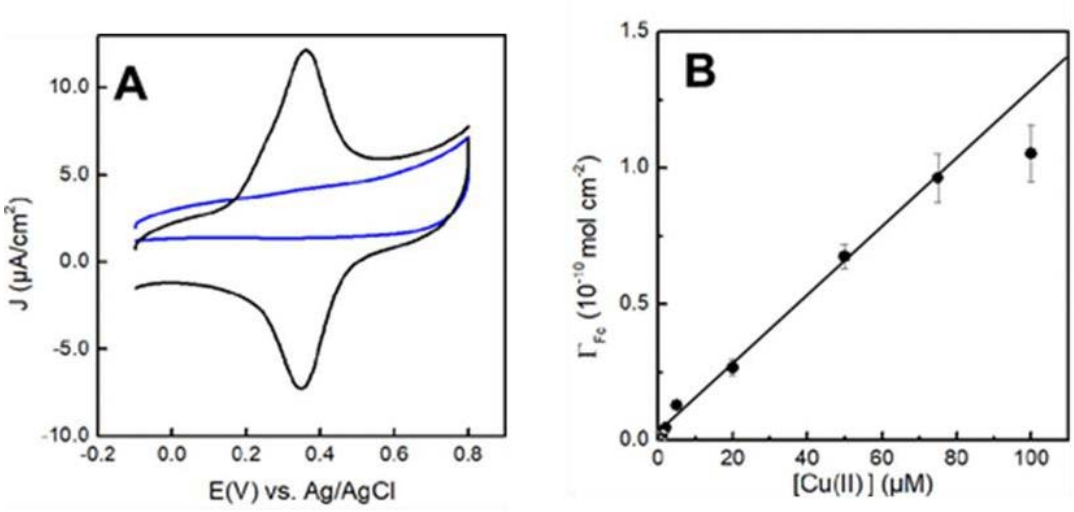

Figure 3.6 (A) CV responses of N3C11S-Au upon reacting with Fc-C≡CH in the presence of 50 μM Cu(II) (blue curve) and 50 μM Cu(II) + 4 μM CLICK-17 DNAzyme (black curve), respectively. (B) Γ_{Fc} as a function of the concentration of Cu(II). Other detailed conditions for the surface reaction and CV measurements are the same as those described in Figure 3.2.

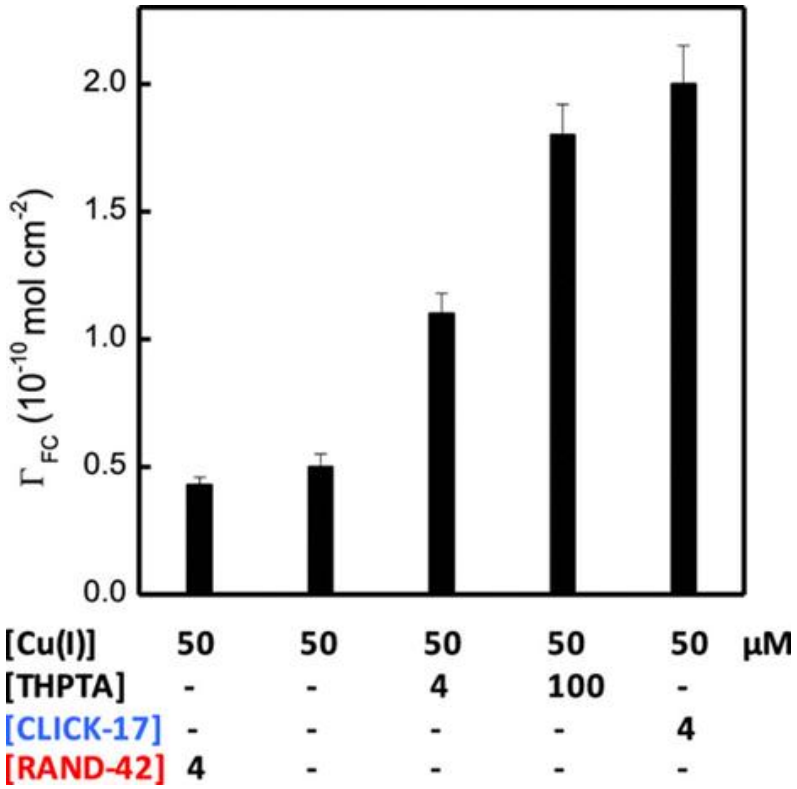

Figure 3.7 Fc surface densities upon derivatization of N3C11S-Au with Fc-C≡CH in the presence of different concentrations of Cu(I), THPTA, CLICK-17 DNAzyme, or a control sequence (RAND-42). Other detailed reaction conditions for the surface reaction and CV measurements are the same as shown in Figure 3.2. The reaction time was kept as 30 min for all these experiments.

We have shown in Chapter 2 that the CLICK-17 DNAzyme can catalyze CuAAC reactions in aqueous solution in the presence of Cu(II), i.e., no explicit reductant was added to convert Cu(II) to Cu(I). Presumably, the catalytic Cu(I) might be generated through the reduction of Cu(II) complexed with CLICK-17 DNAzyme by a mild reductant like HEPES, which is the buffering agent in the reaction mixture, or by consecutive guanines along the absence of a reducing reagent (i.e., AA in this study), we did not observe any change in the CV of the modified electrodes ($N_3C_{11}S$-Au) from representative, capacitive response upon incubation with Fc-C≡CH in the presence of Cu(II) (blue curve in Figure 5A). In contrast, with CLICK-17 DNAzyme added to the derivatization solution and within the same period of reaction time (30 min), we were able to observe a pair of clear-cut redox peaks that correspond to the surface immobilized Fc groups (black curve in Figure 3.6A). The Γ_{Fc} obtained in this case is (1.6 ± 0.5) × 10^{-10} mol/cm^2, which is slightly lower than that (2.1 ± 0.2 × 10^{-10} mol/cm^2) obtained when using the same concentrations of Cu(I) and CLICK-17. With a constant concentration of CLICK-17 DNAzyme, we have

observed a similar dependence of Γ_{Fc} on the concentration of the Cu(II) catalyst (Figure 3.6B). Taking the linear section of the curve as the calibration for Cu(II) quantitation, we can deduce a detection limit (LOD) as low as 1.0 μM. Without any particular enhancement steps or condition optimization. To elucidate the capability of CLICK-17 in facilitating CuAAC on surfaces, we have also compared it with THPTA, the same water soluble CuAAC ligand. In Figure 3.7, it was shown that μM-concentrations of THPTA significantly improve the reaction efficiency, i.e., much higher Γ_{Fc} was obtained in comparison with that of using Cu(I) only. It is remarkable that with as low as 4.0 μM CLICK-17 DNAzyme, we can achieve a Γ_{Fc} value that is almost twice as high as thatwith the same concentration of THPTA, and is 20% higher than that with 100 μM of THPTA. We also tested an unrelated DNA sequence (RAND-42) as the representative of noncatalytic DNA control, which showed no effect on the surface click reaction. In fact, the Γ_{Fc} value obtained is a bit lower than that obtained using 50 μM-concentration of Cu(I) only. A much broader comparison between the DNAzyme facilitated CuAAC on SAMs and other surface click reactions is presented in B1 [128,129,146–151]. It is clear that the use of DNAzyme (CLICK-17) can significantly accelerate the CuAAC reaction at organized molecular interfaces, particularly on functionalized SAMs. The conditions adapted in the present study, not only the ultra-low concentration of Cu(I), but also the capability of using Cu(II) directly, have not been achieved in other studies, either on flat substrates, nanoparticles, or cellulous fibers[152].

It should be noted that, the exact mechanism of this particular DNAzyme enhanced catalytic activity of the CuAAC reaction is yet to be elucidated. As the first study to explore the adaptation of a newly selected DNAzyme for accelerating CuAAC reactions at organized molecular interfaces, multiple aspects of this system deserve further investigation.

3.3. Conclusion

In this study, the fabrication of functionalized surfaces via CuAAC using CLICK-17 DNAzyme together with Cu(I) or Cu(II) has been demonstrated by studying the derivatization of N3C11S-Au with Fc-C≡CH. The catalytic activity of DNAzyme on surface CuAAC can be readily evaluated electrochemically by determining the achieved Fc surface density. Our results confirm that the newly selected CLICK-17 DNAzyme (a 79-nucleotide DNA single strand) can efficiently catalyze CuAAC to tether redox

functionalities on electrode surfaces with ultra-low concentrations (μM) of either Cu(I) or Cu (II). Moreover, the reaction rate constant of the CLICK-17 DNAzyme-facilitated surface CuAAC is 7 times larger than that obtained using Cu(I) alone. In conclusion, the DNAzyme facilitated CuAAC promises a fast, efficient, and reliable means to construct functional molecular interfaces for biosensing and beyond.

3.4. Material and Methods

3.4.1. Chemicals

Fc-C≡CH (97%), 4-(2-hydroxyethyl)-1-piperazineethanesulfonic acid (HEPES), tris(3-hydroxypropyl-triazolylmethyl) (THPTA, 95%), $MgCl_2$, $CuSO_4 \cdot 5H_2O$, and ascorbic acid (AA, 99%) were purchased from Sigma-Aldrich (St. Louis, MO). The CLICK-17 DNAzyme (5′-GGA TCG TCA GTG CAT TGA GAT TAT TAT GCA ACT CTAT GGG TCC ACT CTG TGA ATG TGA CGG TGG TAT CCG CAA CGG GTA-3′) and the control sequence, RAND- 42 (5'-ATC TAC GAA TTC ATC AGG GCT AAA GAG TGC AGA GTT ACT TAG-3′) were synthesized by Integrated DNA Technologies Inc. (Coralville, IA). Ethanol (95%) was obtained from Commercial Alcohols Inc. (Toronto, ON). Gold substrates (glass slides coated first with 5 nm Cr, and then 100 nm Au) were purchased from Evaporated Metal Films Inc. (Ithaca, NY). Deionized water (>18.2 MΩ cm) produced with a Barnstead EASYpure UV/UF compact water system (Dubuque, IA), was used to prepare all aqueous solutions and buffers.

3.4.2. Preparation of N3C11S-Au and the Derivatization with Fc-C≡CH

Precut, small pieces of gold slides (0.7 × 2.5 cm^2) were cleaned by immersing in a Piranha cleaning solution (3,1 mixture of 96% H_2SO_4 and 30% H_2O_2) for 10 min at 95 °C (Caution: the so-called piranha solution is extremely corrosive and reacts violently with organics and should be handled with extreme care) followed by rinsing with a copious amount of deionized water. The gold slides were then immersed in deoxygenated, 0.5 mM N3C11SH/95% ethanol solution for 15 ~ 18 h. After modification, the gold slides were rinsed and sonicated in 95% ethanol, washed with deionized water, and dried with N_2. For the surface click reaction, the gold slides modified with N3C11SH were covered with a 50-μL drop of derivatization buffer (25 mM HEPES, 10% (v/v) ethanol, 250 μM Fc-C≡CH, 20

mM $MgCl_2$, 2.5 mM AA, 10 ~ 100 μM $CuSO_4$, and 4 ~ 100 μM CLICK-17 DNAzyme at pH 7.4) and incubated in a humidity chamber for 30 min unless otherwise noted. After incubation, the gold slides were thoroughly rinsed with deionized water and dried with N2. It should be noted that CLICK-17 DNAzyme was first activated by heating up to 90 °C, and slowly cooling down to room temperature before being added to the derivatization solution to ensure its proper folding

3.4.3. Instrumentation and Characterization.

Water contact angles were determined on a goniometer (AST VCA system, Billerica, MA) using the sessile drop method. Particularly, 2.0 μL of water drop was pipetted on the surface, and the contact angles of both sides of the drop were determined. Typically, water contact angles at three different locations on the same sample and on three independently prepared samples were measured. The reflection adsorption FTIR spectra were obtained using a Nicolet Magna 560 Fourier transform infrared spectrometer (Thermo Nicolet Co., Madison, WI) equipped with a mercury cadmium telluride detector (cooled with liquid nitrogen) and a grazing angle reflectance attachment. The IR spectra of modified gold surfaces were measured with respect to a background spectrum of a freshly cleaned gold slide. CV measurements were performed with a CHI 660D electrochemical workstation and a three-electrode, single chamber cell made of Plexiglas V-series acrylic resin. The working electrode was attached to the opening at the side of the cell (sealed by an O-ring). The real area of the working electrode exposed to the electrolyte solution (0.15 ± 0.01 cm2) was determined from the linear relationship between the measured CV peak current (Ip) of 1.0 mM $K_3Fe(CN)_6$ in 0.1 M KCl solution and the square root of the potential scan rate (v1/2) with the Randles-Sevcik equation. A platinum wire and an Ag | AgCl | 3 M NaCl electrode were used as the counter and reference electrodes, respectively. All electrochemical measurements were performed in 0.1 M NaClO4 under ambient conditions. The electrolyte solution was deoxygenated by bubbling Ar for at least 15 min prior to use, and all measurements were conducted under the protection of Ar.

Chapter 4. Ultrasensitive Detection of Total Copper with an Electrochemical Biosensor Built on the *in cis* Coupling of Hexynyl CLICK-17 DNAzyme with Azido Self-Assembled Monolayers

New methods to detect copper sensitively and specifically are of great practical importance because of its presence in both ecological and biological systems. In this chapter, I am presenting the use of the newly selected DNAzyme, CLICK-17, which catalyzes the azide-alkyne cycloaddition reaction strictly dependent on the presence of copper, as a superior transducer for electrochemical copper quantitation. CLICK-17 offers the following notable advantages as a transducer: it does not require the presence of an unstable reducing agent (detects both Cu(II) and Cu(I) in samples); it offers rapid detection owing to the fast *in cis* coupling kinetics; and, it generates no background because its catalytic activity strictly relies on the presence of copper (signal-on). In our CLICK-17-utilizing electrochemical biosensor, the DNAzyme efficiently couples to a binary 11-azido-1-undecanethiolate/octanethiolate monolayer on gold (N3C11S-/C8S-Au). Such covalently immobilized CLICK-17 DNA is then accurately quantitated by the cyclic voltammetric response of electrostatically bound $[Ru(NH_3)_6]^{3+}$. As the negative charges on the phosphate backbone of surface-bound 79nt-DNA strands are inclusively compensated by the multiply charged redox cations (e.g., $[Ru(NH_3)_6]^{3+}$) at low ionic strength, the electrochemical signal is naturally amplified (~ 30 folds). Without any additional signal amplification steps, the constructed biosensor detects Cu(II) with a LOD of 3.5 nM and Cu(I) with a LOD of 0.8 nM, free of background signals and highly specific against other metal ions. More importantly, we have shown the successful use of this DNAzyme copper sensor to determine copper concentrations in real ore samples from the mining industry, with performance comparable to the gold standard flame atomic absorption spectrophotometry.

---

† Adapted from: Liu, K.; Chen, K. S.; Sen, D.; Yu, H.-Z. Electrochimica Acta 2021, 379, 138125. Copyright 2021 Elsevier Ltd. Yu, H.-Z. supervised the project in all aspects. I conceived the initial concept and performed major parts of the experiments. Chen, K. S helped with some of the surface chemistry and electrochemistry measurements; Liu, K., Sen, D. and Yu, H.-Z. composed the manuscript.

4.1. Introduction

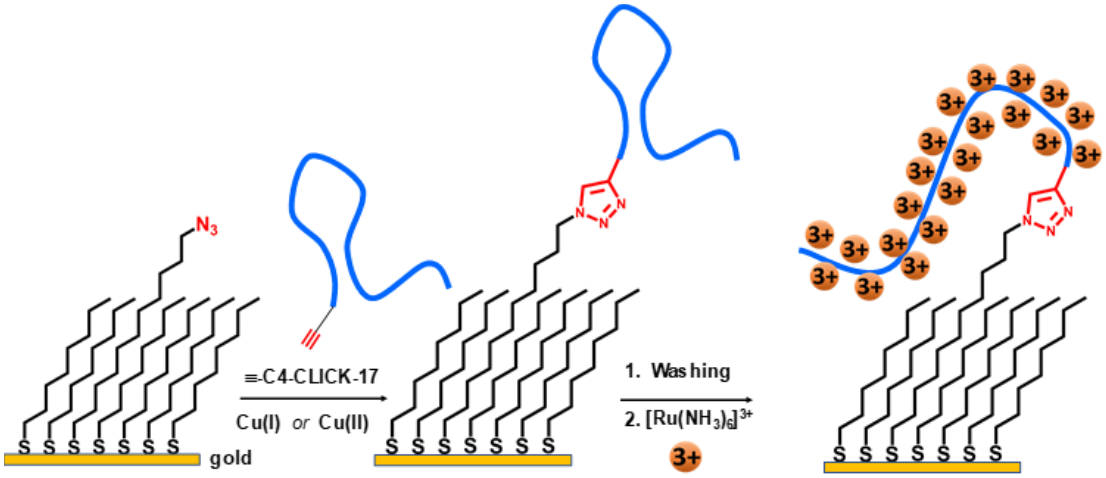

Figure 4.1 Schematic illustration of the electrochemical detection of total copper (Cu(I)/ Cu(II)) based on the *in cis* coupling of hexynyl CLICK-17 DNAzyme (≡-C4-CLICK-17) and binary 11-azido-1-undecanethiolate / 1-octanethiolate self-assembled monolayers on gold (N3C11S-/C8S-Au).

Copper is one of the most important metals present in nature, from many industrial processes to biological systems.[89,153] Traditional instrumental analysis for copper includes atomic absorption spectrometry (AAS), inductively coupled plasma mass spectroscopy (ICP-MS), and inductively coupled plasma atomic emission spectroscopy (ICP-AES).[154,155] Aiming at on-site or point-of-care applications, a number of spectroscopic and electrochemical copper sensing strategies have been recently explored based on various copper-responsive synthetic molecular ligands, functional nucleic acids, or selective reactions.[156–158]

DNAzymes catalyze a broad range of chemical and biochemical processes.[33,36,159] They typically require specific cations for proper structural folding and/or functioning as active sites; several DNAzymes that require copper as an essential co-factor have been isolated, characterized, and adapted for sensor designs.[34,36,93,159] A general strategy is to use a copper-specific DNAzyme as the recognition motif, and a separate module (often, a fluorophore-tagged DNA or a tandem enzyme) to produce signals. As example, Liu and Lu designed a molecular beacon-type sensor that is capable of detecting as low as 35 nM of Cu(I),[160] by adapting the copper-dependent cleaving DNAzyme originally selected by Carmi et al.,[93] and an DNA end-appended fluorophore as the signaling module. Yin et al. fused the same DNAzyme with a G-quadruplex to construct a unimolecular dual-

DNAzyme for directly detecting 1.0 μM (65 ppb) of Cu(II).[161] Quan and co-workers have improved the detection limit to 0.365 nM using graphene as the reaction matrix (functions as both "scaffold" and "quencher" of the same Cu(II)-dependent DNAzyme).[162] Taking advantage of the high affinity of thiol to copper ions, Huang et al. have selected another Cu(II)-dependent DNAzyme (PSCu10, which cleaves an unusual phosphorothioate RNA substrate) and built a sensor for detecting 1.6 nM of Cu(II) without any amplification steps.[163] These sensors may have high background signals due to the nature of the enzymatic reaction, especially for G-quadruplex-hemin systems as hemin (plus H_2O_2) catalyzes the same reaction.[164] Their selectivity can be compromised, as RNA-cleaving DNAzymes are usually activated by more than one type of metal ions, e.g., PSCu10 shows cleavage in the presence of Pb2+ at comparable concentrations at pH 7.5.[163]

In comparison with DNAzyme-enabled platforms described above[162–164] copper-catalyzed aide-alkyne cycloaddition (CuAAC)-based copper sensors are highly sensitive to Cu(I) (i.e., the addition of reducing/stabilizing reagents are mandatory) as such this click reaction strictly requires Cu(I) as the catalyst.[62, 113] Furthermore, the catalytic activity of Cu(I) is poor in water with low turnover cycles at concentrations < 50 μM, and is highly dependent on the metal ion / stabilizing ligand ratio.[67,77] Recently, we have isolated and characterized a new DNAzyme, CLICK-17, which catalyzes CuAAC efficiently with sub-micromolar Cu(I) or Cu(II).[145] We have demonstrated that under multi-turnover conditions, CLICK-17 is efficient at catalyzing the reaction between ethynylferrocene and azido self-assembled monolayers (SAMs) on gold to facilitate the immobilization of 'ideal' electrochemical reporters (ferrocene).[165]

Based on this observation, it is expected that the CLICK-17-catalyzed *in cis* reaction (where the alkyne-tagged DNAzyme itself couples to an azide-derivative and shows ultra-fast kinetics in aqueous solution in a copper concentration-dependent manner) should occur efficiently on surfaces. As depicted in Figure 4.1, such copper-dependent coupling of alkyne-CLICK-17 DNAzyme (a 79nt single-stranded DNA) with azido SAMs on gold can then be readily quantified using electrostatically bound ruthenium hexamine cations (e.g., $[Ru(NH_3)_6]^{3+}$), a protocol that has been established previously.[166] Such a design concept is expected to overcome the limitations of the aforementioned DNAzyme and CuAAC-based copper sensors. Owing to two distinct levels of signal amplification, low background and high specificity, guaranteed by the CLICK-17 DNAzyme, we expect to create a copper sensor that is both highly sensitive and practical.

4.2. Results and Discussion

4.2.1. From *in cis* catalysis of CLICK-17 to electrochemical copper quantitation

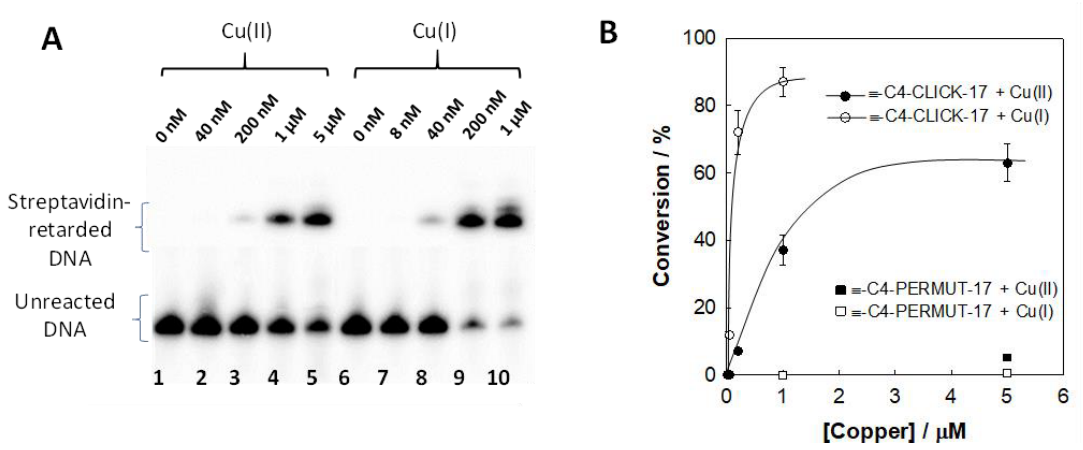

Figure 4.2 Gel electrophoresis assay for quantifying the coupling of ≡-C4-CLICK-17 with azide-PEG3-biotin. (A) 2.0 µM ≡-C4-CLICK-17 reacted with 2 mM azide-PEG3-biotin in the presence of Cu(II) and in situ generated Cu(I) (2.5 mM sodium ascorbate added) at the concentrations listed atop. The reaction time was kept at 30 min for all lanes. (B) plot of conversion percentages of ≡-C4-CLICK-17 and ≡-C4-PERMUT-17 reacted with azide-PEG3-biotin as a function of the copper concentration. The solid lines are to guide the eyes only.

As the performance of DNAzyme biosensors is primarily determined by the catalytic activity of the DNAzyme itself, we first tested the CLICK-17 *in cis* reaction in solution to lay a basis for the electrochemical sensor design. A model system was investigated, in which 5'-hexynyl-labelled DNAzyme was reacted with azide-PEG3-biotin (which possesses a polyethylene glycol linker that structurally resembles an alkanethiol for the surface immobilization, vide infra). The conversion percentage can be readily determined by comparing the band intensity of unreacted DNAzyme in a gel electrophoresis assay relative to that of DNA strands retarded by binding to streptavidin (upon coupling with azide-PEG3-biotin, same method used in chapter 2). Besides the hexynyl CLICK-17 DNAzyme (≡-C4-CLICK-17), we have also tested a control, non-catalytic DNA (≡-C4-PERMUT-17), which is a sequence-permuted version of CLICK-17[145].

Figure 4.2 shows the gel electrophoresis results for the *in cis* coupling of ≡-C4-CLICK-17 with azide-PEG3-biotin. It should be noted that streptavidin was added after the coupling step to amplify the mass/charge differences of the DNA-biotin adduct from the unreacted DNA. It is clear in Fig. 4.2A that the band corresponding to unreacted DNA diminishes with increased concentration of either Cu(I) or Cu(II), while the band for streptavidin-retarded DNA (biotin adducts) becomes much stronger. As shown in Figure 4.2B, the conversion percentage increases with copper concentration to reach 87% in the presence of 1.0 μM of Cu(I), and 63% with 5 μM of Cu(II), respectively. Strikingly, as low as 0.04 μM of Cu(I) or 0.2 μM of Cu(II) is enough to produce a detectable signal in the gel assay within 30 min. More importantly, in the presence of low concentrations (<5.0 μM) of either Cu(II) or Cu(I) (the latter generated in situ and stabilized with a water-soluble chelator, THPTA), no detectable coupling was observed for ≡-C4-PERMUT-17 with azide-PEG3-biotin under the same conditions (Figure 4.2B). Additional control experiments with other DNA sequences (Figure C1) confirmed that the length and sequence of non-catalytic DNA strands do not play any role in the reactivity.

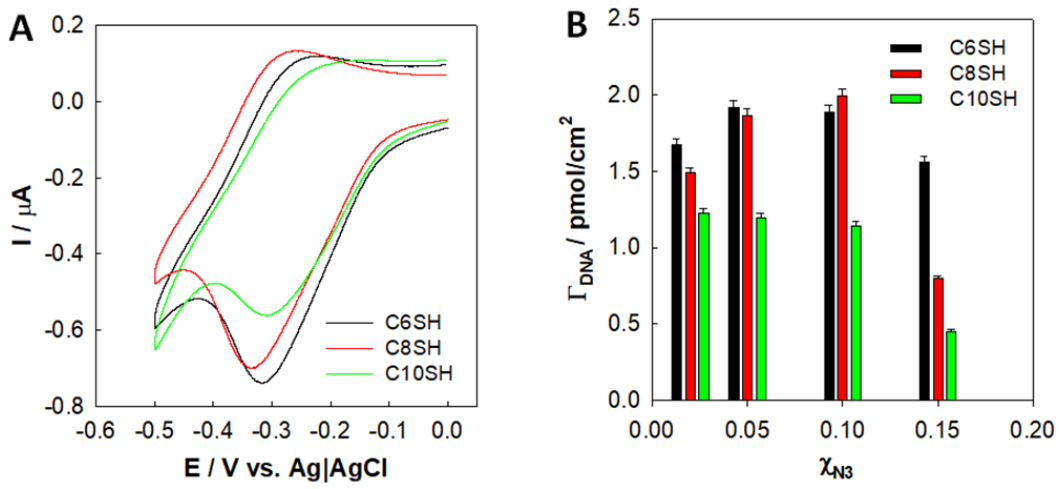

Figure 4.3 Representative CV curves of surface-bound $Ru[NH_3]_6^{3+}$ upon coupling ≡-C4-CLICK-17 DNAzyme on N3C11S-/CnS-Au SAMs (at the same N3C11SH/CnSH mole ratio of 0.05); CVs were measured in 10 mM Tris buffer (pH = 7.4) with 5.0 μM $Ru[NH_3]_6^{3+}$ at a scan rate of 50 mV/s. The potential was held at 0.0 V for 10 sec and then scanned negatively.(B) DNA surface density (Γ_{DNA}) coupled on N3C11S-/CnS-Au SAMs with different mole ratios of N3C11SH (χ_{N3}) in the binary deposition solution. The experimental uncertainties (error bars) in (B) were based on three independently prepared electrodes. A comparative study with the *in trans* reaction,

CLICK-17 catalyzed coupling of ethynylferrocene on N3C11S-/CnS-Au SAMs is presented in the Appendix C (Figure C2).

We have recently confirmed that under *in trans* (multiple turnovers) conditions, CLICK-17 catalyzes the reaction between ethynylferrocene and azide-terminated self-assembled monolayers (SAMs) on gold[145]. We expected that the *in cis* reaction of ≡-C4-CLICK-17 with azide-terminated SAMs on gold would be at least as efficient (Figure 4.1), which motivated us to construct an electrochemical copper sensor built on such a selective surface immobilization protocol. Like proteins, DNAzymes fold into complex 3D structures; the reactivity of a bulky folded DNAzyme towards surface-confined azide functionalities is expected to be sensitive to steric hindrance around the azide functionalities. Thus, careful choice of diluent alkanethiol and its ratio with the azidoalkanethiol is of vital importance when preparing the binary SAMs. No prior reports on crosslinking of a DNAzyme directly on SAMs have been found; however, mixed monolayers of azidoalkanethiol and n-alkanethiol reacted with alkynyl labelled DNA strands, have been exploited to construct DNA monolayers for biosensing[167]. In such cases, the number of DNA strands attached is primarily determined by the azide coverage within the mixed monolayers. Particularly, Barton and co-workers have observed a linear relationship between the DNA surface coverage and mole fraction of azide in the binary monolayer[168].

To construct a mixed monolayer that is able to attach the highest density of CLICK-17, we tested diluent alkanethiol of different lengths (CnSH, n = 6, 8, and 10) at different mole ratios in the deposition solution (χ_{N3} = 0.02, 0.05, 0.10, and 0.15). To quantify the resulting surface attached ≡-C4-CLICK-17, we adapted the established voltammetric procedure that makes use of multiply charged redox cations (e.g., $Ru[NH_3]_6^{3+}$) as the signal readout[166]. Notably, $Ru[NH_3]_6^{3+}$ serves not only as an ideal electrochemical reporter (for its facile and reversible re-dox property) but also as the second level of signal amplification (beyond the intrinsic enzymatic signal amplification by CLICK-17, shown in Figure 4.1). Figure 4.3A shows representative CV curves of 5.0 μM of $Ru[NH_3]_6^{3+}$ upon coupling CLICK-17 onto mixed monolayers with different diluent n-alkanethiols (CnSH, n = 6, 8, and 10) at the same mole ratio of N3C11SH (χ_{N3} = 0.05).

Well-defined peaks for the reduction of $Ru[NH_3]_6^{3+}$ and the re-oxidation of $Ru[NH_3]_6^{2+}$ are observed at 0.31 V (vs. Ag|AgCl) for all three systems (Figure 4.3A). It has been shown that the peak current for the reduction of $Ru[NH_3]_6^{3+}$ to $Ru[NH_3]_6^{2+}$ is proportional to the scan rate, i.e., characteristic of a surface-confined electrochemical

response (Figure C3 in appendix C). The surface density of DNAzyme strands (Γ_{DNA}, mol/cm^2) was calculated using Equation 8:

Equation 8

$$\Gamma_{DNA} = \Gamma_{Ru}\left(\frac{z}{m}\right) = \left(\frac{Q}{nFA}\right)\left(\frac{z}{m}\right)$$

where Q is the charge obtained by integration of the reduction peak, n is the number of electrons in the reaction, F is the Faraday constant, A is the area of the working electrode, m is the number of nucleotides in the DNA, and z is the charge of the redox cations.

As shown in Figure 4.3B, the Γ_{DNA} value is apparently not proportional to the χ_{N3} in the deposition solution. It is also evident that with C8SH or C6SH as the diluting thiol, we can achieve much higher DNA surface density than C10SH; the highest surface density was obtained at a mole fraction of χ_{N3} = 0.05~0.10 for both C6SH and C8SH. When the χ_{N3} increased to 0.15, for all three diluent alkanethiols tested, the DNA attachment was significantly lowered. This is different from the situation of unstructured alkynyl-modified DNA reacting with mixed azide monolayers, as mentioned above.[168] The other important finding is the relatively small standard divisions (as represented by the errors in Fig. 4.3B), which confirms the reproducibility the formation of stable Azido SAMs, the coupling of ≡-C4-CLICK-17, and, in turn, the sensing performance for copper (replicate CVs are presented in Figure C4 in appendix C).

The fact that binary SAMs with low Γ_{N3} (χ_{N3} = 0.05-0.10), react with CLICK-17 much more efficiently than those with higher χ_{N3} (e.g., 0.15) is likely due to the restricted accessibility of azide for DNAzymes. While a linear relationship between Γ_{N3} and χ_{N3} has been confirmed (Figure C2 in appendix C), in the binary SAMs, azidoalkanethiols may form clusters or densely packed domains more so when its mole fraction is high. This issue is also affected by the length of diluent alkanethiols in the binary SAMs.

The efficient *in cis* coupling of ≡-C4-CLICK-17 DNAzyme to the binary N3C11S-/C8S-Au SAMs was also confirmed with other structural characterization techniques. For example, the water contact angle measured for N3C11S-/C8S-Au SAMs (χ_{N3} = 0.05) is 101 ± 3^o, this is much higher than bare gold (<30^o), showing that the surface wettability is dominated by the hydrophobic n-alkanethiols. After coupling the DNAzyme, the water

contact angle decreases to 66 ± 2°, indicating that the surface becomes more hydrophilic owing to the ionic nature of DNA strands (Figure C5 in appendix C).

Although the achieved DNA surface density when using C8SH for dilution is about 5% higher than with C6SH, the mole ratio of N3C11SH in the binary SAMs with C8SH is only half of that with C6SH (Fig. 4.3B). Therefore, we chose C8SH and χ_{N3} = 0.05 for constructing the copper sensor. We also confirmed the specificity of the reaction between ≡-C4-CLICK-17 and the mixed SAMs on gold, as the control strand (≡-C4-PERMUT-17) did not produce any detectable peaks in the presence of 5.0 μM of either Cu(II) or Cu(I) (CVs presented in Figure C6 in appendix C).

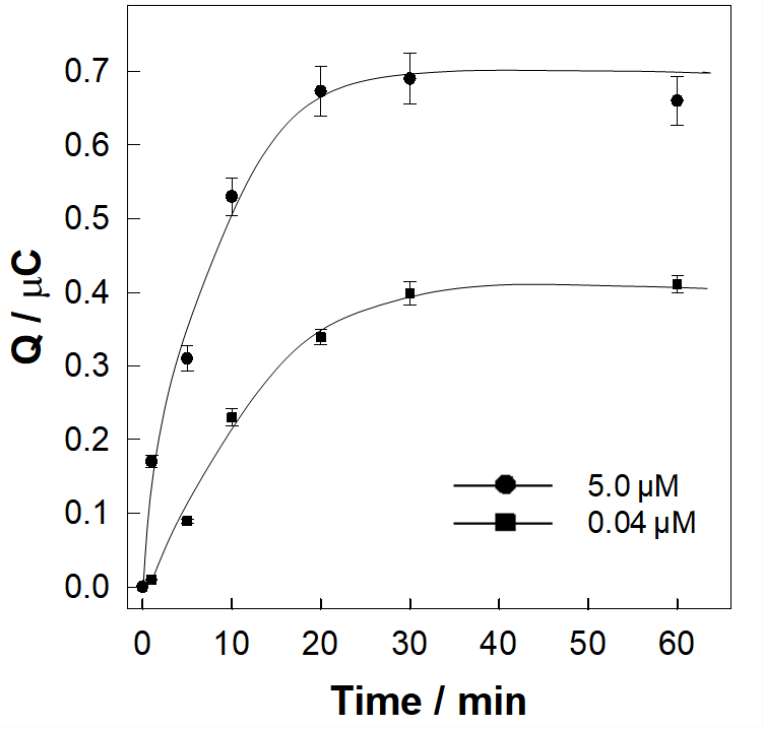

Figure 4.4 Time dependence of the *in cis* reaction between ≡-C4-CLICK-17 with binary N3C11S-/C8S-Au SAMs in the presence of Cu(II) of 5.0 μM (solid circle) and 0.04 μM (solid squares). All data are based on three independent replicates, and the solid lines are to guide the eyes only. The original CV scans are presented in Figure C7 in appendix C.

Another important factor we should consider is how long it takes to obtain an equilibrated (or stable) sensing signal (i.e., the surface coupling kinetics). Often, sensor designs involve enzymatic processes requires quenching steps to terminate the reaction such that quantifiable signals can be obtained [169]. In fact, this procedure can be a source of uncertainty and inaccuracy. In our previous study, we showed that different

concentrations of copper (both Cu(I) and Cu(II)) catalyze the reaction to 'equilibrate' at different final conversion percentages[145]. This is possibly due to the catalytic Cu(I) species being deactivated via complex processes after catalyzing a certain number of conversions. Such a phenomenon was also observed previously by Rodionov et al. in a ligand-free reaction system[67]. As a practical matter, this feature would make quenching steps non-essential, since after the reaction proceeds to 'equilibrium', a stable sensing signal could be read without the need to terminate the reaction. As expected, the *in cis* reaction of hexynyl CLICK-17 with binary SAMs on gold behaves as predicted (Figure 4.4). In the presence of 0.04 μM and 5.0 μM Cu(II), the initial, exponentially rising signals (integrated charge of surface-bound $Ru(NH_3)_6^{3+}$) reach their respective 'plateaus' with different (but stable) final Q values (0.69±0.02 μC and 0.39±0.01 μC, respectively). The time needed in either case for obtaining the 'stabilized' signal is ~ 30 min, which meets the needs.

4.2.2. Sensitivity and selectivity of the CLICK-17-based electrochemical copper Sensor

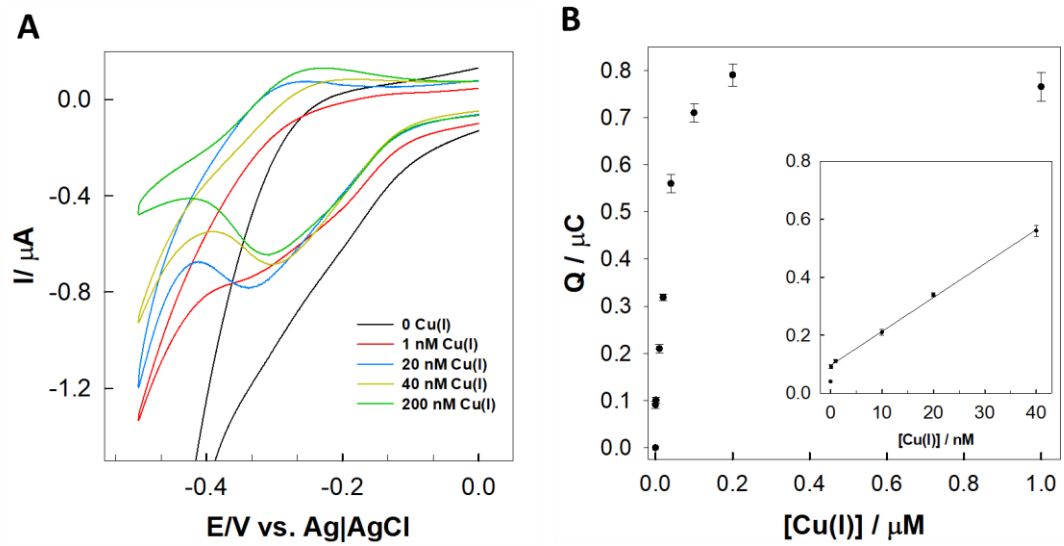

Figure 4.5 (A) Representative CVs of surface-bound Ru[NH3]63+ upon coupling ≡-C4-CLICK-17 DNAzyme on binary N3C11S-/C8S-Au in the presence of Cu(I) of indicated concentrations; the CVs were performed in 10 mM Tris (pH = 7.4) with 5.0 μM $Ru[NH_3]_6^{3+}$ at a scan rate of 50 mV/s. The potential was held at 0.0 V for 10 sec and then scanned negatively. (B) Plot of the integrated charge of surface-confined $Ru[NH_3]_6^{3+}$ (Q) versus the concentration of Cu(I) in the coupling reaction. The dash line is to guide the eyes only. The inset shows the linear response range; the solid line shows the best fit to the experimental data, from which the limit of detection (LOD) was determined. All data presented in (B) were based on at least three independent replicates.

With the sensing principle confirmed and conditions optimized, we proceeded with the quantitation of copper in standard buffer solutions. Figure 4.5A shows representative CV curves for surface-confined $Ru[NH_3]_6^{3+}$ upon coupling ≡-C4-CLICK-17 on binary N3C11S-/C8S-Au SAMs in the presence of different concentrations of Cu(I). Clear-cut redox peaks were observed even with as low as 1.0 nM of Cu(I) present for the coupling reaction, which in turn allowed accurate determination of the charge for the DNA surface-confined, electrostatically bound $Ru[NH^3]_6^{3+}$. We also note that the higher the concentration of Cu(I) in the coupling reaction, the smaller the capacitive charging current was observed (except for copper concentrations that were close to each other). This indicates that the electrode surface was increasingly covered with more DNA strands. No discernible redox peaks were observed in the absence of Cu(I) (i.e., [Cu(I)] = 0, black curve in Figure 4.5A), showing that the DNA attachment is strictly copper dependent. The extremely low background observed indicated that the 'click reaction' on the binary SAMs does not occur without addition of the Cu(I) catalyst. It is significant for a sensor that no baseline correction is needed. We plotted the integrated charge of the surface-confined $Ru[NH_3]_6^{3+}$ (Q) versus the concentration of Cu(I) in the solution (Figure 4.5B). In the Cu(I) concentration range of 0.1 nM-200 nM, the Q value increased monotonically. A satisfactory linearity was found between 0.1 nM - 40 nM Cu(I) (inset of Figure 4.5B); based on the best fit to the experimental data, the limit of detection (LOD) for Cu(I) was

determined to be 0.8 ± 0.1 nM.

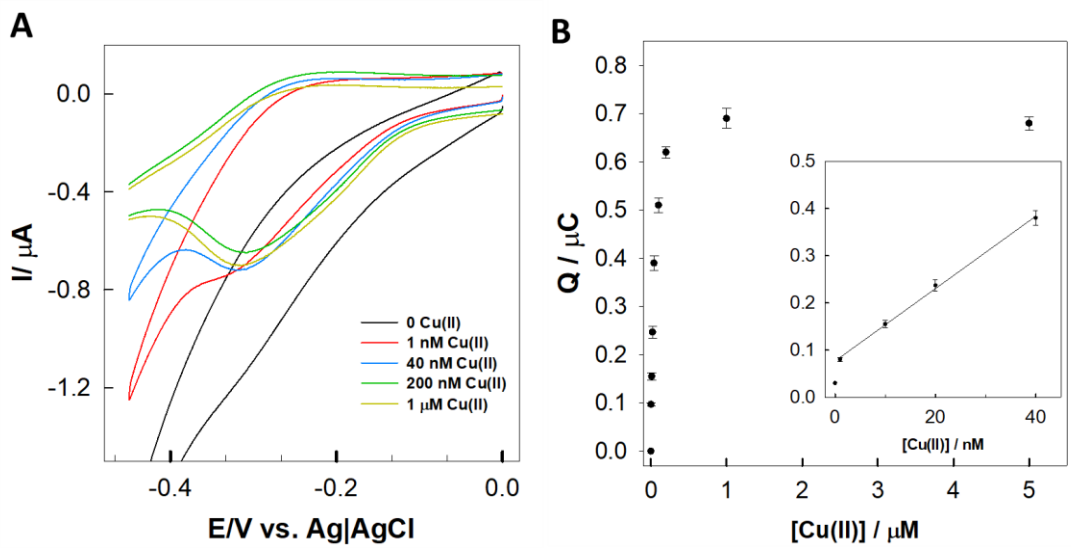

Figure 4.6 (A) Representative CVs of surface-bound $Ru[NH_3]_6^{3+}$ upon coupling ≡-C4-CLICK-17 DNAzyme on binary N3C11S-/C8S-Au in the presence of Cu(II) of listed concentrations; the measurements were performed in 10 mM Tris (pH = 7.4) with 5.0 μM $Ru[NH_3]_6^{3+}$ at a scan rate of 50 mV/s. The potential was held at 0.0 V for 10 sec and then scanned negatively. (B) Plot of the integrated charge of the surface-confined $Ru[NH_3]_6^{3+}$ versus the concentration of Cu(II) in the coupling reaction. The dash line is to guide the eyes only. The inset shows the linear response range, and the solid line is the best to the experimental data, from which the LOD for Cu(II) was determined. The uncertainties presented in (B) were based on at least three independent replicates.

We further tested for the Cu(II)-dependence of the developed CLICK-17-based electrochemical sensor. As shown in Figure 4.6A, the CV curves also showed clear-cut redox peaks for a wide range of Cu(II) concentrations, which now corresponded to surface-bound $Ru[NH_3]_6^{3+}$ enabled by Cu(II)-catalyzed coupling of ≡-C4-CLICK-17 on binary N3C11S-/C8S-Au SAMs (i.e., no reducing reagents were added to the reaction). While we were not able to detect measurable signals in the absence of Cu(II), with increased Cu(II) concentrations from 1.0 nM to 1.0 μM, the redox peaks became more and more pronounced. Figure 4.10B shows the highly sensitive response of the integrated charge of $Ru[NH_3]_6^{3+}$ (Q) at low Cu(II) concentration, a dependence that saturated at or

above 1 μM. The best linear fit to the experimental data between 1.0 nM - 40 nM of Cu(II) (inset of Figure 4.6B), yields a LOD of 3.5 ± 0.4 nM for the direct quantitation of Cu(II).

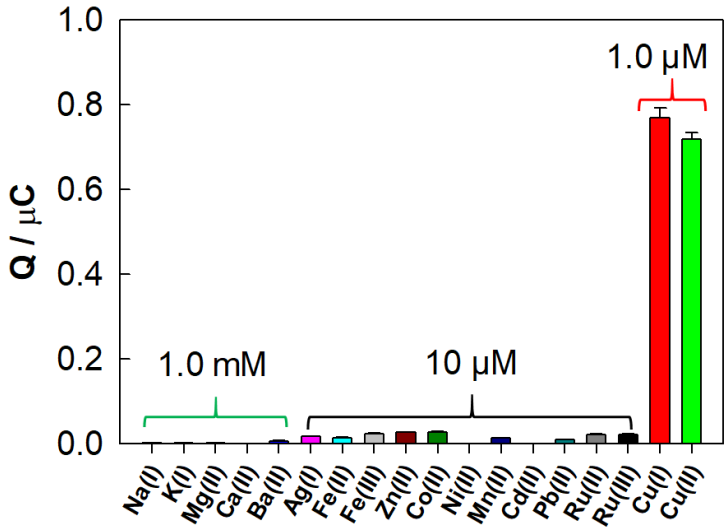

Figure 4.7 Selectivity test of the ≡-C4-CLICK-17 DNAzyme electrochemical sensor for total copper detection. Integrated charge of surface-confined $Ru[NH_3]_6^{3+}$ (Q) upon treating the binary N3C11S-/C8S-Au SAMs with ≡-C4-CLIKC-17 in the presence of different metal ions.

Specificity is of vital importance in metal ion sensing, particularly since DNA, as a polyanion polymer, is known to interact with metal ions through its negatively charged backbone and its nucleobases in some cases[103]. The present CLICK-17-based copper sensor is, nonetheless, highly specific to copper (depicted in Figure 4.7). Out of all metal ions, only certain Ag(I) and Ru(II) complexes have been reported to catalyze the alkyne-azide cycloaddition, and that, too, mostly in organic solvents[170–172]. Along with Ag(I) and Ru(II), we tested 9 other cations at much higher concentration (at least 10 μM) than the saturation concentrations for Cu(I) and Cu(II) (1.0 μM). In fact, Na^+, K^+, Ca^{2+} Mg^{2+} and Ba^{2+} were tested at 1.0 mM, since these are metal ions generally present at high concentrations in many situations. As shown in Figure 4.7, out of all the tested metal ions, only Cu(II) and Cu(I) were able to generate distinct signals, while all the other tested metal cations produced negligible responses.

4.2.3. Industrial Sample Testing and the AAS Validation

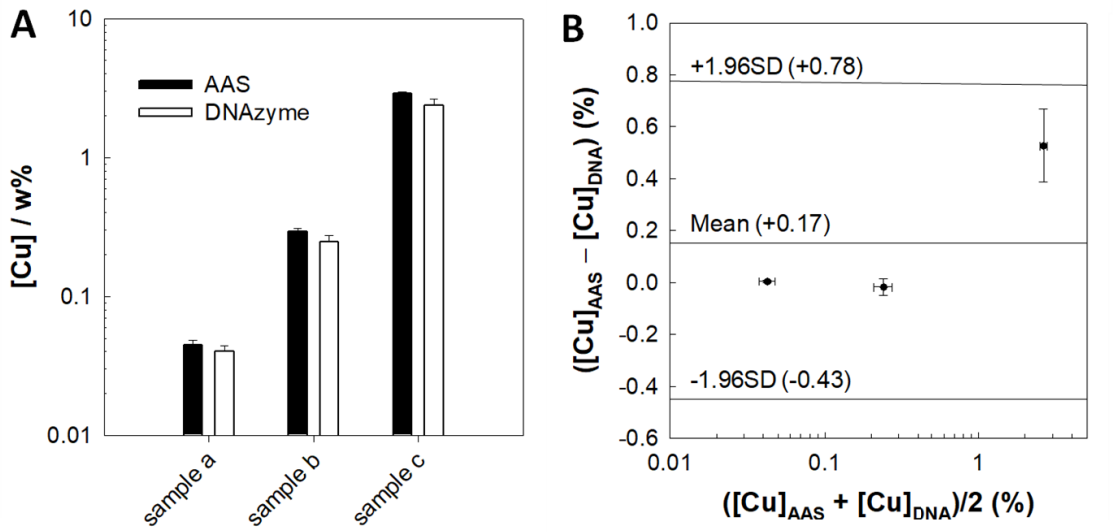

Figure 4.8 (A) Comparison of determined copper concentrations (w%) for three independent ore samples using AAS (black bars) and the CLICK-17 sensor (white bars); (B) Bland-Altman plot based on the data presented in (A).

To further verify the applicability and robustness of the CLICK-17 electrochemical copper sensor, we conducted tests on complex ore extracts. In the mining industry, the abundance of copper in ores needs to be measured routinely, which is performed primarily using the gold standard of flame atomic absorption spectrometry (AAS) at centralized facilities[173]. Besides copper, the ore samples often contain iron, lead, silver, gold, silicate, sulfur, carbon, and other trace amounts of elements. Despite such sample complexity, we decided to test if the present CLICK-17 copper sensor would be able to determine copper concentrations in these samples accurately. We determined copper weight percent (w%) in three different ore samples (S1, S2, and S3) and compared our data side-by-side with the data obtained from AAS measurements (Figure 4.8A). While the abundance of copper was quite different in the three ores examined, the AAS and the new CLICK-17 electrochemical sensor data (representative CV curves are shown in Figure C 8 in appendix C) agreed with each other remarkably well, within the experimental uncertainties. The Bland-Altman plot shown in Fig. 4.8B further validates the agreement between the CLICK-17-electrochemical sensor and AAS.

The successful determination of copper in complex extracts of ore samples confirms that the CLICK-17 electrochemical copper sensor is truly ‘immune’ to interference

from other metal ions and contaminants within a complex industrial sample. Likely, the influence of potential interferences can be further minimized in the CLICK-17 sensor by using large dilution factors, and these are in- deed feasible (and, sometimes required) with this sensor. Given the success of the CLICK-17 copper sensor for the determination of copper in true industrial samples, we strongly believe that it should find convenient applications in point-of-care detection of copper in biological samples (often complex and containing mixtures of several types of macromolecules), for instance, monitoring accumulated copper levels in the brain tissue of patients with Alzheimer's disease.[92]

As described above, our CLICK-17 copper sensor is responsive to both Cu(II) and Cu(I), with Cu(II) being more application relevant owing to the instability of Cu(I) in aqueous solutions. However, the Cu(I) responsive feature is potentially useful for samples containing reducing agents. The test can be done within an hour (30 min reaction, 20 min preparation of the electrochemical cell and 10 min for measurements and data processing), and the entire process can be carried out on benchtop under ambient conditions using conventional electrochemical instruments and accessories. In fact, the present CLICK-17 copper sensor is one the most sensitive DNAzyme-based copper biosensors (a detailed comparison is presented in Table C1).. It is, however, the simplicity and robustness made it particularly suitable for real-life applications.

In its multi-role sensor design, the CLICK-17 DNA functions as an enzymatic (-self) substrate, the copper recognizing motif, and at the same time the signal generating module as well as signal amplifier (the last by virtue of electrostatically binding to it- self multiple redox cations, which serve as the electrochemical reporter). The dramatically simplified design of the electrochemical sensor makes the whole system highly robust. Previously reported highly sensitive copper sensors, by contrast, required complex signal amplification steps.[162] Inevitably, large uncertainty and problematic reproducibility are matters of concern for sensing designs that incorporate multiple steps of reactions and/or incubations. The present CLICK-17 copper sensor, indeed, serves as a pioneering example of how selective sensing of metal ions can be done with a simple, one-step *in cis* catalytic reaction (Figure 4.1), yet offer both high sensitivity and selectivity. We expect the present sensor design to be extendable to the detection of other metal ions that uniquely

catalyze specific crosslinking reactions, and possibly for the detection of many different metallic or bioorganic analytes.

4.3. Conclusion

Based on a pioneering multi-role biosensor design strategy, we have presented a label-free, quenching-free, and background-less electrochemical copper sensor built upon the *in cis* reaction of a catalytic DNA (≡-C4-CLICK-17) with binary N3C11S-/C8S-Au SAMs. This sensor is responsive to both Cu(I) and Cu(II), both within large concentration ranges (0.1 nM–1 μM) and with impressive LODs (0.8 nM and 3.5 nM for Cu(I) and Cu(II), respectively). The measurement can be successively completed within an hour for both Cu(II) and Cu(I) in an add-and-wait manner. The simplicity and the unprecedented multi-role design strategy for the construction and testing of this DNAzyme-based electrochemical sensor exhibits its ease of use, rapidity, and robustness. We have validated its applicability and reproductivity by the successful determination of copper content in real industrial samples. We envision that this CLICK- 17 electrochemical copper sensor will find applications in point-of- care determinations of copper in biological samples, and its unique, multi-role design strategy should be adaptable for sensing many other important analytes.

4.4. Material and methods

4.4.1. Materials and reagents

11-azido-1-undecanethiol (>95%, N3C11SH) was purchased from ProChimia Surfaces Sp. Z. o.o. (Gdynia, Poland); [α-32P]-dCTP labelling kit was purchased from Perkin-Elmer (Hebron, KY); 1-hexanethiol (>97%, C6SH), 1-octanethiol (>97%, C8SH), 1-decanethiol (>97%, C10SH), azide-PEG3-biotin conjugate, sodium ascorbate (98%), hexaammineruthenium (III) chloride (98%, $Ru(NH_3)_6Cl_3$), formamide (≥ 99.5%), potassium chloride (KCl), and all other common salts were purchased from Sigma-Aldrich (St. Louis, MO). Ethanol (95%) was obtained from Commercial Alcohols (Toronto, ON). All chemicals were of ACS-reagent grade and used as received. All DNA strands were purchased from Integrated DNA Technologies (Coralville, IA), which were purified via 7% denaturing PAGE and ethanol precipitation before use. The CLICK-17 DNAzyme has the

nucleotide sequence: 5'-GGATCGTCAGTGCATTGAGATTATTATGCAACTCTATGGGTCCACTCTGTGAATGTGACGGTGGTATCCGCAACGGGTA-3'; the PERMUT-17 DNA has the nucleotide sequence: 5'-GGATCGTCAGTGCATTGAGAGACATACATGTTATCGGTATGTTCGAGCTCT ATA TCTCGTACCCGTTGCGGATACCACC-3'. Gold slides (regular glass slides coated with 5 nm Cr and 100 nm Au) were purchased from Evaporated Metal Films (EMF) Inc. (Ithaca, NY). Deionized water (>18.2 MΩ·cm) was produced with a Barnstead EasyPure UV/UF compact water system (Dubuque, IA).

4.4.2. DNA refolding and coupling with azide-PEG3-biotin

All DNA strands were refolded as previously reported prior to the coupling reactions. Briefly, the DNA in 20 mM HEPES buffer (pH 7.4) was heat-denatured at 100° C for 5 min, then cooled gradually to room temperature over 10 min on a thermal cycler. $MgCl_2$ to a final concentration of 20 mM was then added, followed by the addition of $CuSO_4$ to the designated concentrations. Such a mixture was used directly for the Cu(II)-catalyzed coupling reactions. For the Cu(I) reactions, 2.5 mM sodium ascorbate was added to the mixture.

For the gel electrophoresis study of the solution reactions with azide-PEG3-biotin, the purified DNA was first 3'-end radiolabeled with [α-32P]-dCTP, as previously described. Such ^{32}P-labelled DNA was then mixed with excess amount of unlabeled DNA and refolded as described above. Upon mixing with 2.5 mM of azide-PEG3-biotin, the CuAAC reaction was initiated by adding either $CuSO_4$ alone (for the Cu(II) reaction) or a mixture of $CuSO_4$ with sodium ascorbate (for the Cu(I) reaction). Reactions were terminated by ethanol precipitation of the DNA, which was redissolved in HEPES buffer containing streptavidin (0.5 mg/mL), mixed with denaturing loading dye (8 M Urea, 1.0 mM EDTA in pure formamide) before loaded onto the denaturing gel (10% containing 8 M Urea).

4.4.3. Preparation of binary N3C11S-/CnS-Au SAMs and reaction with DNAzymes

Gold slides were cut into rectangular pieces (0.7 × 1.8 cm^2) and cleaned in a Piranha solution (3:1 (v/v) mixture of 96% H_2SO_4 and 30% H_2O_2, freshly prepared before

use) for 10 min at 100 °C (*CAUTION: Piranha solution reacts violently with organics; thus, it must be handled with extreme caution and appropriate personal protection*). After extensive washing with deionized H_2O, the cleaned gold slides were soaked in an ethanolic solution of N3C11SH/CnSH (n = 6, 8, and 10) at the designated mole ratio overnight. The total concentration of alkanethiols in the deposition solution was kept at 1.0 mM. After SAMs' formation, the slides were washed first with 95% ethanol, then with H_2O. For coupling hexynyl DNA, 50 µL of refolded DNA sample was applied directly onto the slides and incubated in a humidity chamber at room temperature for the designated period of time. After the reaction, the slides were washed with hot H_2O (90 °C) briefly to remove non-specifically adsorbed DNA strands prior to the electrochemical measurements.

4.4.4. Electrochemical measurements

All CV measurements were performed in a three-electrode, single-chamber electrochemical cell, which has an opening at one side for attaching the gold slide (as the working electrode). The electrode area exposed to the electrolyte solution (0.15 ± 0.01 cm2) was confined by an O-ring seal and estimated based on the Randles−Sevcik equation by measuring the CVs of 1.0 mM K3Fe(CN)6 in 0.1 M KCl at varied scan rates . An Ag|AgCl|1 M KCl electrode and a platinum wire were used as reference and counter electrode, respectively. The electrolyte solution for the electrochemical detection, 5.0 µM of $Ru(NH_3)_6Cl_3$ in 10 mM Tris buffer (pH = 7.4) were degassed with Ar (>10 min) before use. All electrochemical measurements were performed with a CHI 1040A Electrochemical Analyzer (Austin, TX) in a Faraday cage at room temperature.

4.4.5. Extraction of copper from ore samples and AAS measurements

Three powdered ore samples were obtained from Copper Mountain Mining Corporation. 50 mg of the ore powder was treated in a mixture of 1 mL of HNO3 (63%, w/w) and 1 mL of HCl (37%, v/v) in a test tube. The mixture was briefly vortexed before boiling for 15 min, and the tube was shaken every 3 min during the boiling. The mixture was then transferred to a 10.0 mL volumetric flask and topped up to the mark with H_2O. Residual solid was removed by filtration with a glass microfiber filters (Whatman® GF/A). The clear solution obtained was further diluted and subjected to either AAS or the CLICK-17 sensor measurements. Three independent extractions and measurements were carried out for each of the samples.

For flame AAS measurements, a standard calibration curve was first constructed with $CuCl_2$ in 0.02 M HNO_3 solution (1 mM EDTA). The detection was performed on an AAnalyst™ atomic spectrometer (PerkinElmer) with a copper hollow cathode lamp (324.75 nm). The settings for the instrument were: oxygen flow rate of 10 mL/min, acetylene flow rate of 2.5 mL/min, and a slit width oμ 0.2 nm.

Chapter 5. *In vitro* selection of DNA aptamers for ferrocene

In this chapter, the *in vitro* selection for DNA aptamers that bind ferrocene will be presented. As an ideal electrochemical reporter, ferrocene has been widely used as the electrochemical signal module in biosensor designs. Till now, no aptamers binding to ferrocene, or to any other organometallic compound, have been reported, possibly due to ferrocene being a refractory target for *in vitro* selection. Taking advantage of a water-soluble ferrocene derivative, adopting a capture selection method, we were able to isolate an aptamer (FcE2) for ferrocene with modest binding affinity.

5.1. Introduction

Ferrocene is the first organometallic compound of its kind. It has unique molecular structure: two cyclopentadienyl rings bound on the opposite sides of a central iron atom to form a 'sandwich' structure.[174] The Nobel Prize in Chemistry in 1973 was awarded to Fischer and Wilkinson for their work on the chemistry of ferrocene and other sandwich complexes.[175] The unique structure of ferrocene makes it ferrocene molecules very stability toward O_2, water, strong base, and high temperature. It keeps unchanged when treated with carbon monoxide at 150 °C.[176] Besides of its high stability, ferrocene can undergo reversible one electron oxidation/reduction reactions. Interestingly, the molecular structure of ferrocene remains unchanged when it is oxidized to form ferrocenium.[177,178] These properties of ferrocene make it an 'ideal' electrochemical reporter to be used in many electrochemical biosensors designs.[179] Ferrocene has also been extensively exploited in many electron transfer systems involve electron transfer between ferrocene units or between ferrocene and other redox centers both intra- and intermolecularly.[180]

DNA aptamer binding to molecules like ferrocene that undergoes ideal reversible redox reactions has not been reported. A DNA aptamer binds ferrocene specifically may make the following studies possible: (1) Studying electron transfer between ferrocene and its DNA aptamer; (2) Studying how DNA aptamer distinguishes ferrocene and its oxidized form ferrocenium, which structurally resembles ferrocene; (3) Designing of new sensing strategies. However, the isolation of DNA aptamers binding to small molecules is generally challenging. Ferrocene is a particularly refractory target due to its lack of chemical functionalities to interact with DNA.

A new *in vitro* selection method, capture selection, has been proposed and proved to be suitable for isolation of DNA aptamers for small molecules.[181-183] Stojanovic and coworkers have optimized this method for the selection of DNA aptamers binding to small molecules such as glucose, serotonin, dopamine and a few amino acids.[181-182] The same method has been adopted by Xiao and coworkers to isolate DNA aptamer binding to cathinone as well.[183] Despite all the success, this method has a intrinsic limitation: it limits the aptamer sequences by the requirement that the ligand binding conflicts with that of a complementary oligonucleotide; this confines the diversity of aptameric structures which

may cause a loss on good binders that bind alternatively. In contrast, the conventional target-functionalized beads based *in vitro* selection method screens the full possibilities of aptameric structure. However, the beads-based method has the concern of steric hindrance originated from the morphology of the bead surface (as reviewed in section 1.1.4). It will be interesting to compare the two methods in isolating aptamers for a challenging target such as ferrocene.

5.2. Results and Discussion

5.2.1. Conventional *in vitro* selection for aptamers bind to ferrocene

To date, aptamers binding to a vast variety of targets have been successfully isolated.[184]Regardless of the specific design and experimental conditions, the vast majority of *in vitro* selections have been performed by following the similar essential procedure: the targets of interest are first immobilized onto certain kinds of solid matrices (agarose and magnetic beads being most commonly used) that facilitate the subsequent separation of active species (the DNA/RNA binding sequences) from those spectator species. We have attempted to isolate a ferrocene binding aptamer by adopting this method initially.

Ferrocene was immobilized onto Sepharose beads to be used as target for the *in vitro* selection (details of the coupling reaction and selection procedure are described in Section 5.4). We carried out 16 rounds of *in vitro* selection. The stringency of selection was gradually increased by decreasing the quantity of ferrocene modified beads, shortening the incubation time and also conducting harsher washing steps. To minimize non-specific binding between DNA library and the Sepharose beads, negative selections with unmodified beads were incorporated every other round of positive selections. The DNA libraries from round 1, 3, 5, 7, 9, 11, 13,16 were tested for binding to ferrocene modified Sepharose beads. Unmodified Sepharose beads were used as negative control. As shown in Figure 5.1, DNA library from early rounds (round 1- round 7) showed baseline binding to both ferrocene-modified or unmodified Sepharose beads. Starting from round 9, a rise in binding was observed for both beads. Negligible binding enhancement was observed after round 13 with increased stringency. The final DNA library (round 16) was

sequenced. We then tested the binding capabilities of the sequences to ferrocene modified beads. However, all the tested sequences bind to ferrocene-modified beads and unmodified beads with same binding affinity. We concluded that no aptamer was selected by the conventional *in vitro* selection method. The increased binding of DNA library (after round 9) may be a result of DNA sequences binding to the beads.

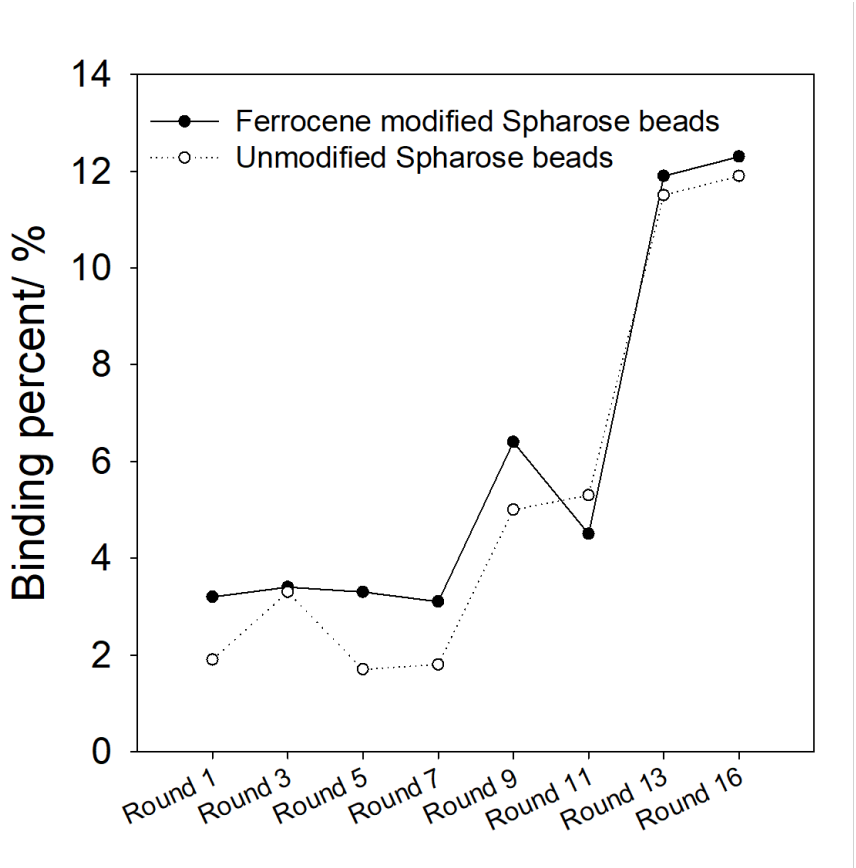

Figure 5.1 Binding profile of DNA library from different rounds of *In vitro* selection. Solid circle: The percentage of DNA library that stays on ferrocene-modified beads after incubation; open circle: the percentage of DNA library that stays on unmodified Sepharose beads after incubation.

Two possibilities might explain the ineffectiveness of conventional *in vitro* selection method in isolating DNA aptamers for ferrocene: (1). The steric hindrance of bead's surface hindered the 'full interaction' between DNA library and the surface-bound ferrocene. Although there is a C6 linker between ferrocene and the Sepharose beads, it may not be sufficient to allow DNA library to approach the ferrocene in the way resulting in binding; (2) Aptamers binding to ferrocene do not exist.

5.2.2. Capture Selection

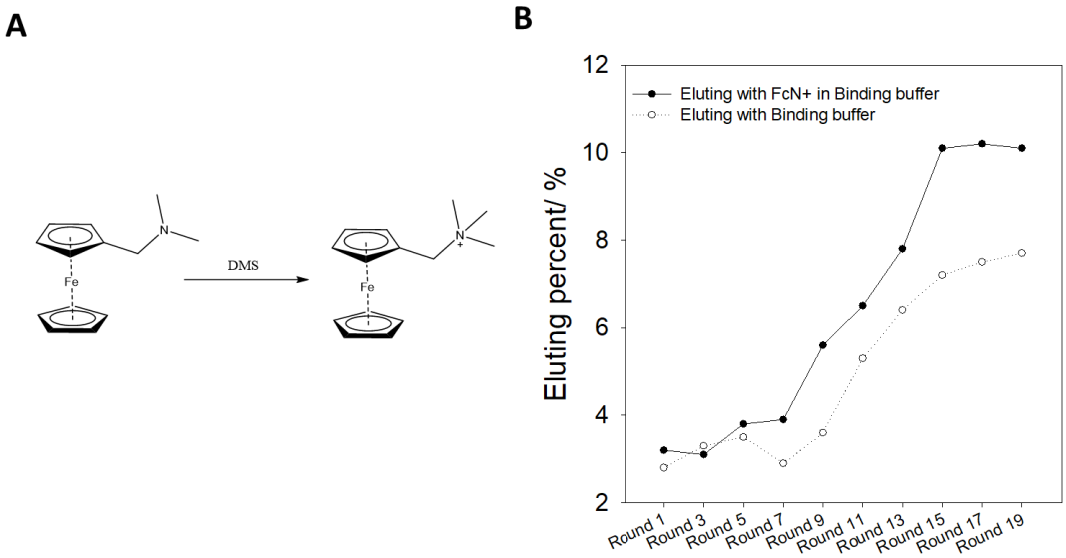

Figure 5.2 (A) The methylation of N,N-dimethylferrocenylmethylamine to form N,N,N-trimethylethanaminium ferrocene (abbreviated as FcN+ thereafter); (B) Eluting (the more binding, the more eluting) of DNA library of different rounds from capture selection with 1mM FcN+ (solid circle) in binding buffer (25 mM Tris, pH 7.4, 10 mM $MgCl_2$, 10 mM KCl, 1000 mM NaCl) or binding buffer alone(hollow circle).

Capture selection, an alternative method for the isolation of aptamers, differs from conventrional *in vitro* selection in that instead of target molecules, the randomized DNA library is immobilized onto beads (more detailed description of capture selection can be found in section 1.1.4). This allows firstly high concentrations of target molecules to be used for the incubation, which increases the chance of weaker binders to be selected. Indeed, DNA aptamers binding to small molecules are expected to be weaker than binding to peptide or proteins;[12] secondly, this method allows the use of unmodified small molecules (need to be relatively water-soluble) as targets, which ensures the resulted aptamer recognize the target itself; and thirdly, it has been shown that the three-way junction structure of the library facilitates hydrophobic interactions.[29] To increase the solubility of ferrocene, a water soluble N,N,N-trimethylethanaminium ferrocene (shown in Figure 5.2A, abbreviated as FcN+ thereafter) was synthesized. With FcN+ as target molecule, we carried out 19 rounds of capture selection. The stringency of selection was gradually increased by decreasing the concentration of FcN+ in the eluting buffer, and shortening the incubation time during the eluting steps. The binding of the DNA library to the target molecule FcN+ can be evaluated by the percentage of bead-bound library that can be eluted off. As shown I n Figure 5.2B the binding remains at baseline level for round

1 until round 7, then an increase in the binding became more profound with more rounds of selections. No matter how the eluting stringency was changed, no further binding enhancement was observed after round 15, We cloned and sequenced the round19 DNA library. 23 unique clones were picked and sequenced (Figure 5.3).

```
Fc-E1       -------AGTGCCCTGGAA--CAATAGTTCGCTCGGTTC--- 30
FcE-16      -------AGTGCCCTGGAA--CAATAGTTCGCTCGGTTC--- 30
FcE-14       -----ATATTGCC---AAC--CGATAACT--GTTGGTTCAT- 29
FcE-12      -----ACGCTTCACTTCTG--CGAGCATCAACTTTGC----- 30
FcE-22      ---------TGCGAATGAAATCTAAAGTTTGAATGAACG--- 30
FcE-1      GAAAAACAATCTA---TAGA-TGAGCGTT---TTGTA----- 30
FcE-23      -TAAACTGTTCTGATTCAGA-TAAG-GTT---TTGG------ 30
FcE-4        --GAAATAGCATACTTGTA------AGTTCGATCGATC---- 30
FcE-11       --AATCTAACTCATCTAGGG----CAGTTATATTGA------ 30
Fc-E2         -----TAAATCCATA-CCATAGTACAAACCCTTTAA------ 30
FcE-15        -----TAAATCCATA-CCATAGTACAAACCCTTTAA------ 30
FcE-24        -----TAAATCCATA-CCATAGTACAAACCCTTTAA------ 30
FcE-9       -------AATCT-----CGTAGCGTAAGCCTATAAAGAATTG 30
FcE-3        -----TATGTCGTCC-GCAT----TTGACCGTTCGATAA--- 29
FcE-5       -----TAGGTGAGTAAGTACGCTACTTAGAGCCAA------- 30
FcE-6       -----TAGGTGAGTAAGTACGCTACTTAGAGCCAA------- 30
FcE-10       ------AGGTAGCTAAGCAC-TTATTTAG--CTAAAATG--- 30
FcE-17      ---TATAAGCGTGTGGGTACCAAACA-AATA-TAG------- 30
FcE-21       --TTATTAG-GTACCAGTAAATGGTA-TGCA-TAA------- 30
FcE-18      -----TAGGTCTGTCAAAATTTGGCAGTGAG-TAGT------ 30
FcE-8        ---AGTTAATGCGCAAGTATCT AAATTAAGCT--------- 29
FcE-7         -----TA---TCGTAATAATCTTG-AAAATTATAAGGTA--- 30
FcE-13        -----TA---TCGTAATAATCTTG-AAAATTATAAGGTA--- 30
```

Figure 5.3 Sequences from Round19 DNA library.

Alignment of the sequences revealed no consensus motifs, which is similar to the observation reported by Yang and Stojanovic in the their selection of DNA aptamers for small molecules.[28] Two aptamer candidates from the sequencing results were selected based on the redundancy of clone copy (FcE2 appeared in three independently picked clones). Both clones were then synthesized and tested for their binding affinities with FcN+.

5.2.3. Binding affinity determined by electrophoresis

We adopted a native PAGE method to determine the binding affinity of the two clones with ferrocene (FcN+). As shown in Figure 5.4, the unbound bands represent the aptamer/capture-18 duplex. Upon binding ferrocene to the aptamer, the capture-18 was ripped off from the aptamer DNA strand (as a result of the formation of aptamer/ferrocene complex; same concept as shown in Figure 1.9). The aptamer/ferrocene complex travels faster than aptamer/capture-18 duplex in the 10% native gel and labelled as Bound in the images. Based on the densitometry analysis of the gel data, the K_d was estimated to be 6.3±0.9 mM for FcE1, and 2.7±0.4 mM for FcE2, respectively.

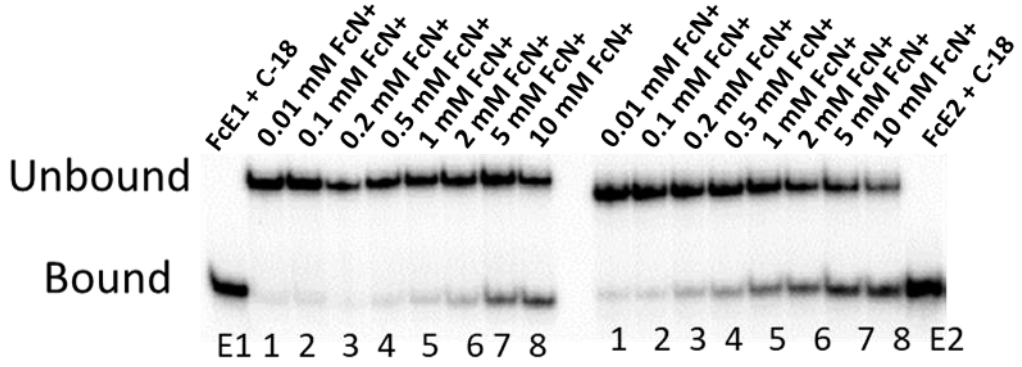

Figure 5.4 PAGE data for the determination of Kd for Clone FcE1 and FcE2. The unbound band represents 32P-labelled FcE1 (or FcE2) and capture strand duplex, the bound band represents FcE1 (or FcE2) and FcN+ complex. E1, FcE1 DNA alone, E2, FcE2 DNA alone. For both FcE1 and FcE2 gels, the concentrations of FcN+ for lane 1 until lane 8 are 0.01, 0.1, 0.2, 0.5, 1, 2, 5, 10 mM. DNA are kept at 2 μM in binding buffer (25 mM Tris-HCl, pH 7.4, 10 mM MgCl2, 10mM KCl, 100 mM NaCl) in all cases.

Both FcE1 and FcE2 bind to ferrocene with moderate (low mM) binding affinity. We ask the question that does this aptamer represent the best possible binder to ferrocene or it is merely the best outcome of this particular *in vitro* selection? Is it possible to find better binders by improving the *in vitro* selection method? We are aware of the following limitation of capture selection method: (1) With conventional *in vitro* selection method, binders with better k_{on} can be selected by reducing the incubation time and binders with better k_{off} can be selected by increasing the washing stringency. However, for capture selection, only the k_{on} can be enhanced by reducing the incubation time or decreasing the target concentration. There is no way to enrich binders with better k_{off}; (2) In our earlier *in vitro* selection experiments for DNAzymes, and many other successful *in vitro* selections,[93,182] the sequencing of the final DNA library generates several families of

aptamers, within each family consensus sequences were observed. However, both our capture selection and those carried out by Stojanovic et al.[93, 181] end up with a DNA library lacking consensus sequences. Instead, aptamers were picked based on their redundancy of clone copies. This might indicate that the final DNA library was not sufficiently forced to evolve toward the best solution for binding to different targets. It may be still possible to improve this method so that better aptamers can be isolated.

5.3. Conclusion

As ferrocene lacks chemical functionalities to interact with DNA, it is challenging to isolate a DNA aptamer for binding with. However, by adopting a capture selection method, in conjunction with a water-soluble ferrocene derivative (FCN+), we were able to isolate an aptamer binding to ferrocene with mM binding affinity. In contrast, our attempt with traditional *in vitro* selection method failed to isolate an aptamer for ferrocene. This finding highlights the necessity of adopting proper *in vitro* selection method for isolating aptamers binding to refractory targets.

5.4. Materials and Methods

5.4.1. Chemicals

(Dimethylaminomethyl) ferrocene (Sigma-Aldrich, 95% purity); Dimethyl sulfide (Sigma-Aldrich, 99.5%); Streptavidin-agarose beads (Sigma-Aldrich); 10K MWCO centrifugal filter units (Sigma-Aldrich); Thiol-activated Sepharose beads (Sigma-Aldrich); (6-Bromohexyl) ferrocene (Sigma-Aldrich); HEPES (Sigma-Aldrich, 99.5%, copper $\leqslant$ 5 ppm); $MgCl_2 \cdot H_2O$ (Sigma-Aldrich, 99%, copper $\leqslant$ 5 ppm); LiOH • H_2O (Sigma-Aldrich, $\geqslant$ 99%, copper $\leqslant$ 5 ppm); sodium ascorbate (Sigma-Aldrich, 98%); NaCl (Sigma-Aldrich, 99%); KCl (ACP Chemicals, 99%); sodium acetate (Bio Basic, 99%); 5-hexyn-1-ol (Sigma-Aldrich, 96%); propargyl alcohol (Sigma- Aldrich, 99%); 3-azido-7-hydroxycoumarin (AKScientific, 98%); azide-PEG3-biotin conjugate (Sigma-Aldrich); NaOH (Sigma-Aldrich, 99%);. The oligonucleotides were from IDT: (1) a random (N30) library (72-mer): 5'-GGAGGCTCTCGGGACGAC(N30)GTCGTCCCGATGCTGCAATCGTAA-3'; (2) forward-primer (18-mer): 5'-GGAGGCTCTCGGGACGAC-3', (3) reverse-primer (22-mer): 5'-TTACGATTGCAGCATCGGGACG-3', (4) Cleavable reverse-primer (22-mer): 5'-biotin-

TTACGATTGCrAGCATCGGGACG-3', (5) biotinylated column immobilizing capture (18-mer): 5'- GTCGTCCCGAGAGCCATA-BioTEG-3'.

5.4.2. Procedure for *in vitro* selections

The procedure for conventional *in vitro* selection has been reported previously by Thomas and Sen.[185] To prepare the ferrocene functionalized beads, 2 mg of (6-Bromohexyl) ferrocene was reacted with thiol-activated Sepharose beads in 10% DMSO in water. The reaction was kept at room temperature for overnight, Then the beads were washed extensively with 10% DMSO in water, followed by incubation with bromoethane to block any remaining thiol groups on beads. Then the beads were washed extensively with 10% DMSO in water. Ferrocene functionalized beads were kept in PBS and equilibrated with selection buffer (20mM Tris-HCl, pH=7.3, 150 mM NaCl, 10 mM $MgCl_2$, 5mM KCl) before used for *in vitro* selection.

For the capture selection, the procedure reported by Yang et al.[28] was followed. For the first round of selection, 0.15 nmol of gel purified N30 (^{32}P-labelled) was mixed with 0.6 nmol of capture-18mer and refolded. The refolded DNA was passed through streptavidin-agarose beads. The beads were washed 10 times with 1× binding buffer (25 mM Tris-HCl, pH 7.4, 10 mM $MgCl_2$, 10 mM KCl, 100 mM NaCl). Then eluted with 5 mM FcN+ in 1× binding buffer for three times. Each eluent was collected and concentrated with 10K centrifugal filters, followed by PCR amplification. PCR conditions: one cycle of 95 °C, 2 min, 15 cycle of [95 °C, 45 sec; 60 °C, 45 sec; 72°C, 45 sec], and one cycle at 72 °C, 2 min. The cloning and sequencing followed the same procedure shown in Section 2.8.3.

5.4.3. Native gel for evaluating FcN+/aptamer binding

2 μM ^{32}P-labelled FcE1 or FcE2 and 8 μM capture-18mer was mixed and refolded in 1× binding buffer. FcN+ of different concentrations was added to the mixture and incubated at room temperature for 30 min before native loading dye was added. Samples were run on native gels with 1 mM $MgCl_2$ in a cold room.

Chapter 6. Concluding remarks and future work

As presented in Chapter 2 to Chapter 4, the success of the isolation of a CuAAC catalyzing DNAzyme (CLICK-17) through properly designed *in vitro* selection opened new avenues for biological conjugation, surface immobilization of redox reporters, and the design of sensitive copper sensors. The DNAzyme has been shown to use both Cu(I) and Cu(II) as its cofactors and works under both *in cis* (single turnover) and *in trans* (multi turnover) conditions. The key improvement is that CLICK-17 only requires copper of either valences lower than 5 μM to achieve ultra-high catalytic efficiency (especially under *in cis* conditions, reaction reaches completion within two min). The high catalytic efficiency with lowered copper requirement allowed us to develop a number of applications based on CLICK-17. Firstly, we have shown that CLICK-17 is a useful tool for the labelling of protein and cell surface. Azide-functionalized lysozyme was prepared as a model protein and the successful labeling was confirmed by mass spectrometry. Secondly, it was demonstrated that the *in trans* reaction of CLICK-17 is a useful tool for introducing electrochemical reporter onto azide-terminated SAMs. Lastly, a copper biosensor using the *in cis* coupling reaction between alkynyl labelled CLICK-17 with azide-terminated SAMs has been developed and tested against industrial samples.

Despite the success of using CLICK-17 in the facilitated immobilization of redox centers and the development of ultrasensitive copper sensors, we have not been able to demonstrate the application of CLICK-17 in labelling live cells, partly due to the challenges in preparing azide-functionalized live cells. As a matter of fact, introducing azide groups onto live cells metabolically has been well established.[187,188] I propose the following experiments (6.1) to elucidate whether CLICK-17 is a superior tool for the labelling of live cells as future work.

As a preliminary test (Chapter 5), the isolation of a DNA aptamer binding to a water-soluble ferrocene derivative (N,N,N-trimethylethanaminium ferrocene) has been explored with both conventional *in vitro* selection and capture selection methods. While the conventional failed, the capture selection has generated an aptamer (FcE2) binding to ferrocene with only mM binding affinity. The second part of the future work (6.2) will describe the idea of a new Exonuclease I (EXO I) assisted *in vitro* selection procedure with ferrocene as a trial target.

6.1. Cell surface labelling using CLICK-17

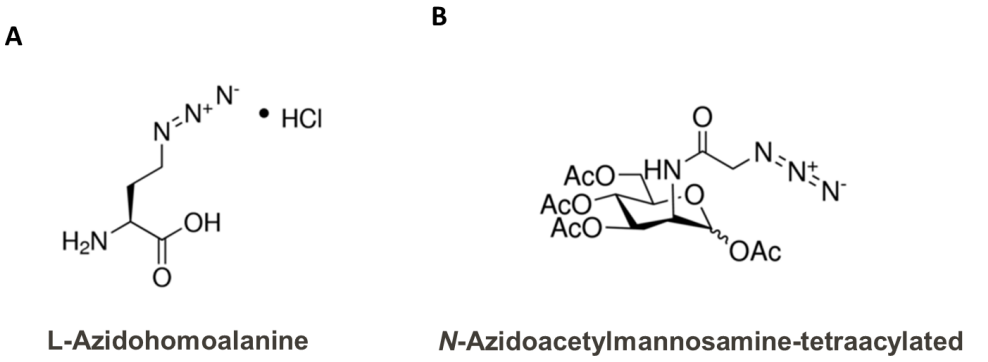

Figure 6.1 (A). L-azidohomoalanine (AHA); (B) N N-Azidoacetylmannosamine-tetraacylated.

Introducing tags, usually fluorophores, onto the cell membrane is a common way to trace and study live cells during many biological processes.[186] The use of CuAAC to label biological samples, either cells directly or cell lysate, has been well documented.[87] CLICK-17 can be used as a highly efficient, low toxicity labeling reagent if azide groups are present on the cell membrane. Actually, a few methods are available to metabolically functionalize cell membrane with azide groups.[187,188] One way is to use a methionine surrogate azidohomoalanine (AHA, Figure 6.3A).[188] When cells are cultured in methionine-free culture medium supplemented with AHA, AHA will be incorporated into nascent proteins in place of methionine residues. The azide groups on cell membranes can then be used for chemoselective labelling. Another method relies on the unnatural sialic acid biosynthesis. Human cells metabolize the unnatural precursor N-azidoacetylmannosamine (Figure 6.3B), an azide-bearing analog of the native sugar N-acetylmannosamine, to the corresponding sialic acid residues on cell surface glycoconjugates. These azide-groups on cells surface can then be used for further click reactions.

As a proof of concept, we have tested CLICK-17 on labelling live E. coli cells on the surface. Culturing a methionine-auxotroph E. coli strain (M15MA, a courtesy of Dr. Tirrell of California institute of technology.) in AHA supplemented culture medium, azide groups were incorporated into newly synthesize membrane proteins. Dual labelled CLICK-17 (modified on 5'-end with alkynyl group and 3'-end with fluorescein) was used to label the E. coli cells at the presence of 5 μM $CuSO_4$ and 0.5 mM ascorbate. Our preliminary

data (Figure 6.2 A and A') shows that CLICK-17 labels the E coli cells successfully. A negative control with M15MA cultured in normal culture medium showed no labelling after reaction with CLICK-17 (Figure 6.2 B and B'), The cytotoxicity of the reaction conditions were tested by examining the growth curve of E. coli, cells treated with copper of different concentration at the presence of either CLICK-17 or other copper ligands. As shown in Figure 6.3, the conditions used in labelling E. coli cells (5 μM of $CuSO_4$ and 0.5 mM ascorbate) was not affecting the growth curve of treated cells, which implies the tested conditions are biocompatible. Based on these preliminary data on E. coli cells, we are planning to test 1). CLICK-17 labelling of cell surface of mammalian cells (azide will be introduced by culturing cells in medium supplemented with N N-Azidoacetylmannosamine-tetraacylated) and ultimately stem cells; and 2). enhancing the signal by introducing short fluorescein labelled oligoes that are complementary to CLICK-17 DNA strand.

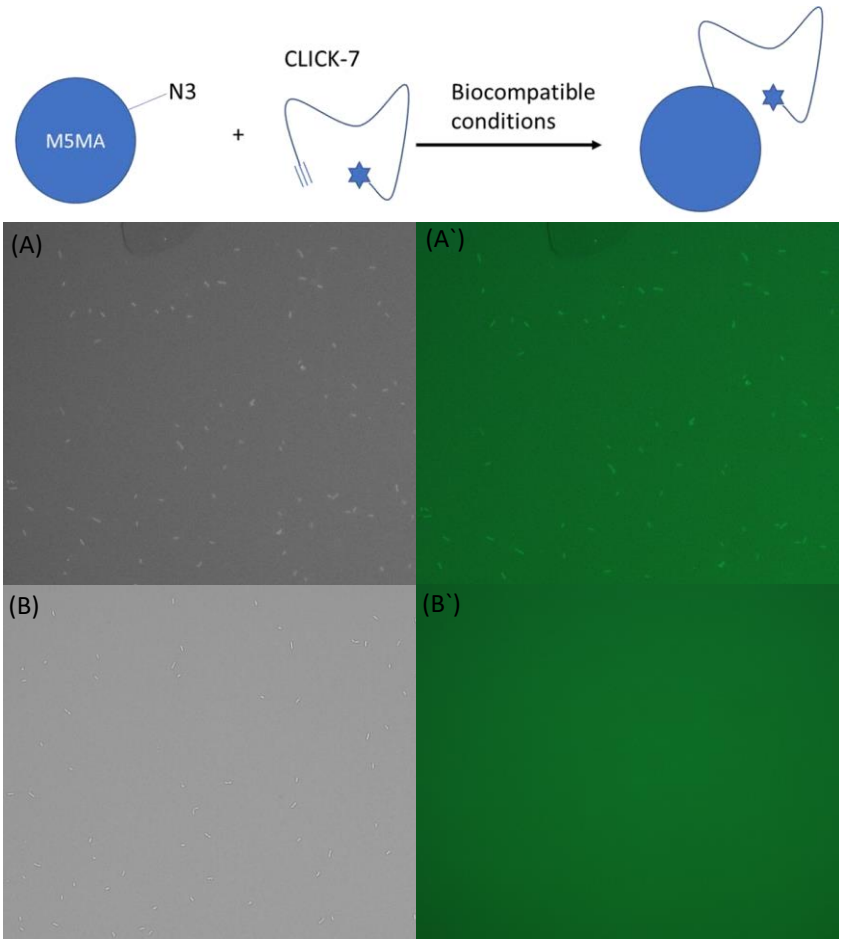

Figure 6.2 Top: a schematic illustrated the labelling reaction of dual labelled CLICK-17 (5' end with alkynyl and 3' end with fluorescein) with azide functionalized E. coli cells

(M15MA). Azide functionalized cells (A and A') or cells without azide functionalization (B and B') were pelleted by centrifugation and washed 3 times with 1x PBS. Cell were resuspended in 1x PBS and the cell density in solutions were determined by absorbance at 600 nm. For each labelling reaction, ~ $1X10^7$ cells were reacted with refolded dual labelled CLICK-17 at the presence of 5 μM $CuSO_4$ and 0.5 mM ascorbate at room temperature for 20 min. Cells were washed with 1x PBS after reaction and applied onto glass slides to be imaged on a fluorescence microscope. A). Cell image of azide containing M15MA reacted with CLICK-17 (dual labelled). Image was taken under white light; A') same cells as A), image was taken with fluorescein filters; B) Cell image of M15MA (no azide) reacted with CLICK-17 (dual labelled). Image was taken under white light; B') same cells as B), image was taken with fluorescein filters. (Due to the size of the E. coli cells, it is difficult to observe the cells in the images, please enlarge the images so that cells can be seen easier)

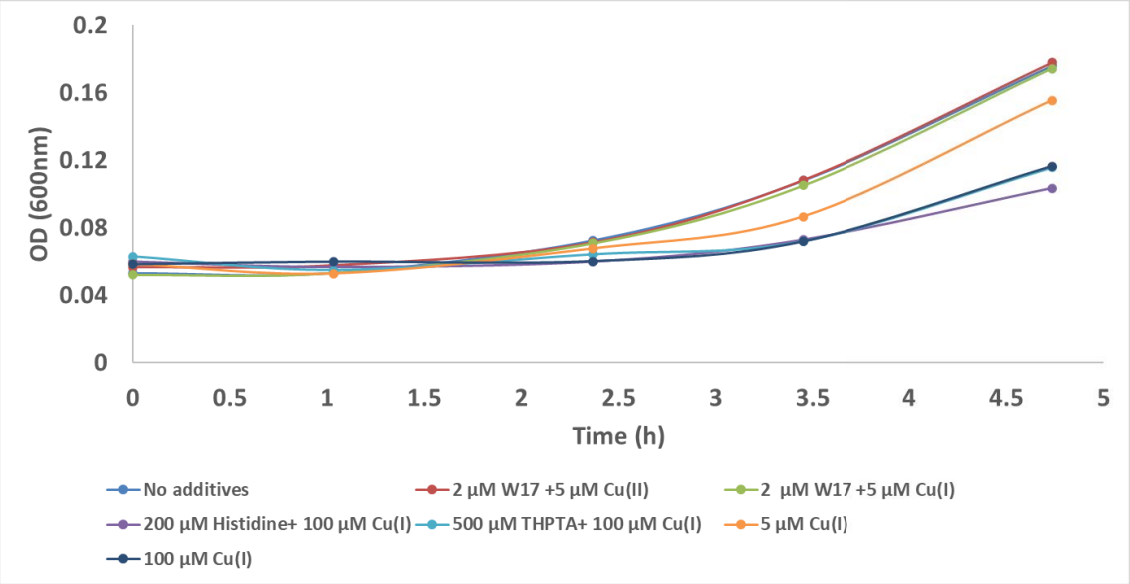

Figure 6.3 Growth curve of M15MA in LB medium after treated with Cu(I) or Cu(II) together with CLICK-17, THPTA, or histidine in 1x PBS buffer for 20 min. Equal number of cells were treated and pelleted by centrifugation before transferred into LB medium. Absorbance at 600 nm were measured at different time points and used for construction of the growth curve. The concentrations of copper and different ligands (CLICK-17, THPTA or histidine) were shown in the figure legend.

6.2. An EXO I-assisted homogenous capture selection

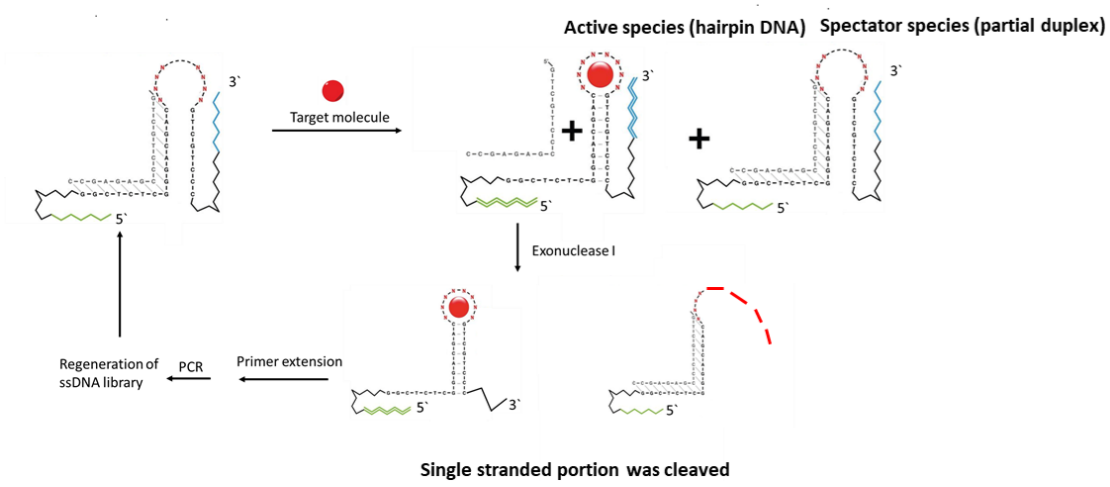

Figure 6.4 EXO I assisted homogenous *in vitro* selection. DNA sequences of the DNA library, primers and capture oligoes are the same as shown in Section 5.4.1. Briefly, target binding induces the formation of hairpin DNA (active species). EXO I treatment cleaves the single stranded portion of active species and spectator species. After cleavage, the active species are still potent template for PCR, while the spectator species are not. The active sequences are then amplified by PCR and regenerated DNA library can be used for further round of selection.

To facilitate the ferrocene aptamer selection, an exonuclease I (EXO I) assisted homogenous *in vitro* selection method is proposed (Figure 6.4). EXO I has the following features: (1). it is a DNA specific exonuclease catalyzes the removal of nucleotides from linear, single-stranded DNA in the 3' to 5' direction. (2) EXO I does not cleave double-stranded DNA. As shown in Figure 6.5, EXO I cleaves the single stranded portion dangling the hairpin DNA and duplex DNA. The single stranded DNA (linear DNA) was completely cleaved within the first 10 min treated with EXO I. These data backed up our proposal of, partitioning active species from spectator species with the help of exonuclease I (after exonuclease I cleavage, the active sequences will have enough prime binding region to allow PCR amplification while the spectators are too short to be potent PCR templates).

There are a few potential advantages of the proposed *in vitro* selection method: (1) It is completely bead-free, *in vitro* selection will be done in homogeneous solutions. It has been shown that *in vitro* selection in homogenous solutions allows better interaction between DNA library and target molecules which will dramatically reduce the number of rounds needed for aptamer isolation;[189] (2) Allow aptamers with good k_{off} to be selected (the cleaving stringency can be adjusted by both the concentration of exonuclease I and

the incubation time in an accurate manner). With this new *in vitro* selection method, aptamers with better binding affinities for ferrocene (and other small molecules) may be selected.

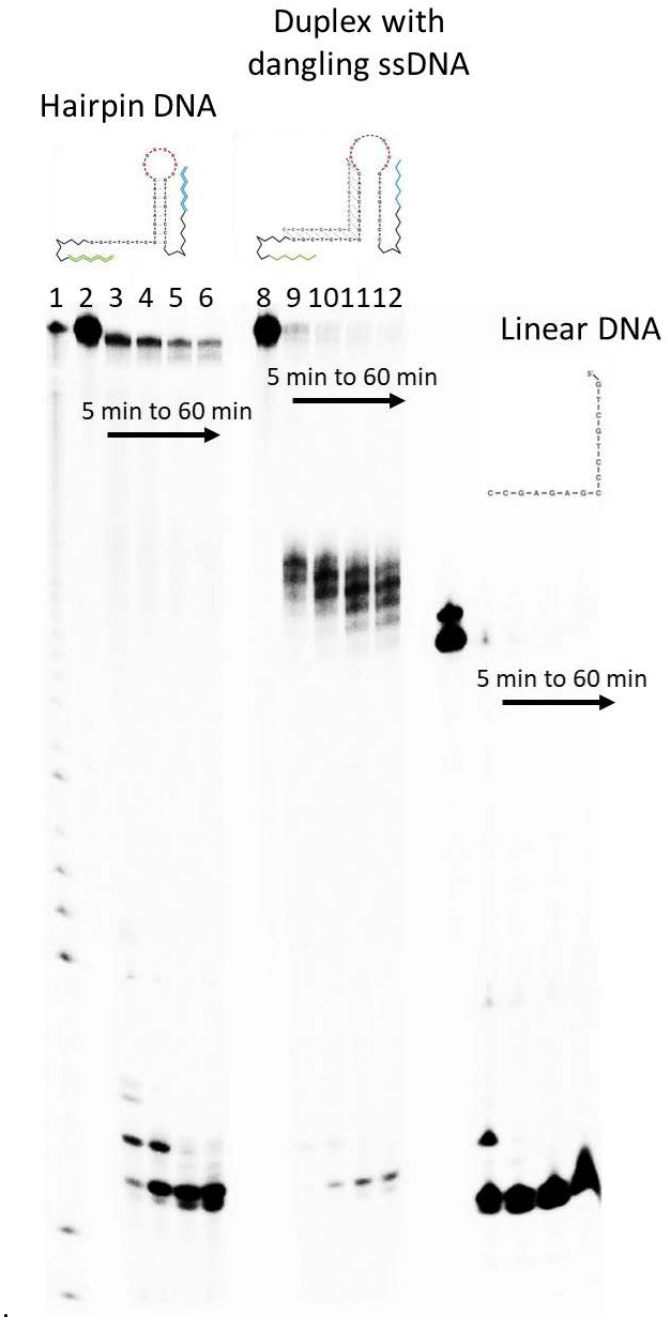

Figure 6.5 EXO I cleavage patter on different DNA constructs. 0.2 μM exonuclease I was incubated with 2 μM DNA at room temperature for different length of time. Lane 1 is a G-ladder prepare by DMS methylation followed by hot base cleavage. The linear DNA (labelled in the figure) was completely cleaved within the first 10 min; the duplex with

dangling ssDNA had the ssDNA portion cleaved within the first 10 min leaving the duplex portion un-cleaved. One interesting observation is that, the cleavage of ssDNA dangling the duplex is not complete and the immediate 5 nucleotide beside the duplex has slow cleaving rate. Similarly, the ssDNA portion of the hairpin DNA was cleaved quickly (within the first 5 min).

References

(1) Pray L. A. Discovery of DNA Structure and Function: Watson and Crick. *Nature Education* **2008**, 6, 134.

(2) Watson J. D.; Crick F. H. C. Molecular Structure of Nucleic Acids: A Structure for Deoxyribose Nucleic. *Nature* **1953**, 171, 737–738.

(3) Neveu, M.; Kim, H.-J.; Benner, S. A. The "Strong" RNA World Hypothesis: Fifty Years Old. *Astrobiology* **2013**, *13* (4), 391–403.

(4) Kruger, K.; Grabowski, P. J.; Zaug, A. J.; Sands, J.; Gottschling, D. E.; Cech, T. R. Self-Splicing RNA: Autoexcision and Autocyclization of the Ribosomal RNA Intervening Sequence of Tetrahymena. *Cell* **1982**, *31* (1), 147–157.

(5) Altman, S.; Baer M.; Guerrier C.-T.; Vioque A. Enzymatic cleavage of RNA by RNA. *Trends Biochem Sci.* **1986**, 11 (12), 515-518.

(6) Wilson, D. S.; Szostak, J. W. In Vitro Selection of Functional Nucleic Acids. *Annu. Rev. Biochem.* **1999**, *68* (1), 611–647.

(7) Breaker, R. R.; Joyce, G. F. A DNA Enzyme That Cleaves RNA. *Chem. Biol.* **1994**, *1* (4), 223–229.

(8) Ellington, A. D.; Szostak, J. W. In Vitro Selection of RNA Molecules That Bind Specific Ligands. *Nature* **1990**, *346* (6287), 818–822.

(9) Andrew D. E.; Szostak J. W. Selection in vitro of single stranded DNA molecules that fold into specific ligand-binding structures. *Nature* **1992**, 355, 850-852.

(10) Li Y.; Sen D. A catalytic DNA for porphyrin metalation. *Nat Strut Mol Biol.* **1996**, 3, 743–747.

(11) Dunn, M. R.; Jimenez, R. M.; Chaput, J. C. Analysis of Aptamer Discovery and Technology. *Nat Rev Chem* **2017**, *1* (10), 0076.

(12) Famulok M.; Hartig J. S.; Mayer G. Functional Aptamers and Aptazymes in Biotechnology, Diagnostics, and Therapy. *Chem. Rev.* **2007**, 107 (9), 3715–3743.

(13) Huizenga, D. E.; Szostak, J. W. A DNA Aptamer That Binds Adenosine and ATP. *Biochemistry* **1995**, *34* (2), 656–665.

(14) Lin, C. H.; Patei, D. J. Structural Basis of DNA Folding and Recognition in an AMP-DNA Aptamer Complex: Distinct Architectures but Common Recognition Motifs for DNA and RNA Aptamers Complexed to AMP. *Chem. Biol.* **1997**, *4* (11), 817–832.

(15) Jiang F.; Kumar R. A.; Jones R. A., Patel D. J. Structural basis of RNA folding and recognition in an AMP–RNA Aptamer Complex. *Nature* **1996**, 382,183-186.

(16) Sazani, P. L.; Larralde, R.; Szostak, J. W. A Small Aptamer with Strong and Specific Recognition of the Triphosphate of ATP. *J. Am. Chem. Soc.* **2004**, *126* (27), 8370–8371.

(17) Shui, B.; Ozer, A.; Zipfel, W.; Sahu, N.; Singh, A.; Lis, J. T.; Shi, H.; Kotlikoff, M. I. RNA Aptamers That Functionally Interact with Green Fluorescent Protein and Its Derivatives. *Nucleic Acids Res* **2012**, *40* (5), e39–e39.

(18) Abeydeera, N. D.; Egli, M.; Cox, N.; Mercier, K.; Conde, J. N.; Pallan, P. S.; Mizurini, D. M.; Sierant, M.; Hibti, F.-E.; Hassell, T.; Wang, T.; Liu, F.-W.; Liu, H.-M.; Martinez, C.; Sood, A. K.; Lybrand, T. P.; Frydman, C.; Monteiro, R. Q.; Gomer, R. H.; Nawrot, B.; Yang, X. Evoking Picomolar Binding in RNA by a Single Phosphorodithioate Linkage. *Nucleic Acids Res* **2016**, *44* (17), 8052–8064.

(19) Pinheiro, V. B.; Taylor, A. I.; Cozens, C.; Abramov, M.; Renders, M.; Zhang, S.; Chaput, J. C.; Wengel, J.; Peak-Chew, S.-Y.; McLaughlin, S. H.; Herdewijn, P.; Holliger, P. Synthetic Genetic Polymers Capable of Heredity and Evolution. *Science* **2012**, *336* (6079), 341–344.

(20) Zandarashvili, L.; Nguyen, D.; Anderson, K. M.; White, M. A.; Gorenstein, D. G.; Iwahara, J. Entropic Enhancement of Protein-DNA Affinity by Oxygen-to-Sulfur Substitution in DNA Phosphate. *Biophys J.* **2015**, *109* (5), 1026–1037.
(21) Taylor, A. I.; Holliger, P. Directed Evolution of Artificial Enzymes (XNAzymes) from Diverse Repertoires of Synthetic Genetic Polymers. *Nat Protoc* **2015**, *10* (10), 1625–1642.
(22) Griffin L. C., Tidmarsh G. F., Bock L. C., Toole J. J., Leung L. L. In Vivo Anticoagulant properties of a novel nucleotide-based thrombin inhibitor and demonstration of regional anticoagulation in extracorporeal circuits. *Blood* **1993**, 81 (12): 3271-3276.
(23) Sefah, K.; Yang, Z.; Bradley, K. M.; Hoshika, S.; Jimenez, E.; Zhang, L.; Zhu, G.; Shanker, S.; Yu, F.; Turek, D.; Tan, W.; Benner, S. A. In Vitro Selection with Artificial Expanded Genetic Information Systems. *Proc. Natl. Acad. Sci. U.S.A.* **2014**, *111* (4), 1449–1454.
(24) Vaught, J. D.; Bock, C.; Carter, J.; Fitzwater, T.; Otis, M.; Schneider, D.; Rolando, J.; Waugh, S.; Wilcox, S. K.; Eaton, B. E. Expanding the Chemistry of DNA for in Vitro Selection. *J. Am. Chem. Soc.* **2010**, *132* (12), 4141–4151.
(25) Mosing, R. K.; Bowser, M. T. Microfluidic Selection and Applications of Aptamers. *J. Sep. Sci.* **2007**, *30* (10), 1420–1426.
(26) Mendonsa, S. D.; Bowser, M. T. In Vitro Evolution of Functional DNA Using Capillary Electrophoresis. *J. Am. Chem. Soc.* **2004**, *126* (1), 20–21.
(27) Lou, X.; Qian, J.; Xiao, Y.; Viel, L.; Gerdon, A. E.; Lagally, E. T.; Atzberger, P.; Tarasow, T. M.; Heeger, A. J.; Soh, H. T. Micromagnetic Selection of Aptamers in Microfluidic Channels. *Proc. Natl. Acad. Sci. U.S.A.* **2009**, *106* (9), 2989–2994.
(28) Yang, K.-A.; Barbu, M.; Halim, M.; Pallavi, P.; Kim, B.; Kolpashchikov, D. M.; Pecic, S.; Taylor, S.; Worgall, T. S.; Stojanovic, M. N. Recognition and Sensing of Low-Epitope Targets via Ternary Complexes with Oligonucleotides and Synthetic Receptors. *Nature Chem* **2014**, *6* (11), 1003–1008.
(29) Yang, K.-A.; Pei, R.; Stefanovic, D.; Stojanovic, M. N. Optimizing Cross-Reactivity with Evolutionary Search for Sensors. *J. Am. Chem. Soc.* **2012**, *134* (3), 1642–1647.
(30) Nutiu, R.; Li, Y. In Vitro Selection of Structure-Switching Signaling Aptamers. *Angew. Chem.* **2005**, *44* (7), 1061–1065.
(31) Song, S.; Wang, L.; Li, J.; Fan, C.; Zhao, J. Aptamer-Based Biosensors. *Trends Anal. Chem.* **2008**, *27* (2), 108–117.
(32) Hoadley, K. A.; Purtha, W. E.; Wolf, A. C.; Flynn-Charlebois, A.; Silverman, S. K. Zn^{2+} -Dependent Deoxyribozymes That Form Natural and Unnatural RNA Linkages. *Biochemistry* **2005**, *44* (25), 9217–9231.
(33) Carmi, N.; Shultz, L. A.; Breaker, R. R. In Vitro Selection of Self-Cleaving DNAs. *Chem. Biol.* **1996**, 3 (12), 1039–1046.
(34) Cuenoud B., Szostak Jack W. A DNA Metalloenzyme with DNA Ligase Activity. *Nature* **1995**, 375, 611–614.
(35) Wang, W.; Billen, L. P.; Li, Y. Sequence Diversity, Metal Specificity, and Catalytic Proficiency of Metal-Dependent Phosphorylating DNA Enzymes. *Chem. Biol.* **2002**, *9* (4), 507–517.
(36) Li, Y.; Liu, Y.; Breaker, R. R. Capping DNA with DNA. *Biochemistry* **2000**, *39* (11), 3106–3114.
(37) Pradeepkumar, P. I.; Höbartner, C.; Baum, D. A.; Silverman, S. K. DNA-Catalyzed Formation of Nucleopeptide Linkages. *Angew. Chem.* **2008**, *47* (9), 1753–1757.
(38) Sheppard, T. L.; Ordoukhanian, P.; Joyce, G. F. A DNA Enzyme with N-Glycosylase Activity. *Proc. Natl. Acad. Sci. U.S.A.* **2000**, *97* (14), 7802–7807.
(39) Chandra, M.; Silverman, S. K. DNA and RNA Can Be Equally Efficient Catalysts for Carbon−Carbon Bond Formation. *J. Am. Chem. Soc.* **2008**, *130* (10), 2936–2937.

(40) Chinnapen, D. J.-F.; Sen, D. A Deoxyribozyme That Harnesses Light to Repair Thymine Dimers in DNA. *Proc. Natl. Acad. Sci. U.S.A.* **2004**, *101* (1), 65–69.
(41) Burmeister, J.; von Kiedrowski, G.; Ellington, A. D. Cofactor-Assisted Self-Cleavage in DNA Libraries with a 3′–5′-Phosphoramidate Bond. *Angew. Chem.* **1997**, *36* (12), 1321–1324.
(42) Li, Y., Sen D. Toward an Efficient DNAzyme. *Biochemistry* **1997**, 36 (18), 5589–5599.
(43) Zhou, C.; Avins, J. L.; Klauser, P. C.; Brandsen, B. M.; Lee, Y.; Silverman, S. K. DNA-Catalyzed Amide Hydrolysis. *J. Am. Chem. Soc.* **2016**, *138* (7), 2106–2109.
(44) Mohan, U.; Burai, R.; McNaughton, B. R. In Vitro Evolution of a Friedel–Crafts Deoxyribozyme. *Org. Biomol. Chem.* **2013**, *11* (14), 2241.
(45) Chandrasekar, J.; Silverman, S. K. Catalytic DNA with Phosphatase Activity. *Proc. Natl. Acad. Sci. U.S.A.* **2013**, *110* (14), 5315–5320.
(46) Walsh, S. M.; Sachdeva, A.; Silverman, S. K. DNA Catalysts with Tyrosine Kinase Activity. *J. Am. Chem. Soc.* **2013**, *135* (40), 14928–14931.
(47) Ibrahim H., Mulyk P., Sen D. DNA G-Quadruplexes activate heme for robust catalysis of carbene transfer reactions. *ACS Omega* **2019**, 4 (12), 15280–15288.
(48) Liu, M.; Chang, D.; Li, Y. Discovery and Biosensing Applications of Diverse RNA-Cleaving DNAzymes. *Acc. Chem. Res.* **2017**, *50* (9), 2273–2283.
(49) Singh, N.; Ranjan, A.; Sur, S.; Chandra, R.; Tandon, V. Inhibition of HIV-1 Integrase Gene Expression by 10-23 DNAzyme. *J Biosci* **2012**, *37* (3), 493–502.
(50) Lermer, L.; Roupioz, Y.; Ting, R.; Perrin, D. M. Toward an RNaseA Mimic: A DNAzyme with Imidazoles and Cationic Amines. *J. Am. Chem. Soc.* **2002**, *124* (34), 9960–9961
(51) Silverman, S. K. Catalytic DNA: Scope, Applications, and Biochemistry of Deoxyribozymes. *Trends Biochem Sci* **2016**, *41* (7), 595–609.
(52) Nowakowski, J.; Shim, P. J.; Prasad, G. S.; Stout, C. D.; Joyce, G. F. Crystal Structure of an 82-Nucleotide RNA–DNA Complex Formed by the 10-23 DNA Enzyme. *Nat Struct Biol* **1999**, 6 (2):151-156.
(53) Ponce-Salvatierra, A.; Wawrzyniak-Turek, K.; Steuerwald, U.; Höbartner, C.; Pena, V. Crystal Structure of a DNA Catalyst. *Nature* **2016**, *529* (7585), 231–234.
(54) Kim, H.-K.; Liu, J.; Li, J.; Nagraj, N.; Li, M.; Pavot, C. M.-B.; Lu, Y. Metal-Dependent Global Folding and Activity of the 8-17 DNAzyme Studied by Fluorescence Resonance Energy Transfer. *J. Am. Chem. Soc.* **2007**, *129* (21), 6896–6902.
(55) Liu, H.; Yu, X.; Chen, Y.; Zhang, J.; Wu, B.; Zheng, L.; Haruehanroengra, P.; Wang, R.; Li, S.; Lin, J.; Li, J.; Sheng, J.; Huang, Z.; Ma, J.; Gan, J. Crystal Structure of an RNA-Cleaving DNAzyme. *Nat Commun* **2017**, *8* (1), 2006.
(56) Fan, H.; Zhang, X.; Lu, Y. Recent Advances in DNAzyme-Based Gene Silencing. *Sci. China Chem.* **2017**, *60* (5), 591–601.
(57) Kolb, H. C.; Finn, M. G.; Sharpless, K. B. Click Chemistry: Diverse Chemical Function from a Few Good Reactions. *Angew. Chem.* **2001**, 40 (11), 2004-2021.
(58) Liang, L.; Astruc, D. The Copper(I)-Catalyzed Alkyne-Azide Cycloaddition (CuAAC) “Click” Reaction and Its Applications. An Overview. *Coord. Chem. Rev.* **2011**, *255* (23–24), 2933–2945.
(59) Hein, C. D.; Liu, X.-M.; Wang, D. Click Chemistry, A Powerful Tool for Pharmaceutical Sciences. *Pharm Res* **2008**, *25* (10), 2216–2230.
(60) Haldón, E.; Nicasio, M. C.; Pérez, P. J. Copper-Catalysed Azide–Alkyne Cycloadditions (CuAAC): An Update. *Org. Biomol. Chem.* **2015**, *13* (37), 9528–9550.
(61) Tornøe, C. W.; Christensen, C.; Meldal, M. Peptidotriazoles on Solid Phase: [1,2,3]-Triazoles by Regiospecific Copper(I)-Catalyzed 1,3-Dipolar Cycloadditions of Terminal Alkynes to Azides. *J. Org. Chem.* **2002**, *67* (9), 3057–3064.

(62) Rostovtsev V. V., Green L., Fokin V. V., Sharpless K. B. A Stepwise Huisgen Cycloaddition Process Copper(I)-Catalyzed Regioselective Ligation of Azides and Terminal Alkynes. *Angew. Chem.* 2002, 114 (14), 2708-2711.
(63) Lutz, J.; Zarafshani, Z. Efficient Construction of Therapeutics, Bioconjugates, Biomaterials and Bioactive Surfaces Using Azide–Alkyne "Click" Chemistry. *Adv. Drug Deliv. Rev.* **2008**, *60* (9), 958–970.
(64) Johnson, J. A.; Finn, M. G.; Koberstein, J. T.; Turro, N. J. Construction of Linear Polymers, Dendrimers, Networks, and Other Polymeric Architectures by Copper-Catalyzed Azide-Alkyne Cycloaddition "Click" Chemistry. *Macromol. Rapid Commun.* **2008**, *29* (12–13), 1052–1072.
(65) Himo, F.; Lovell, T.; Hilgraf, R.; Rostovtsev, V. V.; Noodleman, L.; Sharpless, K. B.; Fokin, V. V. Copper(I)-Catalyzed Synthesis of Azoles. DFT Study Predicts Unprecedented Reactivity and Intermediates. *J. Am. Chem. Soc.* **2005**, *127* (1), 210–216.
(66) Kuang, G.-C.; Guha, P. M.; Brotherton, W. S.; Simmons, J. T.; Stankee, L. A.; Nguyen, B. T.; Clark, R. J.; Zhu, L. Experimental Investigation on the Mechanism of Chelation-Assisted, Copper(II) Acetate-Accelerated Azide–Alkyne Cycloaddition. *J. Am. Chem. Soc.* **2011**, *133* (35), 13984–14001.
(67) Rodionov V. O., Fokin V. V., Finn M. G. Mechanism of the Ligand-Free CuI-Catalyzed Azide–Alkyne Cycloaddition Reaction. *Angew. Chem.* **2005**, 117 (15), 2250-2255.
(68) Rodionov V. O., Presolski S. I., Díaz D. D., Fokin V. V., Finn M. G. Ligand-Accelerated Cu-Catalyzed Azide−Alkyne Cycloaddition A Mechanistic Report. *J. Am. Chem. Soc.* **2007**, 129 (42), 12705-12712.
(69) Worrell, B. T.; Malik, J. A.; Fokin, V. V. Direct Evidence of a Dinuclear Copper Intermediate in Cu(I)-Catalyzed Azide-Alkyne Cycloadditions. *Science* **2013**, *340* (6131), 457–460.
(70) Hein, J. E.; Tripp, J. C.; Krasnova, L. B.; Sharpless, K. B.; Fokin, V. V. Copper(I)-Catalyzed Cycloaddition of Organic Azides and 1-Iodoalkynes. *Angew. Chem.* **2009**, *48* (43), 8018–8021.
(71) Partyka, D. V.; Gao, L.; Teets, T. S.; Updegraff, J. B.; Deligonul, N.; Gray, T. G. Copper-Catalyzed Huisgen [3 + 2] Cycloaddition of Gold(I) Alkynyls with Benzyl Azide. Syntheses, Structures, and Optical Properties. *Organometallics* **2009**, *28* (21), 6171–6182.
(72) Kuang, G.-C.; Guha, P. M.; Brotherton, W. S.; Simmons, J. T.; Stankee, L. A.; Nguyen, B. T.; Clark, R. J.; Zhu, L. Experimental Investigation on the Mechanism of Chelation-Assisted, Copper(II) Acetate-Accelerated Azide–Alkyne Cycloaddition. *J. Am. Chem. Soc.* **2011**, *133* (35), 13984–14001.
(73) Nolte, C.; Mayer, P.; Straub, B. F. Isolation of a Copper(I) Triazolide: A "Click" Intermediate. *Angew. Chem.* **2007**, *46* (12), 2101–2103.
(74) Iacobucci, C.; Reale, S.; Gal, J.-F.; De Angelis, F. Dinuclear Copper Intermediates in Copper(I)-Catalyzed Azide-Alkyne Cycloaddition Directly Observed by Electrospray Ionization Mass Spectrometry. *Angew. Chem.* **2015**, *54* (10), 3065–3068.
(75) Jin, L.; Tolentino, D. R.; Melaimi, M.; Bertrand, G. Isolation of Bis(Copper) Key Intermediates in Cu-Catalyzed Azide-Alkyne "Click Reaction." *Sci. Adv.* **2015**, *1* (5), e1500304.
(76) Ziegler M. S., Lakshmi K. V., T. Tilley D. Dicopper Cu(I)Cu(I) and Cu(I)Cu(II) Complexes in Copper-Catalyzed Azide−Alkyne Cycloaddition. *J. Am. Chem. Soc.* **2017**, 139 (15), 5378–5386.

(77) Hong, V.; Presolski, S. I.; Ma, C.; Finn, M. G. Analysis and Optimization of Copper-Catalyzed Azide-Alkyne Cycloaddition for Bioconjugation. *Angew. Chem.* **2009**, *121* (52), 10063–10067.
(78) Pham, A. N.; Xing, G.; Miller, C. J.; Waite, T. D. Fenton-like Copper Redox Chemistry Revisited: Hydrogen Peroxide and Superoxide Mediation of Copper-Catalyzed Oxidant Production. *J. Catal.* **2013**, *301*, 54–64.
(79) Gaetke, L. M.; Chow-Johnson, H. S.; Chow, C. K. Copper: Toxicological Relevance and Mechanisms. *Arch Toxicol* **2014**, *88* (11), 1929–1938.
(80) Kuwabara, M. D., Sigman D. S. Footprinting DNA-Protein complexes in Situ following gel retardation assays using 1,10-phenanthroline-copper ion: Escherichia Coli RNA polymerase-Lac promoter complexes. *Biochemistry* **1987**, 26 (23), 7234-8.
(81) Agard, N. J.; Prescher, J. A.; Bertozzi, C. R. A Strain-Promoted [3 + 2] Azide−Alkyne Cycloaddition for Covalent Modification of Biomolecules in Living Systems. *J. Am. Chem. Soc.* **2004**, *126* (46), 15046–15047.
(82) Baskin, J. M.; Prescher, J. A.; Laughlin, S. T.; Agard, N. J.; Chang, P. V.; Miller, I. A.; Lo, A.; Codelli, J. A.; Bertozzi, C. R. Copper-Free Click Chemistry for Dynamic in Vivo Imaging. *Proc. Natl. Acad. Sci. U.S.A.* **2007**, *104* (43), 16793–16797.
(83) Jewett, J. C.; Sletten, E. M.; Bertozzi, C. R. Rapid Cu-Free Click Chemistry with Readily Synthesized Biarylazacyclooctynones. *J. Am. Chem. Soc.* **2010**, *132* (11), 3688–3690.
(84) Presolski, S. I.; Hong, V.; Cho, S.-H.; Finn, M. G. Tailored Ligand Acceleration of the Cu-Catalyzed Azide−Alkyne Cycloaddition Reaction: Practical and Mechanistic Implications. *J. Am. Chem. Soc.* **2010**, *132* (41), 14570–14576.
(85) Baskin, J. M.; Bertozzi, C. R. Bioorthogonal Click Chemistry: Covalent Labeling in Living Systems. *QSAR Comb. Sci.* **2007**, *26* (11–12), 1211–1219.
(86) van Geel, R.; Pruijn, G. J. M.; van Delft, F. L.; Boelens, W. C. Preventing Thiol-Yne Addition Improves the Specificity of Strain-Promoted Azide–Alkyne Cycloaddition. *Bioconjugate Chem.* **2012**, *23* (3), 392–398.
(87) Uttamapinant, C.; Tangpeerachaikul, A.; Grecian, S.; Clarke, S.; Singh, U.; Slade, P.; Gee, K. R.; Ting, A. Y. Fast, Cell-Compatible Click Chemistry with Copper-Chelating Azides for Biomolecular Labeling. *Angew. Chem.* **2012**, *124* (24), 5954–5958.
(88) Bevilacqua V., King M., Chaumontet M., Nothisen M., Gabillet S., Buisson D., Puente C., Wagner A., Taran F. Copper-Chelating Azides for Efficient Click Conjugation Reactions in Complex Media. *Angew. Chem.* **2014**, 126 (23), 5982-5986.
(89) Barceloux, D. G. Copper. *Clin. Toxicol.* **1999**, *37* (2), 217–230.
(90) Rubino, J. T.; Franz, K. J. Coordination Chemistry of Copper Proteins: How Nature Handles a Toxic Cargo for Essential Function. *J. Inorg. Biochem.* **2012**, *107* (1), 129–143.
(91) Donnelly, P. S.; Xiao, Z.; Wedd, A. G. Copper and Alzheimer's Disease. *Curr Opin Chem Biol* **2007**, *11* (2), 128–133.
(92) Curtain C. C., Ali F., Volitakis I., Cherny R. A., Norton R. S., Beyreuther K., Barrow C. J., Masters C. L., Bush A. I., Barnham K. J. Alzheimer's Disease Amyloid-β Binds Copper and Zinc to Generate an Allosterically Ordered Membrane-Penetrating Structure Containing Superoxide Dismutase-like Subunits. *J Biol Chem* **2001**, *276* (23), 20466–20473.
(93) Carmi, N.; Balkhi, S. R.; Breaker, R. R. Cleaving DNA with DNA. *Proc. Natl. Acad. Sci. U.S.A.* **1998**, *95* (5), 2233–2237.
(94) Hiai, S. Effects of Cupric Ions on Thermal Denaturation of Nucleic Acids. *J. Mol. Biol.* **1965**, *11* (4), 672–690.

(95) Eichhorn G. L., Clark P. Interaction of metal ions with polynucleotides and related compounds, V. the unwinding and rewinding of the DNA strands under the influence of Cu(II) ions. *Proc. Natl. Acad. Sci. U.S.A.* **1965**, 53 (3), 586–593.
(96) Sissoëff, I.; Grisvard, J.; Guillé, E. Studies on Metal Ions-DNA Interactions: Specific Behaviour of Reiterative DNA Sequences. *Prog. Biophys. Mol. Biol.* **1978**, *31*, 165–199.
(97) Sagripanti J-L., Kraemerll, K. Site-Specific Oxidative DNA Damage at Polyguanosines Produced by Copper Plus Hydrogen Peroxide. *J. Biol. Chem.* **1989**, 264 (3), 1729-1734.
(98) Drouin, R.; Rodriguez, H.; Gao, S.-W.; Gebreyes, Z.; O'Connor, T. R.; Holmquist, G. P.; Akman, S. A. Cupric Ion/Ascorbate/Hydrogen Peroxide-Induced DNA Damage: DNA-Bound Copper Ion Primarily Induces Base Modifications. *Free Radic. Biol. Med.* **1996**, *21* (3), 261–273.
(99) Prütz, W. A.; Butler, J.; Land, E. J. Interaction of Copper(I) with Nucleic Acids. *Int. J. Radiat. Biol* **1990**, *58* (2), 215–234.
(100) Prütz, W. A. The Interaction between Hydrogen Peroxide and the DNA -Cu (I) Complex: Effects of PH and Buffers. *Z. Naturforsch. C* **1990**, *45* (11–12), 1197–1206.
(101) Stoewe, R.; Prütz, W. A. Copper-Catalyzed DNA damage by ascorbate and hydrogen peroxide: Kinetics and Yield. *Free Radic. Biol. Med.* **1987**, *3* (2), 97–105.
(102) Yamamoto, K.; Kawanishi S, S. Hydroxyl Free Radical Is Not the Main Active Species in Site-Specific DNA Damage Induced by Copper(I1) Ion and Hydrogen Peroxide. *J Biol Chem* **1989**, 264 (26), 15435-15440.
(103) Burda, J. V.; Šponer, J.; Leszczynski, J.; Hobza, P. Interaction of DNA Base Pairs with Various Metal Cations (Mg^{2+}, Ca^{2+}, Sr^{2+}, Ba^{2+}, Cu^{+}, Ag^{+}, Au^{+}, Zn^{2+}, Cd^{2+}, and Hg^{2+}): Nonempirical Ab Initio Calculations on Structures, Energies, and Nonadditivity of the Interaction. *J. Phys. Chem. B* **1997**, 101 (46), 9670–9677.
(104) Eichhorn, G. L.; Shin, Y. Ae. Interaction of Metal Ions with Polynucleotides and Related Compounds. XII. The Relative Effect of Various Metal Ions on DNA Helicity. *J. Am. Chem. Soc.* **1968**, *90* (26), 7323–7328.
(105) Aoki, K.; Clark, G. R.; Orbell, J. D. Metal-Phosphate Bonding in Transition Metal·nucleotide Complexes. The Crystal and Molecular Structures of the Polymeric Copper(II) Complex of Guanosine 5′-Monophosphate. *Biochim. Biophys. Acta* **1976**, *425* (3), 369–371.
(106) De Meester, P.; Goodgame, D. M. L.; Skapski, A. C.; Smith, B. T. X-Ray Structure of a Hydrated Nickel Salt of Guanosine 5′-Monophosphate; Evidence for the Absence of Direct Metal-Phosphate Bonding. *Biochim. Biophys. Acta* **1974**, *340* (1), 113–115.
(107) Kagawa T. F., Geierstange B. H., Wang H.-J., Ho P. S. Covalent Modification of Guanine Bases in Double-Stranded DNA. *J Biol Chem* **1991**, 266 (30), 20175-20184.
(108) Rodriguez H., Drouin R., Holmquist G. P., Connor T. R., Boiteux S., Laval J., Doroshow J. H., Akman S. A. Mapping of copper/hydrogen peroxide-induced DNA damage at nucleotide resolution in human genomic DNA by ligation-mediated polymerase chain reaction Mapping Cu(II) H_2O_2 DNA Damage. *J Biol Chem* **1995**, 270 (29),17633-17640.
(109) Sigel, R. K. O.; Sigel, H. A Stability Concept for Metal Ion Coordination to Single-Stranded Nucleic Acids and Affinities of Individual Sites. *Acc. Chem. Res.* **2010**, *43* (7), 974–984.
(110) Knobloch, B.; Sigel, H. A Quantitative Appraisal of the Ambivalent Metal Ion Binding Properties of Cytidine in Aqueous Solution and an Estimation of the Anti–Syn Energy Barrier of Cytidine Derivatives. *J Biol Inorg Chem* **2004**, *9* (3), 365–373.

(111) Da Costa, C. P.; Sigel, H. Acid−Base and Metal Ion Binding Properties of Guanylyl (3'-5')Guanosine (GpG^-) and 2'-Deoxyguanylyl(3'-5')-2'-Deoxyguanosine [$d(GpG)^-$] in Aqueous Solution. *Inorg. Chem.* **2003**, *42* (11), 3475–3482.
(112) Costa, C. P. D.; Sigel, H. Stabilities of Complexes Formed between Lead(II) and Simple Phosphonate or Phosphate Monoester Ligands Including Some Pyrimidine-Nucleoside 5b-Monophosphates (CMP^{2-}, UMP^{2-}, DTMP2–). *J Biol Inorg Chem* **1999**, 4, 508–514.
(113) Haldón, E.; Nicasio, M. C.; Pérez, P. J. Copper-Catalysed Azide–Alkyne Cycloadditions (CuAAC): An Update. *Org. Biomol. Chem* **2015**, 13 (37), 9528–9550.
(114) Appukkuttan, P.; Dehaen, W.; Fokin, V. V.; Van der Eycken, E. A Microwave-Assisted Click Chemistry Synthesis of 1,4-Disubstituted 1,2,3-Triazoles via a Copper(I)-Catalyzed Three-Component Reaction. *Org. Lett.* **2005**, *36*, 10.
(115) Brewer, G. J. Risks of Copper and Iron Toxicity during Aging in Humans. *Chem. Res. Toxicol.* **2010**, *23* (2), 319–326.
(116) Soares, E. V.; Hebbelinck, K.; Soares, H. M. Toxic Effects Caused by Heavy Metals in the Yeast *Saccharomyces Cerevisiae*: A Comparative Study. *Can. J. Microbiol.* **2003**, *49* (5), 336–343.
(117) Wang, Q.; Chan, T. R.; Hilgraf, R.; Fokin, V. V.; Sharpless, K. B.; Finn, M. G. Bioconjugation by Copper(I)-Catalyzed Azide-Alkyne [3 + 2] Cycloaddition. *J. Am. Chem. Soc.* **2003**, *125* (11), 3192–3193.
(118) Tuerk, C.; Gold, L. Systematic Evolution of Ligands by Exponential Enrichment: RNA Ligands to Bacteriophage T4 DNA Polymerase. *Science* **1990**, *249* (4968), 505–510.
(119) Silverman, S. K. Catalytic DNA: Scope, Applications, and Biochemistry of Deoxyribozymes. *Trends Biochem Sci* **2016**, *41* (7), 595–609.
(120) Travascio, P.; Li, Y.; Sen, D. DNA-Enhanced Peroxidase Activity of a DNA Aptamer-Hemin Complex. *Chem. Biol.* **1998**, *5* (9), 505–517.
(121) Zuker, M. Mfold Web Server for Nucleic Acid Folding and Hybridization Prediction. *Nucleic Acids Res* **2003**, *31* (13), 3406–3415.
(122) Brotherton, W. S.; Michaels, H. A.; Simmons, J. T.; Clark, R. J.; Dalal, N. S.; Zhu, L. Apparent Copper(II)-Accelerated Azide−Alkyne Cycloaddition. *Org. Lett.* **2009**, *11* (21), 4954–4957.
(123) Saverot, S.; Geng, X.; Leng, W.; Vikesland, P. J.; Grove, T. Z.; Bickford, L. R. Facile, Tunable, and SERS-Enhanced HEPES Gold Nanostars. *RSC Adv.* **2016**, *6* (35), 29669–29673.
(124) Holman, M. R.; Ito, T.; Rokita, S. E. Self-Repair of Thymine Dimer in Duplex DNA. *J. Am. Chem. Soc.* **2007**, *129* (1), 6–7.
(125) Gao, J.; Berden, G.; Rodgers, M. T.; Oomens, J. Interaction of Cu^+ with Cytosine and formation of i-Motif-like C-M^+-C Complexes: Alkali versus Coinage Metals. *Phys. Chem. Chem. Phys.* **2016**, *18* (10), 7269–7277.
(126) Thirumurugan P., Matosiuk D. Jozwiak K. Click Chemistry for Drug Development and Diverse Chemical–Biology Applications. *Chem. Rev.* **2013**, 113 (7), 4905–4979.
(127) Nicosia, C.; Huskens, J. Reactive Self-Assembled Monolayers: From Surface Functionalization to Gradient Formation. *Mater. Horiz.* **2014**, *1* (1), 32–45.
(128) Collman, J. P.; Devaraj, N. K.; Chidsey, C. E. D. "Clicking" Functionality onto Electrode Surfaces. *Langmuir* **2004**, *20* (4), 1051–1053.
(129) Collman, J. P.; Devaraj, N. K.; Eberspacher, T. P. A.; Chidsey, C. E. D. Mixed Azide-Terminated Monolayers: A Platform for Modifying Electrode Surfaces. *Langmuir* **2006**, *22* (6), 2457–2464.

(130) Devaraj, N. K.; Miller, G. P.; Ebina, W.; Kakaradov, B.; Collman, J. P.; Kool, E. T.; Chidsey, C. E. D. Chemoselective Covalent Coupling of Oligonucleotide Probes to Self-Assembled Monolayers. *J. Am. Chem. Soc.* **2005**, *127* (24), 8600–8601.
(131) Ciampi, S.; Böcking, T.; Kilian, K. A.; James, M.; Harper, J. B.; Gooding, J. J. Functionalization of Acetylene-Terminated Monolayers on Si(100) Surfaces: A Click Chemistry Approach. *Langmuir* **2007**, *23* (18), 9320–9329.
(132) Ciampi, S.; Eggers, P. K.; Le Saux, G.; James, M.; Harper, J. B.; Gooding, J. J. Silicon (100) Electrodes Resistant to Oxidation in Aqueous Solutions: An Unexpected Benefit of Surface Acetylene Moieties. *Langmuir* **2009**, *25* (4), 2530–2539.
(133) Aiello, V.; Joo, N.; Buckley, J.; Nonglaton, G.; Duclairoir, F.; Dubois, L.; Marchon, J. C.; Gély, M.; Chevalier, N.; De Salvo, B. Redox Behavior of a Ferrocene Monolayer on SiO2 Obtained after Click-Coupling. *Surf. Sci.* **2013**, *612*, 57–62.
(134) Mpeta, L. S.; Fomo, G.; Nyokong, T. Click Chemistry Electrode Modification Using 4-Ethynylbenzyl Substituted Cobalt Phthalocyanine for Applications in Electrocatalysis. *J Coord Chem* **2018**, *71* (10), 1623–1638.
(135) Mishyn, V.; Aspermair, P.; Leroux, Y.; Happy, H.; Knoll, W.; Boukherroub, R.; Szunerits, S. "Click" Chemistry on Gold Electrodes Modified with Reduced Graphene Oxide by Electrophoretic Deposition. *Surfaces* **2019**, *2* (1), 193–204.
(136) Qiu, S.; Xie, L.; Gao, S.; Liu, Q.; Lin, Z.; Qiu, B.; Chen, G. Determination of Copper(II) in the Dairy Product by an Electrochemical Sensor Based on Click Chemistry. *Anal. Chim. Acta* **2011**, *707* (1–2), 57–61.
(137) Wei, T.; Dong, T.; Xing, H.; Liu, Y.; Dai, Z. Cucurbituril and Azide Cofunctionalized Graphene Oxide for Ultrasensitive Electro-Click Biosensing. *Anal. Chem.* **2017**, *89* (22), 12237–12243.
(138) Galán, T.; Prieto-Simón, B.; Alvira, M.; Eritja, R.; Götz, G.; Bäuerle, P.; Samitier, J. Label-Free Electrochemical DNA Sensor Using "Click"-Functionalized PEDOT Electrodes. *Biosens. Bioelectron.* **2015**, *74*, 751–756.
(139) Tang, Y.; Zhang, J.; Tang, D.; Teng, L.; Lv, J.; Tang, D. Click-Conjugation of Nanogold-Functionalized PAMAM Dendrimer: Toward a Novel Electrochemical Detection Platform. *Electroanalysis* **2015**, *27* (10), 2280–2285.
(140) Zhou Y., Wang S., Zhang K., Jiang X. Visual Detection of Copper(II) by Azide- and Alkyne-Functionalized Gold Nanoparticles Using Click Chemistry. *Angew. Chem.* **2008**, 47 (39), 7454-7456.
(141) Hong, V.; Steinmetz, N. F.; Manchester, M.; Finn, M. G. Labeling Live Cells by Copper-Catalyzed Alkyne−Azide Click Chemistry. *Bioconjugate Chem.* **2010**, *21* (10), 1912–1916.
(142) Tian, H.; Dai, Y.; Shao, H.; Yu, H.-Z. Modulated Intermolecular Interactions in Ferrocenylalkanethiolate Self-Assembled Monolayers on Gold. *J. Phys. Chem. C* **2013**, *117* (2), 1006–1012.
(143) Qi, L.; Tian, H.; Shao, H.; Yu, H.-Z. Host–Guest Interaction at Molecular Interfaces: Binding of Cucurbit[7]Uril on Ferrocenyl Self-Assembled Monolayers on Gold. *J. Phys. Chem. C* **2017**, *121* (14), 7985–7992.
(144) Good R. J. Contact Angle, Wetting, and Adhesion: a Critical Review. *J Adhes Sci Technol* **1992**, 6 (12), 1269-1302.
(145) Liu, K.; Lat, P. K.; Yu, H.-Z.; Sen, D. CLICK-17, a DNA Enzyme That Harnesses Ultra-Low Concentrations of Either Cu^{+} or Cu^{2+} to Catalyze the Azide-Alkyne 'Click' Reaction in Water. *Nucleic Acids Res* **2020**, 48 (13), 7356–7370.
(146) Hijazi, I.; Jousselme, B.; Jégou, P.; Filoramo, A.; Campidelli, S. Formation of Linear and Hyperbranched Porphyrin Polymers on Carbon Nanotubes via a CuAAC "Grafting from" Approach. *J. Mater. Chem.* **2012**, *22* (39), 20936.

(147) Dördelmann, G.; Meinhardt, T.; Sowik, T.; Krueger, A.; Schatzschneider, U. CuAAC Click Functionalization of Azide-Modified Nanodiamond with a Photoactivatable CO-Releasing Molecule (PhotoCORM) Based on $[Mn(CO)_3(Tpm)]$. *Chem. Commun.* **2012**, *48* (94), 11528.
(148) Toulemon, D.; Pichon, B. P.; Leuvrey, C.; Zafeiratos, S.; Papaefthimiou, V.; Cattoën, X.; Bégin-Colin, S. Fast Assembling of Magnetic Iron Oxide Nanoparticles by Microwave-Assisted Copper(I) Catalyzed Alkyne–Azide Cycloaddition (CuAAC). *Chem. Mater.* **2013**, *25* (14), 2849–2854.
(149) Vega, B.; Wondraczek, H.; Bretschneider, L.; Näreoja, T.; Fardim, P.; Heinze, T. Preparation of Reactive Fibre Interfaces Using Multifunctional Cellulose Derivatives. *Carbohydr. Polym.* **2015**, *132*, 261–273.
(150) Lange, N.; Dietrich, P. M.; Lippitz, A.; Kulak, N.; Unger, W. E. S. New Azidation Methods for the Functionalization of Silicon Nitride and Application in Copper-Catalyzed Azide-Alkyne Cycloaddition (CuAAC): New Azidation Method of Si_3N_4 and Application in Click Chemistry. *Surf. Interface Anal.* **2016**, *48* (7), 621–625.
(151) Gan, W.; Shi, Y.; Jing, B.; Cao, X.; Zhu, Y.; Gao, H. Produce Molecular Brushes with Ultrahigh Grafting Density Using Accelerated CuAAC Grafting-Onto Strategy. *Macromolecules* **2017**, *50* (1), 215–222.
(152) Zaidi, R.; Hadi, S. M. Strand Scission in DNA by Gossypol and Cu(II): Role of Cu(I) and Oxygen-Free Radicals. *J. Biochem. Toxicol.* **1992**, *7* (4), 213–217.
(153) G. Georgopoulos, A. Roy, M. J. Yono, P. ENVIRONMENTAL COPPER: ITS DYNAMICS AND HUMAN EXPOSURE ISSUES. *J TOXICOL ENV HEAL B* **2001**, *4* (4), 341–394.
(154) Reddi, G. S.; Rao, C. R. M. Analytical Techniques for the Determination of Precious Metals in Geological and Related Materials. *Analyst* **1999**, *124* (11), 1531–1540.
(155) Soodan, R. K.; Pakade, Y. B.; Nagpal, A.; Katnoria, J. K. Analytical Techniques for Estimation of Heavy Metals in Soil Ecosystem: A Tabulated Review. *Talanta* **2014**, *125*, 405–410.
(156) Liu, J.; Lu, Y. Colorimetric Cu(II) Detection with a Ligation DNAzyme and Nanoparticles. *Chem. Commun.* **2007**, No. 46, 4872.
(157) Wang, J.; Li, H.; Long, L.; Xiao, G.; Xie, D. Fast Responsive Fluorescence Turn-on Sensor for Cu(II) and Its Application in Live Cell Imaging. *J. Lumin.* **2012**, *132* (9), 2456–2461.
(158) Chai, X.; Zhou, X.; Zhu, A.; Zhang, L.; Qin, Y.; Shi, G.; Tian, Y. A Two-Channel Ratiometric Electrochemical Biosensor for In Vivo Monitoring of Copper Ions in a Rat Brain Using Gold Truncated Octahedral Microcages. *Angew. Chem.* **2013**, *52* (31), 8129–8133.
(159) Sreedhara, A.; Li, Y.; Breaker, R. R. Ligating DNA with DNA. *J. Am. Chem. Soc.* **2004**, *126* (11), 3454–3460.
(160) Liu, J.; Lu, Y. A DNAzyme Catalytic Beacon Sensor for Paramagnetic Cu^{2+} Ions in Aqueous Solution with High Sensitivity and Selectivity. *J. Am. Chem. Soc.* **2007**, *129* (32), 9838–9839.
(161) Yin, B.-C.; Ye, B.-C.; Tan, W.; Wang, H.; Xie, C.-C. An Allosteric Dual-DNAzyme Unimolecular Probe for Colorimetric Detection of Copper(II). *J. Am. Chem. Soc.* **2009**, *131* (41), 14624–14625.
(162) Liu, M.; Zhao, H.; Chen, S.; Yu, H.; Zhang, Y.; Quan, X. A “Turn-on” Fluorescent Copper Biosensor Based on DNA Cleavage-Dependent Graphene-Quenched DNAzyme. *Biosens. Bioelectron.* **2011**, *26* (10), 4111–4116.

(163) Huang, P.-J. J.; Liu, J. An Ultrasensitive Light-up Cu^{2+} Biosensor Using a New DNAzyme Cleaving a Phosphorothioate-Modified Substrate. *Anal. Chem.* **2016**, *88* (6), 3341–3347.
(164) Travascio, P.; Li, Y.; Sen, D. DNA-Enhanced Peroxidase Activity of a DNA Aptamer-Hemin Complex. *Chem. Biol.* **1998**, *5* (9), 505–517.
(165) Gan, N.; Liu, K.; Qi, L.; Zhang, G.; Guo, Y.; Sen, D.; Yu, H.-Z. DNAzyme-Catalyzed Click Chemistry for Facilitated Immobilization of Redox Functionalities on Self-Assembled Monolayers. *J. Phys. Chem. C* **2020**, *124* (35), 19083–19090.
(166) Yu, H.-Z.; Luo, C.-Y.; Sankar, C. G.; Sen, D. Voltammetric Procedure for Examining DNA-Modified Surfaces: Quantitation, Cationic Binding Activity, and Electron-Transfer Kinetics. *Anal. Chem.* **2003**, *75* (15), 3902–3907.
(167) Drummond, T. G.; Hill, M. G.; Barton, J. K. Electrochemical DNA Sensors. *Nat Biotechnol* **2003**, *21* (10), 1192–1199.
(168) Furst, A. L.; Hill, M. G.; Barton, J. K. DNA-Modified Electrodes Fabricated Using Copper-Free Click Chemistry for Enhanced Protein Detection. *Langmuir* **2013**, *29* (52), 16141–16149.
(169) Malvano, R.; Boniolo, A.; Dovis, M.; Zannino, M. Elisa for Antibody Measurement: Aspects Related to Data Expression. *J. Immunol. Methods* **1982**, *48* (1), 51–60.
(170) Boren, B. C.; Narayan, S.; Rasmussen, L. K.; Zhang, L.; Zhao, H.; Lin, Z.; Jia, G.; Fokin, V. V. Ruthenium-Catalyzed Azide−Alkyne Cycloaddition: Scope and Mechanism. *J. Am. Chem. Soc.* **2008**, *130* (28), 8923–8930.
(171) Lamberti, M.; Fortman, G. C.; Poater, A.; Broggi, J.; Slawin, A. M. Z.; Cavallo, L.; Nolan, S. P. Coordinatively Unsaturated Ruthenium Complexes As Efficient Alkyne-Azide Cycloaddition Catalysts. *Organometallics* **2012**, *31* (2), 756–767.
(172) McNulty, J.; Keskar, K.; Vemula, R. The First Well-Defined Silver(I)-Complex-Catalyzed Cycloaddition of Azides onto Terminal Alkynes at Room Temperature. *Chem. Eur. J.* **2011**, *17* (52), 14727–14730.
(173) Rauret, G.; Rubio, R.; López-Sánchez, J. F.; Casassas, E. Determination and Speciation of Copper and Lead in Sediments of a Mediterranean River (River Tenes, Catalonia, Spain). *Water Res.* **1988**, *22* (4), 449–455.
(174) Woodward, R. B.; Rosenblum, M.; Whiting, M. C. A new aromatic system. *J. Am. Chem. Soc.* **1952**, 74 (13), 3458–3459.
(175) Fischer, E. O. Auf dem Weg zu Carben- und Carbin-Komplexen (Nobel-Vortrag). *Angew. Chem.* **1974**, *86* (18), 651–663.
(176) Werner, H. At Least 60 Years of Ferrocene: The Discovery and Rediscovery of the Sandwich Complexes. *Angew. Chem.* **2012**, *51* (25), 6052–6058.
(177) Martinez, R.; Tiripicchio, A. Structure of Ferrocenium Hexafluorophosphate. *Acta Cryst.* **1990**, *46* (2), 202–205.
(178) Dunitz, J. D.; Orgel, L. E.; Rich, A. The Crystal Structure of Ferrocene. *Acta Cryst* **1956**, *9* (4), 373–375.
(179) Heinze, K.; Lang, H. Ferrocene—Beauty and Function. *Organometallics* **2013**, *32* (20), 5623–5625.
(180) Saleem, M.; Yu, H.; Wang, L.; Zain-ul-Abdin; Khalid, H.; Akram, M.; Abbasi, N. M.; Huang, J. Review on Synthesis of Ferrocene-Based Redox Polymers and Derivatives and Their Application in Glucose Sensing. *Anal. Chim. Acta* **2015**, *876*, 9–25.
(181) Yang, K.-A.; Pei, R.; Stojanovic, M. N. In Vitro Selection and Amplification Protocols for Isolation of Aptameric Sensors for Small Molecules. *Methods* **2016**, *106*, 58–65.
(182) Nakatsuka, N.; Yang, K.-A.; Abendroth, J. M.; Cheung, K. M.; Xu, X.; Yang, H.; Zhao, C.; Zhu, B.; Rim, Y. S.; Yang, Y.; Weiss, P. S.; Stojanović, M. N.; Andrews, A.

M. Aptamer–Field-Effect Transistors Overcome Debye Length Limitations for Small-Molecule Sensing. *Science* **2018**, *362* (6412), 319–324.
(183) Yang, W.; Yu, H.; Alkhamis, O.; Liu, Y.; Canoura, J.; Fu, F.; Xiao, Y. In Vitro Isolation of Class-Specific Oligonucleotide-Based Small-Molecule Receptors. *Nucleic Acids Res* **2019**, *47* (12), e71–e71.
(184) Thomas, J. M.; Chakraborty, B.; Sen, D.; Yu, H.-Z. Analyte-Driven Switching of DNA Charge Transport: *De Novo* Creation of Electronic Sensors for an Early Lung Cancer Biomarker. *J. Am. Chem. Soc.* **2012**, *134* (33), 13823–13833.
(185) Puppulin, L.; Hosogi, S.; Sun, H.; Matsuo, K.; Inui, T.; Kumamoto, Y.; Suzaki, T.; Tanaka, H.; Marunaka, Y. Bioconjugation Strategy for Cell Surface Labelling with Gold Nanostructures Designed for Highly Localized PH Measurement. *Nat Commun* **2018**, *9* (1), 5278.
(186) Link, A. J.; Tirrell, D. A. Cell Surface Labeling of *Escherichia c Oli* via Copper(I)-Catalyzed [3+2] Cycloaddition. *J. Am. Chem. Soc.* **2003**, *125* (37), 11164–11165.
(187) Dieck T., S.; Müller, A.; Nehring, A.; Hinz, F. I.; Bartnik, I.; Schuman, E. M.; Dieterich, D. C. Metabolic Labeling with Noncanonical Amino Acids and Visualization by Chemoselective Fluorescent Tagging. *Curr Protoc Cell Biol* **2012**, Chapter 7:Unit7.11.
(188) Yu, H.; Alkhamis, O.; Canoura, J.; Liu, Y.; Xiao, Y. Advances and Challenges in Small-Molecule DNA Aptamer Isolation, Characterization, and Sensor Development. *Angew. Chem.* **2021**, 60, 2–26.

Appendix A: Supporting Information for Chapter 2

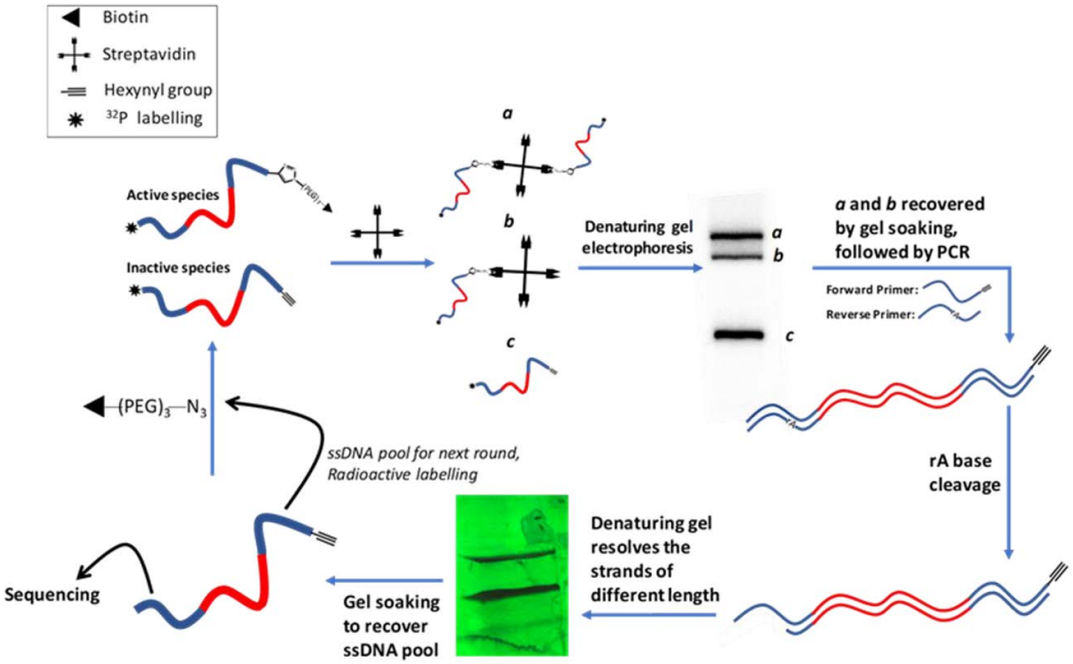

Figure A1 Schematic diagram for the SELEX scheme used in this work. (1) Reaction of a folded, random sequenced ('N40' within 80 nt) 5'-hexynyl single-stranded DNA (ssDNA) pool/library with azide-biotin (the black arrowhead represents the biotin moiety) and in situ generated Cu(I); (2) separation of individual sequences of CuAAC-coupled 5'-hexynyl ssDNAs from unreacted DNAs in the library by binding to streptavidin ('StAv') followed by (3) denaturing (or native) gel electrophoresis; (4) purification from the gel of StAv-retarded DNA bands, and their PCR amplification using a 5'-alkynated forward DNA primer and a reverse DNA primer incorporating a single internal adenine riboside ('rA'). (5) Hot-base cleavage of the ribose-containing DNA strand within the PCR-generated duplex; (6) size-separation and purification of the alkynylated ssDNA from the non-alkynylated ssDNA; and (7) repetition of the selection cycle, or sequencing of the DNA pool (8) to identify individual DNA sequences that promote CuAAC.

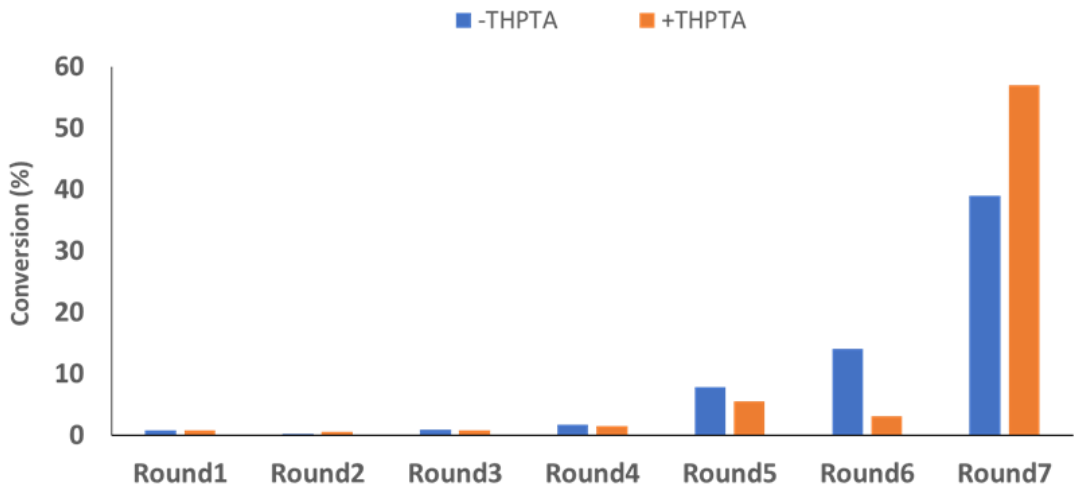

Figure A2 Enrichment of *in cis* CuAAC-catalyzing DNAzymes from the first seven rounds of *in vitro* selection. Enrichment percentages of the evolving random-sequence DNA library is plotted as a function of selection round, following the selection protocol shown in Figure 2.1.

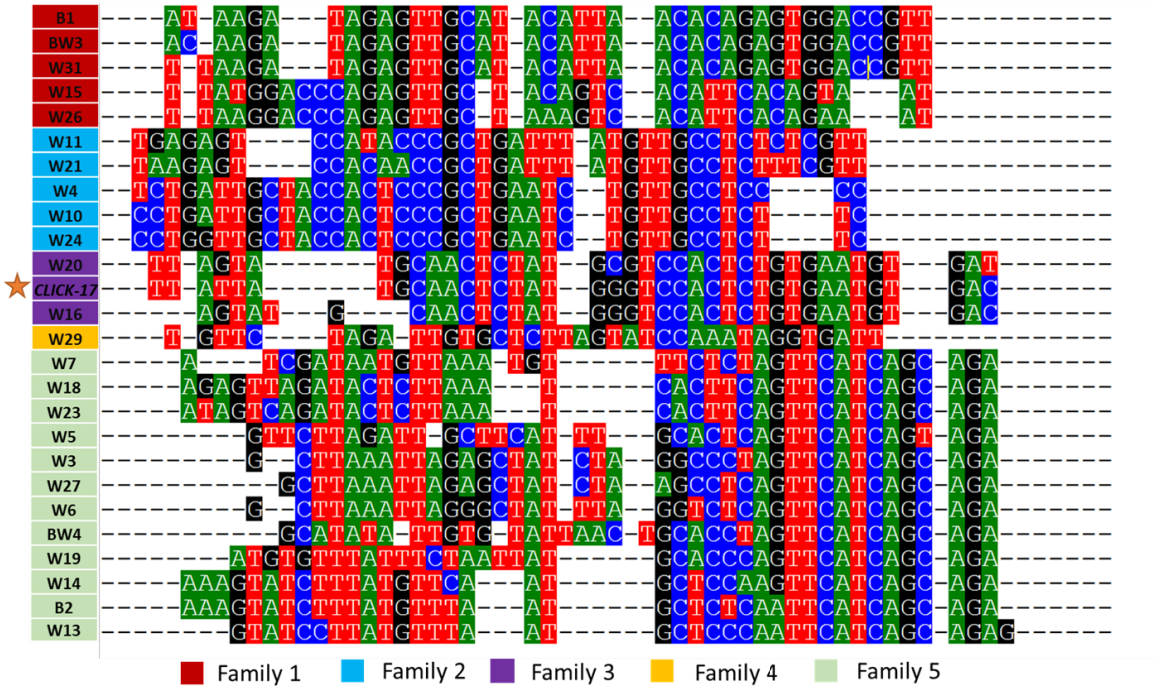

Figure A3 The N40 regions of cloned DNA sequences. 40 clones from Round 25 of the *in vitro* selection experiment are shown. Some of the sequences shown above were present in multiple clones. The clone CLICK-17, used for the bulk of this study, is shown with an asterisk.

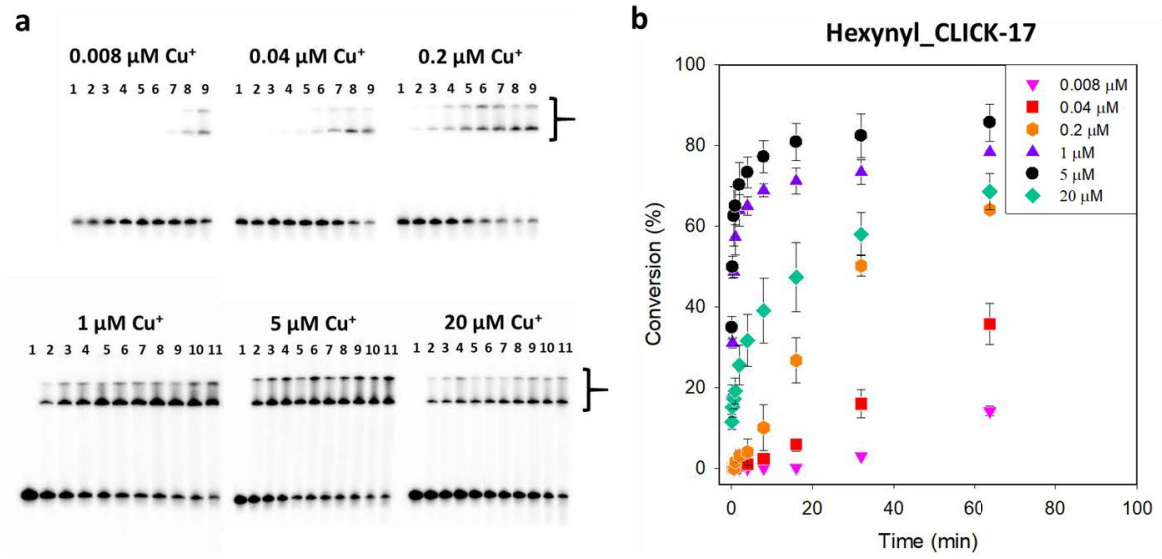

Figure A4 Kinetics for ≡-CLICK-17 biotinylation via CuAAC as a function of Cu(I) concentration. ≡-CLICK-17 DNA concentration was fixed at 2 µM. For the upper panel of three gels, lanes 1-9 show reaction times of: 0 min; 1; 2; 4; 8; 16; 32; 64; and 128 min, respectively. In the lower panel of three gels, lanes 1-11 show: 0 s; 10 s; 20 s; 40 s; then, 1; 2; 4; 8; 16; 32; and, 64 min. The error bars report one standard deviation from two independently collected data sets.

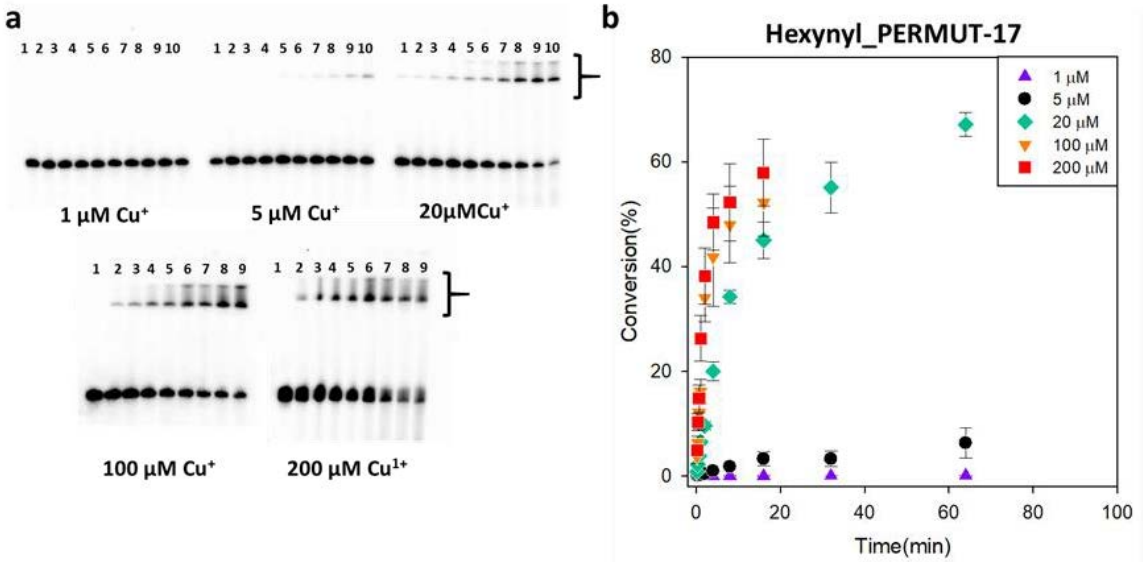

Figure A5 Kinetics for ≡-PERMUT-17 biotinylation via CuAAC as a function of Cu(I) concentration. ≡-PERMUT-17 DNA concentration was fixed at 2 µM. For the upper panel of three gels, lane 1-9 show reaction times of: 0 min; 1; 2; 4; 8; 16; 32; 64; and,128 min. In the lower two gels, lanes 1-11 show: 0 s; 10 s; 20 s; 40 s; 1 min; 2; 4; 8; 16; 32; and 64 min reactions. The error bars report one standard deviation from two independently collected data sets.

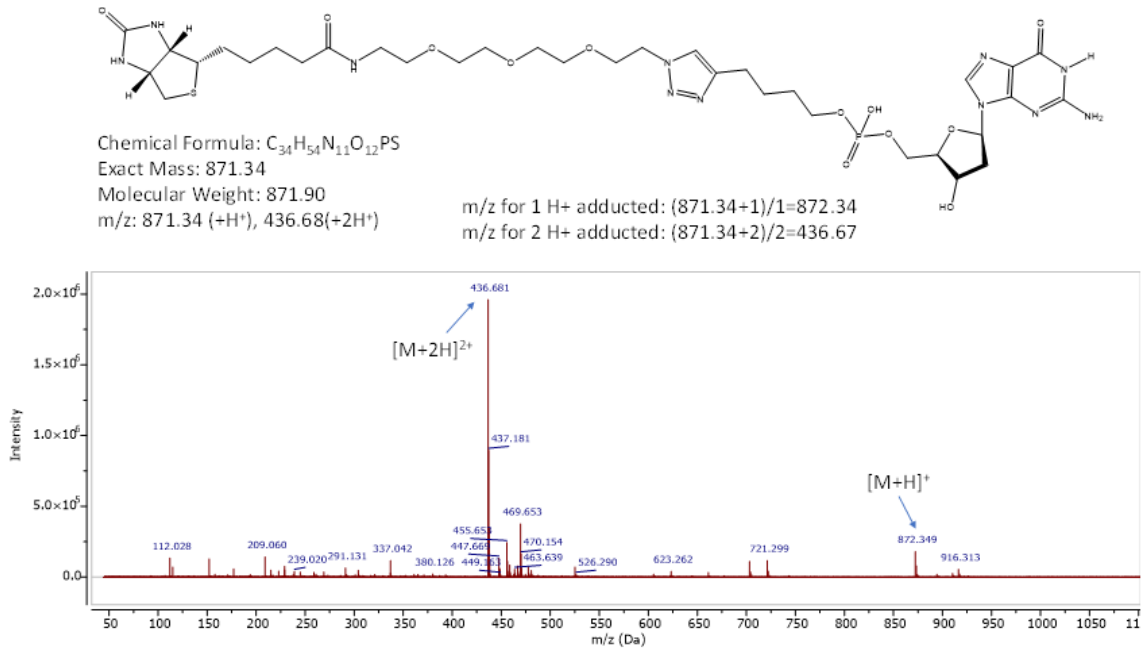

Figure A6 ESI Mass spectrometric analysis of the *in cis* conjugation of ≡-CLICK-17 with azide-biotin. The presumed conjugation product was first treated with Endonuclease P1, which degrades single-stranded DNA to 5'-deoxyribonucleotide monophosphates. Complete digestion of the conjugated product would leave a residual structure that incoporates the 5'-most deoxyriboguanosine monophosphate residue of the CLICK-17 DNA sequence linked to azide biotin via the triazole and linker atoms as shown.

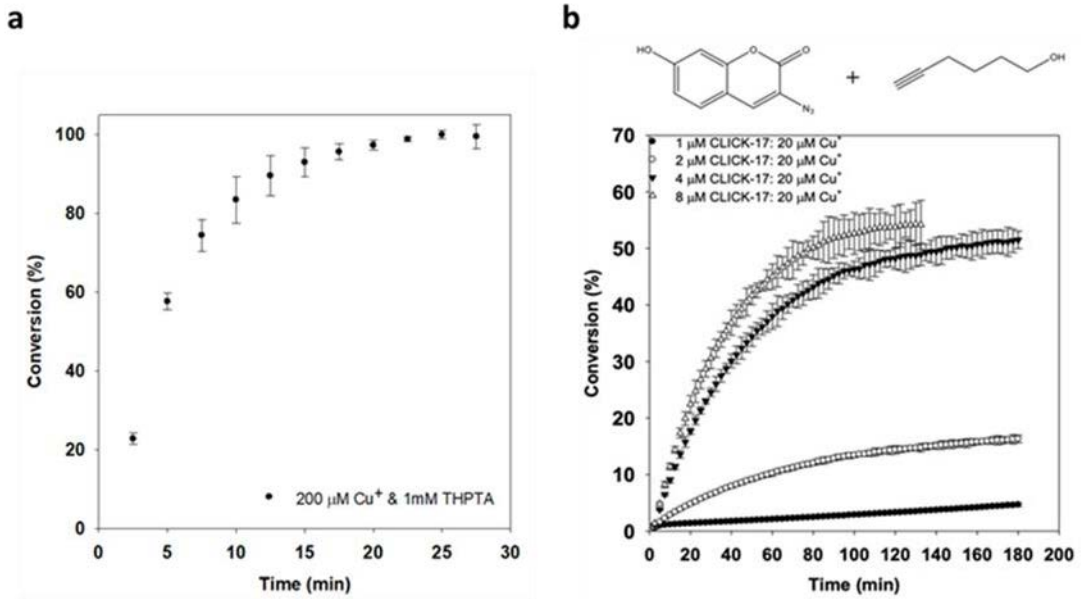

Figure A7 (a) Fluorescence calibration curve. Calibration curve for the CuAAC conversion of 50 μM azide-biotin using 2 mM propargyl alcohol in 50 mM Li-HEPES, pH 7.4; and 200 μM $CuSO_4$ in the presence of 2.5 mM sodium ascorbate and 1 mM THPTA. The DNA and the substrates were mixed in a reaction tube, and the reaction initiated with the addition

of ascorbate and THPTA to a final reaction volume of 40 µl. The solution was quickly transferred into a 384-well plate for fluorescence measurement in an Infinite M200 Pro (Tecan) fluorescence plate reader. The error bars report one standard deviation from three independently collected data sets; (b) The impact of CLICK-17 DNA concentrations on the *in trans* CuAAC reactions catalyzed by CLICK-17. Fixed concentrations of azide-coumarin (50 µM), hexynol (8 mM),and Cu(I) (20 µM) were used in R buffer, at 22 °C, with CLICK-17 DNA concentration varying, as above. The error bars report one standard deviation from three independently collected data sets.

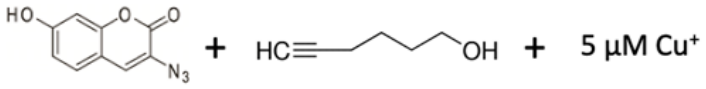

a

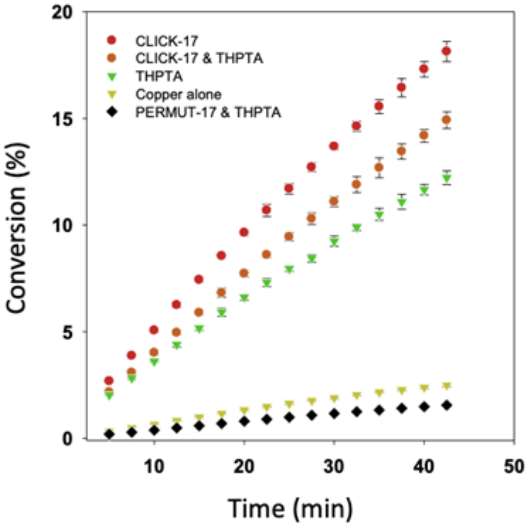

b

	Initial rate (µM/min)
2 µM CLICK-17	0.24
2 µM CLICK-17 + 25 µM THPTA	0.19
25 µM THPTA	0.16
Cu^+ alone	0.03
2 µM PERMUT-17 + 25 µM THPTA	0.02
2 µM PERMUT-17	< 0.01

Figure A8 CLICK-17 is capable of utilizing Cu(I) to catalyze CuAAC *in trans* between freely diffusing hexynol and azide-coumarin substrates. The conditions of reaction consisted of 50 µM 3-azido-7-hydroxycoumarin ('azide-coumarin'), 8 mM hexynol, 5 µM Cu(I), and the different combination of catalysts and reagents shown in the Table. Reactions were started by the addition of sodium ascorbate. The error bars report one standard deviation from three independently collected data sets.

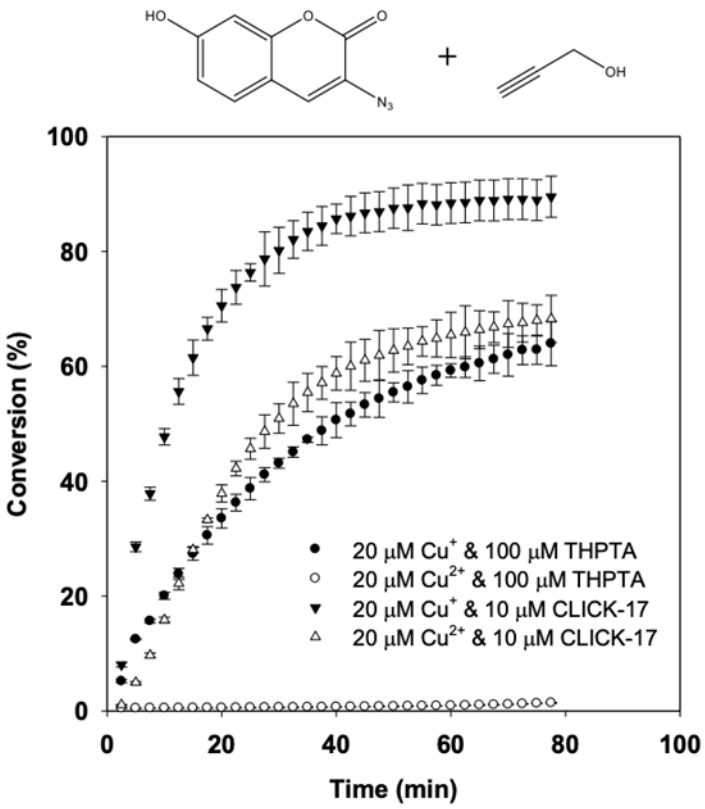

Figure A9 CLICK-17 catalysis with Cu(I) and Cu(II) under optimized conditions. Catalysis *in trans* for quantitative conversion to product was achieved within 40 min in the presence of Cu(I) (20 μM Cu(I), 10 μM CLICK-17, 50 μM azide-coumarin, 20 mM propargyl alcohol) at 22 °C in R buffer. A comparison yield at 40 min with 100 μM THPTA is ~ 55%. In the presence of Cu(II), however, yield over 40 min with 10 μM CLICK-17 is ~60%, while with 100 μM THPTA, only ~2%. In these experiments, azide-coumarin is the limiting subsrate; and with 20 mM propargyl alcohol CuAAC is ~90% complete within 40 min at 22 °C, whereas with 100 μM THPTA ligand replacing CLICK-17, only ~60% of the reaction is completed even after 80 min. The use of Cu(II)instead of Cu(I) gives an even more striking result, with > 60% reaction completion in 80 min with CLICK-17 and no reaction on this timescale with THPTA replacing CLICK-17. The error bars report one standard deviation from three independently collected data sets.

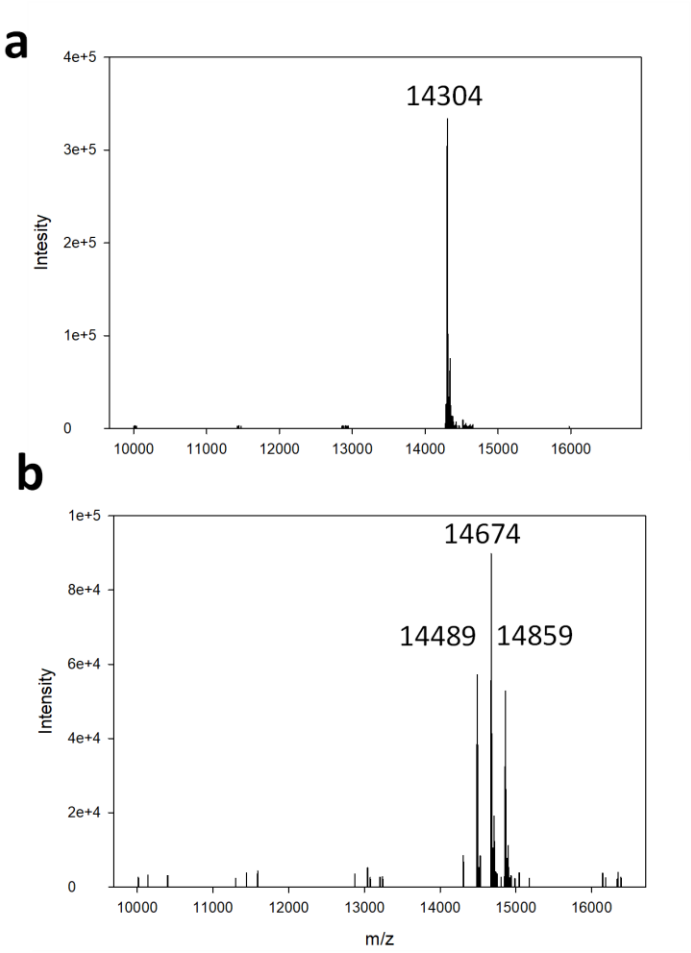

Figure A10 ESI mass spectrometry analysis of the azide labeling of lysozyme. Top, lysozyme protein whole protein LC-mass spectrometry data (ESI). The peak at 14304 Da is consistent with molecular weight of lysozyme. Bottom, lysozyme labelled with N3-PEG2-NHS ester. The peak at 14303 decreased dramatically, and three new peaks appears at 14489, 14674, 14859, which correspond to lysozyme with 1, 2, and 3 N3-PEG2 labels, respectively (each label adds 185 Dato the protein).

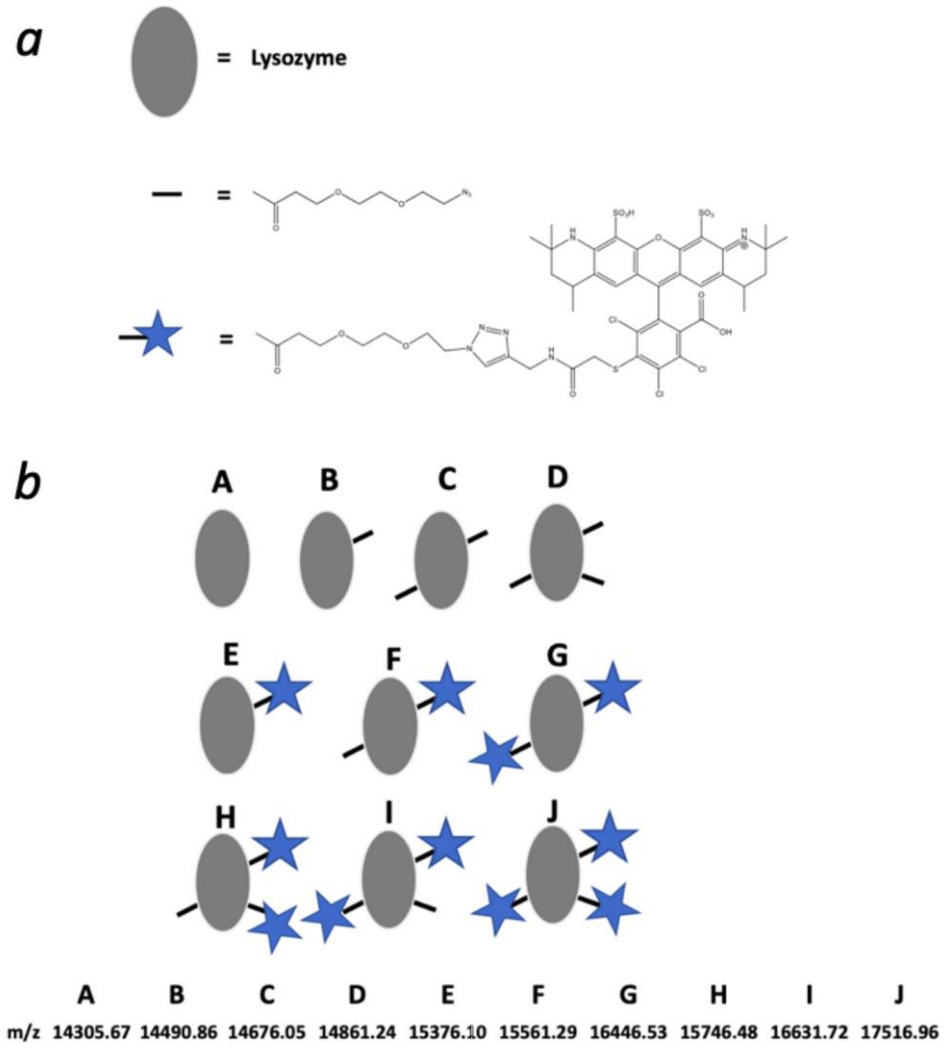

Figure A11 (a, b) Schematic of symbols used for the ESI mass spectrometry data shown in Figure A12. Product A represents unmodified lysozyme; B-D are lysozyme-$(N3)_{1-3}$; whereas, E-J represent different conjugates of lysozyme-$(N3)_{1-3}$ with ≡-AFDye 546.

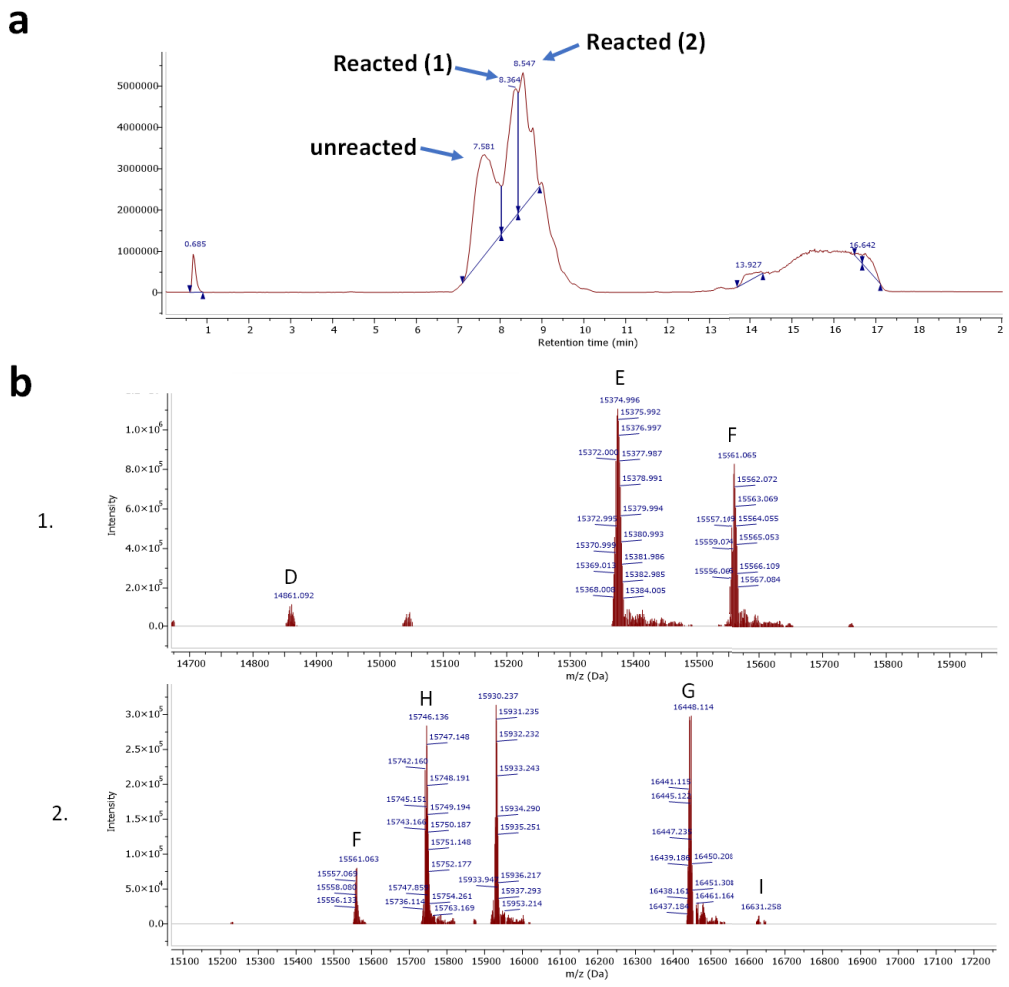

Figure A12 (a) LC Chromatogram, showing two peaks of interest, '1' and '2', with retention times of 8.37 min, and 9.01 min, respectively; (b) m/z profiles of chromatogram peaks '1' and '2 " , representing different lysozyme-(N3)1-3 and ≡ -AFDye 546 conjugates (products D-I shown, defined in Figure A11)

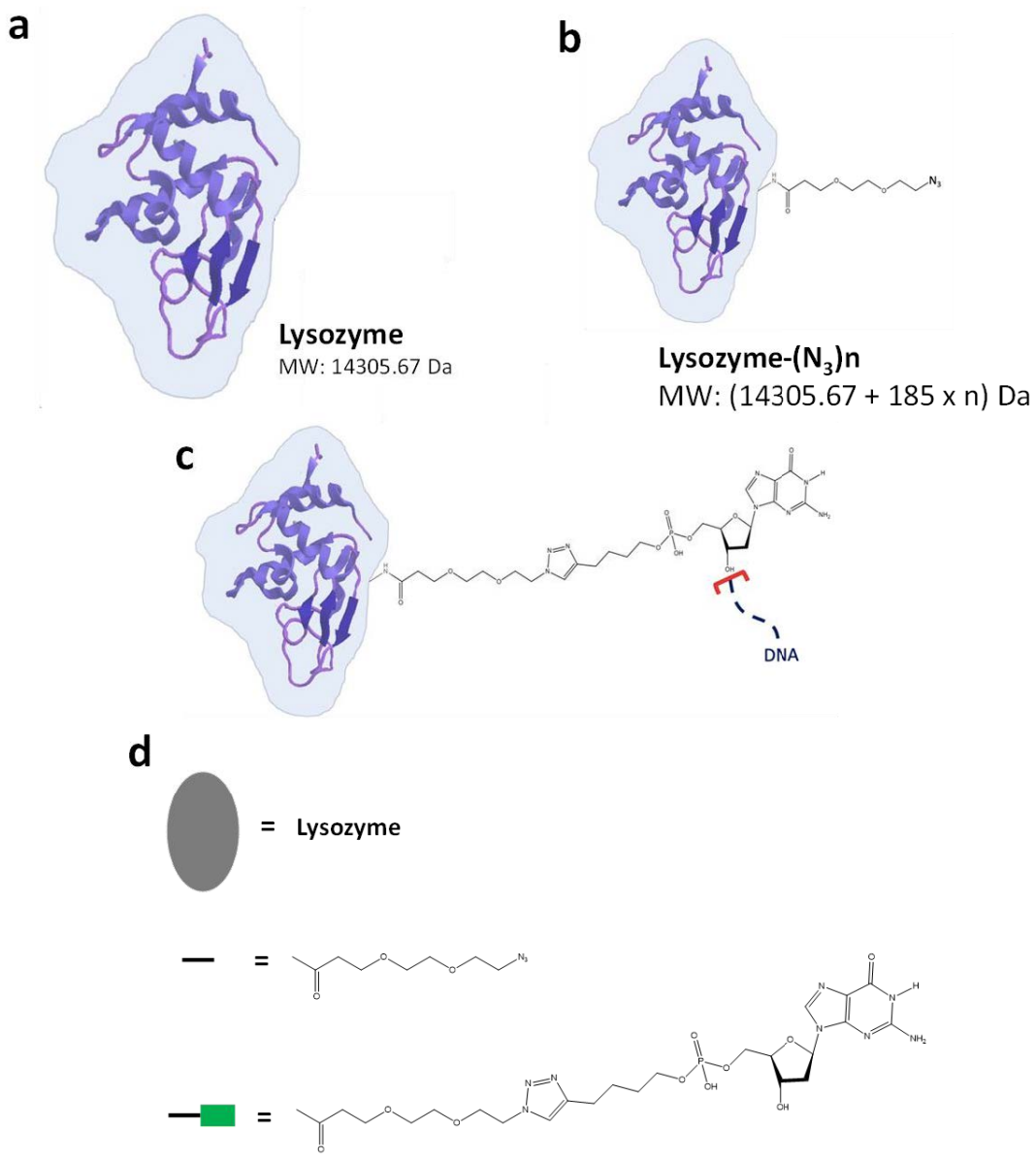

Figure A13 Expected molecular weights of underivatized lysozyme (a), and of azide-containing lysozyme-$(N3)_n$ (b), are shown. (c) Schematic diagram of lysozyme-$(N3)_n$ (where n = 1), and the *in cis* conjugated product of lysozyme-$(N3)_n$ (where n = 1) reacted with ≡-CLICK-17 (the full length of the conjugated CLICK-17 is shown as 'DNA'). For the purpose of ESI mass spectrometry analysis, the DNA was total-digested with Nuclease P1, an endonuclease that generates 5'-deoxyribonucleotide monophosphates. The portion of the appended CLICK-17 DNA removed by the nuclease P1 is shown by the red bracket. The expected structure of the DNA residue, incorporating the 5'-most deoxyriboguanosine of the CLICK-17 nucleotide sequence, is shown. (d) Schematic of symbols used for the ESI mass spectrometry data shown in Figure. A14.

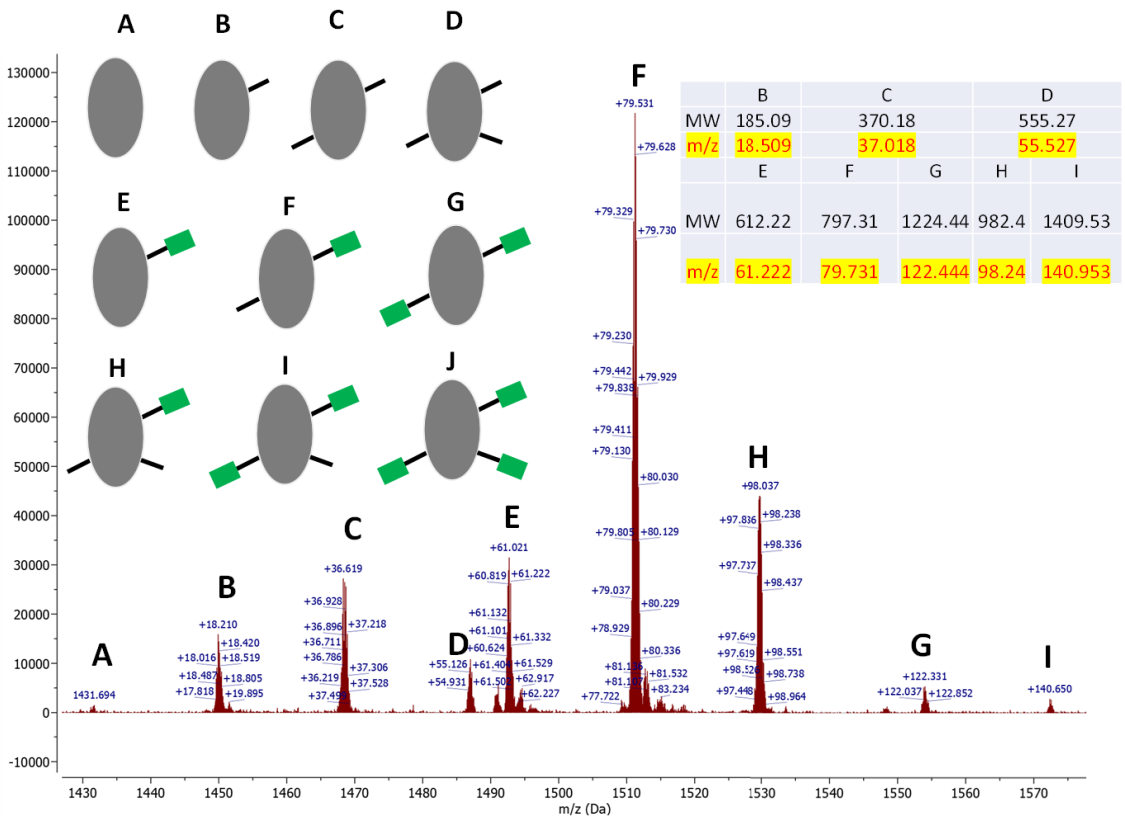

Figure A 14 ESI mass spectrometry data obtained from the Cu(I)-dependent and CLICK-17-catalyzed *in cis* conjugation of lysozyme-$(N3)_{1\text{-}3}$ with ≡-CLICK-17 itself. The various DNA protein conjugate species formed (see Figure A13 for an explanation for the symbols used) were treated with Nuclease P1 to digest away almost the entirety of each conjugated DNA in each case, leaving only the 5'-most deoxyriboguanosine residue behind as a fingerprint of the original DNA attachment.

CLICK-17: GGATC GTCAG TGCAT TGAGA TTATT ATGCA ACTCT ATGGG TCCAC TCTGT GAATG TGACG GTGGT ATCCG CAACG GGTA

CL-17_T24G: GGATC GTCAG TGCAT TGAGA TTAGT ATGCA ACTCT ATGGG TCCAC TCTGT GAATG TGACG GTGGT ATCCG CAACG GGTA

CLICK-16: GGATC GTCAG TGCAT TGAGA - -AGT ATGCA ACTCT ATGGG TCCAC TCTGT GAATG TGACG GTGGT ATCCG CAACG GGTA

CLICK-20: GGATC GTCAG TGCAT TGAGA TTAGT ATGCA ACTCT ATGCG TCCAC TCTGT GAATG TGATG GTGGT ATCCG CAACG GGTA

CL-20_C39G: GGATC GTCAG TGCAT TGAGA TTAGT ATGCA ACTCT ATGGG TCCAC TCTGT GAATG TGATG GTGGT ATCCG CAACG GGTA

CL-20_G24T: GGATC GTCAG TGCAT TGAGA TTATT ATGCA ACTCT ATGCG TCCAC TCTGT GAATG TGATG GTGGT ATCCG CAACG GGTA

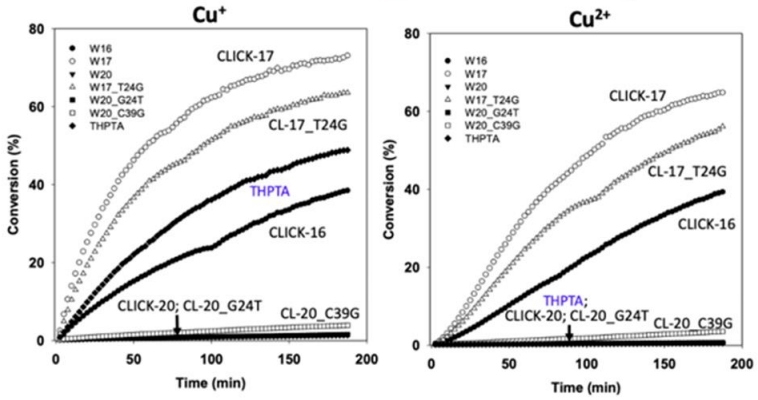

Figure A15 Nucleotide sequences of three of the original DNA clones (CLICK-17, CLICK16, and CLICK-20) obtained from the initial SELEX experiment for DNAzymes catalytic for the CuAAC reaction, as well as nucleotide sequences of three mutants, CLICK-17_T24G, CLICK20_C39G, and CLICK-20_G24T. Below, Cu(I)-dependent (left) and Cu(II)-dependent *in trans* conjugation profiles of hexynol with azide-coumarin.

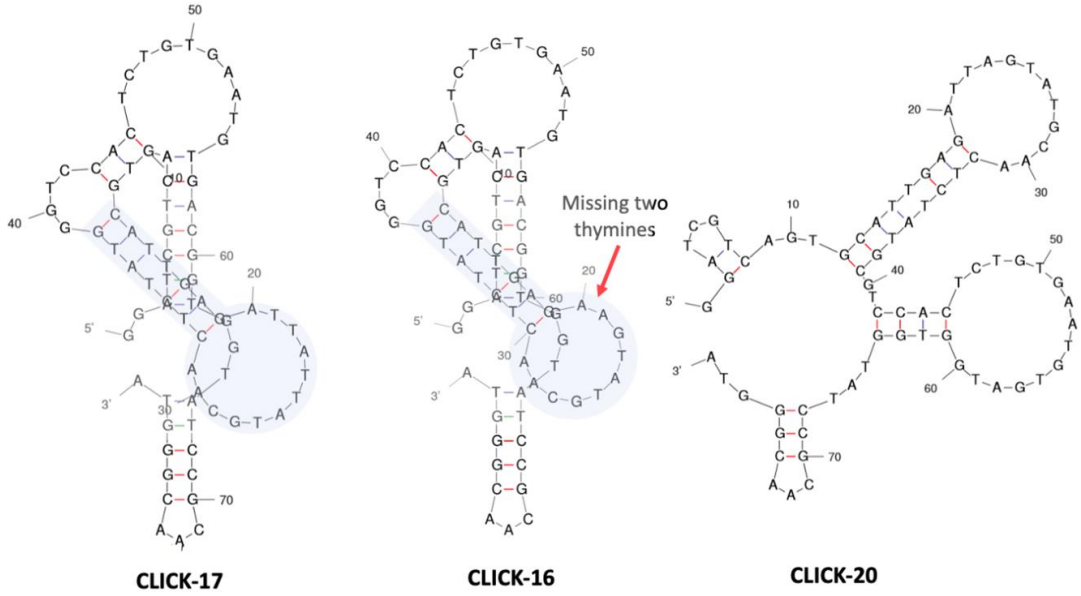

Figure A16 Secondary structure predictions, based on the Mfold program, for the the DNA sequences of clones CLICK-17, CLICK-16, and CLICK-20. The most thermodynamically stable predicted structure for each clone is shown.

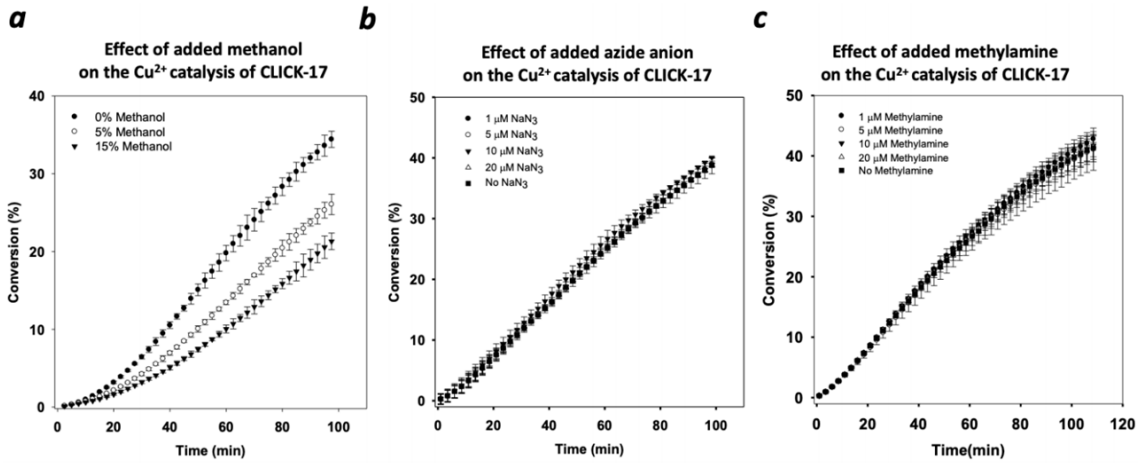

Figure A 17 Effect of supplementations of methanol; azide anion; and methylamine on CLICK-17's 'Cu(II)' catalysis. The data, above, plot averages from three independent experiments carried out for each of the supplementations shown. The error bars for the methanol data report one standard deviation from two independently collected data sets. Error bars for the azide anion and methylamine data report one standard deviation from three independently collected data sets.

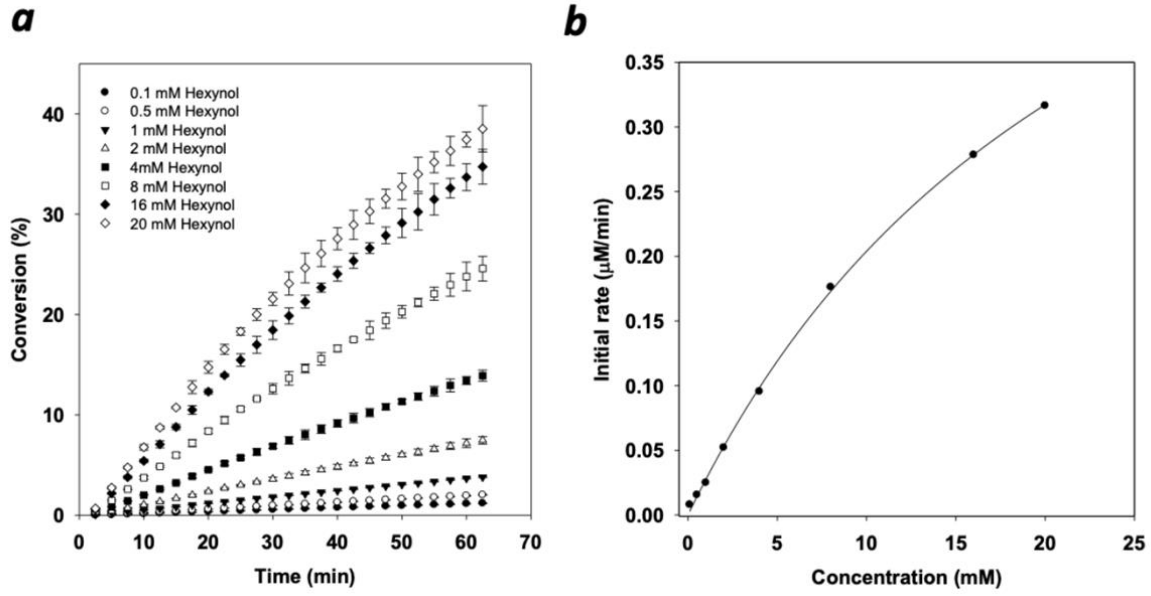

Figure A 18 Does folded CLICK-17 supply a high-affinity binding site for hexynol? Reaction time-dependence profiles of 2 μM CLICK-17 DNA catalyzing the reaction of 5-hexyne-1-ol ('hexynol'; 0.1-20 mM) in R buffer, with a fixed concentration of 3-azido-7-hydroxycoumarin ('azide-coumarin'; 50 μM) and Cu(I) (5 μM). The error bars report one standard deviation from three independently collected data sets.

Appendix B: Supporting Information of Chapter 3

Table B1 Comparison of the Reaction Conditions for Surface CuAAC Reported in Literature

Reference	Precursors	Reaction time	Catalyst
Ref 101	FcCOC≡CH and N3C11S-Au	4 h	10 mol % $CuSO_4$ (1 mM)
Ref 121	Fc-C≡CH and N3C11S-Au	20 min	400 μM Cu(TBTA)BF4)*
Ref 138	Porphyrin with carbon nanotubes	3 h	1 mol/L $Cu(MeCN)_4PF_6$
Ref 139	$[Mn(CO)_3(tpm\text{-}C{\equiv}CH)]PF_6$ w/ nano diamond	4 h	4 mM $CuSO_4$
Ref 140	Azide-terminated iron oxide nanoparticles and 11-(undec-1-ynyl)-S-Au	1 h	1.3 mM $CuBr(PPh_3)_3$
Ref 141	Propargylamine or 1-ethynylpyrene on cellulose fibre	24 h	1 mM Cu(I)TBMA**
Ref 142	Halogenated alkynes with silicon nitride	60 h	4 mM $CuSO_4$
Ref 143	Alkynyl-terminated poly(ethylene oxide) (ay-PEO18) and polymethacrylate	10 min	2 mM Cu(I)/triazole complex
This work	Fc-C≡CH and N3C11S- Au	30 min	50 μM $CuSO_4$

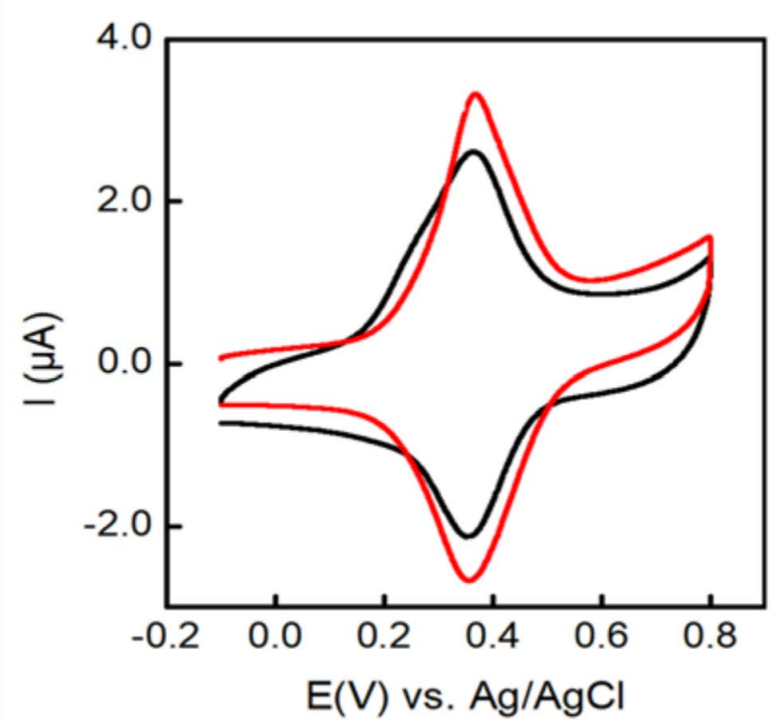

Figure B1 'Complete' derivatization of N3C11S-Au with Fc-C≡CH when catalyzed by Cu(I) only and together with CLICK-17 DNAzyme. Representative CV responses of N3C11S-Au upon derivatization with 50 μM Fc-C≡CH, which were catalyzed with either 50 μM Cu(I) for 4 h (black curve) or 4 μM CLICK-17 + 50 μM Cu (I) for 0.5 h (red curve), respectively. The supporting electrolyte for the CV measurements was 0.1 M $NaClO_4$, and the scan rate (v) was kept at 0.1 V/s. The potential was held at – 0.1 V for 10 sec and then scanned positively. The surface 'click reaction' was carried out in 25 mM HEPES buffer (pH 7.4) containing 50 μM $CuSO_4$, 20 mM $MgCl_2$, and 2.5 mM ascorbic acid (AA), in both cases. In the absence of the CLICK-17 DNAzyme, the reaction takes much longer (4 h vs. 30 min) to reach the maximum surface density of Fc groups. Although the surface densities of Fc groups were determined based on the integration of the anodic peaks to be similar (2.2 ± 0.3 × 10-10 mol/cm^2 for Cu(I) + CLICK-17 and 2.1 ± 0.2 × 10-10 mol/cm^2 for Cu(I) only), the CV peaks obtained from the former are more symmetric.

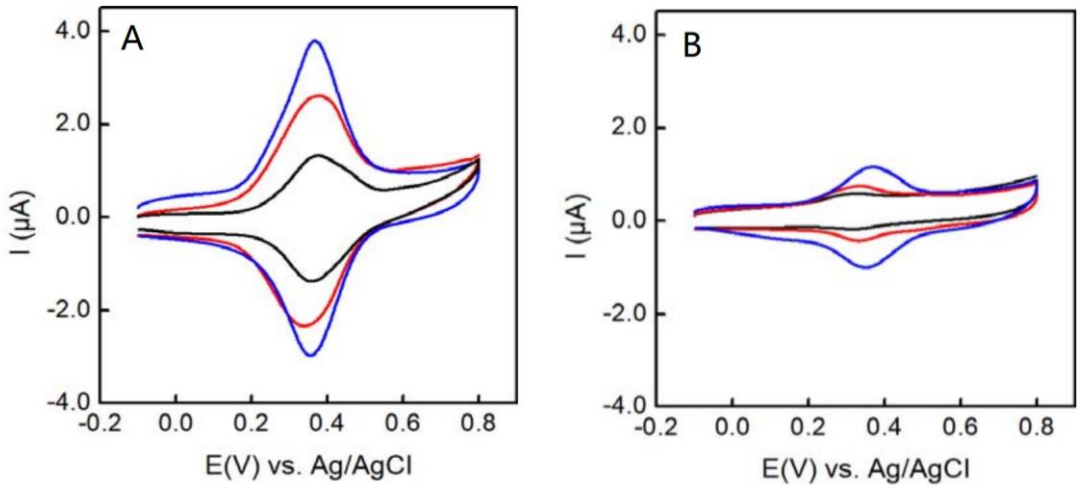

Figure B2 Kinetic studies of the derivatization of N3C11S-Au with Fc-C≡CH catalyzed by Cu(I) and CLICK-17 DNAzyme. (A) Representative CV responses of N3C11S-Au upon reacting with Fc-C≡CH in the presence of 50 μM Cu(I) + 4 μM CLICK-17 for 5 min (black curve), 15 min (red curve) and 30 min (blue curve); (B) Representative CV responses of N3C11S-Au upon derivatization with Fc-C≡CH in the presence of only 50 μM Cu(I) (without adding CLICK-17 DNAzyme) for 5 min (black curve), 15 min (red curve), and 30 min (blue curve). The surface reaction was performed in 25 mM HEPES buffer (pH 7.4) containing 50 μM $CuSO_4$, 2.5 mM AA, 50 μM Fc-C≡CH, 20 mM $MgCl_2$. These CV measurements were performed in 0.1 M $NaClO_4$ at a scan rate of 0.1 V/s. The potential was held at – 0.1 V for 10 sec and then scanned positively. Further analysis of these CV data is presented in Figure 3B in the main text.

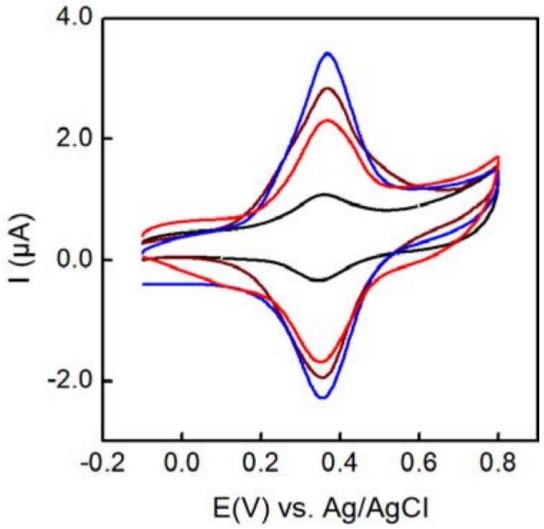

Figure B 3 Comparison of the activities of CLICK-17 DNAzyme and a popularly used organic ligand (THPTA) for the derivatization of N3C11S-Au with Fc-C ≡ CH. Representative CV responses of N3C11S-Au SAMs reacted with 50 μM Fc-C≡CH in the presence of 50 μM Cu(I) for 30 min (black curve), 4 μM THPTA+ 50 μM Cu(I) (red curve), 100 μM THPTA+ 50 μM Cu(I) (brown curve), 4 μM CLICK-17+ 50 μM Cu(I) (blue curve). Other components in the incubation solution are as following: 25 mM HEPES (pH 7.4), 2.5 mM AA, 20 mM $MgCl_2$. The CV measurements were performed in 0.1 M $NaClO_4$ at a scan rate of 0.1 V/s. The potential was held at – 0.1 V for 10 sec and then scanned positively. The quantitative analysis of these CV curves is presented in Figure 6 of the main text.

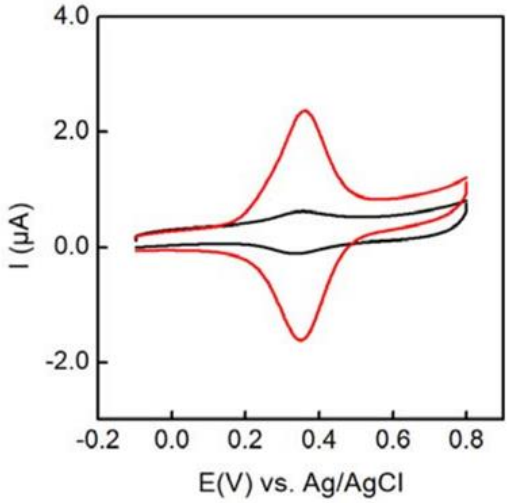

Figure B4 Derivatization of mixed N3C11S-/C8S-Au SAMs with Fc-C ≡ CH. Representative CV responses of N3C11S-/C8S-Au (3:7) SAMs upon derivatization with Fc-C≡CH catalyzed with 50 μM Cu(I) only (black curve) and together with 4 μM CLICK-17 (red curve). Other components in the incubation solution include 25 mM HEPES (pH 7.4), 2.5 mM AA, 20 mM $MgSO_4$. These CV measurements were performed in 0.1 M $NaClO_4$ at a scan rate of 0.1 V/s. The potential was held at – 0.1 V for 10 sec and then scanned positively. Upon 30-min reaction, the achieved Fc surface densities with and without the addition of DNAzyme is 1.45 ± 0.3 $\times 10^{-10}$ mol/cm^{2}and 0.23±0.03 $\times 10^{-10}$ mol/cm^2, respectively.

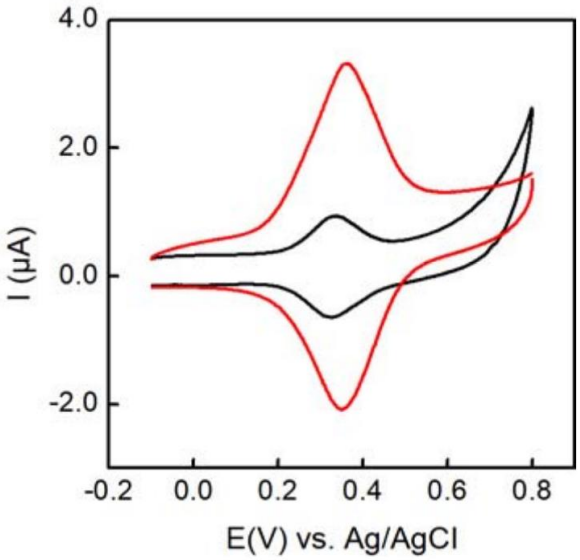

Figure B5 Effect of pre-treatment of the DNAzyme for its catalytic activity. Representative CV responses of N3C11S-/C8S-Au SAMs upon derivatization with Fc-C≡CH in the presence of 50 μM of Cu(I) and 4 μM CLICK-17 for 30 min without (black curve) and with pre-treatment (i.e., the stock solution of 40 μM CLICK-17 was incubated at 100 °C for 5 min, afterwards 200 μM of $MgSO_4$ was added and the solution was cooled gradually over a period of 10 min to room temperature. The CLICK-17 solution was then diluted to the final concentration of 4 μM before being added to the incubation solution). Other composition of the incubation solution includes 25 mM HEPES (pH 7.4), 20 mM $MgSO_4$, and 2.5 mM AA. The determined surface densities of Fc groups without and with the pretreatment is $0.43 \pm 0.05 \times 10^{-10}$ and $2.31 \pm 0.2 \times 10^{-10}$ mol/cm^2, respectively.

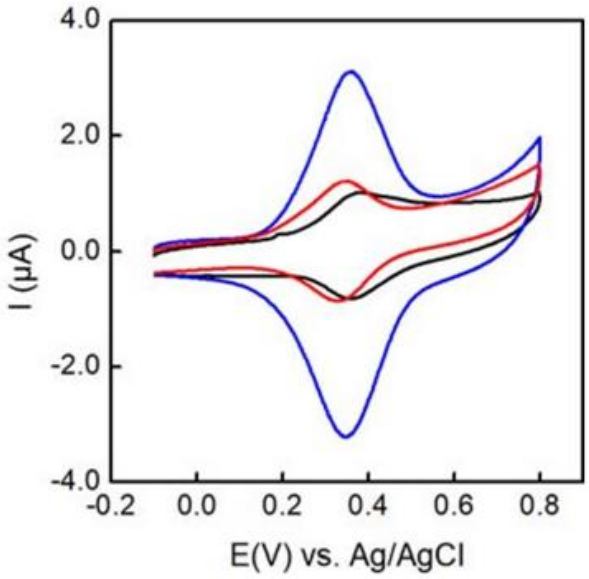

Figure B6 Comparison of control DNA (RAND-42) and the DNAzyme for its catalytic activity. Representative CV responses of N3C11S-Au SAMs upon derivatization with Fc-C≡CH in the presence of 50 μM of Cu(I) (red curve) or 50 μM of Cu(I) together with 4 μM CLICK-17 (blue curve) or with 4 μM of the control DNA (RAND-42) for 30 min. Other composition of the incubation solution includes 25 mM HEPES (pH 7.4), 20 mM $MgSO_4$, and 2.5 mM AA. The determined surface densities of Fc groups upon adding or without adding CLICK-17 was 2.05 ± 0.2×10^{-10} mol/cm^2 and 0.56 ± 0.05 × 10^{-10} mol/cm^2, respectively. While the determined surface densities of Fc groups upon adding RAND-42 DNA is 0.44 ± 0.03 × 10^{-10} mol/cm^2.

.

Appendix C: Supplementary Data for Chapter 4

Supplementary experimental data including gel electrophoresis assay for *in cis* reactions of hexynyl PERMUT-17 and hexynyl 20mer with Azide-PEG3-biotin, water contact angle measurements to follow the surface reaction, and additional CV results to characterize the sensor performance (reproducibility, kinetics, and industrial sample validation).

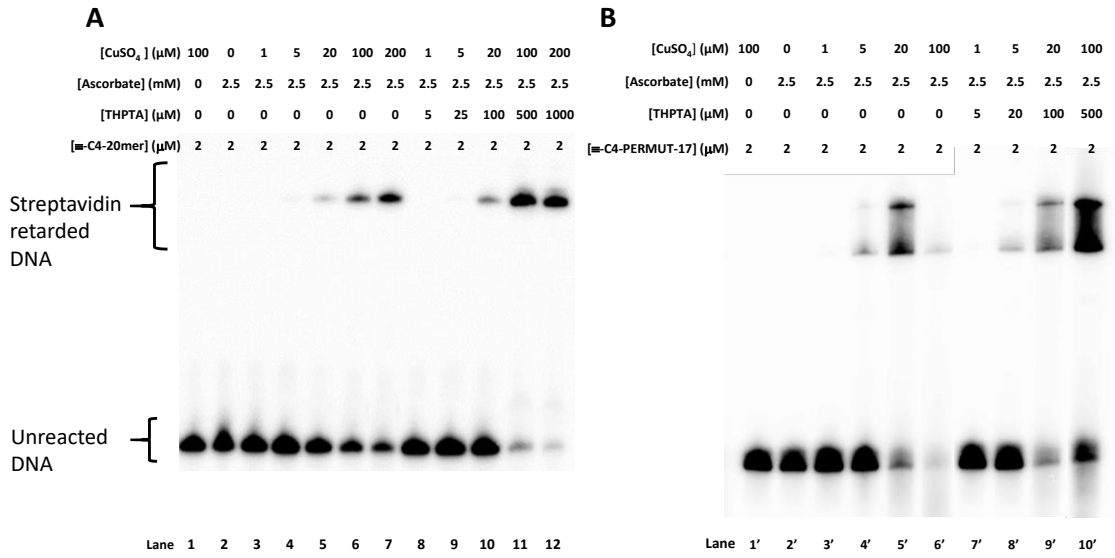

Figure C1 Gel electrophoresis assay for: (A) the *in cis* reaction of hexynyl-20mer (□-C4-20mer, 5'-GGA TCG TCA GTG CAT TGA GA-3') with azide-PEG3-biotin. (B) the *in cis* reaction of hexynyl PERMUT-17 (≡-C4-PERMUT-17) with azide-PEG3-biotin. It is clear that the precence of control DNA strands (≡-C4-20mer and ≡-C4-PERMUT-17) with low concentrations of copper, induced no detectable conversions (lanes 2-3, 8-9, 2'-3', 7'). At least 5.0 μM Cu(I) (lanes 4, 9, 4' and 8') was needed for the generation of detectable conversion. Severe DNA degradation was observed at 100 μM Cu(I) for ≡-C4-PERMUT-17 (Lane 10'), while ≡-C4-20mer, which is shorter, is more resistant to such oxidative damage induced degradation.

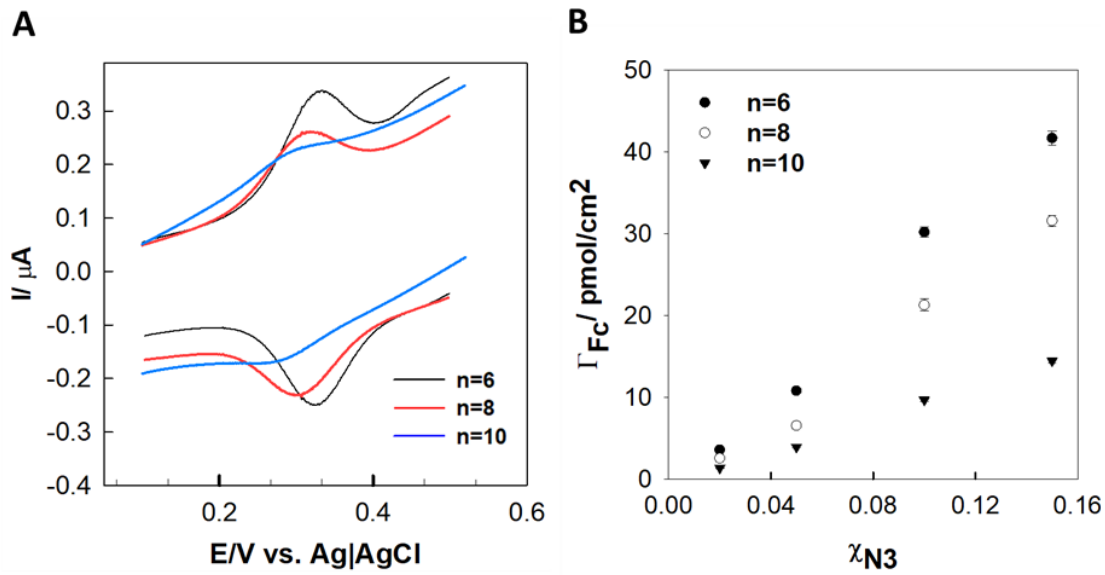

Figure C2 (A) Representative CV curves of binary N3C11S-/CnS-Au SAMs upon coupling ethynylferrocene in the presence of CLICK-17 DNAzyme (*in trans* conditions with unmodified CLICK-17) and Cu(I). Different diluent alkanethiols (CnSH, n = 6, 8, 10) and a low N3C11SH mole fraction (χ = 0.05) were tested. CVs were obtained in 10 mM Tris (pH = 7.4) buffer with 5.0 μM $Ru(NH_3)_6Cl_3$ at a scan rate of 50 mV/s. The potential was held at – 0.1 V for 10 sec and then scanned positively.; (B) plot of the ferrocene surface density Γ_{Fc} = Q/nFA, Q is the integrated charge of the oxidization peak) as a function of the mole fraction of N3C11SH in the deposition solution (χ_{N3} = 0.02, 0.05, 0.10, and 0.15). The uncertainties are based on three independent measurements. For all three different diluting alkanethiols, Γ_{FC} increases proportionally with increasing χ_{N3}. Since ethynylferrocene reacts with azido-terminated SAMs 'quantitatively' (i.e., 1:1 ratio), we can conclude that the surface density of azide groups (Γ_{N3}) is also proportional to the χ_{N3} in the solution. This is different from the case of coupling ≡-C4-CLICK-17 to the azido-terminated, indicative of restricted accessibility of azide groups for DNAzymes (especially in its folded form).

For the CLICK-17 catalyzed reaction between ethynylferrocene and azido SAMs, the experimental procedure from our previous paper was followed [J. Phys. Chem. C. 124 (2020) 19083–19090.]. Briefly, a 50 μl drop of solution (containing 4 μM unmodified CLICK-17, 20 mM HEPES (pH=7.4), 20 mM $MgCl_2$, 20 μM $CuSO_4$, 0.25 mM ethynylferrocene and 2.5 mM sodium ascorbate) was applied directly onto azido SAMs on gold. After incubation in a humidity chamber for 30 min, the gold chip was washed extensively with deionized water and dried by nitrogen gas prior to CV measurement.

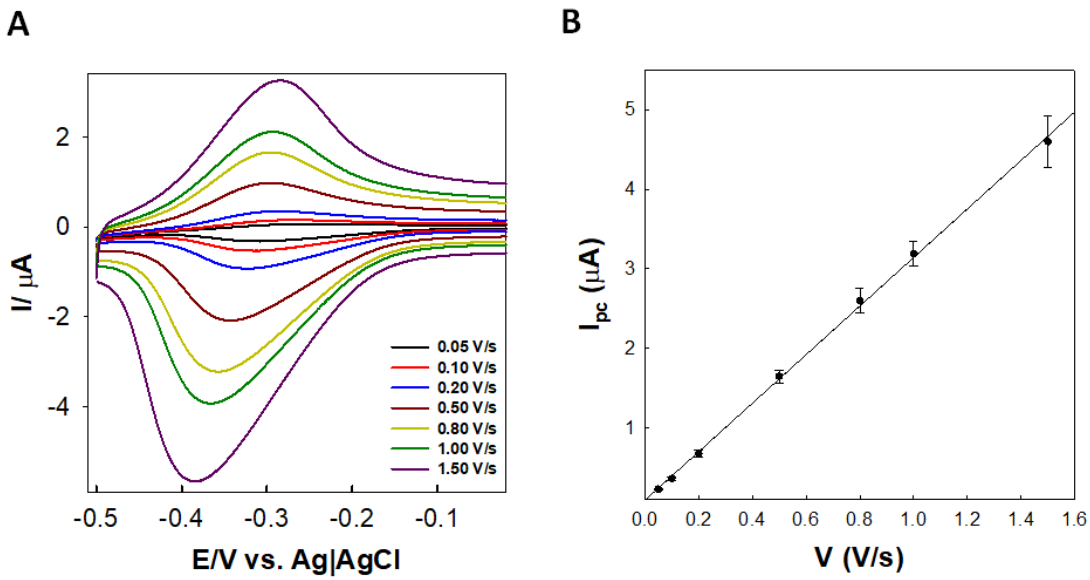

Figure C3 (A) Representative CV curves of 5.0 µM $Ru(NH_3)_6Cl_3$ on N3C11S-/C8S-Au (χ_{N3} = 0.05) upon *in cis* coupling of ≡-C4-CLICK-17 at different scan rates. The potential was held at 0.0 V for 10 sec and then scanned negatively. The coupling was performed with 2.0 µM DNA in 20 mM HEPES (pH 7.4) with 20 mM $MgCl_2$ and 1 µM $CuSO_4$ for 5 min). (B) Plot of the peak current versus the scan rate; the solid line shows the best linear fit to the experimental data. The near ideal linear relationship (R^2 = 0.9990) between Ipc and V confirms that the redox centers are confined on the electrode surfaces (as result of the successful coupling of DNAzymes on the azido SAMs). See, A. J. Bard, L. R. Faulkner, Electrochemical Methods: Fundamentals and Applications, New York: Wiley, 2001, 2nd ed, Page 591.

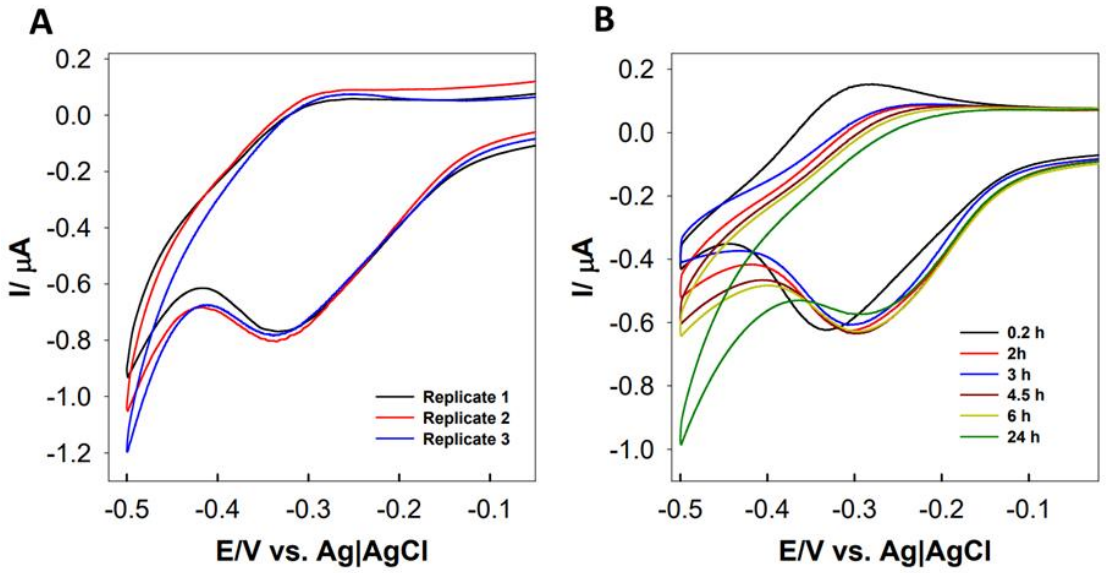

Figure C4 ((A) Representative CV curves of 5.0 µM Ru(NH3)6Cl3 on N3C11S-/C8S-Au (χ_{N3} = 0.05) upon *in cis* coupling of ≡-C4-CLICK-17 with independently prepared electrodes. The coupling was all performed with 2.0 µM DNAzyme in 20 mM HEPES (pH 7.4) with 20 mM $MgCl_2$ and 100 nM $CuSO_4$ for 30 min). The standard derivation of the integrated charges of the cathodic peaks from the three replicates is 0.035 µC (the average charge is 0.520 µC), less than 1%. (B) Representative CV curves of 5.0 µM $Ru(NH_3)_6Cl_3$ on N3C11S-/C8S-Au (χ_{N3} = 0.05) upon *in cis* coupling of ≡-C4-CLICK-17 to N3C11S-/C8S-Au (χ_{N3} = 0.05) scanned at different time after the coupling reaction (i.e., remained in the supporting electrolyte). There was no significant degradation for the first 6 h, i.e., the decrease in the integrated charge is about 10%.

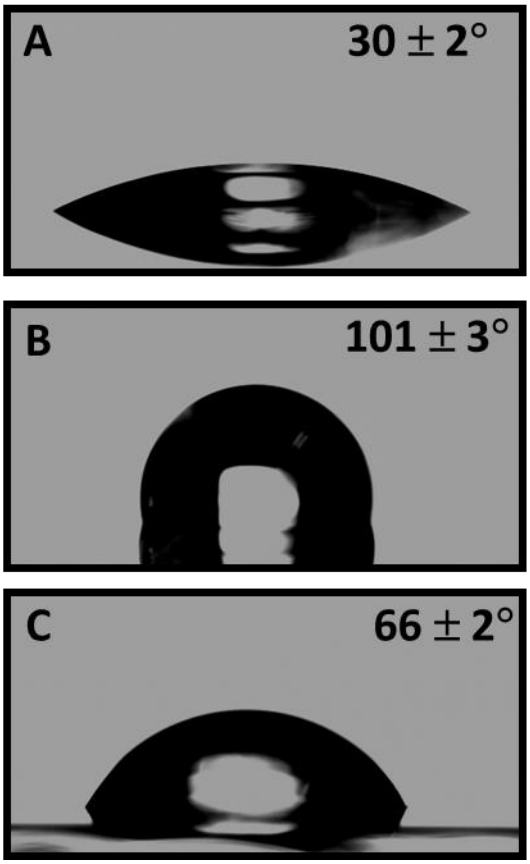

Figure C5 Sessile-drop water contact angle measurements on bare gold (A), N3C11S-/C8S-Au (χ_{N3} = 0.05) SAMs (B) and upon coupling with ≡-C4-CLICK-17 (C). The average contact angles are labelled as the top-right insets. The volume of the deionized water used in each measurement was 1.5 µl.

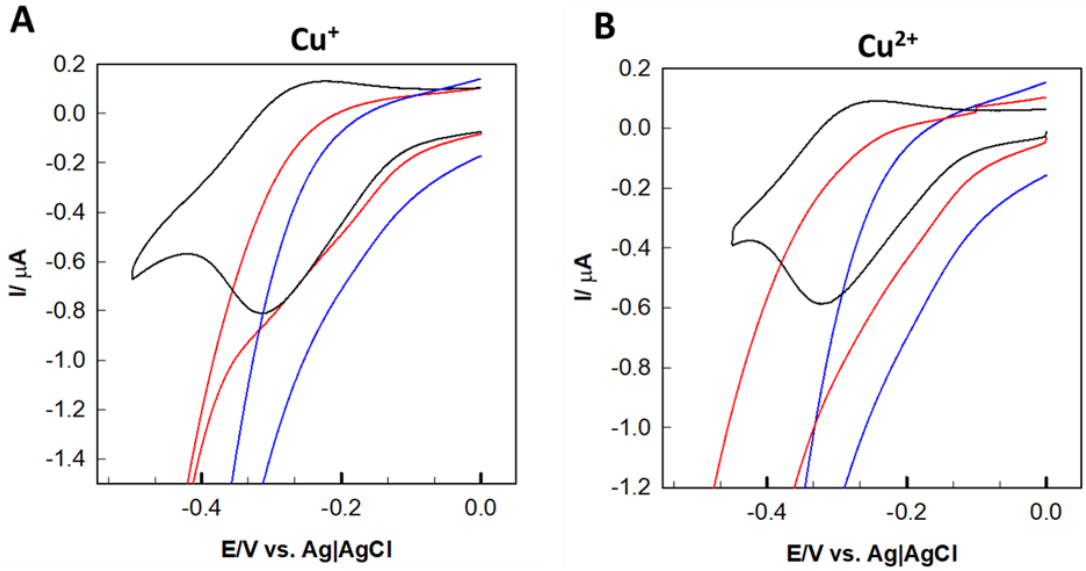

Figure C6 Representative CVs of 5.0 µM $Ru(NH_3)_6Cl_3$ on binary N3C11S-/C8S-Au upon reacting with ≡-C4-20mer (blue curve), ≡-C4-PERMUT-17 (red curve), and ≡-C4-CLICK-17 (black curve) in the presence of 5.0 µM Cu(I) (A) and 5.0 µM Cu(II) (B). The coupling was all performed with 2.0 µM DNA in 20 mM HEPES (pH 7.4) with 20 mM $MgCl_2$ for 30 min. CVs were obtained in 10 mM Tris buffer (pH = 7.4) with 5.0 µM $Ru(NH_3)_6Cl_3$ at a scan rate of 50 mV/s. The potential was held at 0.0 V for 10 sec and then scanned negatively. In both cases, only ≡-C4-CLICK-17 reacted with the binary azido-terminated SAMs to give rise to the well-defined $Ru[NH_3]_6^{3+/2+}$ peaks.

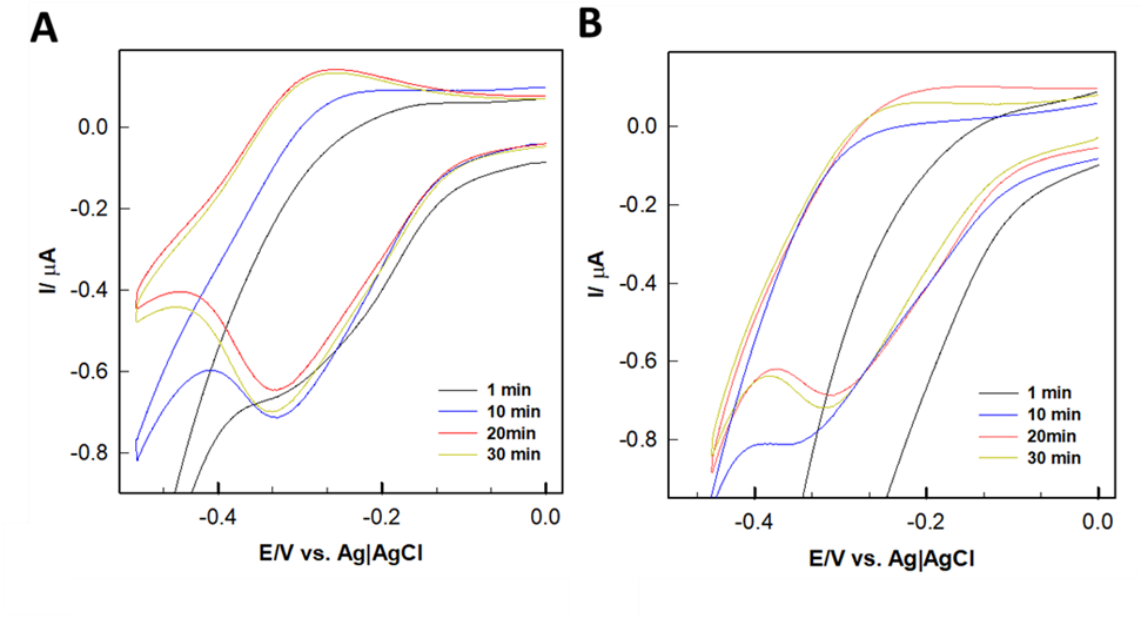

Figure C7 Representative CV curves of 5.0 μM $Ru(NH_3)_6Cl_3$ on N3C11S-/C8S-Au (N3 = 0.05) upon *in cis* coupling of ≡-C4-CLICK-17 to N3C11S-/C8S-Au (χ_{N3} = 0.05) in the presence of (A) 5.0 μM Cu(II); and (B) 0.04 μM Cu(II) for different periods of reaction time. In all cases, the reaction was performed with 2.0 μM DNA in 20 mM HEPES (pH 7.4) and 20 mM $MgCl_2$ for designated periods before quenched by washing with copious amounts of water. CVs were obtained in 10 mM Tris (pH = 7.4) buffer with 5 μM $Ru(NH_3)_6Cl_3$ at a scan rate of 50 mV/s. The potential was held at 0.0 V for 10 sec and then scanned negatively.

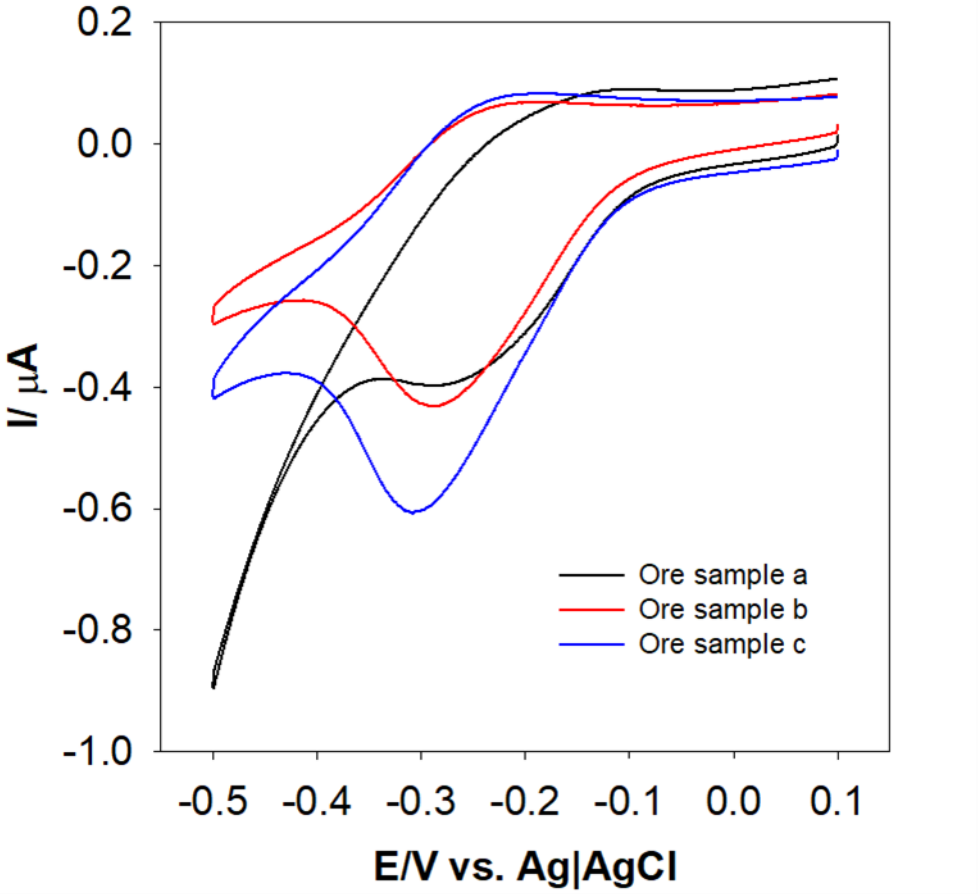

Figure C8 Representative CV curves for testing ore samples with the CLICK-17-based sensor. In all cases, ore extracts were added directly into the refolded ≡-C4-CLICK-17 (2 µM,) in 20 mM HEPES (pH 7.4 with 20 mM $MgCl_2$). The mixture was then used for the surface coupling reaction (30 min). CVs were obtained in 10 mM Tris (pH = 7.4) buffer with 5.0 µM $Ru(NH_3)_6Cl_3$ at a scan rate of 50 mV/s. The potential was held at 0.1 V for 10 sec and then scanned negatively. The weight percent determined by the CLICK-17 copper sensor are: 0.0404% ± 0.0041%, 0.203% ± 0.028%, and 2.37% ± 0.21%, respectively. These values are in excellent agreement with the AAS measurements (0.0374%% ± 0.0031%, 0.194% ± 0.015, and 2.48% ± 0.02%).

Table C1. Comparison of the DNAzyme-based copper detection with methods reported in literature.

Reference	Detection Method	Reagents & Reactions	Linear range & detection limit
[S1] Xu *et al.* Biosens. Bioelectron. 74 (2015) 1–7.	Electrochemical impedance spectroscopy	Cu^{2+} activates the DNA-cleaving DNAzyme to cleave the DNA substrate on a gold electrode. The shortened surface bound DNA then initiates a series of strand-displacement events to assemble duplex DNA bearing multiple G-quadruplex forming sequences. The hemin/G-quadruplex complex oxidized 4-chloro-1-naphthol to form precipitate on surface of gold electrode to induce a conductivity change.	Detection of Cu^{2+} with a linear range of 0.1 pM-5.0 nM, LOD of 0.06 pM
[S2] Liu *et al.* Biosens. Bioelectron. 26 (2011) 4111–4116.	Fluorometric detection in solution using a fluorescence spectrometer	A copper-dependent RNA cleaving DNAzyme (bearing one phosphorothioate linkage) was activated by Cu^{2+} to cleave its substrate. The fluorescence signal is restored upon the cleavage.	Detection of Cu^{+} with a linear range of 0-100 nM, LOD of 1.6 nM
[S3] Huang *et al*. Anal. Chem. 88 (2016) 3341–3347.	Fluorometric detection in solution using a fluorescence spectrometer	Graphene was used as both scaffold and quencher. The graphene bound fluorophore-labeled DNA cleaving DNAzyme was activated by Cu^{+} (Cu^{2+} plus ascorbate) to cleave its substrate. The fluorescence signal is restored upon the cleavage and release of substrate DNA from graphene.	Detection of Cu^{+} with a linear range of 0-0.05 μM, LOD of 0.365 nM
[S4] Yin *et al.* J. Am. Chem. Soc. 131 (2009) 14624–14625.	Colorimetric detection using a UV-Vis spectrophotometer	In the presence of Cu^{2+}, the copper dependent DNA cleaving DNAzyme is activated to cleave its substrate, which induces allosteric transformation of a G-quadruplex forming DNA. The resulted G-quadruplex/Hemin complex functions as a peroxidase	Detection of Cu^{2+} of 1 μM

		to generate a colorimetric signal by the oxidation of TMB.	
[S5] Liu *et al.* Chem. Commun.46 (2007) 4872.	Colorimetric detection using a UV-Vis spectrophotometer	In the presence of Cu^{2+}, the activated copper-dependent DNA ligating DNAzyme catalyzes the cross-linking reaction of DNA-modified AuNP, and induce a color change.	Detection of Cu^{2+} of 5 μM
[S6] Liu *et al.* J. Am. Chem. Soc. 129 (2007) 9838–9839.	Fluorometric detection in solution using a fluorescence spectrometer	In the presence of Cu^{+} (in situ generated by reduction of Cu^{2+} with ascorbate), a copper-dependent DNA-cleaving DNAzyme was activated. The activated DNAzyme then cleaves its substrate to retore the fluorescence of the molecular beacon.	Detection of Cu^{+} with a linear range of 0.1-0.5 μM, LOD of 35 nM
[S7] Situ *et al.* Sens. Actuator B. 240 (2017) 560-565.	Fluorometric detection in solution using a fluorescence spectrometer	In the presence of sodium ascorbate, Cu^{2+} is reduced to Cu^{+} to catalyzed the reaction between azido-functionalized tetraphenylethene (BATPE) and terminal alkyne that leads to the aggregation of fluorescent BATPE.	Detection of Cu^{+} with a linear range of 0.2-12 μM, LOD of 0.2 μM
[S8] Copper Assay Kit (MAK 127)	Colorimetric detection using a UV-Vis spectrophotometer	The formation of a colored complex converted from a chromogen upon the specific addition of copper ions.	Detection of Cu^{+} with a linear range of 1.0-47 μM
[S9] Copper and Iron Test Strip Kit (2994)	Colorimetric, semi-quantitative test in vials by comparing the resulted color with the standard color card	N/A	Detection of Cu^{+} with a linear range 4.7-47 μM
[S10] Copper Detection Assay Kit (K899-100)	Fluorometric detection on 96-well plates	In the presence of sodium ascorbate, Cu^{2+} is reduced to Cu^{+} to catalyze the fluorescent reaction	Detection of Cu^{+} with a linear range of 1.0-10 μM, LOD of

			1.0 μM
The present CLICK-17 based sensor	Cyclic voltammetry	*In cis* coupling alkyne DNAzyme on azido SAMs on gold that is dependent on the copper concentration; electrostatically adsorbed $Ru(NH_3)_6^{3+}$ to provide naturally enhanced signal	Detection of Cu^{+} with a linear range of 0-40 nM, LOD of 0.8 nM. Detection of Cu^{2+} with a linear range of 0-40 nM, LOD of 3.5 nM.

(S1) Xu, M.; Gao, Z.; Wei, Q.; Chen, G.; Tang, D. Hemin/G-Quadruplex-Based DNAzyme Concatamers for in Situ Amplified Impedimetric Sensing of Copper(II) Ion Coupling with DNAzyme-Catalyzed Precipitation Strategy. *Biosens Bioelectron*. **2015**, 74, 1–7.

(S2) Huang, P.J. J.; Liu, J. An Ultrasensitive Light-up Cu 2+ Biosensor Using a New DNAzyme Cleaving a Phosphorothioate-Modified Substrate. *Anal. Chem*. **2016**, 88, 3341–3347.

(S3) Liu, M.; Zhao, H.; Chen, S.; Yu, H.; Zhang, Y.; Quan, X. A 'Turn-on' Fluorescent Copper Biosensor Based on DNA Cleavage-Dependent Graphene-Quenched DNAzyme. *Biosens Bioelectron*. **2011**, 26, 4111–4116.

(S4) Yin, B. C.; Ye, B. C.; Tan, W.; Wang, H.; Xie, C.C. An Allosteric Dual-DNAzyme Unimolecular Probe for Colorimetric Detection of Copper(II). *J. Am. Chem. Soc.* **2009**, 131, 14624–14625.

(S5) Liu, J.; Lu, Y. Colorimetric Cu2+ Detection with a Ligation DNAzyme and Nanoparticles. *Chem. Commun*. **2007**, 46, 4872.

(S6) Liu, J.; Lu, Y. A DNAzyme Catalytic Beacon Sensor for Paramagnetic Cu 2+ Ions in Aqueous Solution with High Sensitivity and Selectivity. *J. Am. Chem. Soc*. **2007**, 129, 9838–9839.

(S7) Situ, B.; Zhao, J.; Lv, W.; Liu, J.; Li, H.; Li, B.; Chai, Z.; Cao, N.; Zheng, L. Naked-Eye Detection of Copper(II) Ions by a 'Clickable' Fluorescent Sensor. *Sens. Actuators B Chem*. **2017**, 240, 560–565.

(S8) *Copper Assay Kit*; Cat. No. MAK127; Sigma-Aldrich: Missouri, USA.

(S9) *Copper and Iron Test Strip Kit*; Cat. No. 2994; LaMotte: Maryland, USA.

(S10) *Copper Detection Assay Kit (Fluorometric)*; Cat. No. K899-100; BioVision: California, USA.